TGP2: 00133

a0010

133 Hotspots, Large Igneous Provinces, and Melting Anomalies

MD Ballmer, University of Hawaii, Honolulu, HI, USA; Tokyo Institute of Technology, Meguro-ku, Tokyo, Japan
PE van Keken, University of Michigan, Ann Arbor, MI, USA
G Ito, University of Hawaii, Honolulu, HI, USA

This article is a revision of the previous edition article by [G Ito and P E van Keken], Volume 7, pp. 371–435, © 2007, Elsevier BV.

s0010

133.1 Introduction

p0010 Volcanism on Earth and the generation of the oceanic and continental crust predominantly occur along divergent or convergent margins. At mid-oceanic ridges, decompression of the upwelling mantle induces magmatism. At subduction zones, the influx of fluids released from the metamorphic dehydration reactions in the downgoing slab leads to partial melting of the overlying hot mantle wedge. In contrast, several forms of volcanism are less readily explained by plate tectonic processes. These include, for example, the formation of intraplate hotspot islands (such as Hawaii) and excessive flood basalt volcanism at plate boundaries (such as at Iceland).

p0015 The most prominent melting anomalies typically occur on top of a broad swelling of topography and are trailed by a volcano chain that parallels plate motion. In some cases, these chains project back to massive volcanic plateaus (large igneous provinces, LIPs), suggesting that hotspot activity began with magmatic outbursts as large as any in the geologic record (Duncan and Richards, 1991; Morgan, 1972; Richards et al., 1989; White and McKenzie, 1989). These observations have led to the establishment of classical 'hotspot' theory proposed by Wilson (1963, 1973), Morgan (1971, 1972), and Crough (1978), who describe hotspots as positive thermal anomalies in the mantle that are fixed relative to the motion of the tectonic plates. These plumes cause excess seafloor elevation and feeding age-progressive volcanism.

p0020 Modern dating techniques, however, recover complex age patterns for many volcano chains and reveal that intraplate volcanism cannot universally be ascribed to activity at localized hotspots (Koppers et al., 2003; McNutt et al., 1997). In addition, some hotspots are not confidently linked to anomalously high mantle temperatures (Klein and Langmuir, 1987; Langmuir et al., 1992). In turn, most hotspots are fed by melting of a source that is geochemically distinct and typically more fertile than 'normal' mantle that feeds mid-ocean ridge (MOR) melting (Hart et al., 1973; Hofmann, 1997; Jackson and Dasgupta, 2008; Schilling, 1971, 1973). Thus, the term 'melting anomaly' may be more general and appropriate to describe the topic of this chapter.

p0025 The differences between the hotspot source and the 'normal' mantle in both major elements and isotopes (Jackson and Dasgupta, 2008) suggest that volcanism at melting anomalies has origins that are at least partly decoupled from plate tectonic processes. A straightforward explanation is that magmatism is sustained by convective upwellings or plumes of unusually hot, buoyant mantle, which rise from the lower mantle (Morgan, 1971, 1972; Whitehead and Luther, 1975; Wilson, 1963, 1973), possibly through a chemically heterogeneous mantle (e.g., Richter and McKenzie, 1981). The morphology of a mantle plume, simulated in laboratory and numerical experiments, is predicted to have a large 'mushroom'-shaped head and a trailing, narrower plume stem. This geometry is similar to that expected for the formation of an LIP followed by a hotspot track (e.g., Campbell and Griffiths, 1990; Richards et al., 1989). Recent regional (e.g., Wolfe et al., 2009) and global seismic studies (e.g., Boschi et al., 2007; Montelli et al., 2006; Zhao, 2007) are providing increasingly convincing evidence for mantle plumes originating in the lower mantle. Another observational link to the deep mantle is the spatial relation of hot spot and LIP locations to the edges of large low-shear-wave-velocity provinces (LLSVPs) imaged at the base of the mantle (Boschi et al., 2007; Burke and Torsvik, 2004; Torsvik et al., 2006).

p0030 Studies of hotspots have flourished over the past few decades. Recent articles and textbooks discuss some of the classic ties of hot spots to mantle plumes (e.g., Campbell, 2007; Campbell and Kerr, 2007; Condie, 2001; Davies, 1999; Foulger and Jurdy, 2007; Foulger et al., 2006; Jackson, 1998; Schubert et al., 2001; Sleep, 2006), the role of mantle plumes in deep mantle convection and chemical transport (e.g., Deschamps et al., 2011; Jellinek and Manga, 2004; Kumagai et al., 2008), and oceanic hot spots (e.g., Ballmer et al., 2011; Hekinian et al., 2004; Ito et al., 2003). It has become apparent that only a few hot spots confidently show all of the previously mentioned characteristics of the classic plume description (Clouard and Bonneville, 2001; Courtillot et al., 2003). The term 'hotspot' itself implies a localized region of anomalously high mantle temperature, but some features that were originally called hotspots may involve little or no excess heat or large distances of coeval volcanism. To understand these discrepancies, there has been significant exploration of the interaction of mantle plumes with plate tectonic processes (e.g., Kincaid et al., 2013; Mittelstaedt et al., 2012), the dynamic effect of compositional heterogeneity (Ballmer et al., 2013b; Davaille, 1999; Kumagai et al., 2008; Lin and van Keken, 2005), and mechanisms that can feed non-hot spot volcanism (Ballmer et al., 2007; Clouard and Gerbault, 2008; Conrad et al., 2011). The progress made in the last decade motivates a comprehensive review on studies of hotspots, LIPs, and melting anomalies. We here summarize the main observations, outline the mechanisms that have been proposed to cause hotspots and other melting anomalies, and pose questions that need quantitative answers.

133.2 Characteristics

s0015

p0035 Guided by the classical description of hot spots, we examine four main characteristics: (1) geographic age progression along volcano chains, (2) initiation by massive flood basalt volcanism, (3) a swell of anomalously shallow topography surrounding volcanoes, and (4) basaltic volcanism with geochemical distinction from most MOR basalts (MORBs). Given the marked progress in seismic methods over the past decade, we also summarize the findings of mantle seismic structure beneath hot spots and surface melt anomalies. **Table 1** provides a compilation of the previously mentioned characteristics for the 67 hot spots and melting anomalies. **Figure 1** shows a global map of their locations with abbreviations and the main LIPs that we will discuss.

133.2.1 Volcano Chains and Age Progression

s0020

133.2.1.1 Long-lived age-progressive volcanism

s0025

p0040 At least 13 hotspot chains record volcanism enduring for more than 50 My. The Hawaiian–Emperor and the Louisville chains, for example, span thousands of kilometers across the Pacific

T0010 **Table 1** Summary of characteristics

Name (abbreviation)	*Hot spot E. long., N. lat.*	*Age progression?*	*Age range*	*Swell? and width (km)*	*Connection to LIP?*	*Geochemically distinct from MORB*
Pacific						
Baja (BAJ)	−113, 27	–	–	No	No	–
Bowie–Kodiak (BOW)	−130, 49.5	Ok	0.1–23.8 Ma	Yes/250 km	No	Maybe $^{206}Pb/^{204}Pb$
Caroline (CAR)	−163, 5.3	Weak	1.4 Ma (east) to 4.7–13.9 Ma (west)	–	No	No
Cobb (COB)	−128.7, 43.6	Good	1.5–29.2 Ma	Yes/370	No	No
Cook (CK)	−149.5, −23.5	No	0.2–19.4 Ma	Yes/500	No	$^{206}Pb/^{204}Pb$
Austral (AU)	−140.0, −29.37	No	0–58.1 Ma	Yes/600	No	$^{206}Pb/^{204}Pb$
Easter (EAS)	−109, −27	Good	0–25.6 Ma	yes/580	Maybe Tuamotu and Mid-Pac	$^{206}Pb/^{204}Pb$
Foundation (FOU)	−111, −39	Good	2.1–21 Ma	Yes/250	No	$^{206}Pb/^{204}Pb$
Galápagos (GAL)	−91.6, −0.4	Yes	0–14.5 Ma offshore; 69–139 Ma, Caribbean LIP	Yes/300	Caribbean LIP	$^{206}Pb/^{204}Pb$
Geologist (GEO)	−157, 19	No	82.7–84.6 Ma	–	No	–
Guadalupe (GUA)	−118, 29	–	$<$3.4 to $\sim$20.3 Ma	Maybe/?	No	–
Hawaii–Emperor (HAW)	−155.3, 18.9	Good	0–75.8 Ma	Yes/920	No	$^{3}He/^{4}He$ and $^{87}Sr/^{86}Sr$ for Hawaiian Islands but not Emperor Seamounts
Japanese–Wake (JWK)	–	No	78.6–119.7 Ma	No	No	$^{206}Pb/^{204}Pb$
Juan Fernandez (JFE)	−79, −34	Weak	1–4 Ma (2 volcanoes dated)	Yes/?	No	$^{3}He/^{4}He$ and $^{87}Sr/^{86}Sr$
Line Islands (LIN)	–	No	35.5–91.2 Ma.	Partially/?	Maybe Mid-Pac	–
Louisville (LOU)	−141.2, −53.6	Good	1.1–77.3 Ma	Yes/540	Doubtfully OJP	$^{206}Pb/^{204}Pb$, maybe $^{87}Sr/^{86}Sr$
Magellan Seamounts (MAG)	–	No	87–118.6 Ma	No	No	$^{87}Sr/^{86}Sr$ and $^{206}Pb/^{204}Pb$
Marquesas (MQS)	−138.5, −11	Ok	0.8–5.5 Ma	Yes/850	Maybe Shatsky or Hess	$^{87}Sr/^{86}Sr$, maybe $^{206}Pb/^{204}Pb$
Marshall Islands (MI)	–	No	68–138 Ma	Maybe/?	No	$^{206}Pb/^{204}Pb$
Mid-Pacific Mountains (MPM)	–	No	73.5–128 Ma	No	It could be an LIP	–
Musician (MUS)	–	Ok	65.5–95.8 Ma	No	No	–
Pitcairn (PIT)	−129.4, −25.2	Good	0–11.1 Ma	Yes/570	No	$^{87}Sr/^{86}Sr$
Pukapuka (PUK)	−165.5, −10.5	Ok	5.6–27.5 Ma	Yes/?	No	$^{206}Pb/^{204}Pb$
Samoa (SAM)	−169, −14.3	Weak	0–23 Ma	400	No	$^{87}Sr/^{86}Sr$, $^{3}He/^{4}He$, and $^{206}Pb/^{204}Pb$
San Felix (SF)	−80, −26	–	–	Yes/?	No	–
Shatsky (SHA)	–	Yes	128–145 Ma	No	It is an LIP	No

(*Continued*)

Table 1 (Continued)

Name (abbreviation)	*Hot spot E. long., N. lat.*	*Age progression?*	*Age range*	*Swell? and width (km)*	*Connection to LIP?*	*Geochemically distinct from MORB*
Society (SOC)	−148, −18	Good	0.01–4.6 Ma	Yes/?	No	$^{87}Sr/^{86}Sr$ and $^{206}Pb/^{204}Pb$
Socorro (SCR)	−111, 19	–	–	Yes/?	No	–
Tarava (TAR)	173, 3	Weak	35.9 Ma and 43.5 Ma	Yes/?	No	–
Tuamotu (TUA)	–	Good	58–74 Ma	Yes/?	No	–
North America						
Yellowstone (YEL)	−111, 44.8	Yes	16–17 Ma	Yes/600	Maybe Columbia River basalts	–
Australia						
Balleny (BAL)	164.7, −67.4	Weak	–	–	Maybe Lord Howe Rise	$^{206}Pb/^{204}Pb$ (2 analyses)
East Australia (AUS)	143, −38	–	–	–	–	–
Lord Howe (LHO)	159, −31	–	–	–	It could be LIP	–
Tasmantid (TAS)	153, −41	Yes	–	Yes/300	Maybe Lord Howe Rise	–
Africa						
Afar (AF)	42, 12	No	–	–	–	–
East Africa/ Lake Victoria (EAF)	34, 6	No	–	–	–	–
Darfur (DAR)	24,13	No	–	–	–	–
Ahaggar (HOG)	6, 23	No	–	–	–	–
Tibesti (TIB)	17, 21	No	–	–	–	–
Ascension/ Circe (ASC)	−14, −8	–	<1 Ma (Ascension) and 6 Ma (Circe)	Yes/800	No	$^{206}Pb/^{204}Pb$
Azores (AZO)	−28, 38	Seafloor spreading	0–20 Ma, possibly ~85 Ma	Yes/2300	No	$^{87}Sr/^{86}Sr$ and $^{206}Pb/^{204}Pb$
Bermuda (BER)	−65, 32	–	–	Yes/500 × 700 (parallel × perp to plate motion)	No	–
Bouvet (BOU)	3.4, −54.4	–	?	Yes/900	Agulhas Plateau?	$^{206}Pb/^{204}Pb$, maybe $^{87}Sr/^{86}Sr$ and $^{3}He/^{4}He$
Cameroon (CAM)	6, −1	No	1–32 Ma	Yes/500–600	No	$^{206}Pb/^{204}Pb$
Canaries (CAN)	−17, 28	Ok	0–68 Ma	No	No	$^{206}Pb/^{204}Pb$
Cape Verde (CAP)	−24, 15	No	Neogene	Yes/800	No	$^{87}Sr/^{86}Sr$ and $^{206}Pb/^{204}Pb$
Discovery (DIS)	−6.45, −44.45	–	35–41 Ma	Yes/600	No	–
Fernando Do Noronha (FER)	−32, −4	–	–	Yes/200–300	–	$^{87}Sr/^{86}Sr$ and $^{206}Pb/^{204}Pb$
Great Meteor (GM)	–	–	–	Yes/800	–	–
Iceland (ICE)	−17.6, 64.6	Yes	0–62 Ma	Yes/2700	N. Atlantic LIP	$^{3}He/^{4}He$
Madeira (MAD)	−17.5, 32.7	Yes	0–67 Ma	No	No	$^{206}Pb/^{204}Pb$
New England (NEW)	−57.5, 35	Yes	81–103, 122–124 Ma	No	No	$^{206}Pb/^{204}Pb$, maybe $^{87}Sr/^{86}Sr$
Shona–Agulhas (SHO)	−4, −52	–	2.5–81 Ma	~900	–	–
Sierra Leone (SL)	−29, 1	–	Not dated	–	It could be an LIP	–

(*Continued*)

Table 1 (Continued)

Name (abbreviation)	*Hot spot E. long., N. lat.*	*Age progression?*	*Age range*	*Swell? and width (km)*	*Connection to LIP?*	*Geochemically distinct from MORB*
St. Helena (SHE)	−10, −17	Yes	3–81 Ma	Yes/720	No	$^{206}Pb/^{204}Pb$
Trindade–Martim Vaz (TRN)	−12.2, −37.5	Probably	<1 Ma to ~85 Ma	Yes/1330	Small eruptions north of Paraná flood basalts and onto Brazilian margin	$^{87}Sr/^{86}Sr$ and $^{206}Pb/^{204}Pb$
Tristan–Gough (TRI)	−9.9, −40.4	Yes	0.5–80 Ma and 130 Ma	Yes/850	Rio Grande–Walvis and Paraná–Etendeka	$^{87}Sr/^{86}Sr$
Vema (VEM)	16, −32	–	>11 Ma	Yes/200–300		–
Amsterdam–St. Paul (AMS)	77, −37	No	–	yes/300–500	Maybe Kerguelen	Maybe $^{87}Sr/^{86}Sr$
Comores (COM)	44, −12	Yes	0–5.4 Ma on island chain and ~50 Ma (Seychelles)	yes/700–800	–	$^{87}Sr/^{86}Sr$ and $^{206}Pb/^{204}Pb$
Conrad (CON)	48, −54	–	Not dated	Half width 400 south of seamounts	It could be an LIP	–
Crozet (CRO)	50, −46	–	Not dated	Yes/1120	Maybe Madagascar	$^{206}Pb/^{204}Pb$, maybe $^{87}Sr/^{86}Sr$ (but few samples)
Kerguelen (KER)	63, −49	Yes	0.1–114 Ma (Kerguelen) and 38–82 Ma (Ninetyeast–Broken Ridge)	Yes/1310	It is an LIP	$^{87}Sr/^{86}Sr$
Marion (MAR)	37.8, −46.8	Weak	<0.5 Ma (Marion) and 88 Ma (Madagascar)	Half width 500 or along axis >1700	Madagascar Plateau and Madagascar island flood basalts	Maybe $^{87}Sr/^{86}Sr$
Réunion (REU)	55.5, −21	Yes	0–70 Ma	Yes/1380	Mascarene, Chagos–Laccadive, and Deccan 30–70 Ma	$^{3}He/^{4}He$ and $^{87}Sr/^{86}Sr$
Eurasia						
Eifel (EIF)	7, 50	No	–	–	–	–

Blanks indicate that there are no data, where we did not find any data, where available data are inconclusive.

Basin (~6000 and >4000 km, respectively), record volcanism starting before 75 Ma (Duncan and Clague, 1985; Duncan and Keller, 2004; Koppers et al., 2004; Watts et al., 1988), and were among the first chains that led to the establishment of the hotspot hypothesis. As both chains terminate at subduction zones, the existing volcanoes likely record only part of the activities of these hot spots (cf. Portnyagin et al., 2009).

p0045 In addition to Hawaii and Louisville, the Galápagos is the third Pacific hotspot with a similar duration. Its interaction with the Galápagos Spreading Center has produced two chains: the Galápagos archipelago–Carnegie Ridge on the Nazca Plate (Sinton et al., 1996) and the Cocos Ridge on the Cocos Plate. The Cocos Ridge records oceanic volcanism for ~14.5 My (Werner et al., 1999) and projects toward the Caribbean LIP (Duncan and Hargraves, 1984) with $^{40}Ar/^{39}Ar$ dates of 69–139 Ma (e.g., Hoernle et al., 2004; Sinton et al., 1997). The geochemical similarity of these lavas with the Galápagos archipelago is a compelling evidence for a total life span for the Galápagos melting anomaly of ~139 My (Hoernle et al., 2002, 2004).

p0050 In the Indian Ocean, at least four hot spots have been related to long-term activity. Muller et al. (1993b) compilation of ages associates the Réunion hotspot to volcanism on the Mascarene Plateau at 45 Ma (Duncan et al., 1990), the Cocos–Laccadive Plateau at ~60 Ma (Duncan, 1978, 1991), and finally the Deccan flood basalts in India with dates as old as ~70 Ma (see also Sheth, 2005). The Comoros hotspot can be linked to volcanism around the Seychelles islands at 63 Ma (Emerick and Duncan, 1982; Müller et al., 1993b). Volcanism on Marion (<0.5 Ma; cf. McDougall et al., 2001) projects along a volcanic ridge to Madagascar (Meert and Tamrat, 2006). While geologic dating is sparse, Storey et al. (1997) inferred

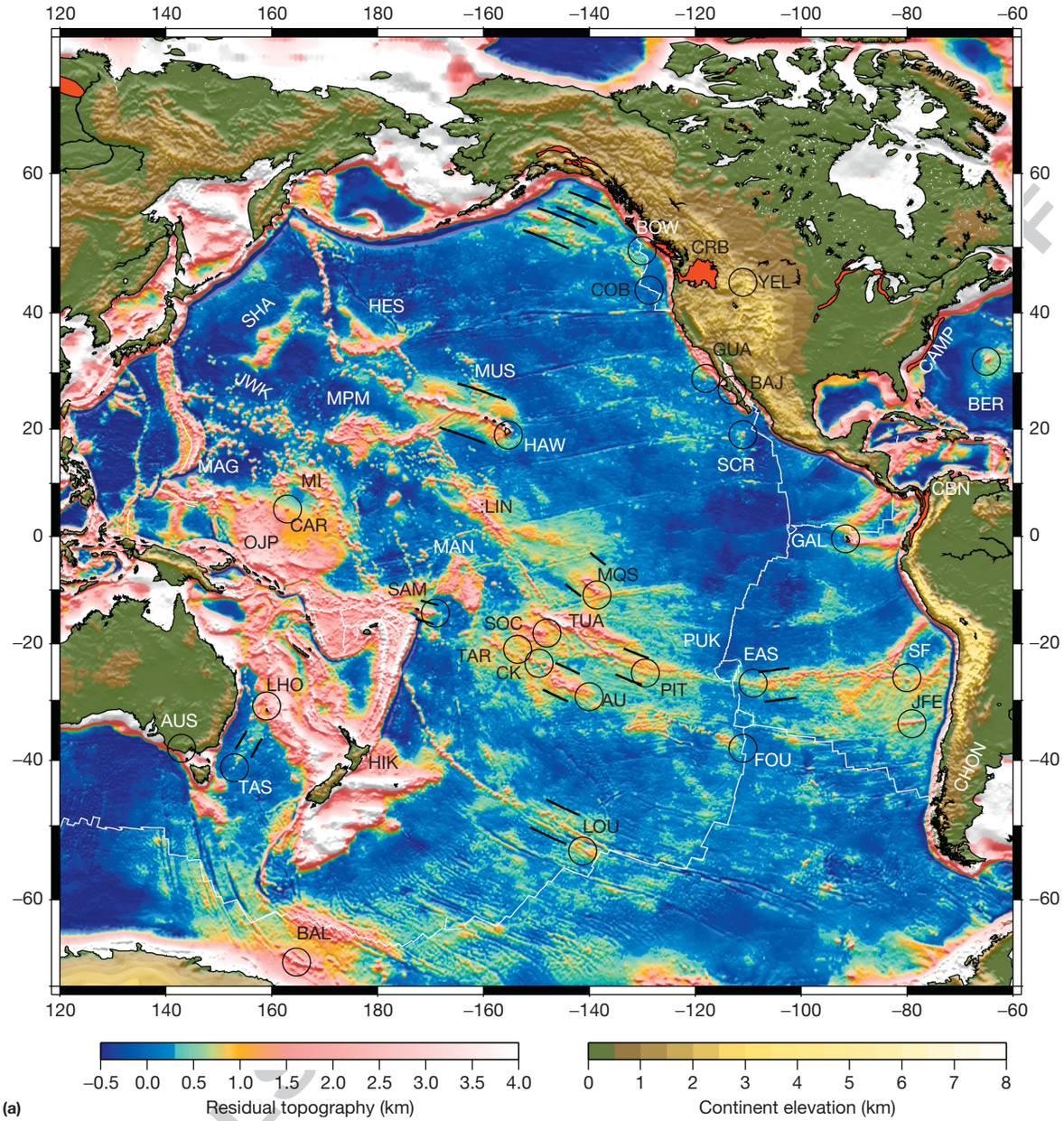

(a)

f0010 **Figure 1** (Continued)

an age progression along this track back to ~88 Ma. The Kerguelen hot spot is linked to Broken Ridge and Ninetyeast Ridge on the Australian Plate and multiple stages of volcanism on the Kerguelen Plateau dating to 114 Ma (Frey et al., 2000; Krishna et al., 2012; Nicolaysen et al., 2000; **Figure 2**).

p0055 In the Atlantic Ocean, at least seven long-lived melting anomalies have been documented. The Tristan–Gough and St. Helena chains record volcanism on the African Plate for ~80 My (O'Connor and Duncan, 1990; O'Connor and Roex, 1992; O'Connor et al., 1999). For Tristan–Gough, a connection to the Paraná flood basalts in South America and the Etendeka basalts in Namibia may even extend the duration of the melting anomaly to ~130 My (O'Connor et al., 2012; Peate, 1997). O'Connor et al. (2012) further proposed a connection of the Shona seamounts with the Agulhas Ridge to form another (zigzag-shaped) long-lived hotspot trail in the South Atlantic (~80 My). The Trindade–Martim Vaz chain on the South American Plate (Fodor and Hanan, 2000) extends to the Alto Paranaiba and Poxoreu volcanic provinces of ages ~85 Ma (Gibson et al., 1997). In the North Atlantic, the Madeira and Canary chains have recorded age-progressive volcanism for nearly 70 My (Geldmacher et al., 2005; Guillou

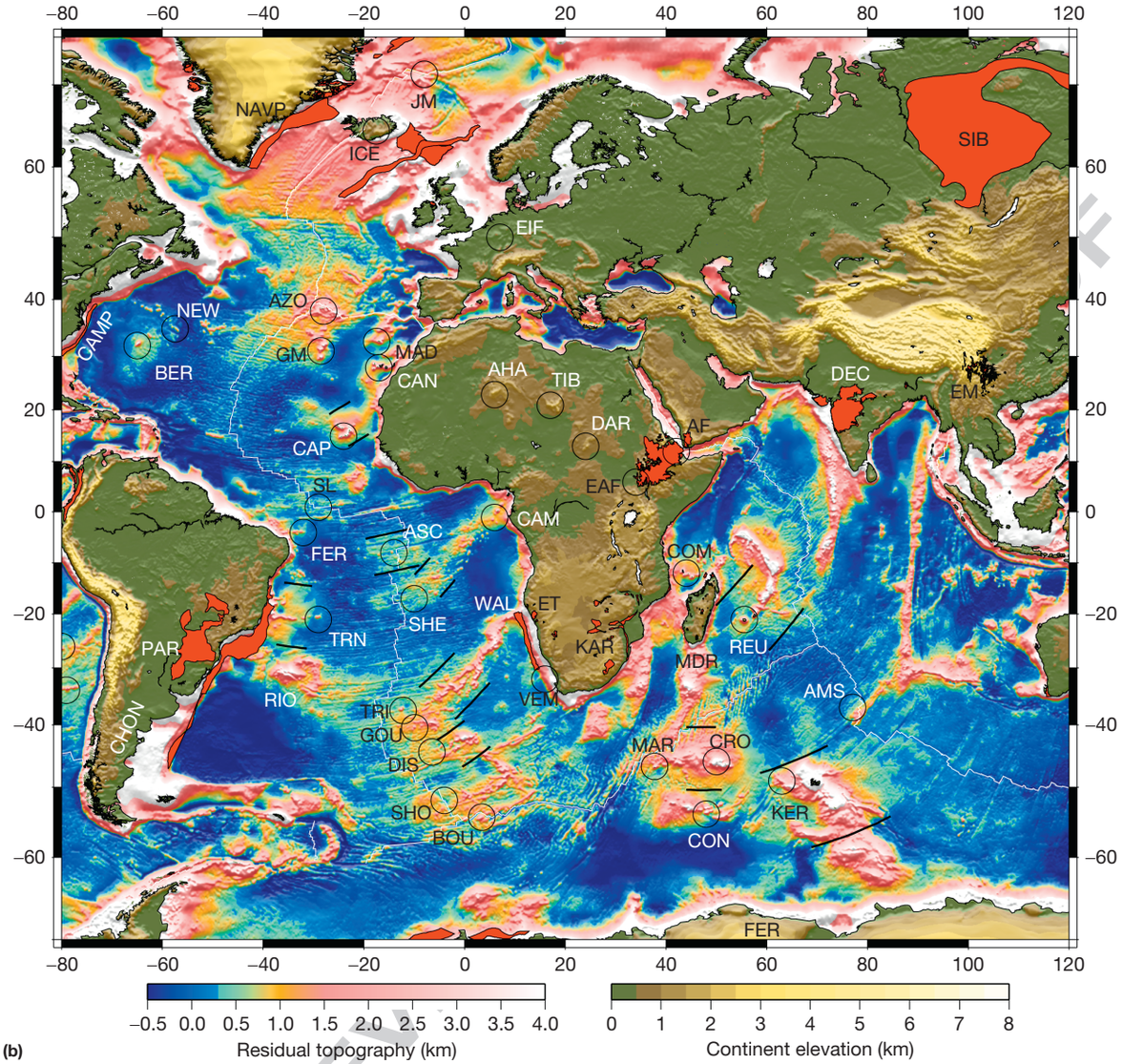

Figure 1 Elevation on the continents and residual topography in the oceans. Residual topography is the predicted bathymetry grid of Smith and Sandwell (1997) corrected for sediment loading and thicknesses (Laske and Masters, 1997) and for seafloor subsidence with age (Stein and Stein, 1992) using seafloor ages from Müller et al. (1993a) (areas without ages are interpolated using cubic splines). Grid processing and display was done using GMT (Wessel and Smith, 1995). Color change from blue to turquoise is at 300 m and delineates the approximate boundaries of anomalously shallow seafloor. Circles mark estimated locations of most recent (hot spot) volcanism. Pairs of lines are used to measure the widths of some of the hot spot swells (**Table 1**). Flood basalt provinces on the continents and continental margins are red. (a) Pacific region and (b) Indo-Atlantic region.

et al., 2004). The Canaries are unusual in that single volcanoes often remain active for tens of My (Geldmacher et al., 2005), much longer than, for example, the typical duration of the Hawaiian volcanoes' shield stage of ~1 My (e.g., Clague and Dalrymple, 1987; Ozawa et al., 2005). The long life span of some of the Canary volcanoes has contributed to uncertainty in defining a geographic age progression but is consistent with the slow motion of the African Plate over the hot spot.

p0060 Finally, Iceland is often cited as a classic Atlantic hotspot with volcanic tracks on two plates due to its location on a MOR (**Figure 3**). The thickest crust of the hotspot tracks occur along the Greenland–Iceland and Faeroe–Iceland Ridges extending NW and SE from Iceland. Anomalously thick oceanic crust immediately adjacent to these ridges shows datable magnetic lineations (Jones et al., 2002b; Macnab et al., 1995; White, 1997). Extrapolating the ages of these lineations onto the Greenland–Iceland and Faeroe–Iceland Ridges suggests the occurrence of age-progressive volcanism with seafloor spreading, which is most easily explained by the Iceland hot spot causing excess magmatism very near to or at the Mid-Atlantic Ridge since the time of continental breakup (White, 1988, 1997; Wilson, 1973). Earlier volcanism occurring as flood

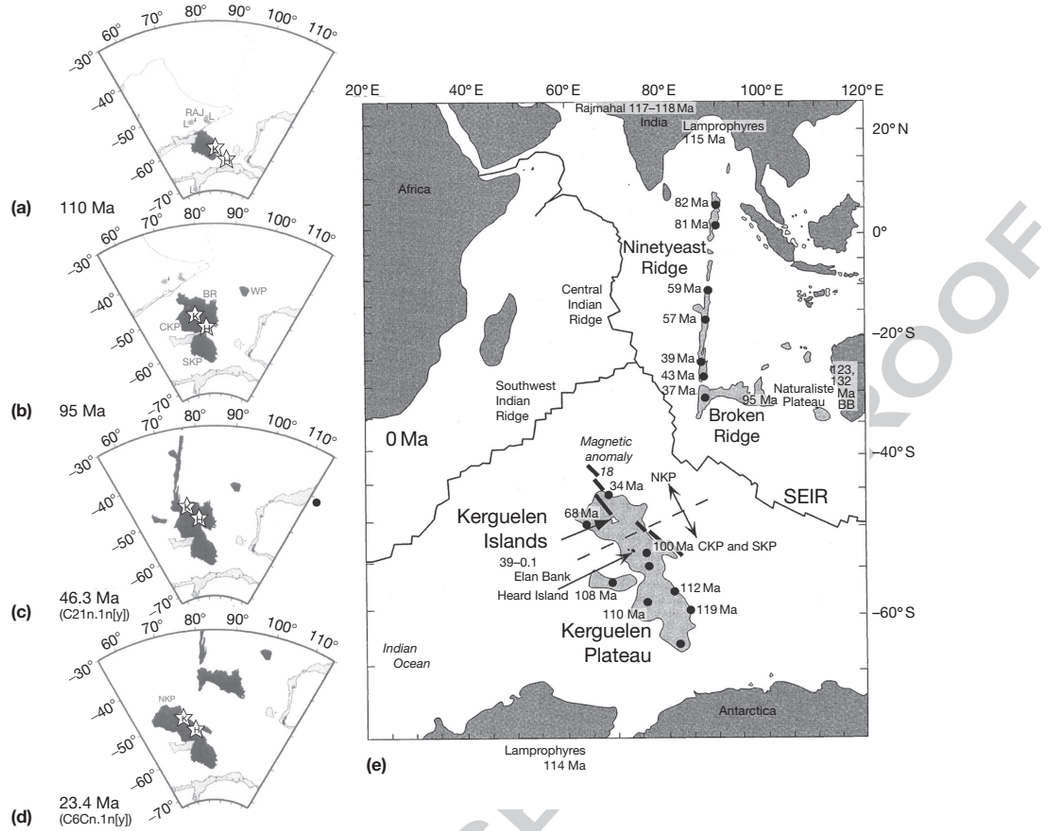

f0015 **Figure 2** Evolution of the Kerguelen Plateau and hot spot track reproduced from (a) to (d) Coffin MF, Pringle MS, Duncan RA, et al. (2002) Kerguelen hotspot magma output since 130 Ma. *Journal of Petrology* 43: 1121–1139. (a) The initial pulse of volcanism formed the Rajmahal Traps (RAJ), lamprophyres (L) and the Southern Kerguelen Plateau (SKP) from ~120 to ~110 Ma. Stars mark reconstructed positions of the hot spot (Müller et al., 1993b) assuming a location at Kerguelen archipelago (K) and Heard Island (H). By 110 Ma, seafloor spreading between India, Antarctica, and Australia is well under way. The formation of the RAJ by the Kerguelen hot spot requires the hot spot to have moved by ~10° relative to the Earth's spin axis (Kent et al., 2002; cf. **Figure 9**). (b) By 95 Ma, central Kerguelen Plateau (CKP) and Broken Ridge (BR) have formed. (c) At 46.3 Ma, northward migration of the Indian Plate formed the Ninetyeast Ridge along a transform fault in the MOR system. (d) The Southeast Indian Ridge has propagated northwestward to separate CKP and BR (by ~42 Ma), which continue drifting apart at 23.4 Ma. (e) Current configuration as shown by Nicolaysen et al. (2000) but with ages from Coffin et al. (2002). Bold line along NE margin of the plateau marks magnetic anomaly 18 (41.3–42.7 Ma).

basalts along the continental margins of Greenland, the British Isles, Norway, and Baffin Island at about 56–62 Ma marks a conservative estimate for the age of the Icelandic melting anomaly (e.g., Lawver and Mueller, 1994; Saunders et al., 1997; White and McKenzie, 1989).

p0065 At a few volcano chains, the continuous record of volcanism is relatively short (a few tens of My) and the full duration of volcanism is poorly constrained. For example, the New England Seamount chain records ~20 My of oceanic volcanism (Duncan, 1984), but an extrapolation to the volcanic provinces in New England could extend the duration by another 20 My (cf. O'Neill et al., 2005). The duration of the Azores hotspot is also unclear. Gente et al. (2003) hypothesized the Azores hotspot and the Great Meteor and Corner Rise Seamounts (~85 Ma) to be conjugate features. Yet, age constraints of these features are poor and any geochemical association with the Azores group remains unknown.

p0070 In the Pacific Ocean (see Clouard and Bonneville (2005) and references therein), the total durations of the Cobb (1.5–29.2 Ma; Desonie and Duncan, 1990; Turner et al., 1980) and Bowie–Kodiak chains (0.2–23.8 Ma; Turner et al., 1980) remain unknown, as they terminate at the subduction zone south of Alaska. The Easter chain extends to at least ~30 Ma on the Nazca Plate (Clouard and Bonneville, 2005; Ray et al., 2012). On the Pacific Plate, the record extends perhaps even further into the past, but the tentative link with the Tuamotu Plateau (Clouard and Bonneville, 2001; Ito et al., 1995) clearly requires further dating.

133.2.1.2 Short-lived age-progressive volcanism

s0030

p0075 At least ten volcanic provinces show age-progressive volcanism lasting less than 25 My (e.g., Clouard and Bonneville, 2005). The Samoan hot spot has been active for 20 My (Hart et al., 2004) and possibly longer (Duncan and Clague, 1985). The hotspot-like age progression along the Samoan track is obscured by voluminous secondary volcanism covering the main islands of the archipelago (e.g., Natland, 1980) but has been revealed by recent sampling of the submarine flanks of the volcanoes (Koppers et al., 2008, 2011b). The Society and Marquesas Islands represent voluminous volcanism but for

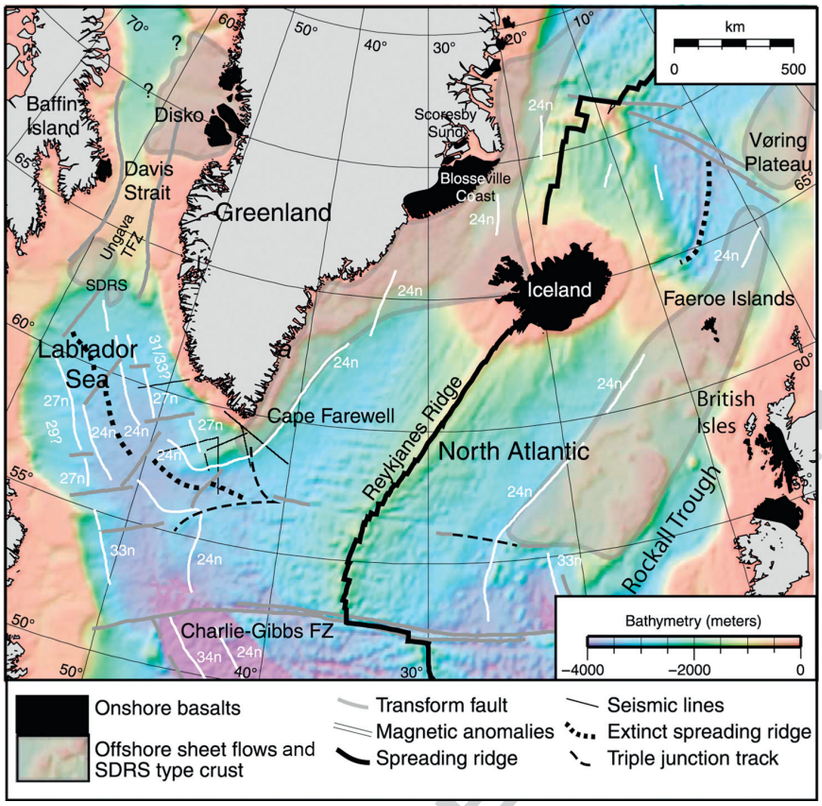

f0020 **Figure 3** From Nielsen et al. (2002). Distribution of Paleogene flood basalts in the North Atlantic Volcanic Province. Selected seafloor magnetic lineations, major transform faults, active and extinct spreading ridges, and seismic lines are marked as labeled.

geologically brief durations of ~4.6 My and ~4.7 My, respectively (Chauvel et al., 2012; Guillou et al., 2005; Legendre et al., 2006). Clouard and Bonneville (2001) argued that the Marquesas hotspot could have formed the Line Islands and Hess Rise based on geometric arguments. If this interpretation is correct, the large gap in volcanism between the three provinces implies strongly episodic volcanism. However, the age trend of the Marquesas volcanoes departs from Pacific Plate motion in both speed and direction and thus contradicts a hot spot origin altogether (cf. Legendre et al., 2006). Similar to the Marquesas, the Foundation chain (duration from 2.1 to 21 Ma) displays an age progression that is somewhat faster than Pacific Plate motion (O'Connor et al., 2004), which could suggest an absolute drift of the underlying melting anomaly (cf. O'Neill et al., 2005). Short hotspot durations of 11–24 My further occur along the Pitcairn (0–11 Ma), Caroline (1.4–13.9 Ma), Tarava (35.9–43.5 Ma; Clouard et al., 2003), Tokelau (58–74 Ma; Koppers et al., 2007), and Japanese seamount (94–118 Ma; Koppers et al., 2003) chains on the Pacific Plate, as well as the Tasmantid seamounts near Australia (7–24.3 Ma; McDougall and Duncan, 1988; Müller et al., 1993b). Such short hotspot durations do not fit in with the classical explanation that hotspots are underlain by long-lived mantle plumes.

p0080 An intriguing yet enigmatic form of age-progressive volcanism is represented by the Pukapuka, Sojourn, and Hotu Matua ridges, which trend WNW–ESE and away from the East Pacific Rise. With respect to its geographic trend and duration, the Pukapuka ridge resembles some of the other volcano chains in the region, such as the Foundation chain (Maia et al., 2001; O'Connor et al., 2002, 2004), but it stands out because of its age pattern as well as its smaller volcanic volume and morphology: the Pukapuka is not built of discrete conical seamounts, but rather of en echelon elongate ridges (Lynch, 1999). Moreover, Pukapuka's rapid and variable rate of age progression (Janney et al., 2000; Sandwell et al., 1995) suggests that the magma source has migrated eastward by rates of ~20 cm year^{-1} (**Figure 4**), which is difficult to reconcile with the concept of a near-stationary hot spot source. While the Sojourn and Hotu Matua ridges lack the lateral extent to robustly define an age progression, they appear very similar to the parallel Pukapuka ridge, not only in terms of the available ages and the morphology of the volcanic edifices (Forsyth et al., 2006) but also in terms of their association with gravity, bathymetry, and seismic wave speed anomalies (**Figure 4**; Harmon et al., 2011).

133.2.1.3 Non-age-progressive volcanism s0035

p0085 An important form of oceanic volcanism does not involve simple geographic age progressions. Amsterdam–St. Paul and Cape Verde are two examples that each represent opposite extremes in terms of size and duration. The Amsterdam–St. Paul hot spot represents a relatively small and short-lived (≤5 My) melting anomaly on the Southeast Indian Ridge that

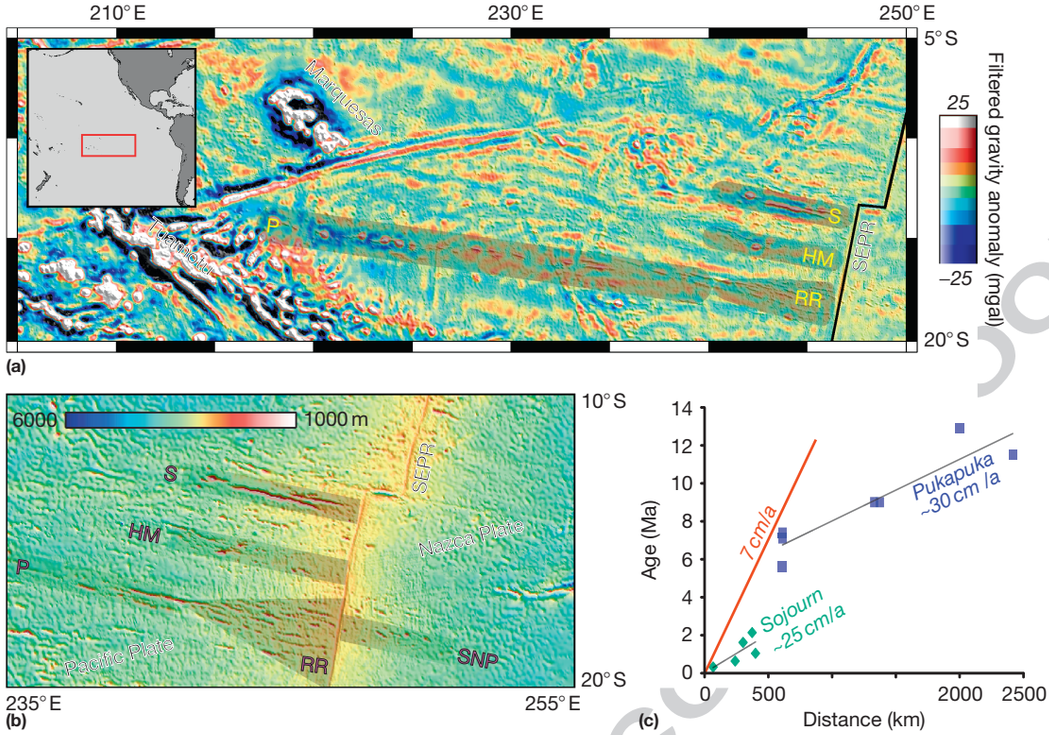

f0025 **Figure 4** From Ballmer et al. (2013a). (a) Filtered gravity anomalies (for filtering scheme, see Harmon et al., 2011) highlighting the east–west trending 'Haxby' gravity lineations (Haxby and Weissel, 1986) and (b) bathymetry in the southeast Pacific (SEPR: southern East Pacific Rise). Volcanic ridges on the Pacific Plate (S: Sojourn; HM: Hotu Matua; and P: Pukapuka), the Rano Rahi seamount field (RR), and a short seamount chain on the Nazca Plate (SNP) are shaded. (c) Ages collected along the Pukapuka and Sojourn ridges scatter about trends that are much faster (by ~20 cm year^{-1}) than Pacific Plate motion (red line). Ballmer et al. (2013a) argued that the Pukapuka source crossed the SEPR at ~5 Ma to form the apparently young (≤3 Ma) SNP.

is geochemically separate from the Kerguelen hot spot (cf. Doucet et al., 2004; Graham et al., 1999) Its small size and duration, as well as its location on a MOR, likely contribute to the lack of an identifiable age progression. The Cape Verde volcanoes, on the other hand, are larger and have likely existed since Early Neogene (e.g., McNutt, 1988). The islands also lack a clear linear age progression, but this can be expected for a hot spot located very close to the Euler pole of the African Plate (McNutt, 1988).

p0090 Examples of volcano chains with complex age–space relations on the rapidly moving Pacific Plate are more difficult to explain within the hot spot framework. While the lack of modern dates on samples of the Mid-Pacific Mountains and the Geologist seamounts precludes robust interpretations, the Marcus–Wake seamounts and Gilbert Ridge, as well as the Marshall, Magellan, and Line Islands, clearly display synchronous or near-synchronous volcanism over large distances of 1500–2000 km (e.g., Davis et al., 2002; Koppers et al., 2003; Clouard and Bonneville, 2005 and references therein). These volcano groups also show long-lived, recurrent activity at individual islands (**Figure 5**). They can thus more reasonably be explained by 'hot lines' or melting anomalies that are elongated in the direction of plate motion (Bonatti and Harrison, 1976; Bonatti et al., 1977) or even by much broader magmatic anomalies with melt extraction limited by the lithosphere (see **Section 133.3.7.3**). The Cameroon volcanic line, which extends from Cameroon to the SW straddling the passive continental margin of Africa (**Figure 6**), may represent an analogue to the Pacific cases of volcanism with coeval activity over distances greater than 1000 km (Marzoli et al., 2000; Montigny et al., 2004).

p0095 Recent volcanism along the prominent Cook–Austral Islands in the South Pacific also displays overall complex geographic age patterns (McNutt et al., 1997) and complex uplift history at individual volcanoes (Adam and Bonneville, 2008; Jordahl et al., 2004). The geographic age pattern of a younger episode of volcanism (0–20 Ma) alone requires either the activity of two parallel hot lines (Ballmer et al., 2009) or that of four closely spaced, short-lived hot spots (representing the Macdonald, Arago/Rurutu, Raivavae and Rarotonga tracks; Bonneville et al., 2002; 2006) (cf. dashed lines in **Figure 5 (c)**). In the framework of a hot spot interpretation, geochemical affinities with seamounts near the Samoan Islands have been suggested to indicate long life spans (of up to ~25 and ~50 My) for some of the tracks (Arago/Rurutu and Macdonald, respectively) (Jackson et al., 2010).

p0100 The remaining oceanic hot spots in **Table 1** do not have sufficient data to define time–space relations. This list includes volcano chains that simply have not yet been adequately dated (Socorro, Tuamotu, and Great Meteor), hot spots that have small footprints (e.g., Discovery, Ascension/Circe, Sierra Leone, Conrad, Bermuda), or spatial patterns

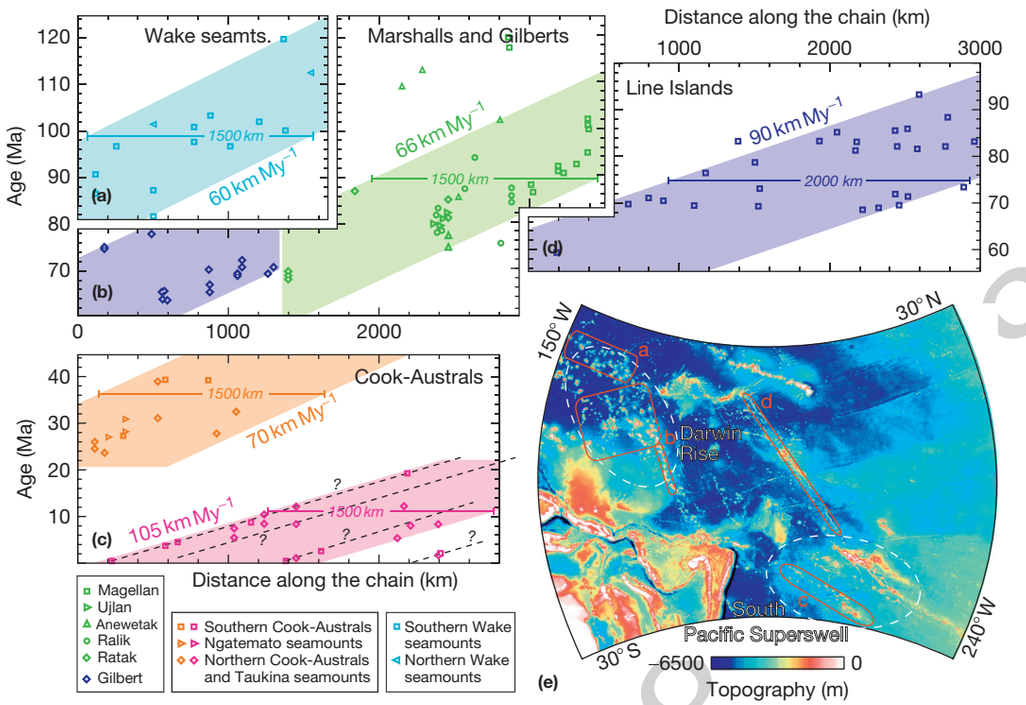

f0030 **Figure 5** Compilation of volcano ages sampled along the (a) Wake seamounts, (b) Marshall Islands and Gilbert Ridge, (c) Cook–Austral Islands, and (d) the Line Islands (see (e) for locations). For (a–c), sample ages collected along each of the subparallel trends (different symbols) are geometrically projected onto the same distance axis. Dashed lines in (c) indicate the putative Macdonald, Raivavae, Arago/Rurutu, and Rarotonga (from left to right) hot spot tracks as identified by Bonneville et al. (2002). As shown by the shaded fields, the scattered volcano ages are alternatively explained by the activity of hot lines of lengths ~1500 km (a–c) or up to ~2000 km (d) for the Line Islands. Modified from Ballmer MD, van Hunen J, Ito G, Bianco TA, and Tackley PJ (2009) Intraplate volcanism with complex age-distance patterns: A case for small-scale sublithospheric convection. *Geochemistry, Geophysics, Geosystems* 10.

controlled by interaction with spreading centers (e.g., Bouvet and Balleny).

s0040 ### 133.2.1.4 Continental hot spots and melting anomalies

p0105 There are a number of continental melting anomalies that are not directly associated with present-day subduction, orogeny, or continental rifting. Such activity occurs, for example, in Mongolia (Hunt et al., 2012), Antarctica (e.g., Giordano et al., 2012), western North America (Lipman and Glazner, 1991; Nelson and Tingey, 1997), eastern Australia (e.g., Griffin and McDougall, 1975), eastern China, Europe, and Africa (Lustrino and Wilson, 2007; green dots in **Figure 7**). A number of these areas are also shown in **Figure 1** and listed in **Table 1**, such as the North American Yellowstone (YEL)–Snake River Plain volcanic progression (YSRP), the European Eifel hot spot (EIF) (cf. Lustrino and Wilson, 2007 and references therein), and the African hot spots such as expressed by the volcanic mountains of Jebel Mara (DAR), Tibesti (TIB), and Ahaggar (HOG) (Burke, 1996).

p0110 The Yellowstone hot spot stands out among these, because it is the only one that displays a clear age progression. It is recorded by silicic caldera forming events starting at 16–17 Ma at the Oregon–Nevada border at a distance of ~700 km. Initial rhyolitic volcanism is followed by long-lived basaltic volcanism along the present-day Snake River Plain (SRP) (**Figure 8**). The effective speed of the hot spot track is 4.5 cm year^{-1}, which includes a component of the present-day plate motion (2.5 cm year^{-1}) and a component caused by the basin and ange extension. The YSRP track appears to be mirrored by the westward-progressing High Lava Plains (HLP) track in southern Oregon (Kincaid et al., 2013; Long et al., 2012; **Figure 8**). The lack of age progression of the other hot spots is usually attributed to the nearly motionless African Plate and the slow motion of the European Plate.

133.2.1.5 The hot spot reference frame

s0045

p0115 The existence of many long-lived volcano chains with clear age progressions led Morgan (1971, 1972) to suggest that hot spots remain relatively stationary to one another and therefore define a global kinematic reference frame separate from plate motions (Duncan and Clague, 1985; Morgan, 1983). Such an absolute reference frame was used to anchor the well-constrained relative motions of the tectonic plates with respect to the lower mantle and to quantify absolute displacements of the Earth's spin axis (i.e., true polar wander) through geologic time (Biggin et al., 2012; Torsvik et al., 2002, 2010b, 2012). The concept of a fixed hot spot reference frame, however, has been challenged by observations that indicate relative motions between hot spots, particularly between the Indo-Atlantic and Pacific hot spot groups (Acton and Gordon, 1994; DiVenere and Kent, 1999; Molnar and Stock, 1987; Raymond et al., 2000; Tarduno and Gee, 1995; Torsvik et al., 2002). Relative motion between these two groups is slow but robust and independent of the plate

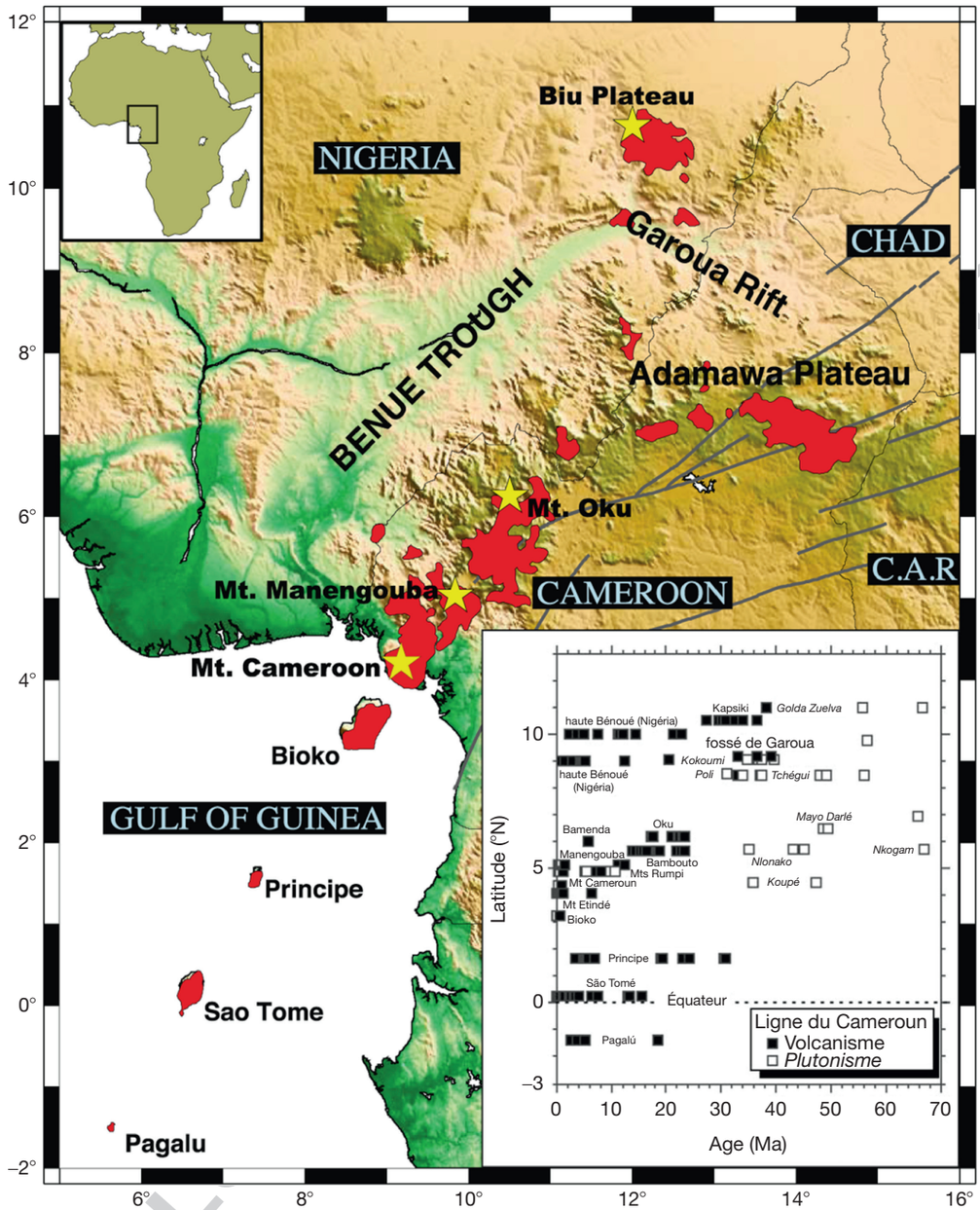

f0035 **Figure 6** Modified from Gallacher RJ and Bastow ID (2012) The development of magmatism along the Cameroon Volcanic Line: Evidence from teleseismic receiver functions. *Tectonics* 31. Sketch map of the Cameroon volcanic line with magmatic provinces shown red. Yellow stars denote selected volcanoes as annotated. Inset (reproduced from Montigny R, Ngounouno I, and Deruelle B (2004) K-Ar ages of magmatic rocks from the Garoua rift: Their place in the frame of the 'Cameroun Line'. *Comptes Rendus Geoscience* 336: 1463–1471) shows age compilation of plutonic and volcanic rocks along the Cameroon Line.

circuit chosen to connect the Indo-Atlantic and Pacific hemispheres. Accordingly, uncertainties in the hot spot reference frame inevitably increase looking back into the geologic past.

p0120 In addition to slow motion between the Pacific and the Indo-Atlantic hot spot groups, somewhat slower relative motion occurs among hot spots within each of the two groups. In the Pacific, relative motion has been inferred for many hot spot pairs but is best documented from interchain distances of coeval volcanoes within the well-sampled Hawaii and Louisville chains (Koppers and Staudigel, 2005; Koppers et al., 1998, 2011a, 2012; Wessel and Kroenke, 2008, 2009). Most importantly, the rapid southward motion of the Hawaiian hot spot while forming the Emperor seamounts before ~50 Ma has been identified to modulate these distances (Pares and Moore, 2005; Tarduno et al., 2003, 2009). In the Indian Ocean, the inferred absolute southward motion of the

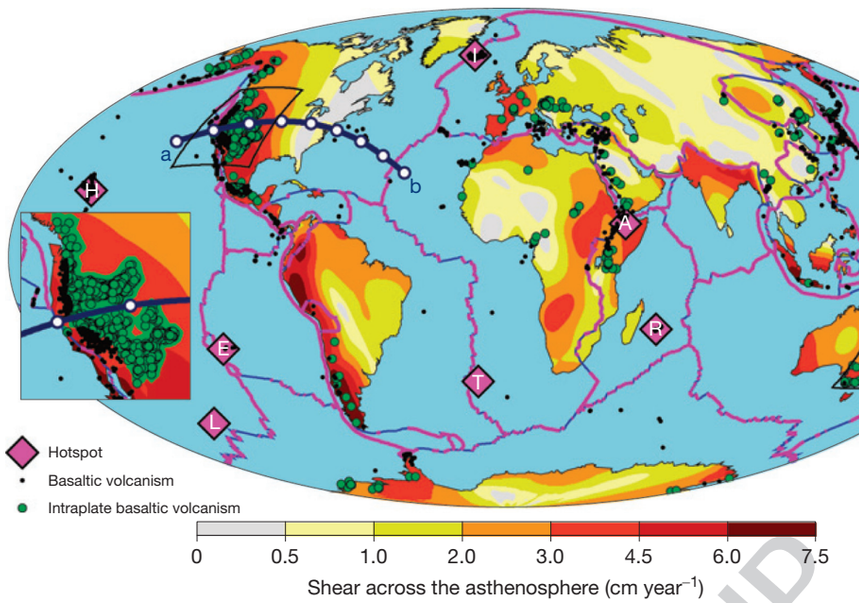

f0040 **Figure 7** From Conrad et al. (2011). Shear across the asthenosphere beneath (colors), and basaltic intraplate volcanism on (green circles) continents. Asthenospheric shear is shown as the amplitude of the vector difference between the motions of the plates and the underlying mantle (i.e., at the base of the asthenosphere as predicted by Conrad and Behn, 2010). Primary (putatively plume-fed) hot spots (Courtillot et al., 2003) are shown as purple squares. Excluding volcanism that is close to plate boundaries or primary hot spots (small black dots), continental intraplate basaltic volcanism (green circles) occurs more frequent where shear across the asthenosphere is large. Reproduced from Conrad CP, Bianco TA, Smith EI, and Wessel P (2011) Patterns of intraplate volcanism controlled by asthenospheric shear. *Nature Geosciences* 4: 317–321.

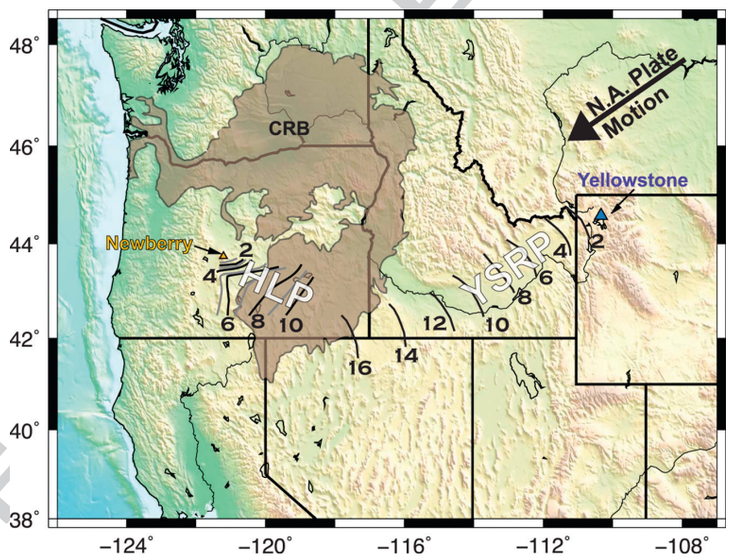

f0045 **Figure 8** Topographic map with age progressions along the Yellowstone–Snake River Plain (YSRP) and High Lava Plains (HLP) tracks. Ages of volcanism are annotated (triangles denote centers of active volcanism). Columbia River basalts (CRBs; age: 16.6–15 Ma) are shown as brown shading. Modified from Long MD, Till CB, Druken KA, et al. (2012) Mantle dynamics beneath the Pacific Northwest and the generation of voluminous back-arc volcanism. *Geochemistry, Geophysics, Geosystems* 13.

Kerguelen hot spot since 100 Ma hinges on the weakly constrained location of its present location (Steinberger and Antretter, 2006; Weis et al., 2002). At or near present day (i.e., <4–7 Ma), motion between hot spots globally is unresolvable or at least much slower than it has been in the geologic past (Gripp and Gordon, 2002; Wang and Wang, 2001). For a more complete description of these issues, we refer the reader to **Chapter 111**.

Whereas fixity of the source of volcanism relative to the drifting plates has been widely used as diagnostic test for a p0125

hot spot origin, slow relative motion of hot spots is naturally expected in the framework of mantle plume theory. Rising plumes are disturbed by large-scale mantle convection that should slowly yet steadily displace their surface expressions. Within this concept, the drift between hot spots is limited due to the relatively sluggish convection in the lower mantle combined with the potential for chemical anchoring of plumes at the base of the mantle (cf. Davaille et al., 2002; Jellinek and Manga, 2002; McNamara and Zhong, 2004; see also **Chapter 136**). Global geodynamic models that simulate plumes rising in a convecting mantle predict directions and amplitudes of motion between hot spots that are consistent with observations for a large range of model parameters (Steinberger, 2000; Steinberger and Antretter, 2006). For example, these models can reproduce the westward motion of the Iceland hot spot relative to both the Indo-Atlantic and Pacific hot spots (Norton, 2000; Raymond et al., 2000) for a relatively shallow plume source near the transition zone (Mihalffy et al., 2008). Also, they routinely predict independent drift for a given hot spot pair (**Figure 9**), as is evident for the Hawaii and Louisville hot spots (Koppers et al., 2012). Such model predictions have been used to define 'moving hot spot' reference frames (Doubrovine et al., 2012). However, these reference frames may have similar results as the single fixed hot spot reference frame in explaining volcano age–distance relations when considering the associated uncertainties (O'Neill et al., 2005). Future work is needed to be able to use hot spot motions as a constraint, for example, to infer mantle properties from the best-fitting geodynamic models.

Sudden changes in the direction of hot spot drift are routinely predicted by many of these models (Steinberger and Antretter, 2006; Steinberger et al., 2004; **Figure 9**), and these can further contribute to bends in hot spot chains, with the Hawaiian–Emperor bend near 50 Ma being a prominent example. The classical explanation for such bends invoked sudden changes in plate motion over fixed hot spots (Andrews et al., 2006; Sharp and Clague, 2006; Whittaker et al., 2007). As a general explanation, however, it is challenged by evidence for prominent bends in seamount chains on the same plate that did not occur at the same time (Koppers et al., 2007). In addition, paleomagnetic evidence along the Hawaiian–Emperor chain indicates a sudden change in hot spot motion from being dominantly southward to being nearly stationary (in the N–S sense) right near the 50 My bend (Kono, 1980; Sager et al., 2005; Tarduno et al., 2009). A combination of changes in both hot spot and plate motion may therefore have occurred during the formation of the Hawaiian–Emperor bend (O'Connor et al., 2013). p0130

133.2.2 Topographic Swells s0050

Figure 1 illustrates that most oceanic hot spots and melting anomalies are associated with anomalously shallow topography that extends several hundred km beyond the area of excess volcanism. For individual hot spots, we identify the presence of such a seafloor swell if residual topography exceeds an arbitrarily chosen value of 300 m and extends appreciably (>100 km) away from the center of volcanism. Such hot spot p0135

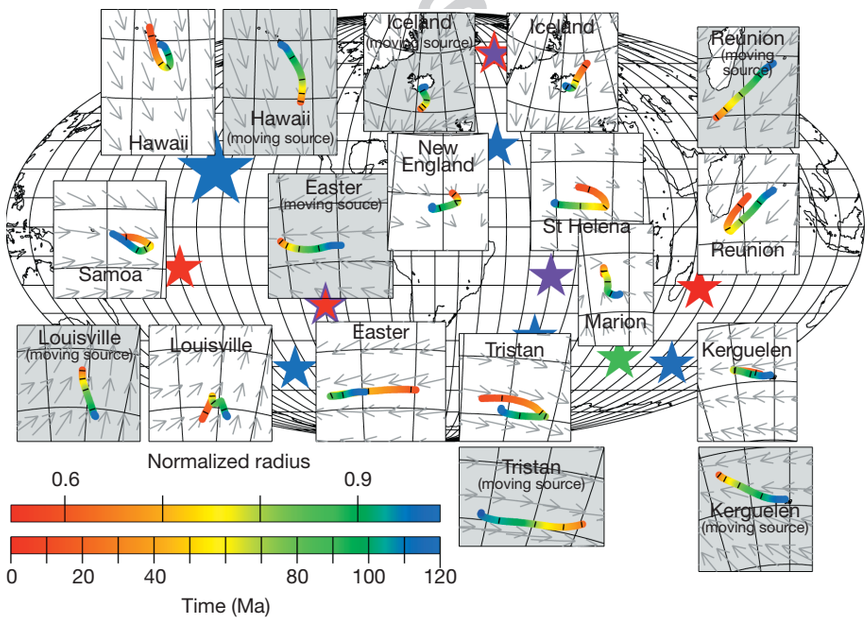

f0050 **Figure 9** Hot spot motions predicted from a global convection model. Hot spot positions today are shown as stars and through time as rainbow-colored bands in insets (scale at the very bottom). Star fill color reflects normalized radius of the plume conduit (top scale). For all hot spots shown, white insets display the predicted hot spot motions for a fixed plume source (i.e., anchored plume). For a subset of hot spots, gray insets display the predicted hot spot motions for a moving plume source. Also shown are the horizontal flow components in the lower mantle (at either 2512 km (gray boxes) or 1918 km depth (white boxes)). Arrow length scale is 5° of arc per cm/year. Reproduced and modified from Steinberger B and Antretter M (2006) Conduit diameter and buoyant rising speed of mantle plumes: Implications for the motion of hot spots and shape of plume conduits. *Geochemistry, Geophysics, Geosystems* 7.

swells are indeed very common. Near major hot spots, they rise to ~2 km above the surrounding seafloor and extend many hundreds of km away from the center of volcanic activity (Crough, 1983). They are also apparent on chains with very small volcanoes such as the Socorro and Tasmantid tracks, as well as the Pukapuka and Sojourn ridges (Harmon et al., 2006, 2011). In contrast, the Madeira and Canary hot spots are two cases that break this pattern. The lack of obvious swells around these large and long-lived hot spots indeed motivates more detailed investigation.

p0140 Hot spot swells are typically restricted to the younger portions of the volcano chain (**Table 1**). The Hawaiian swell, for example, is prominent beneath the youngest (southeast) part of the Hawaiian ridge but begins to fade near ~178°W and disappears near the Hawaiian–Emperor bend (~50 Ma). Swells also decay along the Louisville (near a volcano age of ~34 Ma) and the Tristan chains (on the Walvis Ridge near 62–79 Ma). Similar behavior is seen for the Kerguelen track with shallow seafloor that extends away from the Kerguelen Plateau on the Antarctic Plate juxtaposed to normal topography around the southernmost portion of Broken Ridge (~43 Ma) on the Indian Plate. Swells associated with hot spot tracks in the South Atlantic also systematically decay with age, perhaps except for that associated with the St. Helena track, which however is juxtaposed to the active Cameroon volcanic line. Old chains that lack swells in our analysis include the Japanese–Wake seamounts (>70 Ma), the Magellans (>70 Ma), the Mid-Pacific Mountains (>80 Ma), and the Musicians (>65 Ma). This suggests that if a swell forms at a hot spot, it decreases in height with time until it can no longer be detected at an age of ~50 Ma or less.

p0145 Whereas swells are more difficult to measure on the thick and compositionally heterogeneous continental plates, the Yellowstone hot spot is associated with well-documented excess topography. The measured topographic bulge is 600 m high and ~600 km wide centered around the Yellowstone caldera (cf. **Figure 8**) and is associated with high heat flow, extensive hydrothermal activity, and a 10–12 m positive geoid anomaly (Smith and Braile, 1994). Systematic topographic decay along the track in the SRP is consistent with thermal contraction in response to the progression of the American Plate over a hot spot (Smith and Braile, 1994).

p0150 The South Pacific Superswell is a much larger swell that spans ~3000 km and supports the hot spots in French Polynesia (Adam and Bonneville, 2005; Hillier and Watts, 2004; McNutt and Fischer, 1987). Other swells of comparable size include the ancient Darwin Rise in the northwestern Pacific (McNutt et al., 1990) and the African Superswell (e.g., Nyblade and Robinson, 1994), which encompasses the southern portion of Africa and the South Atlantic down to the Bouvet Triple junction. Both the South Pacific and African Superswells are associated with active volcanism, geoid anomalies (Adam et al., 2010; Cadio et al., 2011), and broad seismically slow structures in the lower mantle (e.g., Dziewonski et al., 2010; Lekic et al., 2012; see also **Section 133.2.5.1** in the succeeding text). While the oceanic hot spots near Africa to first order display the key characteristics predicted by hot spot theory (e.g., O'Connor et al., 2012), the hot spots in the South Pacific are mostly short-lived, including some with extreme geochemical signatures (Konter et al., 2008; Koppers et al., 2003; Staudigel et al., 1991) and complex age progressions (see **Section 133.2.1**; Ballmer et al., 2009; McNutt, 1998; McNutt et al., 1997). The Darwin Rise is often interpreted as the Cretaceous counterpart of the South Pacific Superswell (Cadio et al., 2011; Koppers et al., 2003; McNutt and Judge, 1990). We will discuss the geodynamic mechanisms for swell and superswell support in **Sections 133.3.4** and **133.3.7.1**, respectively.

133.2.3 Flood Basalt Volcanism s0055

p0155 Large igneous provinces provide further constraints on the nature of hot spots and mantle dynamics. LIPs are characterized by massive outpourings and intrusions of basaltic lava, often occurring within a couple of million years. Fundamental reviews of the nature and possible origin of LIPs are provided by Richards et al. (1989), Coffin and Eldholm (1994), Mahoney and Coffin (1997), Courtillot and Renne (2003), and Bryan et al. (2010). As characterized by Coffin and Eldholm (1994), intraplate continental LIPs (such as the Siberian Traps or the Columbia River basalts) often form by fissure eruptions and horizontal flows of massive tholeiitic basalts. Another form of LIP volcanism occurs at passive margins (such as the North Atlantic Volcanic Province or Etendeka–Paraná) that are associated with continental rifting (White and McKenzie, 1989). The initial prerift pulse of volcanism tends to be rapid and often followed by a more prolonged production of thicker-than-normal oceanic crust and sometimes by long-lived hot spot activity. Oceanic LIPs form broad, flat-topped features of anomalously thick crust with some eruptions being subaerial (Kerguelen oceanic plateau). Other eruptions appear to be confined to below sea level (e.g., Ontong Java Plateau and Shatsky Rise). Regional uplift with often rapid onsets commonly accompanies the formation of continental and oceanic LIPs (Saunders et al., 2007). This section reviews some basic geophysical and geologic observations of LIPs that formed since the Permian. For information on older LIPs, we refer the reader to White and McKenzie (1995), Ernst and Buchan (2001; 2003), and Ernst (2007). **Figure 1** shows locations with indicated abbreviations; **Figure 10** summarizes the areas and volumes of the provinces described in the succeeding text.

133.2.3.1 Intraplate continental LIPs s0060

p0160 *Columbia River Basalts* (*CRBs*). The Columbia River basalts erupted a volume of ~0.17 Mkm between 16.6 and 15.3 Ma (Courtillot and Renne, 2003). Excellent exposures provide insights into flow structures and relationships to feeder dikes. Individual eruptions have volumes in excess of 2000 km^3 and flow over distances up to 600 km (Hooper, 1997). The lack of collapse structures suggests that large amounts of magma were rapidly derived from the base of the crust (Hooper, 1997). The volumetrically most important pulse of volcanism is the Grande Ronde basalt that was emplaced in less than 0.5 My (Barry et al., 2010). Detailed geochemical work suggests that the CRBs rose from a centralized magmatic system following crustal assimilation of plume-derived magmas (Wolff et al., 2008).

p0165 *Emeishan* (*EM*). The Emeishan province in western China is estimated to have spanned an area of at least 2 Mkm^2 and volume of 1 Mkm^3 when it first formed (Zhou et al., 2002).

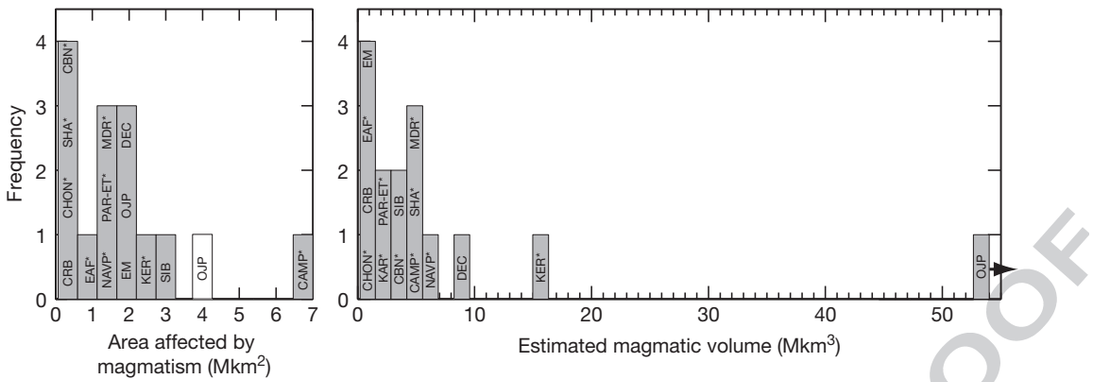

f0055 **Figure 10** Histograms of estimated areas and volumes of the LIPs discussed in the text. The OJP–Manihiki–Hikurangi LIP would have the area shown by white bar and a larger volume than shown, as indicated by arrow.

Eruption ages have been measured at ~258 Ma (Courtillot and Renne, 2003), which is confirmed by a zircon U–Pb date of ~259 Ma (Ali et al., 2005) and by more precise recent U–Pb ages (Shellnutt et al., 2012). Granitic intrusions indicate significant crustal assimilation in magmas that were sourced from the mantle (Shellnutt and Jahn, 2011; Xu et al., 2007; Zhong et al., 2007) A rapid, kilometer-scale uplift preceded the basaltic eruptions by 3 My (He et al., 2003; Sun et al., 2010; Xu et al., 2004). Basalts erupted rapidly (Zheng et al., 2010) and were accompanied by high-MgO basalts (He et al., 2003) and contemporaneous felsic and mafic intrusions (Zhong et al., 2011). Since their eruption, the Emeishan Traps have been fragmented and eroded, currently encompassing an area of ~0.3 Mkm^2 (Xu et al., 2001).

p0170 *Siberia* (*SIB*). The Siberian Traps occupy at present only 0.4 Mkm and have an average thickness of 1 km (Sharma, 1997). There are strong indications, however, that they extend below the sedimentary cover and into West Siberian basin (Reichow et al., 2005). Additional dikes and kimberlites suggest a maximum extent of 3–4 Mkm^2 with possible extrusive volume of >3 Mkm^3. Individual flows can be as thick as 150 m and be traced over hundreds of kilometers. This large eruption took place within only 1 My and coincides with the Permo-Triassic boundary at 250 Ma (Courtillot and Renne, 2003; Reichow et al., 2009). The lack of significant sedimentary rocks or paleosols between flows confirms rapid extrusion (Sharma, 1997). The use of industry seismic and borehole data in the West Siberian basin shows that the basin elevation remained high during rifting, indicating dynamic mantle support (Saunders et al., 2005). Magnetic data elucidate that the eruption took place during oblique rifting (Allen et al., 2006), which may have increased the magmatic output. Petrologic and geodynamic models also agree that lithospheric thinning is required to reconcile the large magmatic output and lava geochemistry (Sobolev et al., 2011; White and McKenzie, 1995). Paleomagnetic reconstructions suggest that the Siberian Traps had erupted over the same part of the mantle where at ~60 Ma the North Atlantic Igneous Province formed (Smirnov and Tarduno, 2010), providing an interesting suggestion for a connection of both LIPs to a long-lived, deep, and nearly stationary source.

p0175 *Yemen/Ethiopian/East African Rift System* (*EAF*). An early volcanic episode in southernmost Ethiopia starting ~45 Ma was followed by widespread flood basalt volcanism in northwestern Ethiopia, Eritrea, and Yemen at ~30 Ma. The 30 Ma event consisted of tholeiites and ignimbrites (Pik et al., 1998) that erupted within 1–2 My (Ayalew et al., 2002; Hofmann et al., 1997). In Yemen, 0.35–1.2 Mkm^3 of mafic magmas were produced within 2 My, followed by less voluminous silicic volcanism starting ~29 Ma (Menzies et al., 1997). Flood volcanism appears to have occurred several My prior to the onset of extension along the East African Rift (EAR) at ~23 Ma (Hendrie et al., 1994; Morley et al., 1992) and in the Gulf of Aden at ~26 Ma (Menzies et al., 1997). Volcanism is bimodal with shield volcanoes forming on top of tholeiitic basalts (Courtillot and Renne, 2003; Kieffer et al., 2004). Currently, the Ethiopian and Kenyan rift systems are on an area of elevated topography of ~1000 km in diameter. A negative gravity anomaly suggests this topography is dynamically supported in the mantle (Stewart and Rogers, 1996). The analysis of primitive magmas indicates that the EAF magmas arise from mantle that is 140–170 K hotter than normal (Rooney et al., 2012).

p0180 *Older continental flood basalts* are often more difficult to detect in the geologic record due to the effects of surface uplift and erosion. For a review, see Ernst (2007). A general characteristic that is attributed to continental LIPs is radiating dike swarms (Mayborn and Lesher, 2004; Mege and Korme, 2004). These dike swarms provide the main pathways for basaltic magmas vertically from the mantle, as well as lateral over distances up to 2500 km (as suggested for the 1270 Ma Mackenzie dike swarm in N. America (Lecheminant and Heaman, 1989; Ernst and Baragar, 1992)).

133.2.3.2 LIPs near or on continental margins

s0065

p0185 *Central Atlantic Magmatic Province* (*CAMP*). The CAMP is primarily delineated by giant dike swarms and is associated with the early breakup of Gondwana between North Africa, eastern United States, and central South America. Ar/Ar dates suggest rapid production from 200 to 202 Ma over an area of 7 Mkm^2 and volume of >2 Mkm^3 (Courtillot and Renne, 2003; Hames et al., 2000; Marzoli et al., 1999), although more recent work puts the CAMP at slightly younger ages of ~199 Ma (Verati et al., 2007; Schaltegger et al., 2008; Jourdan et al., 2009; Marzoli et al., 2011).

p0190 *Chon Aike* (*CHON*). In contrast to the other LIPs discussed in the chapter, the Chon Aike province in Patagonia is primarily silicic with rhyolites dominating over mafic and intermediate lavas. The rhyolites may have formed due to intrusion of basalts into crust that was susceptible to melting. The province is relatively small with an area of 0.1 Mkm^2 and total volume of 0.235 Mkm^3 (Pankhurst et al., 1998). Chon Aike had an extended and punctuated eruptive history from Early Jurassic to Early Cretaceous (184–140 Ma). Pankhurst et al. (2000) recognized episodic eruptions with the first eruptions coinciding with the Karoo and Ferrar LIPs. The province potentially extends into West Antarctica.

p0195 *Deccan* (*DEC*). The Deccan Traps provide one of the most impressive examples of continental flood basalts. It formed by eruptions of primarily tholeiitic basalts over Archean crust over an area of >1.5 Mkm^2 and volume of 8.2 Mkm^3 (Coffin and Eldholm, 1993). The main eruptions straddle magnetic chrons C30*n*, C29*r*, and C29*n* within 1 My around the K–T boundary, as confirmed by Ar/Ar and Re–Os dating (Allegre et al., 1999; Courtillot et al., 2000; Hofmann et al., 2000). The main pulse may have been preceded by a smaller pulse of volcanism at 68–67 Ma (Chenet et al., 2007). An Ir anomaly embedded in the flows suggests that the Chicxulub impact happened while the Deccan Traps were active (Courtillot and Renne, 2003), which is confirmed by stratigraphic work (Keller et al., 2008). Seafloor spreading between India and Seychelles is generally thought to have started in the final stages of flood basalt volcanism (Hooper et al., 2010) at ~63 Ma (Vandamme et al., 1991), although some evidence for an earlier event exists (Collier et al., 2008; Minshull et al., 2008). Unlike older continental flood basalts associated with the breakup of Gondwana, the basalts that are least contaminated by continental lithosphere closely resemble hot spot basalts in oceanic areas with major-element concentrations in agreement with predictions for high-temperature melting (Hawkesworth et al., 1999).

p0200 *Karoo–Ferrar* (*KAR–FER*). The Karoo province in Africa and Ferrar basalts in Antarctica record a volume of 2.5 Mkm^3 combined, which erupted at ~184 Ma (Encarnacion et al., 1996; Minor and Mukasa, 1997), possibly followed by a minor event at 180 Ma (Courtillot and Renne, 2003). The short (<1 My) duration is questioned by Jourdan et al. (2004; 2005), who obtained ages of ~179 Ma for the northern Okavango dike swarm in Botswana and thus inferred long-lived initial activity that propagated northward. More recent zircon U–Pb work on samples collected over an 1100 km range across the Karoo again suggests rapid emplacement (Svensen et al., 2012). In Africa, tholeiitic basalts dominate but some picrites and rhyolites are also exposed (Cox, 1988). The triple-junction pattern of the radiating dike swarm that supplied the Karoo basalt was likely controlled by preexisting lithospheric discontinuities that include the Kaapvaal and Zimbabwe Craton boundaries and the Limpopo mobile belt (Jourdan et al., 2006). The Ferrar province spans an area of ~0.35 Mkm^2 (Elliot and Fleming, 2004) along the Transantarctic Mountains. The two provinces were split by continental rifting and then by seafloor spreading at ~156 Ma.

p0205 *Madagascar* (*MDR*). Widespread voluminous basaltic flows and dikes occurred near the northwestern and southeastern coasts of Madagascar during rifting from India around 88 Ma (Storey et al., 1997). Flood volcanism was probably prolonged as it continued to form the Madagascar Plateau to the south, perhaps 10–20 My later as inferred from the reconstructed positions of Marion hot spot.

p0210 *North Atlantic Volcanic Province* (*NAVP*). The NAVP covers an area of ~1.3 Mkm^2 (Saunders et al., 1997) with an estimated volume of 6.6 Mkm^3 (Coffin and Eldholm, 1993) and is closely linked to continental rifting and oceanic spreading (e.g., Nielsen et al., 2002; White and McKenzie, 1989). Prior to the main pulse of flood volcanism, seafloor spreading was active south of the Charlie–Gibbs Fracture Zone at 94 Ma and propagated northward into the Rockall Trough until the Late Cretaceous near or prior to the earliest eruptions of the NAVP. The early NAVP eruptions occurred as large picritic lavas in western Greenland and Baffin Island (Gill et al., 1992, 1995; Holm et al., 1993; Kent et al., 2004), soon followed by massive tholeiitic eruptions in west and southeast Greenland, the British Isles, and Baffin Island at 61 Ma (2 Mkm^3) as well as in east Greenland and the Faeroes at 56 Ma (>2 Mkm^3) (Courtillot and Renne, 2003; Storey et al., 2007). These initial episodes were succeeded by rifting between Greenland and Europe (recorded by chron 24, 56–52 Ma), continental margin volcanism, and oceanic crust formation, which included the formation of thick seaward-dipping reflector sequences. Spreading slowed in the Labrador Sea at ~50 Ma, stopped altogether at 36 Ma, but continued further to the east on the Aegir Ridge and eventually along the Kolbeinsey Ridge at ~25 Ma, where it has persisted since (Breivik et al., 2006; Mosar et al., 2002). This provides an intriguing suggestion that the presence of hot spots can guide the location of passive ridges during continental breakup.

p0215 Many of the volcanic margin sequences erupted subaerially or at shallow depths, suggesting widespread regional uplift during emplacement (Clift and Turner, 1995; Hopper et al., 2003). Uplift in the early Tertiary is documented by extensive erosion and changes in the depositional environments as far as the North Sea basin (e.g., Mackay et al., 2005; Nadin et al., 1997 and references therein). Reconstructions from drill cores elucidate that uplift was rapid and synchronous and preceded the earliest volcanism by >1 My (Clift et al., 1998).

p0220 *Paraná–Etendeka* (*PAR–ET*). Paraná and Etendeka are conjugate volcanic fields split by the breakup of South America and Africa. The Paraná field in South America covers 1.2 Mkm^2 with estimated average thickness of 0.7 km (Peate, 1997). Extensive dike swarms surrounding the provinces suggest the original extent could have been even larger (Trumbull et al., 2004). Tholeiitic lavas and rhyolites cause a bimodal distribution of eruptives and intrusives. Ar/Ar dates indicate that volcanic activity peaked at ~133–130 Ma (Courtillot and Renne, 2003; Renne et al., 1996; Turner et al., 1994), preceded by minor eruptions in the northwest of the Paraná Basin at 135–138 Ma (Stewart et al., 1996). Younger magmatism persisted along the coast (128–120 Ma) and into the Atlantic Ocean, forming the Rio Grande (RIO) and Walvis (WAL) oceanic plateaus.

p0225 The Etendeka province covers 0.08 Mkm^2 and is very similar to the Paraná flood basalts in terms of eruptive history, petrology, and geochemistry (Ewart et al., 2004; Renne et al., 1996). Seafloor spreading in the South Atlantic progressed northward, with the oldest magnetic anomalies on the seafloor near Cape Town (137 or 130 Ma). The oldest seafloor near

Paraná is >127 Ma. The formation of onshore and offshore basins suggests a protracted period of rifting well in advance of the formation of oceanic crust and the emplacement of the Paraná basalts (Chang et al., 1992).

s0070 ### 133.2.3.3 Oceanic LIPs

p0230 *Caribbean* (*CBN*). The Caribbean LIP is a Late Cretaceous plateau, which is now partly accreted onto the continental margin in Colombia and Ecuador. Its present area is 0.6 Mkm^2 with oceanic crust thicknesses ranging from 8 to 20 km. A volume of 4 Mkm^3 of extrusives erupted in discrete events during 91–88 Ma (Courtillot and Renne, 2003). The full range of $^{40}Ar/^{39}Ar$ dates of 69–139 Ma (e.g., Hoernle et al., 2004; Sinton et al., 1997) suggests a protracted volcanic history that is poorly understood. The origin of the volcanism is likely in the eastern Pacific with a subsequent highly mobile evolution. Clogging of eastward subduction in the Caribbean likely led to reversal with westward subduction in the Antilles trench. The accretion of terranes in Ecuador and Colombia, which started in the Late Cretaceous and early Tertiary, led to westward stepping of the subduction zone (Kerr et al., 1997). A 5 km lava succession in Curaçao contains picrites with up to 31 wt% MgO.

p0235 *Kerguelen* (*KER*). The Kerguelen hot spot has a complex history of continental and oceanic flood eruptions, rifting, and prolonged volcanism (**Figure 2**). The breakup of India, Australia, and Antarctica coincided closely with the eruption of the Bunbury basalts in southwest Australia, dated at 123 and 132 Ma (Coffin et al., 2002). The first massive volcanic episode formed the southern Kerguelen Plateau at 119 Ma, the Rajmahal Traps in India at 117–118 Ma, and the lamprophyres in India and Antarctica at 114–115 Ma (Coffin et al., 2002; Kent et al., 2002). The central Kerguelen Plateau and Broken Ridge formed at ~110 Ma and 95 Ma, respectively (Coffin et al., 2002; Duncan, 2002; Frey et al., 2000). These edifices represent the most active period of volcanism with a volcanic area and volume of 2.3 Mkm^2 and 15–24 Mkm^3 (Coffin and Eldholm, 1993), but unlike many other flood basalt provinces, volcanic activity spanned tens of millions of years. Another unusual aspect is the presence of continental blocks within the plateau as suggested from wide-angle seismics (Operto and Charvis, 1996) and geochemical data of xenoliths and basalts from southern Kerguelen Plateau and Broken Ridge (Benard et al., 2010; Frey et al., 2002; Mahoney et al., 1995; Neal et al., 2002). During 82–43 Ma, northward motion of the Indian Plate formed the Ninetyeast Ridge on young oceanic lithosphere, suggesting that the Kerguelen hot spot remained close to the Indian–Antarctic spreading center (Kent et al., 1997; Krishna et al., 2012; Silva et al., 2013; Singh et al., 2011). The influence of the Kerguelen hot spot can be even traced as far as northeastern India (Ghatak and Basu, 2011). At ~40 Ma, the Southeast Indian Ridge formed and separated Kerguelen Plateau and Broken Ridge. Volcanism has since persisted on the northern Kerguelen Plateau until 0.1 Ma (Nicolaysen et al., 2000). Dynamic uplift of the plateau in the Cretaceous is indicated by evidence for a subaerial environment, but subsidence since then appears to be similar than for normal oceanic crust (Coffin, 1992).

p0240 *Ontong Java Plateau* (*OJP*). Overviews of the origin and evolution of the Ontong Java Plateau are provided by Fitton et al. (2004) and Neal et al. (1997). This plateau extends across 1.5–2 Mkm^2, has crust as thick as 36 km, and has volume estimated at ~50 Mkm^3 (Gladczenko et al., 1997; Korenaga, 2011). The majority of the basalts were erupted in relatively short time (~1–2 My) near 122 Ma as revealed by Ar/Ar (Tejada et al., 1996) and Re–Os isotope (Parkinson et al., 2002), paleomagnetic (Tarduno et al., 1991), and biostratigraphic data (Sikora and Bergen, 2004). Basalts recovered from the Ocean Drilling Program (ODP) Site 803 and the Santa Isabel and Ramos Islands indicate a smaller episode of volcanism at 90 Ma (Neal et al., 1997). Age contrasts between the surrounding seafloor and OJP suggest it erupted near an MOR. Furthermore, rifting is evident on some of its boundaries. Accordingly, Taylor (2006) and Chandler et al. (2012) suggested that the OJP is only a fragment of what was originally an even larger LIP that included Manihiki (MAN) and Hikurangi (HIK) Plateaus. This idea is supported by geochemical similarities between OJP and Manihiki lavas (Hoernle et al., 2010). Given recent evidence for partial subduction of HIK beneath New Zealand, current estimates for the extent of the combined LIP should be regarded as lower bounds (Reyners et al., 2011). The estimated original size of the combined LIP makes it, by far, the largest of all flood basalt provinces in the geologic record, approaching an order of magnitude larger in volume than any continental flood basalt.

p0245 The plateau has been sampled on the tectonically uplifted portions in the Solomon Islands (e.g., Petterson, 2004; Tejada et al., 1996, 2002) and by ocean drilling (Mahoney et al., 2001). The volcanics are dominated by massive flows of tholeiitic basalts with low potassium contents. Petrologic modeling is consistent with primary magmas formed by 30% melting of a peridotitic source (Chazey and Neal, 2004; Fitton and Godard, 2004; Herzberg, 2004b), which would require a hot (1500 °C) mantle source beneath thin lithosphere. The low volatile content of volcanic glasses (Roberge et al., 2004, 2005) and Pb, Sr, Hf, and Nd isotope characteristics (Tejada et al., 2004) resemble MORB.

p0250 Besides its gigantic volume, another enigmatic aspect is that the OJP appears to have erupted below sea level with little evidence for uplift (Coffin, 1992; Ingle and Coffin, 2004; Ito and Clift, 1998; Korenaga, 2005; Roberge et al., 2005). This observation has to be explained by any successful model for the origin of Ontong Java.

p0255 *Shatsky Rise–Hess Rise* (*SHA–HES*). Shatsky Rise is one of the large Pacific oceanic plateaus with an area of 0.48 Mkm^2, a thickness of 9–30 km, and a volume of 4.3 Mkm^3 (Korenaga and Sager, 2012; Sager et al., 1999). The most voluminous portion of the plateau extends from its center to the SW (**Figure 1**). This whole portion has recently been proposed to be made up of a single volcanic edifice with very low slopes, something that would probably make it the largest volcano on Earth (Sager et al., 2013). Initial eruption at Shatsky is associated with a jump of the triple junction between the Pacific, Izanagi, and Farallon Plates toward the plateau (Nakanishi et al., 1999; Sager, 2005) near 145 Ma (Mahoney et al., 2005). Subsequently, volcanism progressed northeast together with the triple junction (which migrated with repeated jumps as indicated by seafloor magnetic lineation) until ~128 Ma. Thus, Shatsky appears to show short-lived age-progressive volcanism on timescales much like many smaller volcano groups (e.g., Society).

Volcanism, however, may have continued with a renewed pulse starting some 10–20 My later with the formation of the Hess Rise, which is comparable in area to Shatsky. Age constraints on Hess Rise are poor due to the lack of sampling and its location on Cretaceous quiet zone seafloor. The possible coincidence of both plateaus at an MOR suggests a dynamic linkage between their formation and seafloor spreading. Another notable aspect is that Pb and Nd isotope compositions for Shatsky are indistinguishable from those of the present-day East Pacific Rise (Mahoney et al., 2005; Sager, 2005).

s0075 ### 133.2.3.4 Connections to hot spots

p0260 The possible links between hot spots and LIPs are important for testing the mechanism of origin for both phenomena, with particular regard to the concept of a starting mantle plume head and trailing, narrower plume stem. While linkages are clear for some cases, a number of proposed connections are obscured by ridge migrations or breakup of the original LIP. In the succeeding text, we list the connections of hot spots to LIPs, in approximate order of decreasing clarity.

p0265 At least six examples have strong geographic, geochronological, and geochemical connections between hot spot volcanism and flood basalt provinces. These are (1) Iceland and the North Atlantic Volcanic Province, including Greenland, Baffin Island, Great Britain volcanics, and Greenland–United Kingdom (Faeroe) Ridge (Saunders et al., 1997; Smallwood and White, 2002); (2) Kerguelen, Bunbury, Naturaliste, and Rajmahal (E India) and Broken Ridge and Ninetyeast Ridge (Kent et al., 1997); (3) Réunion and Deccan (Roy, 2003), W. Indian, Chagos–Laccadive, Mascarene, and Mauritius; (4) Marion and Madagascar (Meert and Tamrat, 2006; Storey et al., 1997); (5) Tristan da Cunha and Paraná, Etendeka, Rio Grande, and Walvis Ridge (Peate, 1997); and (6) the Galápagos and Caribbean (Feigenson et al., 2004; Hoernle et al., 2004).

p0270 In addition to these six examples, a tentative link exists between Yellowstone and the early eruptive sequence of the Columbia River basalts (CRBs) based on geochemistry (Dodson et al., 1997). The paleogeographic connection is somewhat indirect since main CRB eruptions occurred up to 500 km north of hot spot track. This offset may suggest a mechanism for the formation of the flood basalts that is independent of the Yellowstone hot spot (Camp and Hanan, 2008; Hales et al., 2005; Long et al., 2012). Yet, the earliest manifestation of the CRB (at Steens Mountain) is indeed close to the proposed paleolocation of the Yellowstone hot spot (Hooper, 1997; Hooper et al., 2002), implying a south-to-northward propagation of CRB volcanism (Coble and Mahood, 2012) and supporting the suggestion that melts may have been forced sideways from their mantle source by lithospheric structure (Thompson and Gibson, 1991). In turn, it has been suggested that the lithospheric structure forced the Yellowstone plume away from the flood basalt province after ~12 Ma (Shervais and Hanan, 2008).

p0275 For other flood basalt provinces, the links are less clear – in part due to the lack of data. The Bouvet hot spot has been linked to the Karoo–Ferrar; the Balleny hot spot may be connected to the Tasmanian province or the Lord Howe Rise (Lanyon et al., 1993); and the Fernando hot spot has been linked to the Central Atlantic Magmatic Province. Only three Pacific hot spots possibly link back to LIPs: Louisville–OJP, Easter–Mid-Pac, and Marquesas–Hess–Shatsky (Clouard and Bonneville, 2001). The Louisville–OJP connection is highly tenuous: Kinematic arguments against such a link have been made (Antretter et al., 2004), and geochemical differences between the oldest Louisville seamounts and OJP would require distinct chemistry between plume head and tail or a difference in melting conditions (Mahoney et al., 1993; Neal et al., 1997). Nevertheless, some hot spots such as Hawaii, Bowie–Kodiak, and Cobb terminate at subduction zones, so any record of a possible connection to an LIP has been destroyed.

p0280 It is interesting to note that the strongest connections involve flood basalt provinces near continental margins. The possible exceptions are Kerguelen and Marion–Madagascar, which also involve continental lithosphere, as well as the tentative links in the Pacific. The presence of continents may indeed play a large role in the origin of flood basalt volcanism (Anderson, 1994b).

s0080 ### 133.2.3.5 Connections to climate crises and mass extinction

p0285 The eruption of LIPs has been a leading explanation for a number of climate crises and mass extinctions. This volcanic cause of mass extinctions poses an alternative to extraterrestrial causes such as impacts by asteroids or comets, which are probably best documented to be associated with the K–T mass extinction (Schulte et al., 2010). The connection between mass extinctions and LIPs is generally justified by the coincidence of LIP formation and extinctions as well as the ability of rapid and massive extrusions to dramatically change climate and the chemistry of the atmosphere and oceans. The episodicity of mass extinction events and their correlation with LIPs lead to the speculation that the slow convection and heat release from the solid Earth control evolutionary patterns at the Earth's surface (e.g., Courtillot and Olson, 2007). Increasingly, a connection is seen between flood basalts and other transient episodes in the global climate system. Aside from direct effects on ocean and atmospheric chemistry due to volcanic outgassing, the igneous intrusions associated with LIPs can lead to significant release of CO_2 and methane (i.e., major greenhouse gases) from metamorphic interactions with coal, evaporates, and other sedimentary rocks (e.g., Ganino and Arndt, 2009; Retallack, 2013). Such links are also suggested for flood basalts that occur during continental breakup, as illustrated by the correlation between North Atlantic flood basalts with the Paleocene–Eocene thermal maximum at ~55 Ma (Storey et al., 2007) and the Caribbean and Madagascar flood basalts with the Late Cretaceous anoxic event (Kuroda et al., 2007). Interestingly, while the short-term effect of CO_2 release from flood basalt volcanism is likely to lead to global warming, the longer-term effect may be global cooling due to more efficient silicate weathering that acts as a carbon sink (Schaller et al., 2011, 2012).

p0290 Significant recent work has refined early indications that mass extinctions coincide with LIP formation. Indications have indeed been strengthened for the four major extinctions that pair up with LIP formation since the Permian: the end of Cretaceous extinction with the Deccan Traps at ~65 Ma, the end of Triassic extinction with the CAMP at ~200 Ma, the end of Permian extinction with the Siberian Traps at ~250 Ma, and the end of Guadalupian (an epoch in the Permian) extinction with the Emeishan at ~258 Ma (for reviews, see Courtillot and

Renne, 2003; Bryan et al., 2010). In some cases, the suggested temporal coincidence has been questioned because of inherent uncertainties in magnetostratigraphy and geochronological techniques (Whiteside et al., 2007). Yet, future geochronological work using high-precision dating tools is expected to resolve these discrepancies. For example, Blackburn et al. (2013) demonstrated using a new zircon U–Pb methodology that the end of Triassic extinction coincides with four episodes of magma release in the CAMP and atmospheric changes that have occurred over a short period of only 0.6 My. A combination of multiple geochronological techniques further confirms the connection between CAMP and the end of Triassic extinction (Deenen et al., 2010).

p0295 The LIP–extinction connection is further strengthened by a better quantification and qualification of the duration and chemical output of eruptions, as well as a better understanding of the impact of flood volcanism on the global climate system (e.g., Black et al., 2012; Kidder and Worsley, 2010; Payne and Clapham, 2012; Self et al., 2006) and ocean geochemistry (Brand et al., 2012). This understanding is enhanced by a better physical description of the interaction between magmas and sediments (Aarnes et al., 2010; Ogden and Sleep, 2012). Some of this work indicates intriguing differences in magmatic composition between LIPs, such as the anomalously high concentration in sulfur and halogens observed in the Siberian Traps flood basalts (Black et al., 2012), which may have significantly contributed to the dramatic deterioration of the environment at the end of the Permian. The anomalous impact of the Siberian Traps is generally attributed to the intrusion of the basalts into a deep sedimentary basin with significantly higher gas release (Ganino and Arndt, 2009; Svensen et al., 2009) although differences in the source have also been noted (Carlson et al., 2006; Sobolev et al., 2009, 2011).

s0085 ## 133.2.4 Geochemistry and Petrology of OIB

s0090 ### 133.2.4.1 Isotope geochemistry

p0300 Studying the geochemistry of MORB and basalts from oceanic hot spots and melting anomalies (often referred to as ocean island basalts, OIBs) has played a central role in understanding mantle dynamics and heterogeneity. Isotope ratios of key trace elements reflect long-term (10^2–10^3 My) concentration between parent and daughter elements. As they remain unaffected by mantle metasomatism and melting, they have been used to 'fingerprint' source materials. We will focus on three commonly used ratios: $^{87}Sr/^{86}Sr$, $^{206}Pb/^{204}Pb$, and $^{3}He/^{4}He$. High (or low) $^{87}Sr/^{86}Sr$ is associated with long-term enrichment (or depletion) in highly incompatible elements relative to moderately incompatible elements (e.g., Rb/Sr). High (or low) $^{206}Pb/^{204}Pb$ ratios are associated with mantle with a long-term high (or low) U/Pb. The $^{3}He/^{4}He$ ratio is a measure of the amount of primordial ^{3}He, which has been lost to space during the Earth's evolution via degassing but not generated in the mantle, in contrast to radiogenic ^{4}He.

p0305 MORB is characterized by low values of, and small variability in, the ratios mentioned earlier. Figure 11 shows frequency distributions of MORB and OIB from the three major oceans. The data are from http://www.petdb.org/; all data are included so there is no filtering due to affiliation with hot spots or any tectonic features. One standard deviation about the median for all three datasets combined defines the MORB range for $^{87}Sr/^{86}Sr$ of 0.7025–0.7033, for $^{206}Pb/^{204}Pb$ of 17.98–18.89, and for $^{3}He/^{4}He$ of 7.08–10.21. Excluding hot spot-influenced MORB would further reduce these ranges (e.g., to a narrow range in $^{3}He/^{4}He$ of 7.68–9.82 (Graham, 2002)). In contrast, OIBs have a larger variability, extending from MORB values to much higher values (http://georoc.mpch-mainz.gwdg.de/georoc/; Figure 11). By comparing the median hot spot compositions (solid bar) with the MORB ranges, it becomes clear that, with few exceptions, the hot spots and melting anomalies have compositions that are distinguishable from MORB by at least one of the three isotope ratios (see also Table 1). This result appears to be independent of the duration of age progression (e.g., Tristan vs. Marquesas), the presence or absence of a swell (Hawaii vs. the Canaries), or even volcanic flux (Kerguelen vs. Pukapuka and Foundation).

p0310 There are at least four possible exceptions: Shatsky Rise (not shown in Figure 11), Cobb, Bowie–Kodiak, and the Carolines. Helium isotopes are not yet available at these locations, but $^{87}Sr/^{86}Sr$ and $^{206}Pb/^{204}Pb$ compositions for each case fall within or very near to the MORB range. These examples span a wide range of forms, from a small, short-lived seamount chain (the Carolines), to longer-lived, age-progressive volcanism (Bowie–Kodiak and Cobb), to an oceanic LIP (Shatsky). The possibility that these cases are geochemically indistinguishable from MORB may have far-reaching implications for mantle processes and composition and thus clearly motivates further sampling and analysis.

s0095 ### 133.2.4.2 Major-element geochemistry

p0315 In contrast to isotopic ratios, major-element signatures of OIB lavas do not directly reflect that of the mantle source. Major-element concentrations in primary magmas (i.e., magmas that segregated from the mantle melting zone without further modification by shallow processes) are sensitive to the depths and extents of melting. Moreover, they are affected by magma mixing, interaction with the wall rock, and fractional crystallization during ascent. The effects of fractional crystallization are not only large but also relatively well understood and thus can be corrected for when estimating the composition of primary magmas. Alternatively, primary magma compositions can be inferred from melt inclusions or olivine phenocrysts that are estimated to have been in equilibrium with the primary magma when they were formed. However, such analyses are laborious and costly compared to whole rock analysis and hence form just a small portion of the global dataset.

p0320 Despite the difficulties mentioned earlier, major-element signatures of OIB and MORB can be clearly distinguished in properly selected and corrected datasets of whole rock analyses. For example, these datasets are usually restricted to samples with MgO contents between >5 wt% (or even >10 wt%) and $<\sim$15 wt% in order to exclude lavas that have experienced significant fractional crystallization of clinopyroxene (Dasgupta et al., 2010; Jackson and Dasgupta, 2008; Pilet et al., 2008). Fractional crystallization of olivine instead is routinely corrected for by retroactive incremental addition or subtraction of olivines that have been in equilibrium with the corresponding liquid. Similar to isotope datasets, such corrected major-element datasets show that OIB global trends overlap with MORB, but display a much greater variability in all oxides and oxide ratios (Figure 12). In contrast to MORB,

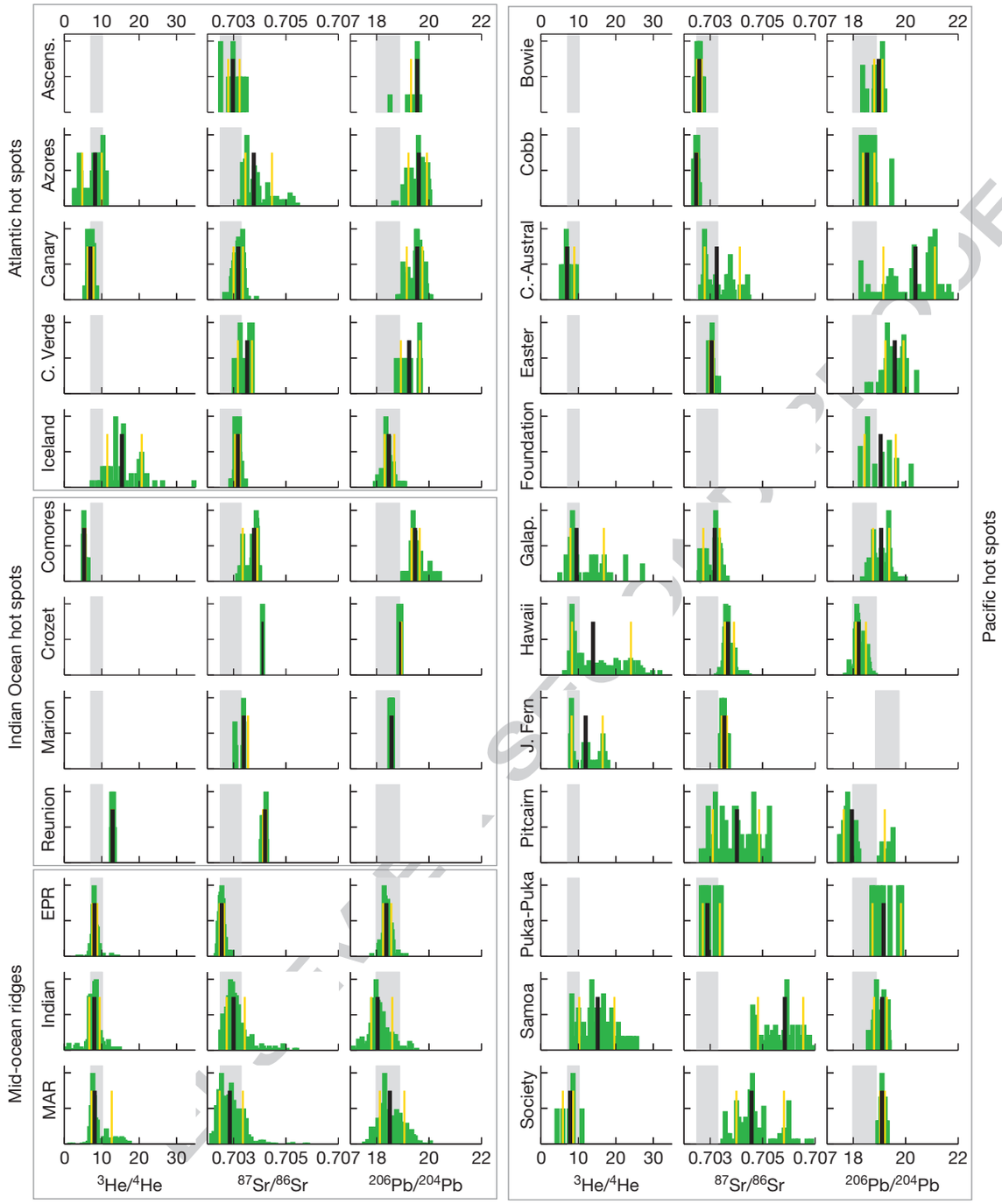

f0060 **Figure 11** Frequency distributions (green, normalized by maximum frequency for each case) of isotope measurements taken for each of the oceanic hot spots shown and for MORs (lower left). Bold black lines mark median values, and yellow lines encompass 68% (i.e., one standard deviation of a normal distribution) of the samples. Light gray bars denote the range of values encompassing 68% of all of the MORB measurements (sum of the three ridges shown). Most of these data are from the GEOROC database (http://georoc.mpch-mainz.gwdg.de/georoc/) with key references for $^{3}He/^{4}He$ data given in Ito and Mahoney (2006). Data for Pukapuka are from Janney et al. (2000) and for the Foundation chain from Maia et al. (2000).

OIB commonly follows an alkalic differentiation trend (except for shield lavas from Hawaii, the Galápagos, and Iceland) due to systematically higher K_2O+Na_2O at a given SiO_2 in the primary magmas. This subset of alkalic OIB is hence nepheline-normative, that is, highly undersaturated in SiO_2. They also display higher concentrations of K_2O, MgO, FeO_X, and TiO_2, as well as lower concentrations of Al_2O_3 at a given SiO_2 (e.g., Pilet et al., 2008), than tholeiitic OIB or even MORB. These characteristics are important constraints for the makeup of the OIB mantle source (see **Section 133.3.6**).

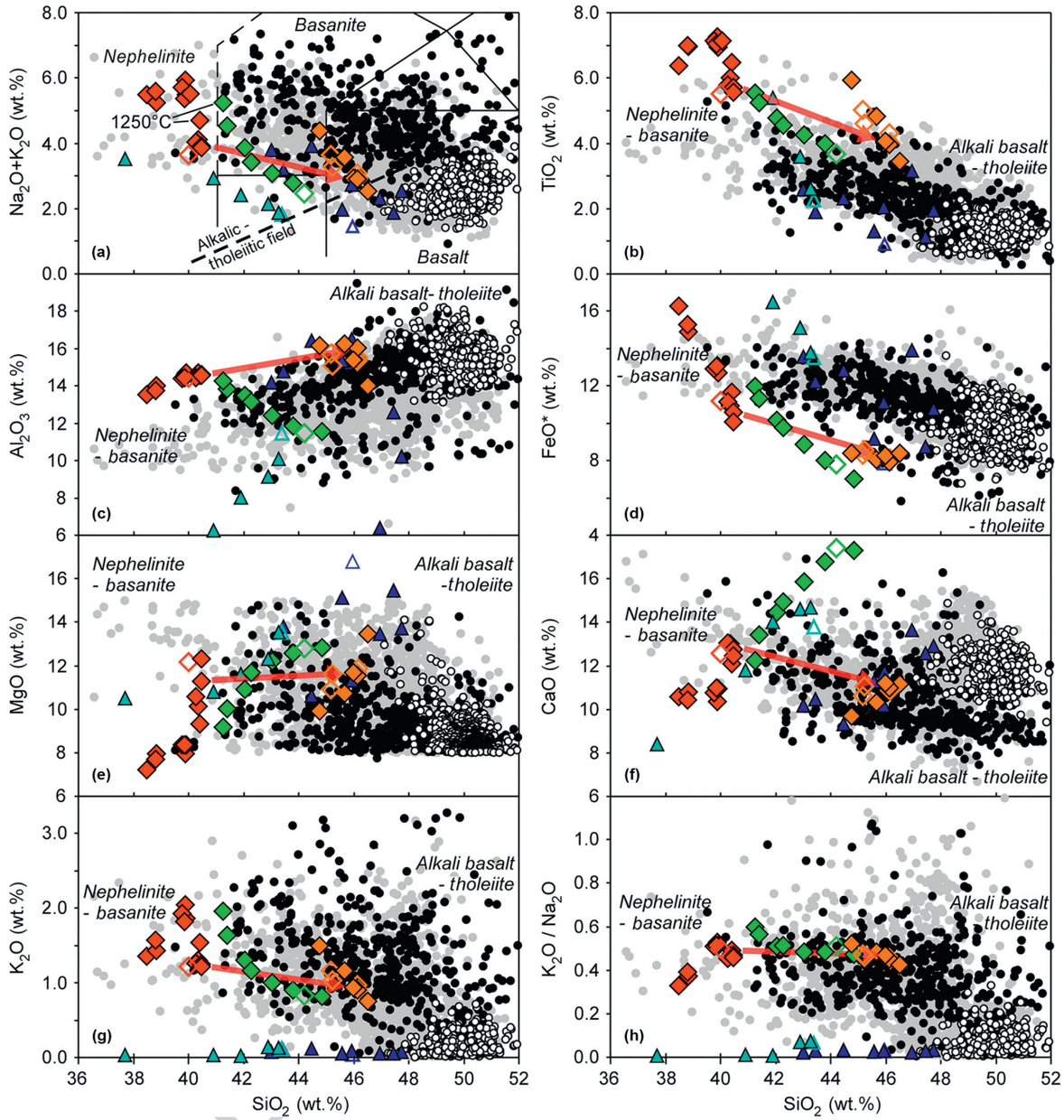

f0065 **Figure 12** From Pilet et al. (2008) with minor modifications. Select major-element concentrations (a–g) and oxide ratios (h) of basalt samples and experimental melts. Solid gray circles, OIB; solid black circles, continental intraplate basalts; open circles, MORB. Solid diamonds are experimental hornblenditic liquids from three different starting compositions (open diamonds) at various experimental conditions (Pilet et al., 2008); triangles are experimental liquids derived from silica-deficient pyroxenites with (dark blue; Dasgupta and Hirschmann, 2006) or without (light blue; Hirschmann et al., 2003; Kogiso et al., 2003) the addition of CO_2.

s0100 ## 133.2.5 Mantle Seismic Anomalies

s0105 ### *133.2.5.1 Global seismic studies*

p0325 Seismic wave propagation in the mantle is generally slowed by elevated temperature, volatile content, and the presence of melt (e.g., Anderson, 1989). In addition, it is affected by the content of mafic materials, such as eclogite (Xu et al., 2008; Zhang and Green, 2007). Seismology is therefore the primary geophysical tool for probing the physical signature of hot spots and melting anomalies and for identifying their depths of origin.

Seismic tomography uses seismic delay times and waveform deviations to map velocity anomalies relative to a particular background model. Applications of these techniques have seen wide popularity as velocity variations can be directly related to chemical and thermal variations in the Earth. Yet, it should be considered that any tomographic image is in fact a p0330

model of the Earth that is strongly dependent on the method of inversion, choice of damping parameters, and background model and can be quite sensitive to the lack of global coverage of earthquakes and seismometers, as well as standard consequences of wave propagation such as wave-front healing or those associated with finite-frequency effects.

p0335 Global seismic tomography has been able to confidently image the remnants of slabs as high-velocity and presumably cold anomalies (e.g., Bijwaard et al., 1998; Grand et al., 1997). The hot mantle upwellings hypothesized to be associated with hot spots are instead expected to be narrow, localized, and much less voluminous than slabs. Any associated low-velocity anomalies may further be obscured by the effects of wave-front healing. Combined, these effects should make plumes very difficult to be imaged with seismic tomography, especially in the lower mantle (Hwang et al., 2011; Nolet et al., 2007; Ritsema and Allen, 2003; Styles et al., 2011). Structures in the lower mantle that are most robustly imaged and likely associated with upwelling are the (1000s of km across) LLSVPs below the South Pacific and African Superswell regions (e.g., Breger et al., 2001; Ni et al., 2005; Trampert et al., 2004; van der Hilst and Karason, 1999). The sharp edges of these anomalies (Ni et al., 2002; To et al., 2005) and their reproduction in dynamic models (McNamara and Zhong, 2005; Tan and Gurnis, 2007) suggest that these features are anomalous in terms of both composition and temperature (see also **Chapter 136**).

p0340 The use of global tomography to probe the existence and nature of smaller-scale (100 s of km across) upwellings associated with individual hot spots continues to be a challenge, but substantial progress has been made with improved resolution in global seismic models (e.g., Boschi et al., 2007; Montelli et al., 2006; Nataf, 2000; Nolet et al., 2007; Ritsema and Allen, 2003; Zhao, 2007 and references therein). Numerous hot spots have been shown to overlie low-velocity anomalies in the upper mantle, and a subset of these anomalies have been argued to extend into the deep lower mantle based on visual inspection (Montelli et al., 2006; Zhao, 2007; **Figure 13**) or on various statistical tests (Boschi et al., 2007, 2008). Two research groups (Boschi et al., 2007; Zhao, 2007) emphasize that many lower mantle, plume-like anomalies are best explained by plumes, which tilt and whose sources migrate due to flow of the ambient mantle. In addition, evidence shows that lower mantle plumes tend to originate from around the edges of the LLSVPs beneath the South Pacific and Africa (Boschi et al., 2007; Thorne et al., 2004; **Figure 13(e)**).

p0345 The passage of mantle plumes from the lower mantle into the upper mantle can also be detected by measuring the depths of the seismic discontinuities bounding the mantle transition zone. Excess temperature is expected to cause the phase change near 410 km with a positive Clapeyron slope to occur deeper and the phase change near 660 km with a negative Clapeyron slope to occur shallower. In both the cases, the olivine system is assumed to dominate the phase changes (Helffrich, 2000; Ito and Takahashi, 1989). Hot mantle plumes that pass through both phase changes should therefore be associated with unusually thin transition zones. Some global-scale studies suggest this is indeed the case (e.g., Lawrence and Shearer, 2008; Li et al., 2003; Schmerr et al., 2010; Tauzin et al., 2008). In some cases, most of the variations in transition zone thickness to topography are suggested at 660 km (Lawrence and Shearer, 2008; Schmerr et al., 2010), whereas many others attributed most of the variations to topography at 410 km (Li et al., 2003; Tauzin et al., 2008). The evidence for the transition near 660 km tending to remain flat or deepen – not shoal – in some regions where the mantle is expected to be unusually hot could indicate that the phase change effects are locally dominated by the garnet system (postgarnet to perovskite, with a positive Clapeyron slope) (Cao et al., 2011; Houser and Williams, 2010; Tauzin et al., 2008).

p0350 Results about the depth of origin of plumes beneath many of the Earth's major hot spots are beginning to show some consistencies. Between the studies of Montelli et al. (2006) and Zhao (2007), 19 hot spots are associated with plumes originating in the deep lower mantle, but only four (Tahiti, Kerguelen, Hawaii, and Cape Verde) are recognized as such in both of the studies (**Figure 14**). These four hot spots also show continuity of low-velocity material extending through most of the mantle according to Boschi et al.'s (2007) objective analysis (i.e., normalized vertical extent >0.5 in **Figure 14**). An additional seven other hot spots (East Africa/Afar, Réunion, Macdonald/Cook, Samoa, the Canaries, the Azores, Iceland, and Easter) identified as deep plumes by either Montelli et al. (2006) or Zhao (2007), but not by both, are also likely to extend through most of the mantle according to Boschi et al. (2007). Of the 19 identified by Montelli et al. (2006) and Zhao (2007), 6 hot spots (Tahiti, Samoa, the Canaries, the Azores, Iceland, and Hawaii) are further associated with anomalously thin mantle transition zones, but 1(Easter) is associated with a transition zone that is as thick or thicker (246 ± 3 km) than the global average (242 ± 2 km) (Courtier et al., 2007). Six of these nineteen hot spots (Easter, Hawaii, Iceland, Réunion, East Africa, and Louisville) were identified by Courtillot et al. (2003) as being 'primary plumes' from the deep mantle on the basis of their association with a buoyancy flux $>10^3$ kg s^{-1}, a flood basalt province, and magmas with high ^{3}He/^{4}He (see also purple squares in **Figure 7**).

p0355 Along these lines, at least three research groups agree that ~11 or so hot spots originate as hot mantle upwellings rising from the deep lower mantle (**Figure 14**): Tahiti, East Africa, Réunion, Samoa, Kerguelen, the Canaries, the Azores, Iceland, Hawaii, Cape Verde, and Easter Island. A critical shortcoming is that the resolution of seismic tomography in the lower mantle is probably insufficient to seismically resolve slow mantle upwellings with lateral dimensions of hundreds of kilometers (Styles et al., 2011). The regions of the lower mantle most reliably imaged as being seismically slow have widths of 1000 km or more (Boschi et al., 2007). This leads to the unresolved question whether any lower mantle plumes (100 s of km wide) originate individually from the core–mantle boundary (CMB) or whether all lower mantle plumes rise out of much broader (1000s of kilometer wide) dome-like LLSVPs (Courtillot et al., 2003; Schubert et al., 2004; Torsvik et al., 2006). Of course, the lack of visibility of a narrow plume in the lower mantle may also just indicate its absence and an origin within or near the transition zone (Courtillot et al., 2003; Cserepes and Yuen, 2000).

133.2.5.2 Seismic studies of major hot spots

s0110

p0360 Regional studies of the seismic structure of the mantle beneath hot spots are often at higher resolution than global studies. We will discuss the main results of these in geographic order.

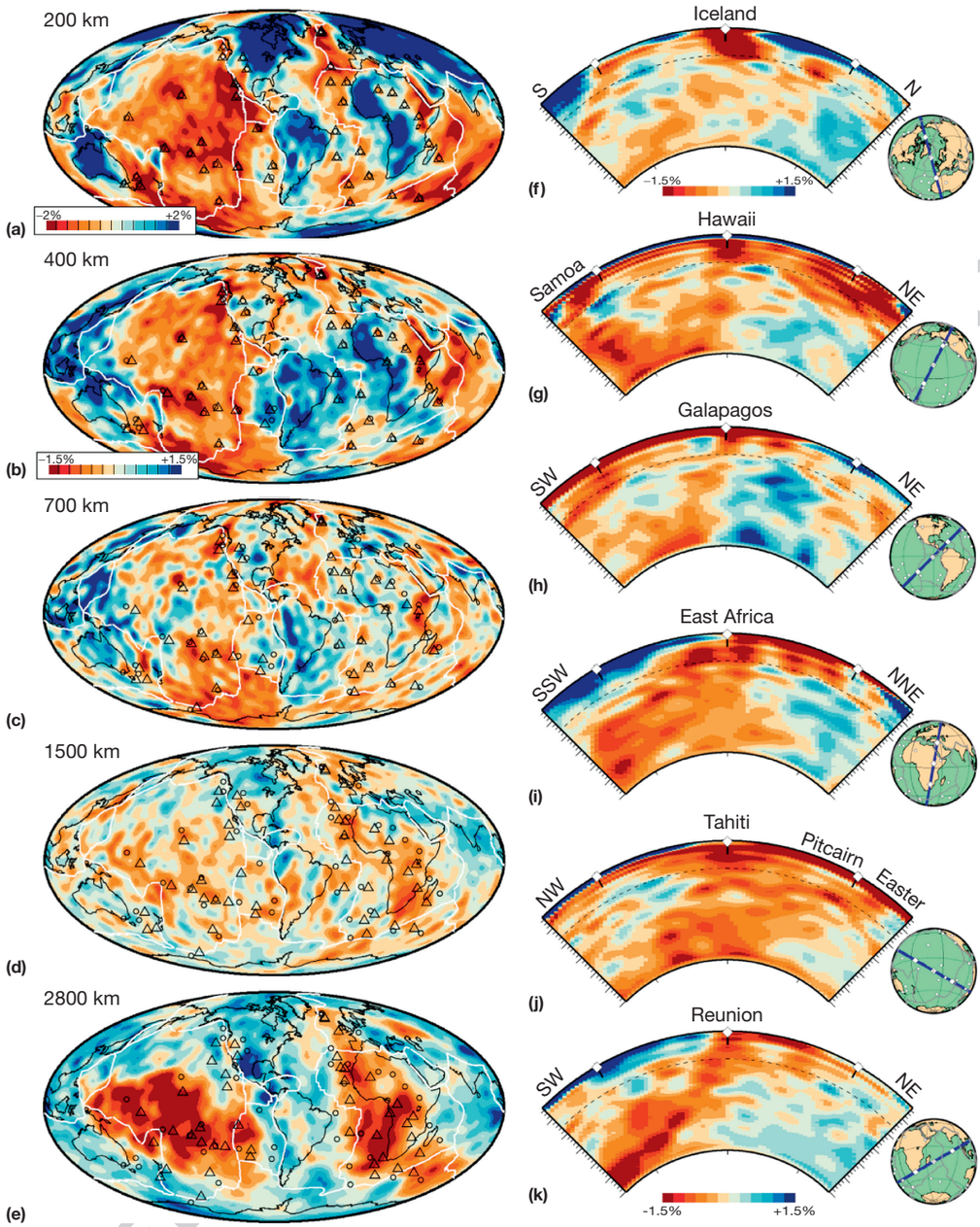

f0070 **Figure 13** (a)–(e) Maps of shear-wave velocity anomalies at different depths (as denoted) in tomography model S40RTS (Ritsema et al., 2011) (all have the same color scale except (a)). Circles mark locations of hot spots (Steinberger, 2000). Estimated plume locations at the different depths (triangles) vary because plumes are modeled as swaying with predicted mantle flow and rising from source locations at the CMB, which also move with the mantle (Boschi et al., 2007; Steinberger and Antretter, 2006). (f)–(k) 90° cross sections beneath several hot spots with low-velocity zones in the upper mantle that appear to extend into the lower mantle. Insets show location and orientations of the cross sections. Diamonds mark three points along each cross section for orientation.

p0365 *Iceland*: Regional seismic studies have confidently imaged a body of anomalously slow seismic wave speeds in the upper mantle beneath Iceland. Conventional ray theory was used to first image the anomaly (Allen et al., 1999, 2002; Foulger et al., 2001; Wolfe et al., 1997). A subsequent study using an improved finite-frequency technique (Allen and Tromp, 2005) resolves the feature to be roughly columnar with lateral dimensions of 250–300 km with peak P- and S-wave anomalies of −2.1% and −4.2%, respectively (Hung et al., 2004; **Figure 15**). Recent studies using full-waveform tomography (Rickers et al., 2013) or Rayleigh waves and local earthquakes (Li and Detrick, 2006; Yang and Shen, 2005) confirm these high amplitudes, which most likely require a combination of excess temperature and melt.

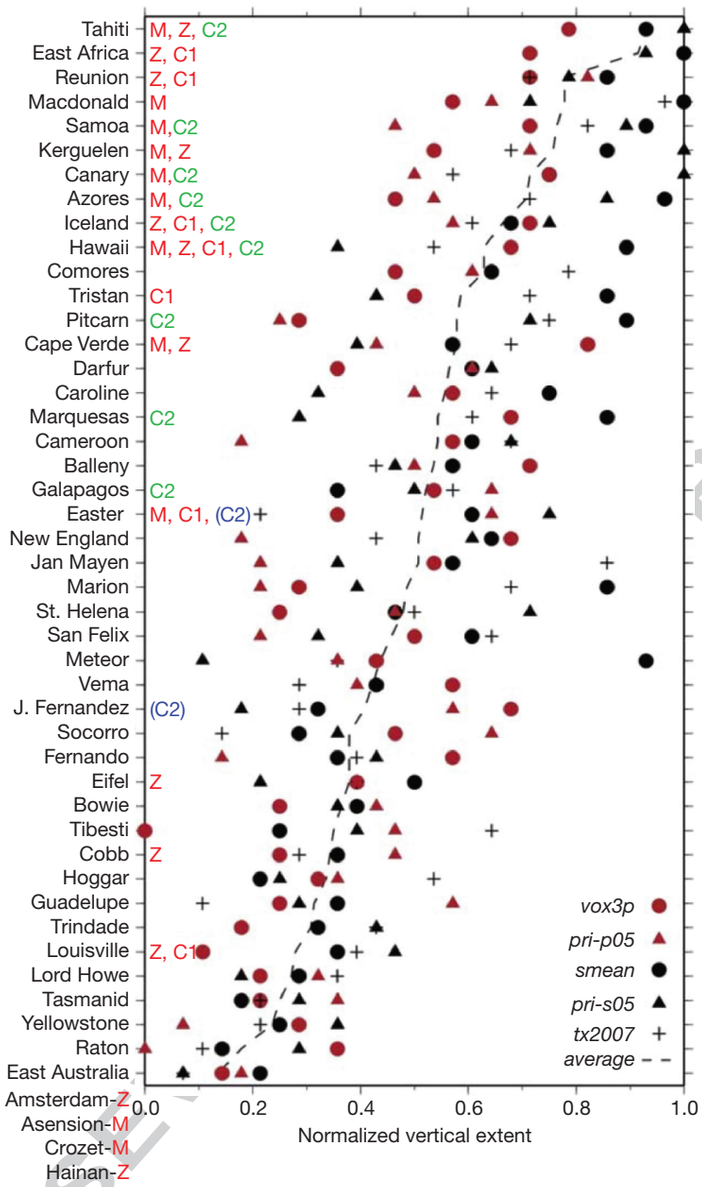

f0075 **Figure 14** Continuity of plumes in seismic tomography models; modified from Boschi L, Becker TW, and Steinberger B (2007) Mantle plumes: Dynamic models and seismic images. *Geochemistry, Geophysics, Geosystems* 8. Each point in a seismic tomography model was examined along the predicted trajectory of a plume that rises from the CMB, is deflected by mantle flow, and surfaces at a given hot spot (listed above). If the point was seismically slow by $\geq|1.5\%|$, it was assigned a value 1.0; otherwise, it was assigned a 0.0. The points were then averaged along the plume trajectory to yield 'normalized vertical extents.' A value of 1.0 indicates that the plume-like anomaly in the tomography model extends across the whole mantle. A value near 0.0 indicates the plume-like anomaly is restricted to shallow depths. Symbols denote values from three S-wave models (tx2007 (Simmons et al., 2006), smean (Becker and Boschi, 2002), and pri-s05 (Montelli et al., 2006) and two P-wave models (pri-p05 (Montelli et al., 2006) and vox3p (Boschi et al., 2007)). Dashed profile shows the average of all the points. Beyond this analysis, red letters indicate studies ('C1,' Courtilot et al. (2003); 'M,' Montelli et al. (2006); and 'Z,' Zhao (2007)), which identify a deep lower mantle origin for a given hot spot. 'C2' (green) and '(C2)' (blue) indicate hot spots overlying a mantle transition zone that is anomalously thin or normal, respectively (Courtier et al., 2007).

p0370 In addition, studies of surface and S-waves reveal seismic anisotropy in the Icelandic upper mantle. Shear-wave splitting of the SKS phase measures the integrated effects of seismic anisotropy along nearly vertical ray paths across the mantle and is detected at a number of locations on Iceland with the fastest S-waves generally being polarized NW–SE (Bjarnason et al., 2002; Li and Detrick, 2003; Xue and Allen, 2005). Azimuthal anisotropy of Rayleigh waves has also been measured. Along the zones of active rifting and volcanism on Iceland, this anisotropy is strong at shallow depths <50 km with fast directions NNE–SSW and weak when somewhat deeper (Li and Detrick, 2006). West of the rift zones, fast

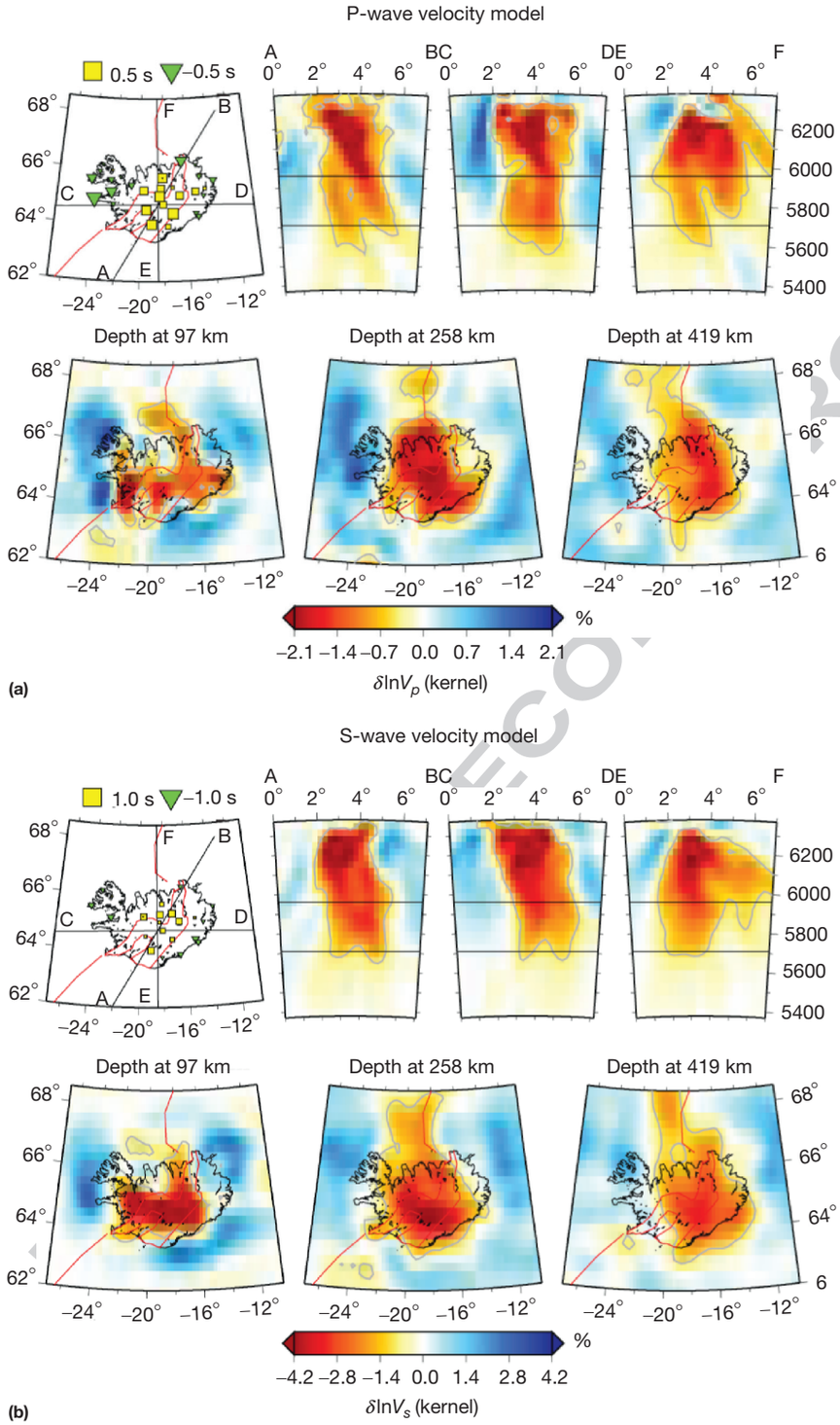

f0080 **Figure 15** Tomographic inversions of the mantle below the Iceland hot spot (Hung et al., 2004) for (a) P-waves and (b) S-waves. Top row shows vertical cross sections along three transects (see insets). Bottom row shows horizontal sections at depths as labeled.

directions are instead oriented NW–SE at shallow depths and more variably at depth. Taken together, the S-wave splitting and surface-wave results are not straightforward to interpret and lead to different conclusions about the cause of seismic anisotropy beneath Iceland. Li and Detrick (2006) interpreted the NNE–SSW Rayleigh wave anisotropy as being caused by a preferential alignment of melt channels or by lattice-preferred orientation (LPO) of olivine induced by mantle flow that roughly parallels the NNE–SSW-trending Northern Volcanic Rift Zone and South Iceland Seismic Zone. In contrast, Xue and Allen (2005) interpreted the S-wave splitting to indicate LPO due to flow from the center of the hot spot in eastern Iceland to the Kolbeinsey Ridge north of Iceland.

p0375 The vertical extent of the Iceland mantle plume has been examined in a variety of studies. Receiver function studies show that the Iceland plume extends well below 410 km as shown by the thinning of the transition zone beneath Iceland (Du et al., 2006; Shen et al., 1998, 2002). While Shen et al. (1998, 2002) showed evidence for both a deepening of the 410 and a shoaling of the 660 km discontinuity SE of Iceland, Du et al. (2006) argued that the 660 km is instead flat. The precise nature of both discontinuities is important in determining whether the Iceland seismic anomaly initiates in the lower mantle. A recent regional full-waveform tomography model (Rickers et al., 2013) is in agreement with Shen et al. (1998; 2002) and suggests that the anomaly is tilted to the SE and extends into the lower mantle. At least three global tomography models are consistent with such a deep-rooted anomaly (Bijwaard and Spakman, 1999; Boschi et al., 2007; Zhao, 2007; see also **Figure 14**). A separate study identifies an ultralow-velocity zone near the CMB below Iceland (Helmberger et al., 1998). An updated global tomography model S40RTS (Ritsema et al., 2011) shows that the lower mantle is seismically slow in a broad zone beneath Iceland but with weak and variable amplitude, suggesting difficulty in resolving the continuity of the Iceland plume from the CMB (**Figure 13(f)**). A more robust determination of the depth of origin of the Iceland plume probably requires a regional seismic experiment spanning a wider geographic area than just the island of Iceland.

p0380 *The Azores*: Evidence for anomalously hot mantle beneath the Azores hot spot comes from a locally broad area of anomalously slow surface-wave speeds identified in the upper 200 km of the mantle, which appears as a perturbation of the generally low-velocity structure extending along the Mid-Atlantic Ridge (Pilidou et al., 2004). Finite-frequency body-wave tomography reveals an irregularly shaped anomaly of low P-wave speeds beneath the Azores archipelago in the shallowest 200 km, which slants northeast and downward to ~400 km depth (Yang et al., 2006).

p0385 *Cape Verde*: Two groups find conflicting results for the mantle structure beneath the Cape Verde hot spot, while both use receiver function methods. The first group finds that the uppermost mantle beneath Cape Verde has anomalously high seismic velocity and low density (Lodge and Helffrich, 2006) and that the transition zone has a normal thickness (Helffrich et al., 2010). The former result was interpreted as revealing a layer of depleted residue from hot spot melting and the latter as indicating that the mantle upwelling sustaining the hot spot originates in the upper mantle. In contrast, Vinnik et al. (2012) found low seismic velocities and normal densities in the shallow upper mantle, as well as a ~30 km thinning of the transition zone, due to a deepening of the 410 km discontinuity and a shoaling of the 660 km discontinuity. These results are consistent with the seismic structure being controlled by temperature in the presence of a hot mantle plume rising from the lower mantle. Vinnik et al.'s (2012) study was based on a larger dataset than used in the two studies of the first group (see preceding text). Vinnik et al. (2012) also argued that frequency-dependent effects may contribute to the discrepancies between the two groups.

Bowie: The presence of a narrow, low-velocity zone near the base of the transition zone below the Bowie hot spot is based on delays in seismic records of Alaskan earthquakes measured in the NW United States (Nataf and VanDecar, 1993). The delays are consistent with a zone of 150 km diameter and an excess temperature of 200 K. p0390

Hawaii: Early tomography studies of the Hawaiian hot spot revealed the presence of anomalously slow seismic velocities in the upper mantle beneath the Hawaiian hot spot swell (Laske et al., 2007) and beneath the Hawaiian Islands (Priestley and Tilmann, 1999; Tilmann et al., 2001; Wolfe et al., 2002). Additional evidence for an upper mantle melt anomaly was provided by a seafloor magnetotelluric study (Constable and Heinson, 2004), which suggests a columnar zone of 5–10% partial melting with a radius <100 km and a depth extent of 150 km. Ritsema et al.'s (2011) global tomography model shows a broad volume of low velocities in the upper mantle beneath Hawaii that appears to connect to a low-velocity body extending through and to the base of the lower mantle (**Figure 13(g)**). p0395

More recently, the Hawaiian Plume-Lithosphere Undersea Melt Experiment (PLUME) (Wolfe et al., 2009) involved one of the largest deployments of ocean bottom and land seismometers to image the seismic structure of the upper mantle and shallow lower mantle beneath the Hawaiian hot spot. Rayleigh wave tomography from the PLUME project reveals low velocities within the lithosphere at depths of 10–60 km beneath the island chain and the surrounding hot spot swell (Laske et al., 2011). Separate tomographic inversions of Rayleigh waves (Laske et al., 2011), S-waves (Wolfe et al., 2009), and P-waves (Wolfe et al., 2011) all image a volume of relatively low seismic velocities in the upper mantle underlying the Hawaiian swell (**Figure 16**). The volume is asymmetrical and irregular in shape. Lower seismic velocities SW of the island of Hawaii than NE correlate with an asymmetrical bathymetric swell, which is shallower to the SW than the NE (Crosby and McKenzie, 2009; Wessel, 1993), and with variations in the depth of seismic converters constrained by receiver functions (Rychert et al., 2013). These observations indicate that the Hawaiian swell is supported by hot and buoyant mantle interpreted to be plume material ponding beneath the lithosphere (Olson, 1990; Sleep, 1990) like a 'pancake' (**Section 133.3.4**). This pancake-shaped feature is asymmetrical about the axis of the volcano chain and appears to be hotter in – or to extend further to – the SW than the NE. In addition, all three tomography studies show that the low-velocity body is surrounded by seismically fast material, which is interpreted to be relatively cool, sublithospheric material that is sinking like a curtain around the plume pancake. The asymmetry as well as short-wavelength variability of the Hawaiian plume pancake is not p0400

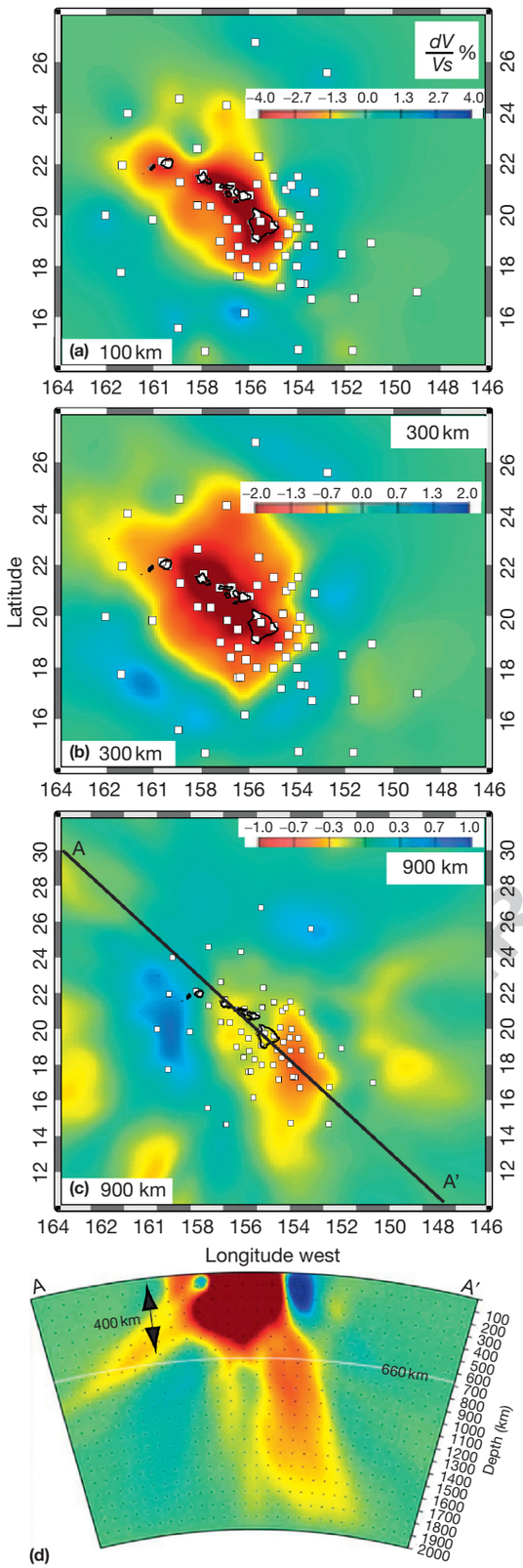

f0085 **Figure 16** The Hawaiian PLUME S-wave tomography model (Wolfe et al., 2009). Horizontal cross sections at depths of (a) 100 km, (b) 300 km, and (c) 900 km of velocity variations displayed as colors with percentages labeled on the color bars. Seismometer locations are denoted with white boxes. (d) Vertical cross section along the diagonal line in and with color scale as in (c).

predicted by models of steady-state plume–plate interaction (Ribe and Christensen, 1994, 1999).

p0405 Another surprising finding of the body-wave studies (Wolfe et al., 2009, 2011) is that the low velocities underlying the Hawaiian swell are present from the base of the lithosphere all the way down to the transition zone (**Figure 16**). If these low velocities indeed identify ponding plume material, the inferred plume pancake is several times thicker than predicted by the classical models of thermally buoyant mantle plumes (e.g., Ribe and Christensen, 1999; van Hunen and Zhong, 2003). A possible explanation is that the Hawaiian plume contains compositionally dense mafic materials that reduce the net buoyancy of plume material to the degree that the rise of the plume temporarily stalls at the depths of 300–410 km, forming a 'deep eclogite pool' (Ballmer et al., 2013b; see **Section 133.3.3.3**). This explanation is supported by joint surface-wave and body-wave tomography (Cheng et al., in press) as well as independent constraints from receiver functions (Huckfeldt et al., 2013).

p0410 Below the upper mantle, the tomography studies image a vertically elongated body of low velocities near the southeast end of island chain that extends into the lower mantle (**Figure 16**; Wolfe et al., 2009; 2011). This feature is interpreted to be the stem of the Hawaiian mantle plume with an estimated thermal anomaly of 250–300 °C, confirming prior discoveries of transition zone thinning by 40–50 km beneath Hawaii (Li et al., 2000, 2004; Collins et al., 2002). A still deeper origin is suggested by a tomographic study that incorporates core phases (Lei and Zhao, 2006). Compelling evidence for an origin at CMB is the imaging of an ultralow-velocity zone (ULVZ) at the base of the mantle having one of the largest known velocity reductions (~20%) yet documented (Cottaar and Romanowicz, 2012).

p0415 *The Galápagos*: The Galápagos hot spot is part of a broad region in the Nazca–Cocos basin with significantly reduced long-period Love and Rayleigh wave speeds (Heintz et al., 2005; Vdovin et al., 1999). The mantle transition zone in the region has a similar thickness as that of the rest of the Pacific Basin except for a narrow region of ~100 km in radius slightly to the west of the Galápagos archipelago, where it is thinned by ~18 km (Hooft et al., 2003). This amount of thinning suggests an excess temperature of ~130 K. A regional body-wave tomography study detected a low-velocity feature of comparable dimension, extending from above the transition zone into the shallow upper mantle (Toomey et al., 2001). Rayleigh wave tomography (Villagomez et al., 2007) shows laterally averaged S-wave velocities at depths 75–150 km that are 0.05–0.2 km s^{-1} lower than that beneath normal Pacific mantle with comparable seafloor ages. This velocity anomaly is consistent with excess temperatures of 30–150 °C, plus ~0.5% melt. The low-velocity material appears to trend diagonally from its greatest depth beneath the Galápagos archipelago upward and to the NE, interpreted to reflect the flow of plume material from the plume stem toward the Galápagos Spreading Center. Ritsema et al.'s (2011) global tomography

model suggests that the upper mantle anomaly connects to a broader plume-like feature extending all the way down to the CMB (**Figure 13(h)**).

p0420 To examine seismic anisotropy in the mantle, shear-wave splitting was also studied (Fontaine et al., 2005). At the western edge of the archipelago, splitting of up to 1 s with fast polarizations directed E–W is consistent with LPO and mantle deformation being dominated by the eastward motion of the Cocos Plate. Directly beneath the archipelago and within the upper mantle seismic anomaly, however, there is no clear splitting, which suggests that melt or complex flow beneath the hot spot superimposes plate motion-derived anisotropy.

p0425 *Yellowstone*: Our understanding of the mantle seismic structure in the area of the Yellowstone hot spot track has evolved dramatically as the data coverage has increased. Early tomographic studies revealed a complex velocity structure in the upper mantle beneath the SRP (which marks the hot spot track), interpreted to represent compositional heterogeneity associated with melting, without a deep-seated mantle plume (Saltzer and Humphreys, 1997). A subsequent study using data from local seismic networks identified low velocities in the upper mantle beneath the SRP, suggesting the presence of a plume-like feature extending as deep as 400 km to the west of Yellowstone (Waite et al., 2006; Yuan and Dueker, 2005).

p0430 The strongest constraints on mantle seismic structure near Yellowstone have been derived from data collected with Earthscope's USArray (http://www.earthscope.org) with dense seismic coverage over the whole area of the western United States. Such a dense coverage provides the opportunity to image the structure beneath Yellowstone at much higher resolution and to greater depths than beneath any other hot spot on Earth. The aperture of the seismic array provides good resolution down to depths of ~1000 km or more. Several groups produced P- and S-wave tomography models of the mantle beneath the western United States (Darold and Humphreys, 2013; Fouch, 2012; James et al., 2011; Obrebski et al., 2010; Schmandt et al., 2012; Sigloch, 2011; Tian and Zhao, 2012). The images differ in detail but common elements related to the Yellowstone hot spot include low velocities in the shallowest 300 km of the upper mantle below the SRP and a relatively narrow (<200 km wide) low-velocity feature beneath Yellowstone that extends continuously through the upper mantle and connects to a broader (~300–500 km across) low-velocity zone in the shallow lower mantle (**Figure 17**). These studies suggest that the deep low-velocity anomaly is irregular in shape, with variable amplitude, and surrounded by seismically fast material without a clear extension to depths greater than 900 km depth.

p0435 Earlier receiver function studies of the mantle transition zone found a depression of the 410 km discontinuity near Yellowstone but did not image an upward deflection of the 660 km discontinuity, as expected for the effect of high temperatures on phase changes in the olivine system (Fee and Dueker, 2004; Yuan and Dueker, 2005). The most recent receiver function study using data from the USArray, however, shows that the 660 km discontinuity shoals by 12–18 km over an area ~200 km wide and centered on the low-velocity feature (Schmandt et al., 2012). In contrast, the 410 km discontinuity appears to be only marginally perturbed (<5 km) (**Figure 17(b)**).

p0440 Interpretation of the seismic structures beneath Yellowstone remains controversial. On the one hand, there is agreement concerning the shallower structure. The seismically slow material just beneath the SRP is interpreted to be a zone of partial melting and to be bound to the NW and from below by the seismically fast remnants of the subducted Farallon Plate and to the SE by foundering lithospheric material. On the other hand, there is disagreement concerning the deeper structure, with one group (James et al., 2011) dismissing a plume origin for the seismic and volcanic anomaly altogether (see **Section 133.3.7.2**).

p0445 Despite these controversies, the good resolution of the seismic structure well into the lower mantle beneath both Yellowstone and Hawaii motivates a brief comparison between the two. Common features involve a horizontal low-velocity anomaly beneath the hot spot tracks that extends in the direction of plate motion, as well as a narrow vertical anomaly near the leading edge of the hot spots that protrudes into the lower mantle. The simplest explanation for these two common features is a plume rising from the lower mantle and ponding beneath the lithosphere. A notable difference is that the deep anomaly beneath Yellowstone is not clearly continuous with depth compared to the inferred continuity for that beneath Hawaii. Another difference concerns the depth extent of the horizontal upper mantle anomaly, which is completely contained in the shallowest 200–300 km beneath Yellowstone's hot spot track (SRP), whereas it extends through most of the upper mantle (Wolfe et al., 2009) or even splits up into two separate layers (Cheng et al., in press) beneath the Hawaiian Islands.

p0450 *Eifel*: The Eifel region in western Germany is characterized by numerous but small volcanic eruptions with contemporaneous uplift of 250 m in the last 1 My. Tomographic imaging indicates a mantle low-velocity anomaly extending to depths of at least 200 km (Passier and Snieder, 1996; Pilidou et al., 2005). Inversions using a high-resolution local array study indicate a fairly narrow (100 km) P-wave anomaly of 2% that possibly extends to 400 km (Keyser et al., 2002; Ritter et al., 2001). The connection with the deep mantle is unclear but has been suggested to include the low-velocity structure that is imaged in the lower mantle below central Europe (Goes et al., 1999). Shear-wave splitting measurements show the largest split times for S-waves polarized in the direction of absolute plate motion, but the pattern is overprinted by complex orientations, suggestive of parabolic mantle flow around a plume stem with the overlying plate moving to the SW (Walker et al., 2005).

p0455 *Cameroon Volcanic Line*: Body-wave tomographic studies using global data and those obtained from the recent Cameroon Broadband Seismic Experiment show that the Cameroon volcanic line (CVL) is underlain by a fingerlike low-velocity anomaly that extends from the Gulf of Guinea in the SW to the Chad–Cameroon border in the NE (e.g., Reusch et al., 2010; Ritsema et al., 2011). The anomaly ranges from ~100 to ~400 km depth with the depth of peak amplitudes shoaling toward the SW, and is juxtaposed by a high-velocity anomaly associated with the Congo Craton (and subcratonic mantle) toward the SE (Reusch et al., 2010). The peak-to-peak difference between the two anomalies is ~5%, corresponding to a temperature contrast of >280 °C (Reusch et al., 2010).

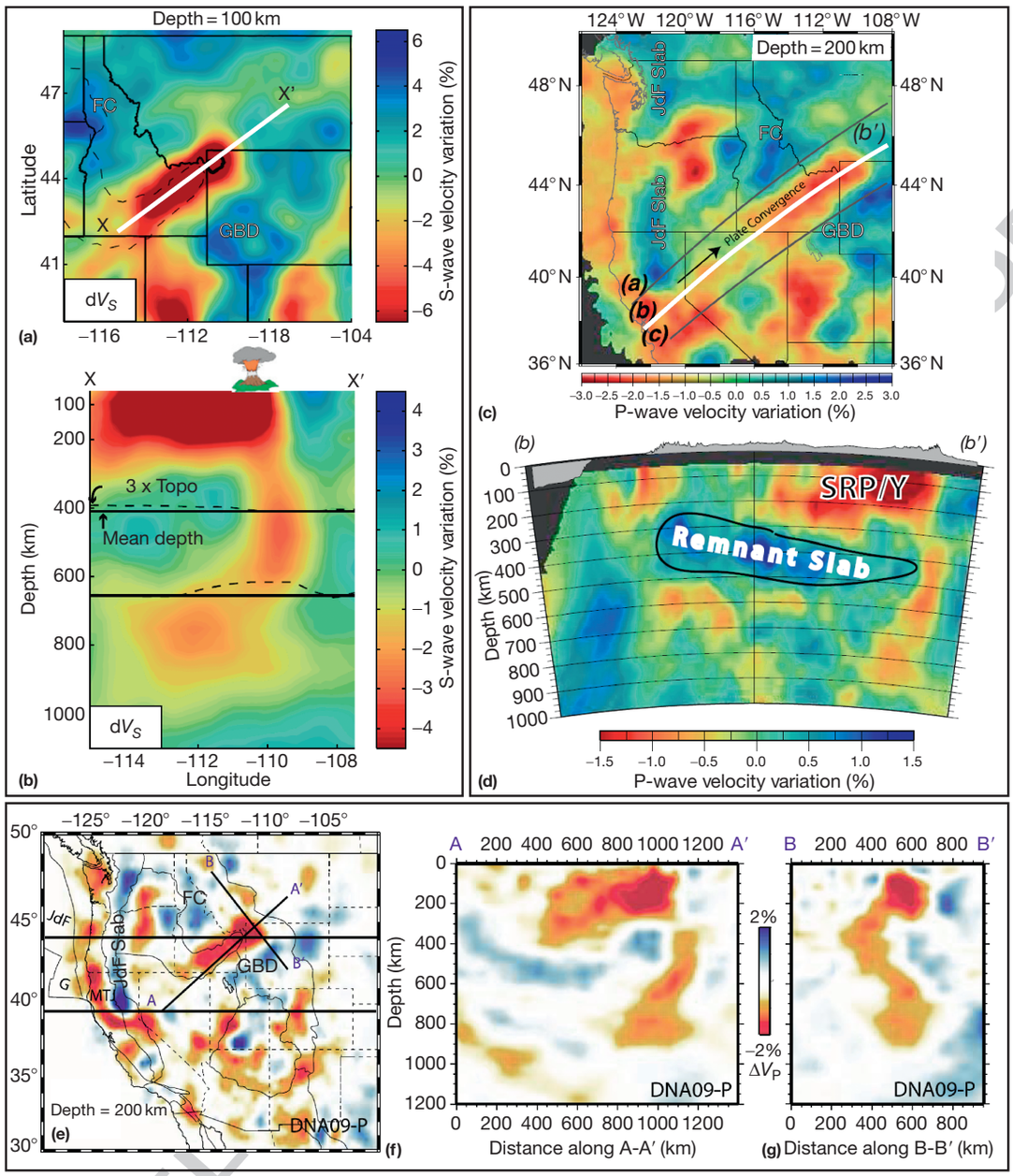

f0090 **Figure 17** Tomography results for (a) and (b) S-waves by Schmandt et al. (2012), (c) and (d) P-waves by James et al. (2011), and (e)–(g) P-waves by Obrebski et al. (2010). For each tomography model, a horizontal cross section at a given depth (labeled) is shown, along with a SW–NE, vertical cross section along the Snake River Plain (SRP) and through the Yellowstone (Y) hot spot (locations labeled on maps). For one model, a NW–SE vertical cross section is also shown (g). GBD = Great Basin (lithospheric) drip (West et al., 2009); FC = Farallon 'curtain' (Darold and Humphreys, 2013); JdF, Juan de Fuca; G, Gorda Plate; 'MTJ', Mendocino triple junction. (b) Depth variations (dashed curves) of seismic discontinuities indicate a shoaling at 660 km and no change at 410 km beneath Yellowstone compared to the mean depths of the discontinuities (solid).

This contrast may suggest anomalously hot mantle beneath the CVL, anomalously cool mantle beneath the Congo Craton (e.g., due to downwelling; King and Ritsema, 2000), or both. A rather moderate thermal anomaly beneath the CVL itself is consistent with receiver function constraints on the ratio of P- to S-wave speed (VP/VS), which indicate the presence of only very small fractions of melt in the asthenosphere (Gallacher and Bastow, 2012).

Shear-wave splitting measurements display fast directions p0460 dominantly parallel or subparallel to the CVL (Koch et al., 2012). These directions are consistent with a strong component of local northeastward asthenospheric flow, as is

predicted by numerical simulations to result from large-scale mantle convection patterns (Conrad and Behn, 2010; Forte et al., 2010). A weaker component of flow perpendicular to the CVL, perhaps related to small-scale convection along the edge of the Congo Craton (cf. King and Ritsema, 2000), may contribute to subparallel (i.e., dominantly N–S) splitting directions measured by Koch et al. (2012) at a subset of stations. Such edge-driven convection (see **Section 133.3.3.5**) may also provide a good explanation for volcanism itself (King and Ritsema, 2000). An alternative plume origin for volcanism is ruled out by nonanomalous transition zone thicknesses (Reusch et al., 2011) and the lack of hot spot-like age–distance relations (**Figure 6**, inset).

p0465 *East Africa*: The hot spots in East Africa overlie the northeastern flank of the African LLSVP (**Figure 13(e)**). The African LLSVP is rooted at the CMB beneath southern Africa (Helmberger et al., 2000). It is a large low-velocity body (~4000 km by ~2000 km) that tilts up and to the northeast beneath East Africa (Forte et al., 2010; Ritsema et al., 1999) (**Figure 13(i)**). The relationship of the African LLSVP to volcanism and rifting in East Africa remains controversial. One suggestion is that volcanism is not attributed to the LLSVP at all, but instead to small-scale, sublithospheric convection along the edges of the African Craton (King and Ritsema, 2000). Another idea attributes the numerous volcanic centers to one or more mantle plumes of ~100 km in width rising from the top of the LLSVP to the base of the lithosphere (e.g., Chang and Van der Lee, 2011; Ebinger and Sleep, 1998; Montelli et al., 2006). A third concept attributes volcanism directly to the rise into the shallow upper mantle and decompression melting of a 'superplume' (cf. Davaille, 1999) as a whole, which would be imaged as an extension of the LLSVP itself (Bastow et al., 2005; Benoit et al., 2006; Park and Nyblade, 2006).

p0470 With the arrival of data from permanent and temporary seismic arrays of the AfricaArray (http://www.africaarray.psu.edu/), a general consensus is forming among the most recent studies (Hansen and Nyblade, 2013; Hansen et al., 2012). S-wave tomography (Nyblade, 2011) and surface-wave (Adams et al., 2012) tomography reveal that the shallow upper mantle in East Africa from just south of the Tanzania Craton to NE of the Ethiopian Rift is seismically slow (**Figure 18**). Associated with this low-velocity anomaly, the 410 km seismic discontinuity is 30–40 km deeper than normal suggesting excess temperatures of >250 °C (Cornwell et al., 2011; Huerta et al., 2009). The seismically slow material in the upper mantle is therefore too thick, geographically broad, and pervasive to be explained by the shallow process of edge-driven convection or by separate, smaller-scale mantle plumes. The observed seismic structure appears to be most consistent with the penetration of a large and broad (super)plume into the upper mantle where it causes decompression melting. Fast polarization directions of shear-wave splitting that are dominantly oriented NE–SW have been interpreted to reflect

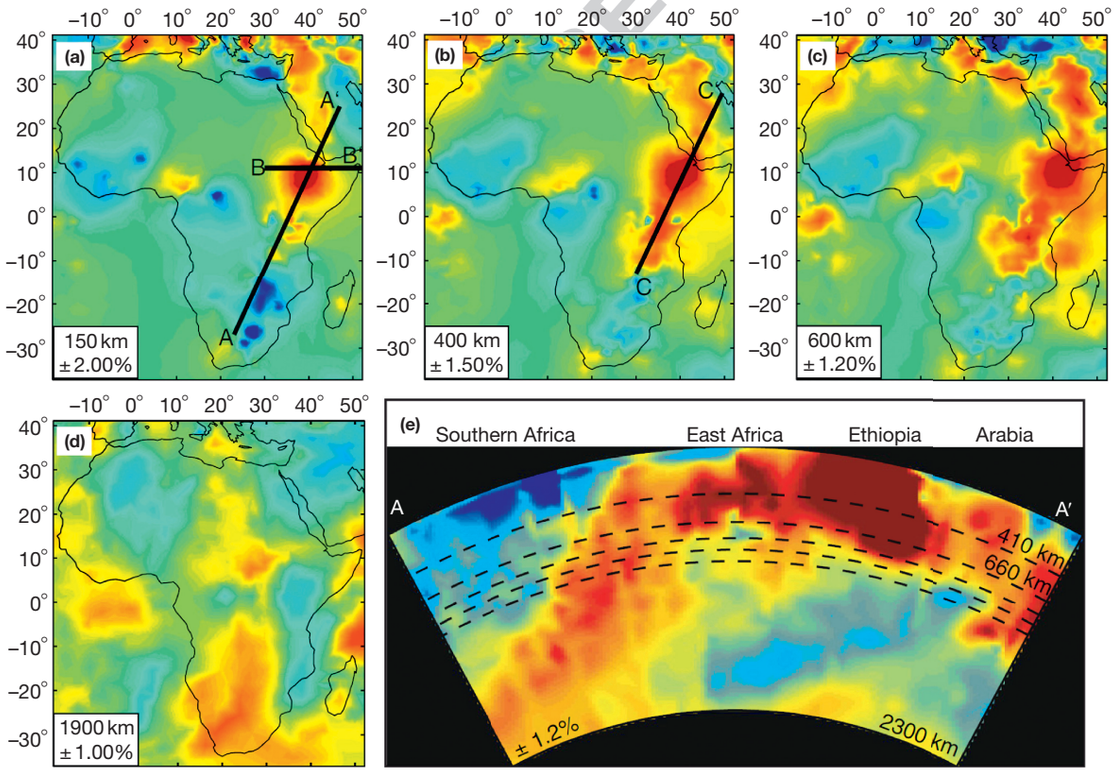

f0095 **Figure 18** Tomography images of the mantle beneath Africa from P-wave inversions of Hansen et al. (2012). (a)–(d) Horizontal cross sections of P-wave velocity perturbations at the labeled depths. (e) Vertical cross section along the profile A–A′ as marked in (a). The ± values indicate the bounds of the color scales in each corresponding panel; blue is fast, while red is slow. Dashed lines in (e) mark depths of 410, 660, 800, 900, and 1000 km.

LPO due to dominantly northeastward flow of the superplume in the upper mantle (Bagley and Nyblade, 2013), an interpretation that is supported by geodynamic models (Forte et al., 2010).

p0475 Potential challenges for a superplume origin arise from a recent S-wave tomography study that images vertically elongate low-velocity bodies beneath Afar and Kenya that protrude downward below the low-velocity upper mantle to at least midmantle (~1400 km) depths (Chang and Van der Lee, 2011). Also, the 660 km seismic discontinuity beneath East Africa is regionally abnormally deep (Cornwell et al., 2011; Huerta et al., 2009). In the context of the superplume hypothesis, this observation would require the presence of eclogitic materials to activate the majorite–perovskite phase change at ~720 km depth (Cornwell et al., 2011; Huerta et al., 2009). A SW–NE shoaling of the discontinuity from northern Ethiopia to Afar would then reflect a decrease in the garnet concentration (Cornwell et al., 2011).

p0480 *South Pacific Superswell*: Approximately antipodal to East Africa is a cluster of hot spots in the area of the South Pacific Superswell (McNutt and Fischer, 1987), which overlies the Earth's other LLSVP in the lower mantle (e.g., Breger et al., 2001; Ni et al., 2005; Trampert et al., 2004; van der Hilst and Karason, 1999). Ritsema et al.'s (2011) S40RTS model shows that the whole area of the South Pacific Superswell is underlain by low seismic velocities in both the lower and the upper mantles (**Figure 13(j)**).

p0485 A recent deployment of temporary seismometers on the seafloor and a number of islands enabled a regional tomographic study of the middle and upper mantle beneath the South Pacific Superswell. The P-wave and S-wave tomography results reveal that the area is underlain by multiple low-velocity regions in the depth range from 400 to 1600 km (Tanaka et al., 2009). Two low-velocity regions at 1200 km depth are centered beneath the Society and Pitcairn hot spots, while two at 800 km depth are located beneath the Tuamotu and Austral Islands. There are also relatively short-wavelength (hundreds of km across) variations at 400 km depth. A prior study of underside reflections of S-waves at the 410 and 660 km discontinuities found the mantle transition zone to have normal thicknesses, except in a ~500 km wide area beneath the Society hot spot (Niu et al., 2002a).

p0490 The incorporation of Rayleigh wave tomography highlights the presence of short-wavelength variability in the upper mantle, showing that the Society, Pitcairn, Macdonald, Marquesas, and Arago hot spots are underlain by low velocities in the depth range of 60–180 km (Suetsugu et al., 2009). Only the low-velocity bodies beneath Society and Macdonald appear to connect to the low-velocity anomalies in the lower mantle. The shallow anomalies beneath the other hot spots appear to be restricted to the upper mantle. Suetsugu et al. (2009) interpreted this structure as reflecting the presence of a number of small-scale (hundreds of km across), plume-like upwellings emanating from the south Pacific LLSVP, some of which having risen above and become separated from the LLSVP. This conclusion is in contrast to the conclusions for the African LLSVP rising as a whole superplume into the shallow upper mantle. These contrasting results lead to questions about the dynamics of LLSVPs. For example, are the contrasting dynamics related to internal forces (differences in composition and temperature) or instead driven by external ones (ambient mantle flow shaping the LLSVPs; McNamara and Zhong, 2005; Steinberger and Torsvik, 2012)?

133.2.6 Summary of Observations

s0115

p0495 Intraplate volcanic activity can be mainly grouped in three categories: long-lived age-progressive volcanism, short-lived age-progressive volcanism, and volcanism with complex age patterns (Courtillot et al., 2003). Long-lived (>50 My) age-progressive volcanism is documented for at least 13 hot spots. At present day, these hot spots define a global kinematic reference frame that is deforming slower than average, present-day plate velocities. Over geologic time, however, the motion between the Indo-Atlantic hot spots, the Pacific hot spots, and Iceland has been significant. Short-lived (≤24 My) age-progressive volcanism is documented along at least ten volcano chains. The directions and rates of age progression in the short-lived chains suggest relative motion between these hot spots, even on the same plate. Finally, the available dates of rocks from a number of volcano groups (e.g., Line and Cook–Austral Islands and Cameroon volcanic line) do not show evidence for simple age–distance relations but instead suggest these groups to have formed by episodic volcanism over tens of millions of years with coeval volcanism over large distances.

p0500 Hot spots are commonly associated with topographic anomalies (i.e., swells). These swells are usually centered by the most active volcanoes, span distances of hundreds of km to >1000 km, and rise hundreds of meters above the surrounding seafloor. Hot spot swells usually diminish with time or distance from the center of active volcanism and exclusively support volcanoes no older than ~50 My.

p0505 LIPs display a huge range in magmatic volumes and durations and have been related to climate change and mass extinction events. They represent the largest outpourings of magma from as large as 50 Mkm^3 (OJP) to <2 Mkm^3 (CRB) (see **Figure 10**). This voluminous magmatism can occur in a dramatic short bursts, lasting 1–2 My (CAMP, CRB, EM, OJP, and SIB), or can be prolonged over tens of My (e.g., CHON, CBN, KER, NAVP, and SHA). Main eruptive products are tholeiitic basalts that, on the continents, typically are transported through radiating dike swarms. High-MgO basalts or picrites are found in a number of provinces (NAVP, OJP, and CAR) indicating high degrees of mantle melting. Smaller rhyolitic eruptions in continental flood basalts (KAR, PAR, CHON, and EARS) instead suggest secondary melting of the continental crust. Dynamic topographic uplift (analogous to hot spot swells) is evident around the main eruptive stages of some LIPs (EME, NAVP, SIB, and KER) but may not have occurred at others (OJP and SHA). While an appreciable amount of the geologic record is lost to subduction, about six active hot spots are confidently linked to LIPs. Most of these hot spots are currently located at or very close to an oceanic spreading center with the Kerguelen hot spot being a notable exception. Flood basalt volcanism itself is also typically associated with rifting, either between continents (PAR, KAR, CAMP, NAVP, DEC, and MAD) or at MORs (OJP–MAN–HIK, KER, and SHA–HES). These links between LIPs and plate tectonics compel substantial revisions or alternatives to the hypothesis of an isolated head of a starting mantle plume as the sole origin of LIPs.

p0510 Basalts from hot spots and other sites of intraplate volcanism, commonly referred to as OIB, are geochemically distinct from MORB. Both isotope ratios and major elements display a much greater variability among OIB than among MORB. Generally, OIBs are more mafic (i.e., lower SiO_2 content) and alkalic (higher $Na_2O + K_2O$) than MORB. For the most part, they also differ in at least one of three commonly analyzed isotope ratios: $^{87}Sr/^{86}Sr$, $^{206}Pb/^{204}Pb$, and $^{3}He/^{4}He$. Exceptions are the Bowie–Kodiak, Cobb, and Caroline chains, which show MORB-like $^{87}Sr/^{86}Sr$ and $^{206}Pb/^{204}Pb$ compositions (but lack $^{3}He/^{4}He$ data). In terms of major elements, the most productive hot spots (Hawaii, Iceland, and the Galápagos) overlap most heavily with MORB.

p0515 Hot spots are typically associated with anomalously low seismic-wave speeds below the lithosphere and in the upper mantle. Transition zone thicknesses are often anomalously thin by tens of km. The previously mentioned findings are consistent with elevated mantle temperature (by 150–200 K) and with the abundance of partial melt in the shallow upper mantle. Improved understanding of mineral physics at appropriately high pressure and temperature is needed to better constrain the magnitude of the putative temperature anomalies and to quantify the potential contribution of compositional heterogeneity. Especially with recent regional studies and the availability of EarthScope data, we have seen increasing evidence for a lower mantle origin for a selected number of hot spots.

p0520 The key characteristics described earlier provide important constraints to test dynamic mechanisms proposed for the origin of melting anomalies. It seems unlikely that a single overarching mechanism can account for the diversity seen in the geologic record. In the next section, we discuss the implications and predictions of each of these mechanisms.

s0120 133.3 Dynamic Mechanisms and Their Implications

p0525 This section reviews the mechanisms proposed to generate intraplate volcanism. We begin with a summary of methods that are used to quantitatively explore dynamic mechanisms (**Section 133.3.1**). We then discuss the geodynamic processes for generating mantle upwelling (**Section 133.3.3**) and related magmatism (**Section 133.3.2**). Candidate mechanisms to compensate hot spot swells and to sustain flood basalt volcanism are explored in **Sections 133.3.4** and **133.3.5**, respectively. In the context of the discussed geodynamic processes, we continue revisiting the geochemical and petrologic signatures of hot spot lavas and their distinctions from MORB (**Section 133.3.6**). Finally, we discuss these processes in the broader context of mantle convection and plate tectonics (**Section 133.3.7**).

s0125 133.3.1 Methods

p0530 The origin and evolution of hot spots and melting anomalies can be constrained by systematically comparing predictions of geodynamic models with observations. Such models simulate the transport of energy, mass, and momentum in the solid mantle that may have local patches of partial melt. They indeed provide a means to directly test conceptual ideas against the basic laws of physics and to delineate the conditions under which a proposed geodynamic mechanism can operate.

p0535 Key aspects of material and energy transport in the mantle can be described mathematically and solved by analytic or numerical approaches or can be studied in laboratory experiments using analogue materials. Analytic approaches provide scaling laws that reveal relationships between phenomena and key parameters for simple or simplified problems (see also **Chapter 129**). Numerical simulations can address much more complex problems. Their accuracy, however, may be limited by the discretization of the differential equations and the parameterizations made (see also **Chapter 130**). Laboratory experiments (see also **Chapter 128**) involving analogue materials such as sucrose syrup and silicon putty instead provide natural experiments that do not suffer from numerical discretization but require significant extrapolation over length scales and timescales. For simplified cases, such as the ascent of plumes through a nearly isoviscous or Newtonian fluid, benchmarks have revealed good agreement of numerical and analogue simulations (e.g., van Keken's (1997) numerical benchmark of the classic Griffiths and Campbell (1990) laboratory experiments; see also Vatteville et al. (2009), van Keken et al. (2013)). It is nevertheless essential to resort to computational modeling to simulate some of the complexities that arise with the features of the Earth's mantle such as compressibility, phase transitions, melting, and realistic rheology dependent on grain size, pressure, and stress (see also **Chapter 127**).

s0130 133.3.2 Generating Magmas for Volcanism

p0540 Understanding the causes for melt generation is essential for studying the origin of hot spots and intraplate volcanism. Partial melting of rocks can conceptually occur due to (1) a change in temperature, (2) a closed-system decompression, and (3) an open-system change in composition. While the scenarios (1) and (3) are relevant for melting the crust (e.g., near intrusions) and the mantle wedge (i.e., at subduction zones), respectively, isentropic decompression melting (2) is the dominant process of melt generation at MORs, hot spots, and other melting anomalies.

p0545 For decompression melting, the total volumetric rate of melt generation is approximately proportional to the rate of decompression (or mantle upwelling) and the melt productivity at constant entropy $(-\partial F/\partial P)_S$ integrated over the volume V of the melting zone:

$$Q_M = \frac{\rho_c}{\rho_c}\int_V \left(-\frac{\partial F}{\partial P}\right)_S \left(-\frac{\mathrm{D}P}{\mathrm{D}T}\right)\mathrm{d}V \qquad [1]$$

where ρ_m is mantle density and ρ_c is igneous crustal density. $(-\partial F/\partial P)_S$ is generally positive above the solidus and zero otherwise. The solidus temperature and $(-\partial F/\partial P)_S$ depend on the equilibrium composition of the solid and liquid at a given pressure (e.g., Hirschmann et al., 1999; McKenzie, 1984; Phipps Morgan, 2001). Mantle magmatism thus requires some combination of excess temperature, presence of fertile or fusible material, and mantle upwelling. Higher temperatures boost melting by increasing the pressure range over which the solidus is exceeded, composition controls melting by changing both this pressure range and $(-\partial F/\partial P)_S$, and both factors may influence the rate of decompression $(-\mathrm{D}P/\mathrm{D}T)$ through their effects on mantle buoyancy and upwelling rate.

s0135 #### 133.3.2.1 Temperature

p0550 Excess melting sustained by elevated temperatures has been a major focus of previous studies. Mantle-source temperatures are commonly estimated from the Fe–Mg content of primary magmas and the olivine phenocrysts with which they equilibrate. One group suggests that the mantle is no hotter beneath Hawaii than beneath many MORs (Falloon et al., 2007; Green et al., 2001). Other groups, however, suggest elevated temperatures of, for example, 100–300 °C beneath Hawaii, 50–100 °C beneath Iceland or the Azores, and ~150 °C beneath Afar (Beier et al., 2012; Herzberg, 2004a; Herzberg and Gazel, 2009; Herzberg et al., 2007; Lee et al., 2009; Putirka, 2005; Putirka et al., 2007, 2011; Rooney et al., 2012). Most, if not all, lavas sampled at hot spots have evolved to varying degrees after leaving the mantle source, and it is therefore difficult to estimate the parental liquids' MgO content. For example, Putirka (2005) argued that the lower MgO contents derived by Green et al. (2001) for Hawaii could lead to an underestimate of temperature. Restricting the analyses to melt inclusions would mitigate this uncertainty, but such an approach is intricate.

p0555 Complementary methods rely on peridotite melting models that invert or forward model a whole suite of major-element and/or minor-element concentrations, sometimes including crustal thicknesses as an additional constraint. Beneath Iceland, estimates for excess mantle temperatures based on such methods range from ~100 to ~250 °C (e.g., Herzberg and O'Hara, 2002; Klein and Langmuir, 1987; Langmuir et al., 1992; Maclennan et al., 2001; McKenzie and Bickle, 1988; Presnall et al., 2002; Shen and Forsyth, 1995; White and McKenzie, 1995). Excess temperatures are further estimated at 200–300 °C beneath Hawaii, based on a combination of geodynamic and melting models (Ribe and Christensen, 1999; Watson and McKenzie, 1991), and at ~100 °C beneath Afar, based on incompatible trace-element forward modeling (Ferguson et al., 2013). Along these lines, most of the studies appear to converge to high thermal anomalies beneath Hawaii and moderate thermal anomalies at other hot spots, but discrepancies between methods remain large.

s0140 #### 133.3.2.2 Composition

p0560 An additional source of uncertainty for the previously mentioned temperature estimates is the composition of the mantle source. Volatile species such as H_2O and CO_2 can dramatically reduce solidus temperatures even in small proportions, as are present in the MORB source (Asimow and Langmuir, 2003; Dasgupta and Hirschmann, 2006; Dasgupta et al., 2007; Hirschmann, 2010). While such small concentrations of volatiles are not likely to increase the total extent of melting significantly, they can enhance the amount of melt produced for a given temperature by expanding the volume of the melting zone. As the mantle beneath hot spots is thought to be more volatile-rich than beneath MORs, temperature estimates based on dry peridotite may be too high. For example, excess temperatures beneath the hot spot-influenced Galápagos Spreading Center may be reduced from ~50 °C for anhydrous melting models to <40 °C when water is considered (Asimow and Langmuir, 2003; Cushman et al., 2004). Similarly, estimates for the mantle excess temperature beneath the Azores have been revised from ~75 to ~55 °C (Asimow and Langmuir, 2003). Hydrous melting models have yet to be explored in detail for the larger Iceland and Hawaii hot spots.

p0565 The mantle beneath hot spots may also contain more fusible, mafic lithologies, such as those generated by the recycling of subducted oceanic crust. The presence of more fusible or 'fertile' mantle has been suggested for hot spots such as Hawaii (Hauri, 1996; Herzberg, 2006; Sobolev et al., 2005; Takahashi, 2002), Iceland (Korenaga and Kelemen, 2000), the Columbia River basalts (Takahashi et al., 1998), the Galápagos (Sallares et al., 2005), the Canaries (Day et al., 2009; Gurenko et al., 2009; Herzberg, 2011), and others (Hofmann, 1997). Mafic lithologies tend to have a lower solidus and much greater isentropic melt productivity $(-\partial F/\partial P)_S$ than peridotite (Pertermann and Hirschmann, 2003; Spandler et al., 2008; Yasuda and Fujii, 1994) and therefore require significantly lower temperatures to produce the same volume of magma compared to peridotite.

p0570 Some have argued that such fertile mantle melting could generate large melting anomalies with very small or even no excess temperatures (Korenaga, 2005). An important difficulty with this hypothesis is that mafic materials will tend to form eclogite, which is significantly denser than lherzolite throughout the upper mantle (Aoki and Takahashi, 2004; Hirose et al., 1999; Irifune et al., 1986). To undergo decompression melting, this material would therefore have to be supported by rapid ambient mantle upwelling. Korenaga proposed that rapid upwelling driven by shallow small-scale convection (cf. **Section 133.3.3.5**) or fast seafloor spreading could entrain eclogite upward from the uppermost lower mantle (Korenaga, 2004, 2005), where eclogite becomes positively buoyant (Hirose et al., 1999) and hence perhaps accumulates. More recent experiments, however, suggest that the excess density of quartz-normative eclogites is actually near doubled in the depth range of 300–410 km (Aoki and Takahashi, 2004), which would make it difficult for plate-driven mantle flow to entrain significant amounts of eclogite into the asthenosphere. A more complete understanding of the properties and phase relations of different lithologies at a range of mantle pressures and temperatures is needed to test the ability of fertile materials to give rise to mantle melting without thermal anomalies.

133.3.2.3 Mantle upwelling

s0145

p0575 The final major factor that can lead to melting anomalies is enhanced mantle upwelling (which determines the decompression rate, $-DP/Dt$). Not only thermal buoyancy but also compositional buoyancy may fuel upwelling. However, compositionally lighter materials such as those with less iron and garnet than the ambient mantle, perhaps due to prior melting (Jordan, 1979; Oxburgh and Parmentier, 1977), are typically less fertile than dense, undepleted materials.

p0580 Behaving in complementary fashion to fertile mantle, depleted mantle must be light enough such that the associated increase in upwelling ($-DP/Dt$) overcomes the reduction in fusibility $(-\partial F/\partial P)_S$ (cf. eqn [1]).

133.3.3 Dynamics of Mantle Upwellings

s0150

p0585 Geodynamic modeling studies have explored a wide range of processes that can create and influence mantle upwellings. Upwellings may occur in columnar plumes or diapirs. The

style of ascent of such upwellings can be greatly affected by variable rheology, thermal expansivity, and conductivity. Compositional heterogeneity can further complicate ascent styles if entrained by plumes. Alternatively, upwelling may be passively driven, for example, by downwellings that remove the cool and negatively buoyant base of the lithosphere or by vertical motion of the whole lithosphere itself. Another form of vertical motion in the mantle, shear-driven upwelling, is independent of density variations as an energy source, but is rather induced by shearing of a rheologically variable mantle.

s0155 ### 133.3.3.1 Thermal boundary layer instabilities

p0590 Density variations near thermal boundary layers can become convectively unstable and lead to plume-like upwelling. In the simplest case of a thermally stratified mantle, the energy source comes from a density inversion with cool rocks overlying hot rocks. Upwelling thermal instabilities develop from small anomalies within such a hot thermal boundary layer as long as they grow faster by advection than they dissipate by thermal diffusion. In the Earth's mantle, the core–mantle boundary (CMB) is the main candidate for a plume-generating thermal boundary layer (e.g., Boehler, 2000), but other boundary layers may exist at locations where sharp transitions in material properties or composition occur, such as the bottom of the transition zone at 670 km depth or the top of a proposed thermochemical layer in the deep mantle.

p0595 In its simplest form, the growth of an upwelling from a hot boundary layer can be approximated as a Rayleigh–Bénard instability with the onset time and growth rate controlled by the local (or boundary) Rayleigh number:

$$Ra_\delta = \frac{\rho g \alpha \Delta T \delta^3}{\mu \kappa} \quad [2]$$

p0600 The instability is enhanced by larger thermal expansivities α, temperature jumps across the boundary layer ΔT, or layer thicknesses δ and hampered by higher viscosities μ and effective thermal diffusivities κ. Of all these parameters, mantle viscosity μ is the least well constrained and thus μ is the largest source of uncertainty in Ra_δ. For more specifics on the governing equations for boundary layer instabilities and examples of their modeling with laboratory and numerical techniques, see **Chapters 6** and **11** of Schubert et al. (2001). Analytic methods provide important insights into the rate of formation of the instability and the dependence on ambient conditions (see, e.g., Whitehead and Luther, 1975; Ribe and de Valpine, 1994). The growth of the instability to a full diapir or plume can be understood with nonlinear theory. For example, Bercovici and Kelly (1997) showed that growth may be retarded due to draining of the source layer by an intermittently stalling diapir. Experimental and numerical work confirms and expands on these predictions (e.g., Olson et al., 1988; Ribe et al., 2007). In general, most studies find that for reasonable lower mantle conditions, boundary layer instability will grow on a timescale of about 10–100 My (e.g., Christensen, 1984; Olson et al., 1987; Ribe and de Valpine, 1994; see also **Chapter 129**).

s0160 ### 133.3.3.2 Thermal plumes

p0605 Laboratory experiments in the absence of large-scale ambient mantle flow show that an unstable boundary layer can lead to numerous simultaneous plumes that interact with each other as they rise through the fluid (e.g., Kelly and Bercovici, 1997; Lithgow-Bertelloni et al., 2001; Manga, 1997; Olson et al., 1987; Whitehead and Luther, 1975). To study the dynamics of a single plume, it has become common to use a more narrow, point-like source of heat, which in laboratory experiments can be achieved by inserting a small patch heater at the base of the tank (e.g., Davaille and Vatteville, 2005; Kaminski and Jaupart, 2003) or alternatively by injecting hot fluid through a small hole (Griffiths and Campbell, 1990). These single-plume experiments predict the formation of a broad rounded head that leads the rising thermal instability and is trailed by a (usually) thinner columnar tail that connects to the deep source of the plume.

p0610 The morphology of the plume head and tail is controlled by the viscosity contrast between the hot plume and the ambient fluid (see Ribe et al. (2007) for a thorough review). A more viscous plume will tend to form a head with approximately the same width as the tail (a 'spout' or 'finger' morphology), whereas a lower-viscosity plume will tend to form a voluminous plume head much wider than the tail (a 'mushroom' or 'balloon' morphology). Since mantle viscosity is a strong function of temperature, the mushroom or balloon geometry should dominate thermal plumes (Kellogg and King, 1997; Olson and Singer, 1985; Richards and Griffiths, 1989; Whitehead and Luther, 1975).

p0615 The rise speed of plumes is proportional to its buoyancy and the square of its radius and inversely proportional to viscosity. Uranium-series geochemistry provides constraints for ascent rates near the base of the lithosphere; these upwelling speeds are often found to be comparable to plate velocities (Bourdon et al., 1998, 2005, 2006; Kokfelt et al., 2003), except for the much faster (i.e., by 1–2 orders of magnitude) rising Hawaiian plume (Pietruszka et al., 2001; Sims et al., 1999).

p0620 A range of instabilities, however, can induce oscillations in rise speeds and mass fluxes of thermal plumes. For example, perturbations within or above the deep thermal boundary layer can induce solitary waves that travel up the plume conduit much faster than average plume ascent rates for strongly temperature-dependent rheology (Olson and Christensen, 1986; Olson et al., 1993; Schubert and Olson, 1989; Scott et al., 1986; Whitehead and Helfrich, 1988). Other experiments have shown that a strongly tilted plume tends to break up into multiple diapiric upwellings (Olson and Singer, 1985; Richards and Griffiths, 1989; Skilbeck and Whitehead, 1978).

p0625 Such instabilities can have important implications for thermal entrainment of ambient mantle materials, through which the plume rises. In contrast to the classic work by Griffiths (1986), Richards and Griffiths (1989), and Griffiths and Campbell (1990, 1991), numerical models have revealed that thermal entrainment is generally limited to the periphery of plume tails (and even of plume heads) and hence insufficient to allow for partial melting of entrained materials beneath the hot spot (Farnetani and Hofmann, 2009; Farnetani and Richards, 1995; Farnetani et al., 2002). Solitary waves traveling rapidly and in isolation up the plume conduit moreover preclude any mixing of the hottest plume pulses with the ambient mantle (e.g., Whitehead and Helfrich, 1988). In contrast, strongly tilted plumes may be able to entrain ambient material more efficiently, perhaps even into the hot center of the

conduit (Richards and Griffiths, 1989). Understanding thermal entrainment is essential for constraining the depths of origin of geochemical signatures identified in hot spot lavas (cf. **Section 133.3.6**).

s0165 ### *133.3.3.3 Thermochemical plumes*

p0630 Thermal plumes rising from deep boundary layers have certainly guided much of our understanding of the causes for the largest hot spots. It is nevertheless likely that the density of many plumes is influenced by composition in addition to temperature. A large volume of compositionally dense but still hot and thermally buoyant material is thought to be present in the deep part of the lower mantle (Kellogg et al., 1999; McNamara and Zhong, 2005) and feed rising thermochemical plumes (e.g., Deschamps et al., 2011).

p0635 The structure of the thermochemical boundary layer at the base of the mantle can control the thermal, compositional, and rheological structure of the rising plumes. Without rapid ambient flow, materials originating from deeper versus shallower parts of the layer are expected to be entrained into the more central versus more peripheral plume conduit, respectively (Farnetani and Hofmann, 2009). If the layer is compositionally stratified, the deepest (i.e., densest albeit hottest) parts of the layer tend to remain stable and not rise into the plume (Farnetani, 1997; Lenardic and Jellinek, 2009). In addition to effects on plume composition and rheology (and therefore ascent style), such a situation may result in plume temperatures significantly smaller than CMB temperatures. These moderately hot plumes, further cooling along an adiabat that is steeper than that of the ambient mantle (Leng and Zhong, 2008), may reconcile the discrepancy between temperature anomalies at hot spots (e.g., Herzberg et al., 2007) and the much larger estimates for the temperature jump across the CMB (e.g., Boehler, 2000).

p0640 In addition, ambient mantle flow can trigger the creation of a plume and influence its thermochemical structure. For example, large-scale mantle convection tends to modulate the topography of the thermochemical boundary layer to focus plume upwellings (Steinberger and Torsvik, 2012). On a more regional scale, Tackley (2011) showed that the impingement of downgoing slabs on a thermochemical boundary layer can trigger plumes of various types (**Figure 19**). The angle of slab impingement influences the amount of mafic (and harzburgitic) materials entrained by, and the distribution of these materials within, the plume (e.g., the presence of mafic and/or refractory harzburgitic materials in the plume head). These predictions are relevant for the geochemical expression of LIP and hot spot volcanism, as well as LIP–hot spot connections (see **Chapter 134**).

p0645 Due to a competition between negative chemical and positive thermal buoyancy forces, entrainment of compositionally dense (e.g., mafic) materials strongly affects thermochemical-plume behavior (**Figure 20**). Plume behavior is predominantly controlled by the lateral thermal and compositional buoyancy profiles across the plume. These profiles depend on the temperature and density contrasts across the boundary layer from which they rise, the thickness of the chemical layer, and the contrast in compressibility between the two materials (Huang et al., 2010; Lin and van Keken, 2006a,b,c; Samuel and Bercovici, 2006; Tan and Gurnis, 2007). Predicted plume

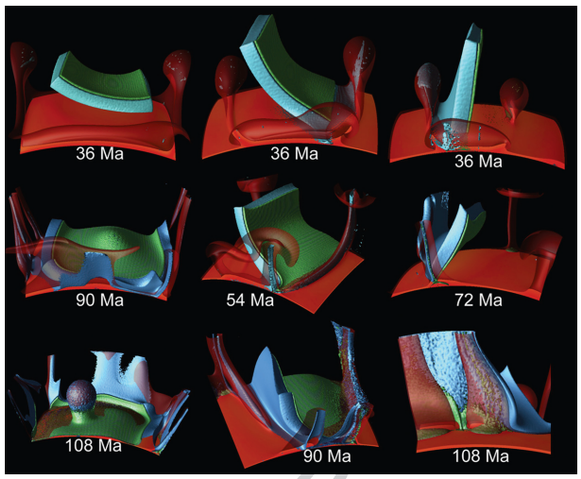

f0100 **Figure 19** From Tackley (2011). Thermochemical plumes triggered by downgoing slabs that interact with a thermochemical boundary layer for three different initial slab angles (different columns). Green and blue isosurfaces denote eclogitic and harzburgitic material, respectively. The red isosurface is the 3000 K isotherm.

ascent styles for different density (**Figure 20(e)–20(l)**) and compressibility contrasts range from nearly stagnant, wide plumes in the lower mantle ('domes' or 'superplumes') to fast episodic pulsations traveling up the plume conduit (e.g., Davaille, 1999; Kumagai et al., 2008; Lin and van Keken, 2005). For somewhat lower density contrasts, the dense layer may get entrained into the plume and then cause the ascent of the plume to stall in the lower mantle (Samuel and Bercovici, 2006) or to oscillate for a range of conditions (Davaille, 1999; Lin and van Keken, 2006b,c; Huang, 2008). The large range in predicted morphologies combined with the potential for stalling or sinking of thermochemical plumes at different depths (**Figure 20(e)–20(l)**) will complicate identifications of mantle upwellings in seismic images (Farnetani and Samuel, 2005; Kumagai et al., 2008; Lin and van Keken, 2006b,c), independent of how chemically dense materials (such as eclogite) influence seismic wave velocities (cf. Abalos et al., 2011; Connolly and Kerrick, 2002; Xu et al., 2008; Zhang and Green, 2007).

p0650 Further complexities arise from the interaction of thermochemical upwellings with mantle phase transitions. Farnetani and Samuel (2005) showed that the endothermic phase transition (and the associated viscosity jump) between the lower mantle and the upper mantle can alter thermochemical plume morphologies, for example, by promoting spout morphologies in the upper mantle (**Figure 20(a)–20(d)**). Furthermore, the density maximum of eclogite relative to peridotite in the depth range of 300–410 km (Aoki and Takahashi, 2004) can cause mantle upwellings to intermittently stall in the mid-upper mantle (Ballmer et al., 2013b; **Figure 20(m)**), which as discussed in **Section 133.2.5.2** can address the seismic structure of the Hawaiian plume (Cheng et al., in press; Wolfe et al., 2009).

p0655 The characteristics of thermochemical plume dynamics are relevant for our understanding of hot spot and flood basalt volcanism. The gravitational pull exerted by high-density eclogites in thermochemical plumes may account for the lack of

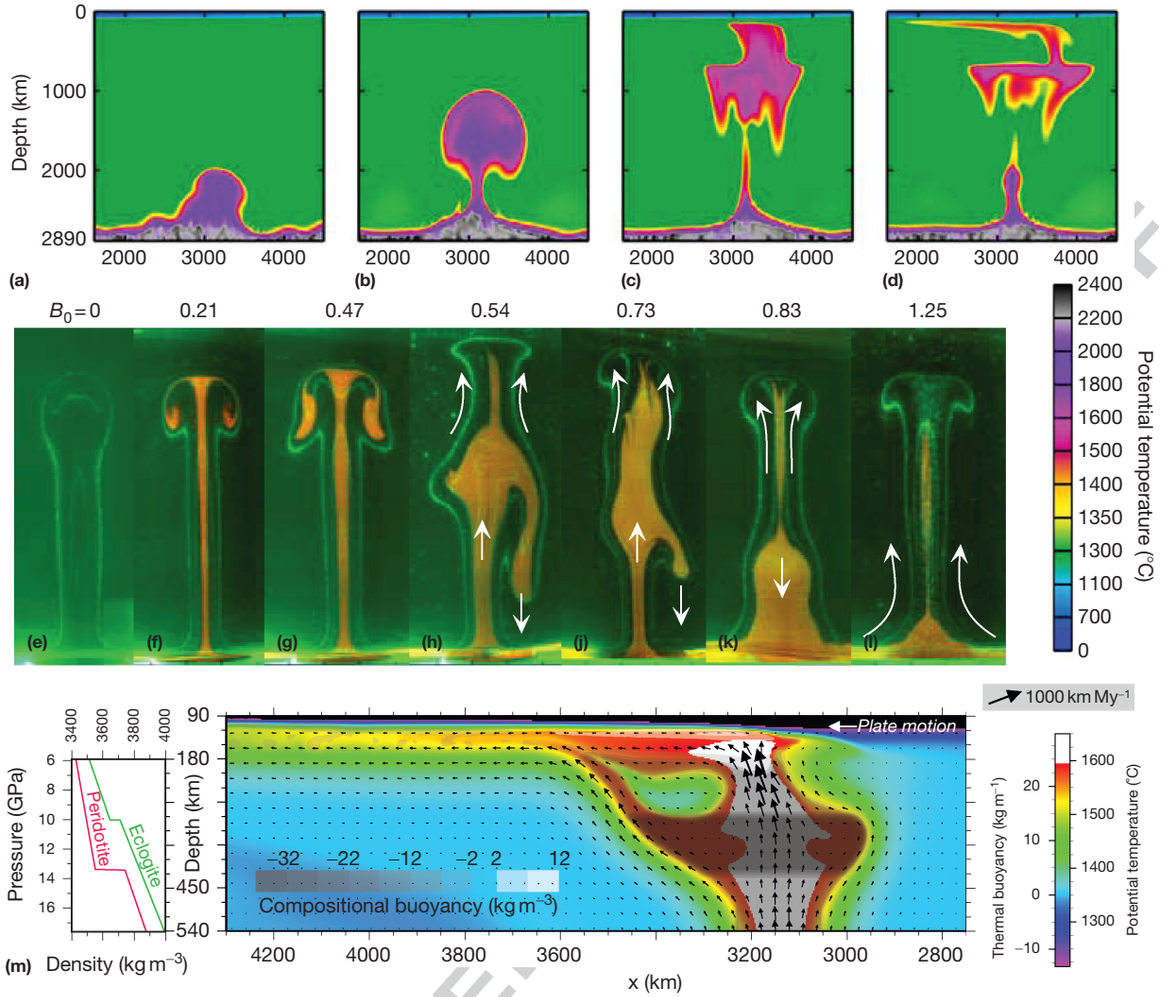

f0105 **Figure 20** Complexity of thermochemical plume dynamics in vertical cross sections through three-dimensional geodynamic models. (a–d) Time series of a plume rising from a deep thermochemical boundary layer and interacting with a viscosity jump at 660 km depth. Colors denote temperature (scale displayed on central right). (e–l) Diverse plume shapes (as snapshots) for different compositional densities of the dense material (i.e., different buoyancy numbers B_0). The dense material is light orange; isotherms are light green. The case with $B_0 = 0$ (e) corresponds to a purely thermal upwelling. (m) Snapshot of a thermochemical plume in the upper mantle. The ascending plume with an eclogite content of 15% interacts with phase changes that modulate the excess density of eclogite relative to peridotite (see inset at bottom left as modified from Aoki and Takahashi (2004)). Potential temperatures and compositional buoyancy are displayed as colors and shadings, respectively. Black arrows show mantle flow velocities. (a–d) Reproduced from Farnetani CG and Samuel H (2005) Beyond the thermal plume hypothesis. *Geophysical Research Letters* 32: L07311, http://dx.doi.org/07310.01029/02005GL022360. (e-l) Reproduced from Kumagai I, Davaille A, Kurita K, and Stutzmann E (2008) Mantle plumes: Thin, fat, successful, or failing? Constraints to explain hot spot volcanism through time and space. *Geophysical Research Letters* 35. (m) Reproduced from Ballmer MD, Ito G, Wolfe CJ, and Solomon SC (2013b) Double layering of a thermochemical plume in the upper mantle beneath Hawaii. *Earth and Planetary Science Letters* 376: 155–164.

premagmatic uplift for the Siberian Traps (Sobolev et al., 2011) and other flood basalt provinces (see **Section 133.2.3**). Oscillatory plume behavior may not only explain the episodicity of LIP emplacement (Lin et al., 2005) but also reconcile magmatic-flux variations evident in the geologic record along many hot spot tracks (e.g., Adam et al., 2007; Mjelde et al., 2010; Zhang et al., 2011) such as Hawaii (van Ark and Lin, 2004; Vidal and Bonneville, 2004) and Iceland (Ito et al., 1999; Parnell-Turner et al., 2013; Poore et al., 2011). Finally, small plumes are predicted to rise intermittently from large, stagnant thermochemical domes (Davaille, 1999) to provide an explanation for short-lived hot spot activity as evident in the S and W Pacific (Clouard and Bonneville, 2005; Courtillot et al., 2003; Koppers et al., 2003).

133.3.3.4 Effects of variable mantle properties on plume dynamics s0170

In addition to thermochemical effects, variations in mantle material properties can lead to complex forms and time dependence of mantle plumes. For example, a combination of increasing ambient mantle viscosity and thermal conductivity and decreasing thermal expansivity with depth has been shown p0660

to cause plumes to be relatively broad in the deep mantle but become thinner when migrating upward (Albers and Christensen, 1996; Leng and Gurnis, 2012). Several effects that are often ignored in geodynamic models, such as those related to radiative heat transport (Matyska et al., 1994), the postperovskite transition (Matyska and Yuen, 2005, 2006), and/or the iron spin-state crossover (Matyska et al., 2011), also tend to increase plume widths in the deep mantle, perhaps to extents comparable to thermochemical domes.

p0665 The largest variations in mantle material properties occur at the upper mantle-to-lower mantle transition at 660 km depth. The sharp decrease in viscosity from the lower to upper mantle causes a sudden drop in the width of rising plumes, as well as a related increase in ascent rate (Kumagai et al., 2007; Leng and Gurnis, 2012; van Keken and Gable, 1995). The density contrasts associated with the 660 km discontinuity can further contribute to acceleration and episodicity of plume flow (Brunet and Yuen, 2000; Nakakuki et al., 1997). Tosi and Yuen (2011) showed that plumes with strongly temperature-dependent rheology may be deflected horizontally just below the 660 km discontinuity, which itself has been identified as a potential source region for plumes (Cserepes and Yuen, 2000).

p0670 An important aspect of mantle rheology is that under high-strain-rate conditions, the rheology is dominated by non-Newtonian effects with a nonlinear dependence of viscosity on stress. Such a rheology can dramatically enhance the deformation rate of boundary layer instabilities and lead to much higher rise speeds than is observed in Newtonian fluids (Larsen and Yuen, 1997; Larsen et al., 1999; van Keken, 1997). Starting plume heads can rise sufficiently fast to almost completely separate from the narrower (and thus slower) tail, a behavior that may form an alternative explanation for the observed LIP episodicity (van Keken, 1997). In turn, nonlinear yield-stress rheology has been shown to promote spoutlike instead of mushroomlike plume morphologies (Davaille et al., 2013; Massmeyer et al., 2013).

p0675 In summary, the classical descriptions of plumes as cylindrical, axisymmetric, continuously rising features from the CMB to the lithosphere captured many of the first-order physical processes and thus provided a powerful framework for understanding localized upwellings that give rise to hot spots. New observations and more sophisticated models, however, have shown that plume-like upwellings are likely to take on complex morphologies, be time-dependent, and originate from different depths in the mantle. Systematic comparison of model predictions with observations, as well as new constraints from mineral physics, is required to identify the range of behaviors that are most applicable to the Earth's mantle.

s0175 133.3.3.5 Small-scale sublithospheric convection

p0680 Beyond the complexities of active plume ascent, other forms of upwelling have been proposed to sustain intraplate volcanism. While plumes rise from a hot thermal boundary in the deep mantle, passive upwelling can be triggered by instabilities dripping down from the cold thermal boundary layer at the base of the lithosphere. Analogous to bottom-up Rayleigh–Bénard instabilities discussed earlier, such top-down-driven small-scale convective instabilities are promoted by the thickening of the cool material at the base of the lithosphere and low viscosities of the underlying asthenosphere. Small-scale convection (SSC) has been shown to be typically organized as rolls (**Figure 21(a)**), aligned by the direction of plate motion (Richter, 1973). Rolls are at first limited to the asthenosphere with typical wavelengths of 200–300 km but may extend deeper beneath mature plates (Korenaga and Jordan, 2004). In both cases, SSC acts to remove the cool base of the lithosphere and to replace it by warm materials from below.

p0685 Such a process can provide an explanation for the observed flattening of seafloor bathymetry (and of surface heat flux) in ocean basins of ages >70 Ma (Davaille and Jaupart, 1994; Doin and Fleitout, 1996; Stein and Stein, 1994; Zlotnik et al., 2008). Instead, SSC beneath young seafloor may be restricted due to the presence of the residual harzburgite from previous MOR melting (Afonso et al., 2008; Hirth and Kohlstedt, 1996; Lee et al., 2005). The occurrence of SSC can further be tested using seismic observables (cf. Sleep, 2011). For example, it is consistent with the seismically derived thermal structure of the Pacific lithosphere (Ritzwoller et al., 2004; van Hunen et al., 2005).

p0690 The removal of the base of the cool (and depleted) lithosphere by SSC may moreover act to induce decompression melting (**Figure 21(b)**; Ballmer et al., 2007; Buck and Parmentier, 1986). According to the geometry typical for SSC (**Figure 21(a)**), magmatism is predicted to emerge along one or multiple hot lines parallel to the direction parallel to plate motion (Bonatti and Harrison, 1976; Bonatti et al., 1977), rather than at localized hot spots. Associated volcanic activity can thus occur coevally over distances of up to 1000–2000 km (Ballmer et al., 2009). Such extensive volcanism can create complex age–distance patterns such as those observed among various seamount chains in the western and southern Pacific (cf. shaded fields in **Figure 5**).

p0695 An important limitation for this mechanism involves that significant decompression melting requires SSC to occur beneath thin lithosphere of moderate or young ages (Ballmer et al., 2007; Buck and Parmentier, 1986; Harmon et al., 2011; Haxby and Weissel, 1986). Seafloor flattening, instead, indicates that SSC is typically restricted to thick lithosphere of ages >70 Ma, mostly due to the presence of the dehydrated harzburgitic residuum from MOR melting to delay SSC (Afonso et al., 2008; Hirth and Kohlstedt, 1996; Lee et al., 2005). Accordingly, SSC would likely have to stir up fertile or excessively hot materials to feed significant volcanism (Ballmer et al., 2010). Alternatively, SSC may be advanced toward younger lithospheric ages near fracture zones (Dumoulin et al., 2008; Huang et al., 2003).

p0700 Adjacent to larger steps in lithospheric thickness, convection is expected to be triggered almost independently of the thickness of the thermal boundary layer. This form of 'edge-driven' thermal convection can spawn decompression melting along rifts, as well as parallel to the edges of thick continental lithosphere (**Figure 22**) with opportunities for volcanism (Buck, 1986; Hardebol et al., 2012; King, 2007; King and Anderson, 1998; King and Ritsema, 2000; Missenard and Cadoux, 2012; Till et al., 2010; van Wijk et al., 2010). Recently, Milelli et al. (2012) showed in analogue experiments that convective instability may also form perpendicular to continental margins, a configuration that could provide an explanation for mantle melting beneath the Cameroon volcanic line (cf. **Figure 6**). Edge-driven convection along rifted margins, alone or in combination with elevated mantle temperatures,

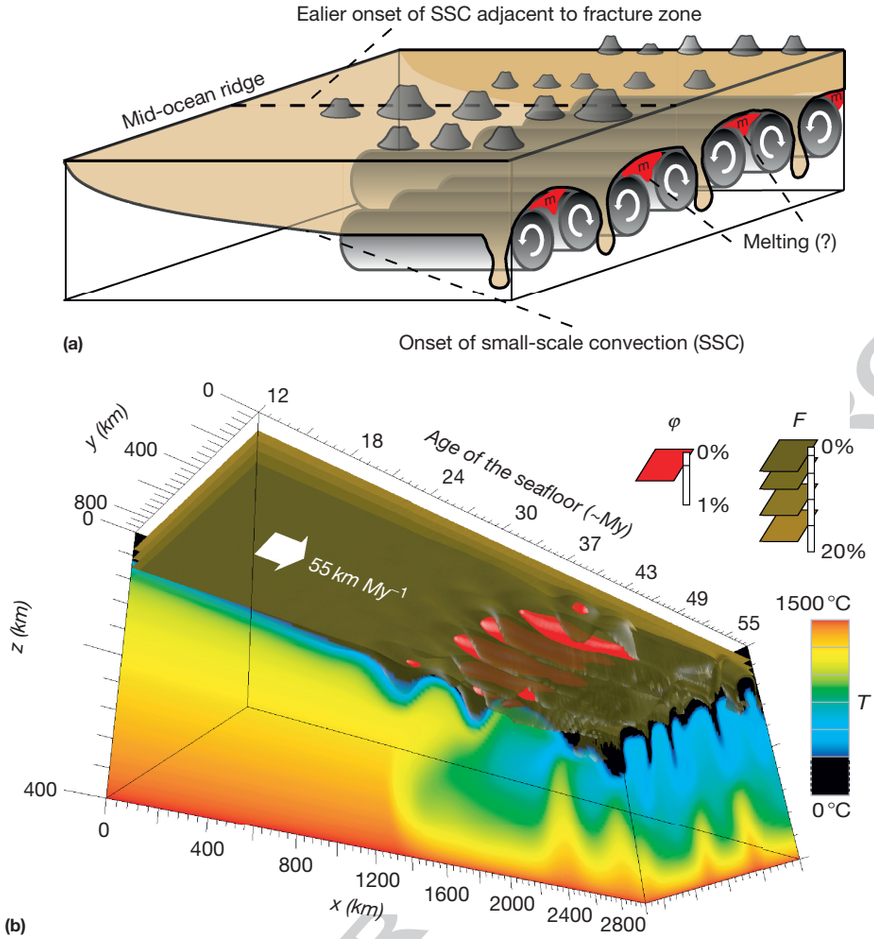

f0110 **Figure 21** (a) Conceptual cartoon of the dynamics of small-scale convection (SSC). Any decompression melting ('*m*') associated with SSC is expected to occur along multiple parallel 'hot lines' associated with the upwelling limbs of SSC. (b) Temperature, melting, and depletion predicted by a three-dimensional geodynamic model of SSC. Retained melt (φ) is labeled by red, and depletion in peridotite (F) by brown isosurfaces. Rainbow colors show temperature (T) along two cross sections. The flow field is not shown but is similar to that sketched in (a). SSC dynamically removes the base of the cool harzburgitic layer (brown) and replaces it by warm and undepleted peridotite to spawn decompression melting (red). Reproduced with minor modifications from Ballmer MD, van Hunen J, Ito G, Bianco TA, and Tackley PJ (2009) Intraplate volcanism with complex age-distance patterns: A case for small-scale sublithospheric convection. *Geochemistry*, *Geophysics*, *Geosystems* 10.

has been even identified as a possible mechanism for flood basalt volcanism (Korenaga, 2004; Mutter and Zehnder, 1988; Nielsen and Hopper, 2004; Nielsen et al., 2002; Sleep, 2007). Spatially and temporally more restricted convective processes such as the return flow associated with local foundering and delamination of the lower continental lithosphere have also been proposed to account for intraplate volcanism (e.g., in western North America) and flood volcanism without elevated mantle temperatures (Crow et al., 2011; Elkins-Tanton, 2007; Gogus and Pysklywec, 2008a,b; Hales et al., 2005; Houseman et al., 1981; Le Pourhiet et al., 2006; Levander et al., 2011; Paczkowski et al., 2012; Reid et al., 2012; van Wijk et al., 2001; West et al., 2009).

s0180 ### 133.3.3.6 Buoyant decompression melting

p0705 A separate form of convective instability can occur in response to melting itself. Partial melting reduces the density of the solid residue (Jordan, 1979; Oxburgh and Parmentier, 1977; Schutt and Lesher, 2006) and generates intergranular melt. Both factors can reduce the bulk density of the partially molten mantle and drive 'buoyant decompression melting' (**Figure 23**). Buoyant decompression melting has been shown to be relevant near MORs, for example, in supporting off-axis melting anomalies (e.g., Jha et al., 1994; Scott and Stevenson, 1989; Sparks et al., 1993; VanDecar et al., 1995). It has also been proposed to be relevant for intraplate volcanism, on both continental and oceanic plates (Hernlund et al., 2008a,b; Raddick et al., 2002; Tackley and Stevenson, 1993). The key ingredients for buoyant decompression melting to occur well away from MORs are an asthenosphere close to or at its solidus and a perturbation that locally initiates melting. Such a perturbation could be caused by extension of the overlying lithosphere (Hernlund et al., 2008b), the flow of mantle across a step in lithospheric thickness (Raddick et al., 2002), or some form of passive mantle

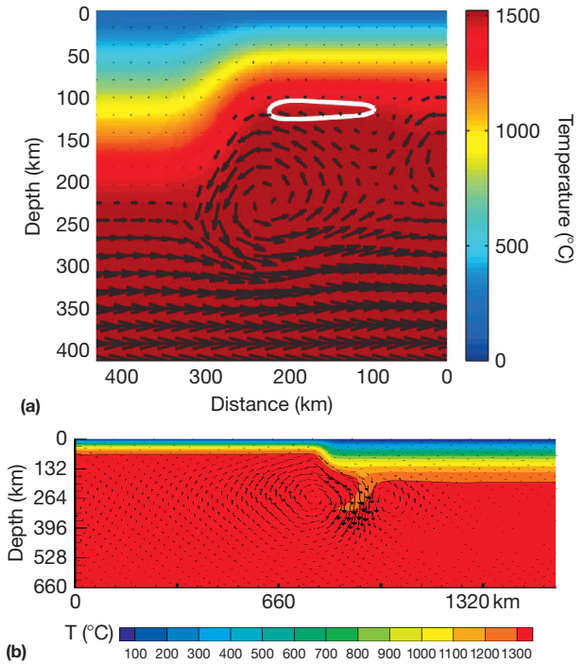

f0115 **Figure 22** Numerical model predictions for two different simulations of edge-driven convection along steps in lithospheric thickness. Colors represent temperatures, and arrows mantle flow velocity vectors. Mantle flow in (a) has a strong component of horizontal shear flow that contributes to drive upwelling (cf. **Figure 24(a)**). White line highlights the mantle domain, in which the solidus temperature is exceeded and melting may occur. Upwelling in (b) is predominantly passively driven by delamination near the sublithospheric step. In both (a) and (b), upwelling occurs >100 km away from the step in lithospheric thickness. (a) Reproduced from Till CB, Elkins-Tanton LT, and Fischer KM (2010) A mechanism for low-extent melts at the lithosphere-asthenosphere boundary. *Geochemistry, Geophysics, Geosystems* 11. (b) Reproduced from van Wijk JW, Baldridge WS, van Hunen J, et al. (2010) Small-scale convection at the edge of the Colorado Plateau: Implications for topography, magmatism, and evolution of Proterozoic lithosphere. *Geology* 38: 611–614.

flow. Significant retention of buoyant melts and low mantle viscosities tend to promote this convective instability. Since higher mantle water contents act not only to reduce the viscosity of the solid mantle but also to mobilize the equilibrium liquid, its effects on buoyant decompression melting remain unclear and thus motivate future studies.

133.3.3.7 Shear-driven upwelling and viscous fingering

s0185

All processes for decompression melting described so far require an inversion in density stratification (e.g., cool mantle overlying hot mantle) as the (potential) energy source of upwelling. Alternatively, vertical flow can result from horizontal shearing of the asthenosphere independent of mantle density variations (Bianco et al., 2011a; Conrad et al., 2010). Asthenospheric shearing is commonly imposed by the motion of the tectonic plates relative to that of the mesosphere and can drive upwelling in two different situations. First, (1) horizontal shear flow is predicted to be guided upward (or downward) at a step in lithospheric thickness (**Figure 24(a)**). Second, (2) redistribution of horizontal shear flow due to strong viscosity heterogeneity is predicted to be accommodated by local upwellings and downwellings (**Figure 24(b)**); vertical motion arises as shear flow is guided around a high-viscosity anomaly or focused within a low-viscosity anomaly.

p0710

Shear-driven upwelling due to the presence of a low-viscosity anomaly (situation (2); **Figure 24(b)**) is an attractive scenario for intraplate volcanism, since such anomalies are likely to be damp or warm and therefore close to the solidus. Regions of anomalously low seismic-wave speeds in the upper mantle (Laske et al., 2011; Schmandt and Humphreys, 2010; Weeraratne et al., 2007) provide evidence for low-viscosity pockets due to excess temperature, partial melt, elevated water content, or a combination thereof. Shear-driven upwelling at the edges of such pockets can support moderate magmatism (**Figure 24(c)**). Associated age progressions are predicted to be similar to those of (rapidly) drifting hot spots but with more variability (Ballmer et al., 2013a; Bianco et al., 2011a), similar to that evident along, for example, the Pukapuka ridge (cf. **Figure 4(c)**). Global mantle convection models predict

p0715

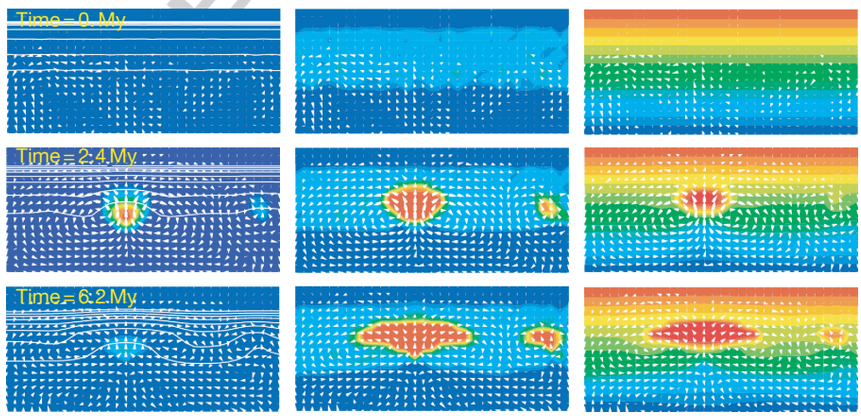

f0120 **Figure 23** From Raddick et al. (2002). Predictions of 2-D numerical models that simulate buoyant decompression melting for 3 time steps (different rows as labeled). Left column shows fractional melting rate (red = 0.0021/My, blue = 0), middle column shows melt fraction retained in the mantle φ (red = 0.02), and right column shows depletion of the residue F (red = 0.108). Density decreases as linear functions of both φ and F, and lateral density variations are what drive upwelling. Melting is therefore limited by the accumulated layer low-density and high-solidus residue.

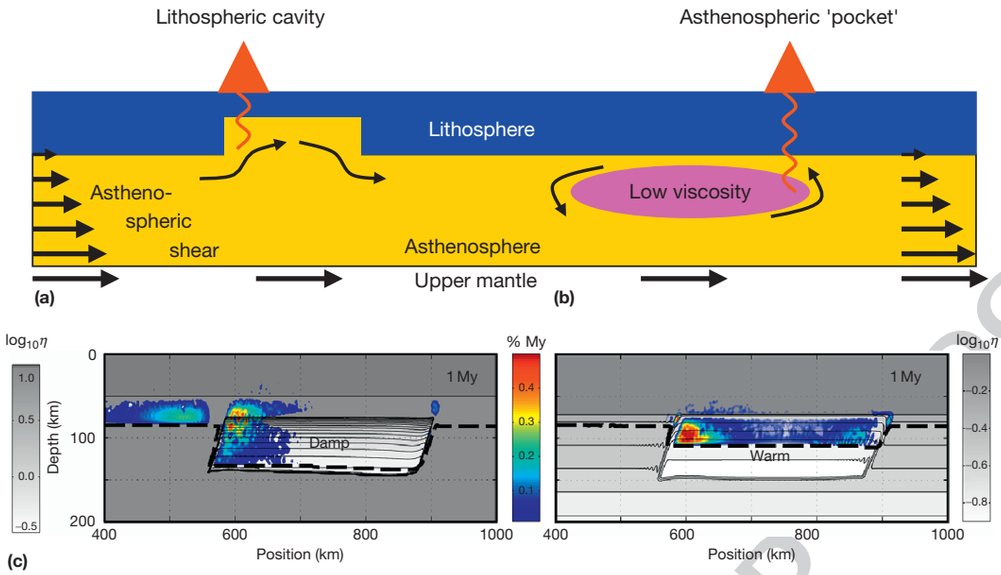

f0125 **Figure 24** Adapted from (a–b) http://www.mantleplumes.org/ShearDrivenUpwelling.html; and reproduced from (c) Bianco TA, Conrad CP, and Smith EI (2011a) Time dependence of intraplate volcanism caused by shear-driven upwelling of low-viscosity regions within the asthenosphere. *Journal of Geophysical Research* 116. (a–b) Cartoon showing two end-member scenarios, in which shear-driven upwelling is expected to occur (see text). Horizontal shear flow in the asthenosphere may be redirected into vertical flow when entering a cavity (a) or a pocket of anomalously low viscosity (b). (c) Snapshot of a numerical model (model time 1 My) quantifying the effects of shear-driven upwelling for the scenario shown in (b). Both damp and warm pockets locally reduce the viscosity η (shading and contours) to induce upwelling (not shown) and decompression melting (colors).

that intraplate regions with excessive intraplate volcanic activity, such as the eastern Pacific (**Figure 4**), western North America, and northeastern Australia (**Figure 7**), are indeed underlain by a strongly sheared asthenosphere (Conrad et al., 2011).

p0720 Identifying shear-driven upwelling as the dominant mechanism for decompression melting in a given volcanic province, however, requires careful analysis of the tectonic setting. In both situations (1) and (2), in which shear-driven upwelling is predicted to occur (near steps in lithospheric thickness and low-viscosity anomalies; **Figure 24(a)** and **24(b)**), alternative mechanisms for decompression melting, such as buoyant decompression melting and (edge-driven) small-scale convection, are also expected to be relevant (e.g., Huang et al., 2003). Increasing asthenospheric background viscosities and/or the rate of asthenospheric shearing promotes shear-driven upwelling relative to convective instabilities.

p0725 Future efforts should be specifically directed at testing the general significance of shear-driven upwelling along the margins of low-viscosity anomalies (situation (2); **Figure 24(b)**). Geophysical studies are needed to assess whether anomalies imaged by tomography can provide sufficient viscosity contrasts (i.e., 1–2 orders of magnitude at a given rate of asthenospheric shearing). Whereas deformation of the pocket in the large-scale flow field has been shown to be less of an issue (cf. Ballmer et al., 2013a; Bianco et al., 2011a), the persistence of magmatism should be limited by the progressive consumption of volatiles or fertile rocks in the pocket. Accordingly, it is imperative to address the origin of the pocket together with that of melting.

p0730 A mechanism that can spawn viscosity heterogeneity in the asthenosphere and that may even lead to excess volcanism by itself has been suggested to be operant in the South Pacific. When two fluids are contained in a thin layer and one fluid displaces a more viscous fluid (driven by a pressure gradient), the boundary between the two becomes unstable and undulates with increasing amplitude (Saffman and Taylor, 1958). Such viscous fingering instabilities may occur in nature, where warm and fertile material diffusely rising beneath the South Pacific Superswell is injected into the ambient asthenosphere. This process may account for the apparent 'Haxby' gravity lineations (Goodwillie, 1995; Harmon et al., 2011; Haxby and Weissel, 1986; Sandwell et al., 1995; Weeraratne et al., 2007) and associated volcanism (e.g., along the Pukapuka ridge) as warm and buoyant fingers travel along the base of the oceanic lithosphere (Sleep, 2008; Weeraratne et al., 2007; **Figure 4**). Whereas related rates of decompression melting should be rather small beneath the quasiflat lithospheres of fast or old plates, a combination with shear-driven upwelling at the tips of the fingers is expected, as both mechanisms are driven by similar physics.

p0735 Similarly, material injected into the asthenosphere by mantle plumes (Phipps Morgan et al., 1995b; Yamamoto et al., 2007) may feed warm low-viscosity channels. Geodynamic models predict that the pressure low expected beneath MORs can assist in drawing material from nearby plumes toward ridges in relatively narrow channels (e.g., Sleep, 1996; Yale and Phipps Morgan, 1998), as was originally hypothesized by Morgan (1978). Channeling of plume material is consistent with hot spot-flavored geochemical fingerprints of basalts formed near or at MORs (Geldmacher et al., 2013; Haase et al., 1996; Niu et al., 1999; Vlastelic and Dosso, 2005), as well as between the Canary hot spot and a subduction zone near Gibraltar (see Duggen et al. (2009) and **Figure 25**), respectively.

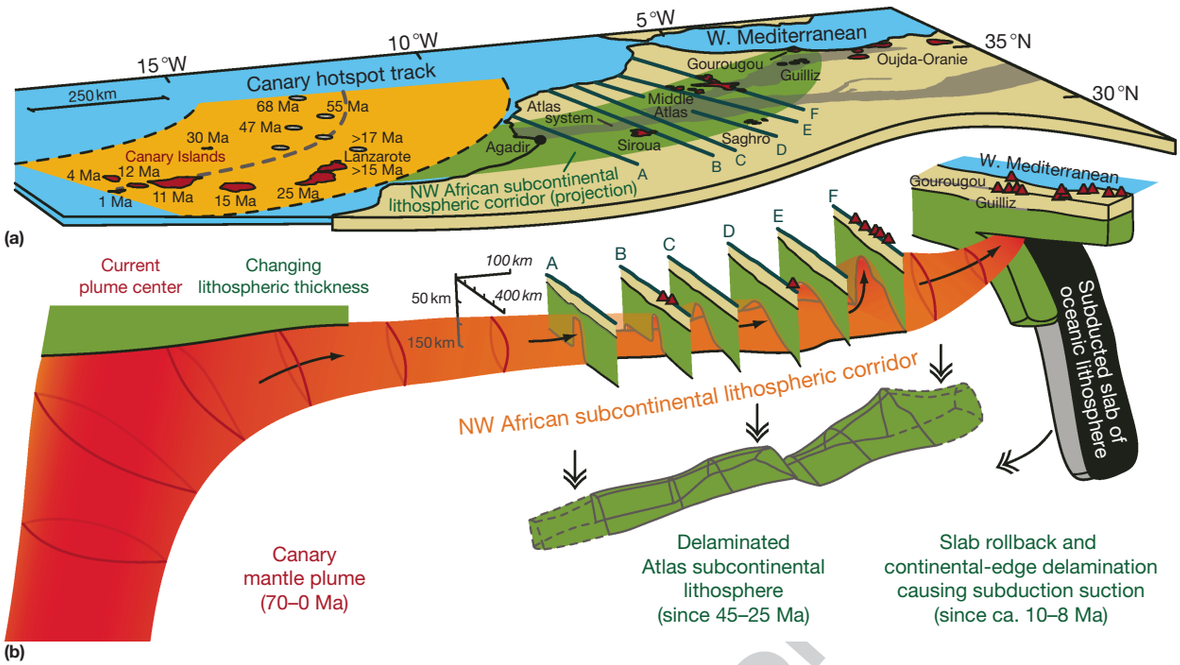

f0130 **Figure 25** From Duggen et al. (2009). Conceptual model for the channeling of plume material from the Canary hot spot through the northwest African subcontinental lithospheric corridor to the mantle wedge of a subduction zone near Gibraltar. Upward flow along the base of the lithosphere, perhaps assisted by shear-driven upwelling (cf. **Figure 24**), may have contributed to sustain Cenozoic basaltic volcanism along the corridor (red triangles in (b)).

s0190 ### *133.3.3.8 Vertical motion of the lithosphere*

p0740 Finally, vertical motion of the whole lithosphere and surface of the Earth can cause mantle upwelling and melting. For example, volcanism off southern Greenland (Uenzelmann-Neben et al., 2012) and peaks in volcanic activity in Iceland (Slater et al., 1998) have been attributed to glacial rebound. Another opportunity for mantle decompression is offered by the growth of large volcanoes (created by another mechanism such as a plume), which not only causes the underlying lithosphere to sink downward but also leads to flexure-induced upwarping in a donut- or arch-shaped zone around the volcano. The small amounts of decompression associated with this flexural uplift are only expected to give rise to magmatism as long as an appreciable portion of the asthenosphere is already near or at its solidus (Bianco et al., 2005). Flexural decompression may thus explain secondary (or rejuvenated-stage) volcanism near the Hawaiian and other major hot spots (e.g., Bianco et al., 2005; Garcia et al., 2010). Upward flexural bulging also occurs on the seaward side of subduction zones and may sustain the activity of 'petit-spot' volcanism off the Japan Trench (Hirano et al., 2001, 2008), as well as contribute to extensive rejuvenated volcanism at the Samoan hot spot (Konter and Jackson, 2012).

s0195 ## 133.3.4 Swells

s0200 ### *133.3.4.1 Swell support mechanisms*

p0745 The origin of hot spot swells was initially attributed to heat anomalies in the mantle that effectively rejuvenate or thin the overriding lithosphere (Crough, 1978; Detrick and Crough, 1978; Crough, 1983). The evidence for such thermal rejuvenation is somewhat ambiguous, as heat flow data fail to show evidence for heated or thinned lithosphere (DeLaughter et al., 2005; Stein and Stein, 1993, 2003). However, it is likely that any such evidence would be obscured by shallow hydrothermal circulation (Harris and McNutt, 2007; McNutt, 2002). Seismic studies, in turn, are able to provide evidence for lithospheric thickness variations at some hot spots. For example, Rayleigh-wave tomography reveals strong variations in lithospheric thickness at the Galápagos hot spot (Villagomez et al., 2007). At the Hawaiian hot spot, S-wave receiver functions indicate substantial lithospheric thinning of 50–60 km from the hot spot toward the NW (Li et al., 2004), whereas recent evidence from regional surface-wave tomography as well as SS precursors suggests only modest thinning (by about 10–20 km) (Laske et al., 2011; Schmerr, 2012).

p0750 Perhaps, the more prevalent view at this point is that hot spot swells are primarily dynamically supported by the hot and buoyant plume layer that is predicted to pond beneath the lithospheric plate (Cadio et al., 2012; Cserepes et al., 2000; Olson, 1990; Parsons and Daly, 1983; Ribe and Christensen, 1994). For example, dynamic support by anomalously hot mantle (as evident from seismic tomography) can explain excess topography associated with the Yellowstone hot spot (Becker et al., 2013). In addition to the thermal buoyancy of a plume, compositional buoyancy associated with melt extraction may also be important in creating hot spot swells (Phipps Morgan et al., 1995a).

p0755 Evidence for such compositional contributions to swell support has been revealed at various hot spots. Exposures of harzburgite along the rifted Marion and Azores Rises, for

instance, indicate compensation by buoyant melt residuum (Zhou and Dick, 2013). Uplift histories and receiver function measurements argue for a combination of buoyant melt residuum and magmatic underplating to support the ~2 km high Cape Verde swell (Lodge and Helffrich, 2006; Ramalho et al., 2010). For the Marquesas swell, geoid observations and seismic reflections also suggest a role for magmatic underplating (Caress et al., 1995; McNutt and Bonneville, 2000).

p0760 A viable tool to quantify the compensation depth of the swell and thus to distinguish between crustal (e.g., magmatic underplating), lithospheric (e.g., lithospheric thinning), and mantle (e.g., dynamic support and buoyant melt residuum) contributions is the analysis of the geoid-to-topography ratio (Marks and Sandwell, 1991; Parsons and Daly, 1983; Ribe and Christensen, 1994). For example, once the local effects of volcanic loading are removed (cf. Cserepes et al., 2000), wavelet analysis of the geoid-to-topography ratio reveals that the Hawaiian swell is predominantly compensated at sublithospheric depths (Cadio et al., 2012). The best candidate for such a deep compensation is dynamic support by a mantle plume.

s0205 ### *133.3.4.2 Plume models and hot spot swells*

p0765 The dynamic support hypothesis for the generation of hotspot swells has been quantitatively tested by geodynamic models. Three-dimensional plume models, for example, have successfully predicted the shape and uplift history of the Hawaiian swell (Asaadi et al., 2011; Cadio et al., 2012; Ribe and Christensen, 1994; van Hunen and Zhong, 2003; Zhong and Watts, 2002): they predict that the plume pushes up the plate by ponding like a 'pancake' of hot material (cf. red layer in **Figure 26(a)**). They also predict the eventual waning of swell topography to occur due to spreading and thinning as well as cooling of the plume pancake. Consideration of stress-dependent rheology appears to be critical to match the plan-view shape of the swell to the NW of Hawaii (Asaadi et al., 2011). The additional effects of small-scale convection in the pancake removing the base (about 15–20 km) of the lithosphere (Agrusta et al., 2013; Ballmer et al., 2011; Moore et al., 1998) can account for the systematic decrease of the geoid-to-topography ratio that is evident along the Hawaiian swell (Cadio et al., 2012). These predictions provide a straightforward explanation for the decay of hot spot swells along the Hawaiian and Louisville chains as well as the lack of swells around very old portions of other volcano chains.

s0210 ## 133.3.5 Large Igneous Provinces

p0770 The rapid and massive magmatic production of LIPs, combined with their strong connection to continental breakup and present-day hot spot volcanism, provides major challenges for our understanding of planetary volcanism. The wide range of eruptive volumes (**Figure 10**) and differences in tectonic style (**Section 133.2.3**) appear to suggest that multiple mechanisms account for flood basalt volcanism.

p0775 The observation of large plume heads followed by thin tails in fluid dynamic experiments has traditionally been used to explain LIP–hot spot connections (Richards et al., 1989) and remains, because of its simplicity and plausibility, an attractive base model for the formation of LIPs. Its strengths include that

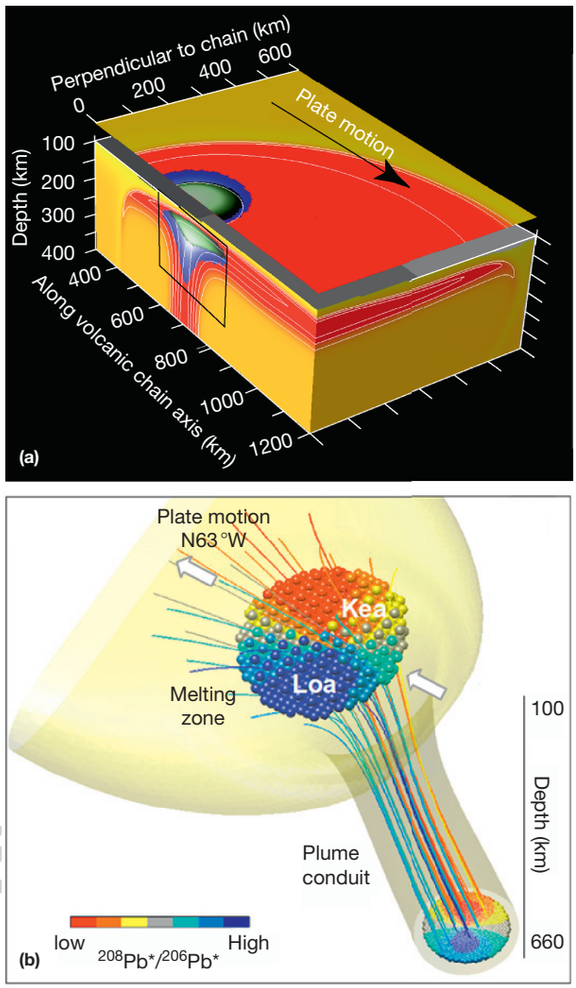

Figure 26 Three-dimensional images (in angled views from above) of plume dynamics and the expressions of compositional heterogeneity in magmatism. Whereas melting is affected by both temperature and composition in the geodynamic models shown, plume dynamics are governed by thermal effects only. (a) From Bianco et al. (2008). White contours (isotherms), as well as red-to-yellow colors, denote temperature. The blue and light green fields show the melting zones of a fertile and refractory compositional component, respectively. The compositional heterogeneity is assumed to be in the form of evenly dispersed fine-scale fertile veins in a refractory matrix. A horizontal cross section through the box at 150 km depth is lifted from the top for visibility. (b) From Farnetani et al. (2012). The isosurface outlines the hot plume; the colored lines denote streamlines tracking large-scale compositional heterogeneity. Heterogeneity is assumed to be distributed bilaterally asymmetrically in the deep plume stem (as represented by $^{208}Pb^*/^{206}Pb^*$ signatures in a cross section at 660 km depth (colors)). The expression of heterogeneity in magmatism is expressed by sphere colors. f0135

(1) it is supported by fluid dynamic experiments with increasingly realistic assumptions about mantle composition and rheology (see **Section 133.3.3**; in fact, modifications to the base model (cf. **Figure 20**) can reconcile the diversity seen in the geologic record), (2) it can explain the natural link between LIP and hot spot volcanism, (3) it reconciles the early occurrence of high-MgO basalts in the LIP record (as the hottest

material is predicted to erupt first), and (4) it implies contemporaneous uplift and extension as is observed in the geologic record of many LIPs (see Section 133.2.3). The main weaknesses of this model involve that the strong correlation of LIPs and continental breakup and the lack of uplift during OJP formation (d'Acremont et al., 2003) are not explained.

p0780 There are a number of alternatives that can address some of the weaknesses of the plume model that include assumptions that LIPs may be generated by processes occurring near the surface of the Earth or by extraterrestrial processes. While the plume model has received significant attention and quantitative hypothesis testing, the majority of the alternatives are currently still in rather qualitative form.

p0785 The first alternative involves that the accumulation of heat below the insulating continent or supercontinent during tectonic quiescence provides warmer than normal mantle and significantly larger eruptive volumes during continent breakup (Anderson, 1994b; Coltice et al., 2007; Grigne et al., 2007; Coltice et al., 2009). While this hypothesis addresses the correlation between LIPs and continental breakup, it does not clarify why flood volcanism does not generally occur along all rifted margins. Also, the connection to a long-lived hot spot trail remains unpredicted. Nevertheless, the correlation between the LIPs and the continental breakup is intriguing, and it is quite likely that regional variations in the composition and strength of the lithosphere have an important control on the location of magma eruption (King and Anderson, 1995, 1998).

p0790 A second alternative is that compositional, rather than thermal, effects cause the generation of excessive melt by, for example, the presence of eclogite or volatiles in the source rock (e.g., Anderson, 1994a, 2005; Cordery et al., 1997; Korenaga, 2004, 2005; Sobolev et al., 2011). Its strengths include that the lack of uplift at some LIPs, including the OJP, could be explained for the presence of dense eclogite. The main weakness of eclogite as the primary source of melting is that eclogite is dense and requires some mechanism to stay near or be brought back to the surface. It would be more than likely in this case that emplacement of the OJP involved both a thermal origin and a compositional origin. For purely compositional effects, the common LIP–hot spot connection (requiring continuous upwelling of more fertile mantle) further remains unexplained. An interesting alternative to a compositional cause for the lack of significant uplift at some LIPs, including the OJP, is the potential for lower crustal flow during magma emplacement (Flament et al., 2011).

p0795 The enigmatic nature of the OJP has also led to the suggestion that meteorite impacts could have been responsible for LIP emplacement (Ingle and Coffin, 2004; Rogers, 1982). A possible strength of this hypothesis is that the decompression of mantle following impact may generate extensive melting (Jones et al., 2002a). A weakness is that the strong connections with continental breakup and hot spot volcanism are unexpected. Furthermore, direct evidence for meteorite impact during LIP emplacement is rare. One of the few convincing observations is the Ir anomaly embedded in the Deccan Traps, but this impact signal postdates the start of volcanism and is most likely related to the Chicxulub impact located on the other side of the planet. There are also doubts whether the dynamics of meteorite impact can indeed cause sufficient melting, unless the mantle is already anomalously hot or fusible (Ivanov and Melosh, 2003). Another issue is that it has been shown to be statistically unlikely that the majority of Phanerozoic LIPs originated as impacts (Elkins-Tanton and Hager, 2005; Ivanov and Melosh, 2003).

Finally, delamination of continental lithosphere and secondary convection at rifted margins have been suggested as alternatives for LIP formation (Anderson, 2005; Hales et al., 2005; van Wijk et al., 2001). While these processes are likely to have occurred regularly in the past, the extent to which they can provide a consistent explanation for the rapid and massive outpourings of flood basalts remains to be quantitatively evaluated. p0800

133.3.6 The Origin of OIB Geochemical Signatures s0215

133.3.6.1 Tracing mantle heterogeneity by isotopic signatures of OIB s0220

The geochemical signatures of ocean island basalts (OIBs) may provide key constraints on the composition of mantle reservoirs. Highlighting the differences between OIB and MORB, we have focused on $^{87}Sr/^{86}Sr$, $^{206}Pb/^{204}Pb$, and $^{3}He/^{4}He$ (Table 1). These ratios are key to tracing five different geochemical flavors in the OIB dataset, which have been associated with five different mantle reservoirs, each with distinct time-averaged, chemical histories (e.g., Hanan and Graham, 1996; Hart et al., 1992; Zindler and Hart, 1986). Lavas with low $^{3}He/^{4}He$ and minimal $^{87}Sr/^{86}Sr$ and $^{206}Pb/^{204}Pb$ are derived from depleted mantle material (DM), referring to depletion in incompatible elements. Enriched (EM1 or EM2, i.e., high $^{87}Sr/^{86}Sr$) and HIMU (i.e., high $^{206}Pb/^{204}Pb$) mantle sources are instead thought to be derived from subducted material – the former from ancient oceanic sediments or metasomatized lithosphere and the latter from oceanic crust – that has evolved in the mantle for >1 Gyr and subsequently been recycled (e.g., Cohen and O'Nions, 1982; Hanyu et al., 2011; Hart et al., 1992; Hofmann, 1997; Hofmann and White, 1982; Sobolev et al., 2008; Zindler and Hart, 1986). p0805

High $^{3}He/^{4}He$, moderately low $^{87}Sr/^{86}Sr$, and intermediate-to-high $^{206}Pb/^{204}Pb$ compositions mark the fifth geochemical end-member, which we will here refer to as FOZO (Hart et al., 1992). Its origin is perhaps least well understood. The 'standard' hypothesis implies that the high $^{3}He/^{4}He$ fingerprints primordial and relatively undegassed mantle material (Hart et al., 1992; see also Gonnermann and Mukhopadhyay, 2009). In a variant of this standard hypothesis, FOZO is not just a leftover of quasihomogenous primordial mantle, but has been enriched through a differentiation process occurring early in the Earth's history (Coltice et al., 2011; Davies, 2010; Lee et al., 2010). The standard hypothesis, however, has recently altogether been challenged by suggestions that FOZO, in fact, has been depleted in highly incompatible elements during partial melting processes. In this scenario, helium degasses only incompletely during partial melting (Class et al., 2005), and FOZO's high $^{3}He/^{4}He$ ratio reflects a low ^{4}He concentration as a result of low U and Th content (with U and Th being more incompatible than helium) (Coltice and Ricard, 1999; Meibom et al., 2005; Parman et al., 2005; Stuart et al., 2003). However, any alternatives to the standard hypothesis do not satisfy constraints from other noble-gas systems such as $^{129}Xe/^{130}Xe$ and $^{20}Ne/^{22}Ne$, which require that the relatively undegassed reservoir (i.e., FOZO) p0810

formed within the first 100 million years of the Earth's history and since then has not been homogenized with the other mantle reservoirs (Mukhopadhyay, 2012; Peto et al., 2013).

p0815 The key observation is that MORB appears to be characteristically similar to DM and to be relatively less influenced by subducted materials and FOZO, whereas hot spot lavas and many other intraplate basalts appear to be influenced substantially by all five components (albeit to different degrees for different volcano groups; cf. **Figure 11**). The dominant explanation for this observation is that the pressure/temperature dependence of mantle viscosity and mineralogy, as well as density differences between the different mantle materials, promotes large-scale (partial) layering in mantle geochemistry. DM is likely to be compositionally light and may tend to concentrate in the upper mantle where it is sampled by MOR magmatism (cf. Nakagawa et al., 2010) Mantle plumes, which feed hot spots, rise from deeper levels in the mantle and hence may incorporate the other materials in addition to DM. For example, geochemical reservoirs associated with subducted slabs that evolved in the mantle for >1 Gyr (EM, HIMU) or even the more ancient FOZO are likely to be stored in the lowermost mantle (e.g., Brandenburg et al., 2008; Christensen and Hofmann, 1994; Coltice and Ricard, 1999).

s0225 ### *133.3.6.2 Constraining source materials from major-element characteristics of OIB*

p0820 While the various mantle reservoirs are well traced by their isotopic signatures in OIB, understanding their major-element signatures is needed to define their physical properties as well as melting behaviors. As a first step toward this goal, Jackson and Dasgupta (2008) demonstrated that major-element concentrations of OIB are correlated with isotopic ratios using a global dataset. At a given MgO, HIMU-flavored volcano chains are systematically lower in SiO_2 and Al_2O_3 and higher in TiO_2, Na_2O, FeO_X, and CaO than EM-flavored volcano chains, and both are distinct from MORB (**Figure 27**). Tholeiitic basalts from Hawaii, the Galápagos, and Iceland display major-element compositions intermediate to these two OIB subgroups and MORB. Thus, mantle reservoirs can in principle be distinguished not only by OIB isotopic signatures but also by OIB major-element concentrations.

p0825 To understand the composition of mantle reservoirs and OIB source lithologies, petrologists have compared experimental melts with typical alkalic OIB signatures. Although low-degree melting of 'common' mantle peridotites is able to produce alkalic melts, experimental evidence is so far lacking that such melts can match the specific major-element signature of OIB (Davis et al., 2011; Hirose and Kushiro, 1993; Mueller et al., 1998; Takahashi and Kushiro, 1983) Addition of CO_2-rich liquid to peridotites would be required to better match these signatures (blue triangles in **Figure 12**; Dasgupta et al., 2007). The characteristic HIMU isotopic fingerprint of most alkalic OIB further calls for a subduction-related origin for the CO_2-rich liquid (Jackson and Dasgupta, 2008).

p0830 Alternative materials for the OIB source are subduction-related lithologies such as basaltic oceanic crust that has transformed to eclogite and evolved in the mantle. While direct eclogite melting produces liquids that are much too high in SiO_2, two-stage eclogite melting can reconcile the major-element characteristics of OIB. In the first step, highly silicic

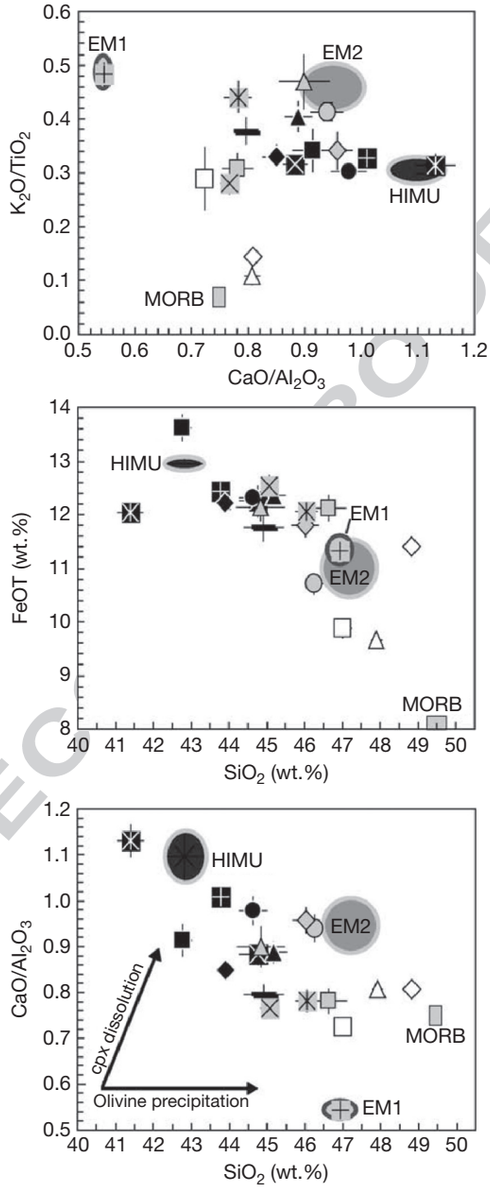

Figure 27 Separation of isotopically flavored OIB subsets in major-element space. Symbols (with ±1σ error bars) show select average major-element concentrations and ratios of fractionation-corrected lavas (10% ≤ gO ≤ 16%) from various island groups. EM-flavored and HIMU-flavored island groups are the gray and black symbols, respectively; their overall averages are represented by ellipses (Pitcairn–Gambier is the sole EM1-flavored island group). Open symbols represent the dominantly tholeiitic lavas from Hawaii, the Galápagos, and Iceland, which plot closer to MORB (cf. gray rectangle) than alkalic OIB. Arrows in (c) elucidate that neither dissolution of clinopyroxene nor precipitation of olivine can account for the global trend in CaO/Al_2O_3 vs. SiO_2. Reproduced from Jackson, and Dasgupta R (2008) Compositions of HIMU, EM1, and EM2 from global trends between radiogenic isotopes and major elements in ocean island basalts. *Earth and Planetary Science Letters* 276: 175–186. f0140

liquids react with the wall rock (i.e., ambient mantle peridotites) to form hybrid lithologies such as pyroxenites (Yaxley and Green, 1998). In a second step, these hybrid lithologies can produce OIB-like liquids as they melt (they do so at lower pressures than eclogites themselves) (Kogiso and Hirschmann, 2006). Oxide ratios in olivine phenocrysts of Hawaiian lavas have indeed been interpreted as evidence for such a two-stage melting process (Sobolev et al., 2005; 2007). Alternatively, incomplete reaction of eclogitic melts with the wall rock (e.g., along melt channels) can leave a modified liquid that satisfies a range of OIB compositions (Mallik and Dasgupta, 2012). Depending on the extent of wall-rock reaction, either alkalic or tholeiitic liquids are generated.

p0835 Hornblendite veins are another viable source lithology for OIB (Pilet et al., 2008; **Figure 12**). Their origin is thought to be a near-ridge environment, where low-degree peridotitic melts freeze into the lithospheric mantle (Pilet et al., 2010). Hornblendite or similar metasomatic lithologies (Halliday et al., 1995; Niu et al., 2002b) have indeed been mapped in peridotite massifs and sampled as xenoliths (Frey et al., 1985; O'Reilly and Griffin, 1988; Takazawa et al., 2000). The metasomatized base of the oceanic lithosphere may contribute to producing OIB-like liquids as it is moved over a hot spot or as it is decompressed as part of a mantle upwelling after recycling. In particular, the rather high K_2O/Na_2O and Al_2O_3/MgO ratios in OIB may indicate the presence of hornblendite in the source or at least provide evidence for the equilibration of the rising magmas with hornblendite.

s0230 #### *133.3.6.3 The origin of geographic variations in OIB geochemistry*

p0840 The variability of hot spot geochemical signatures has typically been ascribed to mantle source heterogeneity. In the framework of plume theory, geographic patterns in OIB geochemistry, such as the large variability of isotopic signatures among South Pacific and Darwin Rise OIB (Koppers et al., 2003; Staudigel et al., 1991) or the distinction between the 'Loa' and the 'Kea' trends of Hawaiian volcanism (Abouchami et al., 2005), are thought to reflect heterogeneity in the deep mantle (Farnetani and Hofmann, 2009; Huang et al., 2011; Konter et al., 2008; Koppers and Watts, 2010; Weis et al., 2011). For example, deep mantle heterogeneity is expected to be directly reflected as lateral zonation of the plume conduit (Farnetani and Hofmann, 2009, 2010; Farnetani et al., 2012; **Figure 26(b)**). However, as major-element variations associated with such compositional zonation can severely affect the dynamics of the rising plume (see **Section 133.3.3.3**), mapping the deep mantle from geographic patterns of lava compositions is not straightforward (cf. Ballmer et al., in press). Moreover, plume pulsations in general and those induced by solitary waves (e.g., Whitehead and Helfrich, 1988) in particular may tend to homogenize material within the hottest parts of the plume.

p0845 Another important aspect to consider is the melting behavior of a heterogeneous source (Phipps Morgan, 1999). Geochemical evidence indicates that such source heterogeneity is present over a range of spatial scales, including scales much smaller than the size of upper mantle melting zones (e.g., Ellam and Stuart, 2004; Ingle et al., 2010; Jackson et al., 2012; Kogiso et al., 2004; Koornneef et al., 2012; Marske et al., 2007; Niu et al., 1996; Phipps Morgan, 1999; Reiners, 2002; Saal et al., 1998; Salters and Dick, 2002; Stracke et al., 2003). As different materials melt over different depth ranges for a given mantle temperature (cf. **Figure 26(a)**), spatial differences in mantle temperature, lithospheric thickness, and the rate of mantle flow through the melting zone can influence the proportions, to which the materials are represented in the lavas. For example, MOR melting is expected to be dominated by the peridotitic DM matrix, a refractory yet the most abundant component, because the thin lithosphere at and near MORs allows for the greatest amount of decompression. Mainly due to the effects of a thicker lithosphere, hot spot magmatism away from MORs is instead predicted to be more heavily influenced by the less abundant but more fertile components, something that may reconcile the difference between OIB and MORB (Ito and Mahoney, 2005a; 2006). In such a framework, mechanisms for non-hot spot volcanism (see **Sections 133.3.3.5–133.3.3.8**) occurring well away from MORs would similarly generate OIB-like liquids (e.g., Ballmer et al., 2010). First-order global trends indeed display significant correlations of major and trace-element compositions of OIB with the thickness of the lithosphere at the time of volcanism (Dasgupta et al., 2010; Humphreys and Niu, 2009; Ito and Mahoney, 2005b; Keller et al., 2004).

p0850 At the regional scale of an individual island group, lateral gradients in temperature and mantle upwelling rate can also give rise to systematic geographic variations in lava chemistry, independent of any lateral compositional zonation of the mantle source (Bianco et al., 2008, 2011b, 2013; Ballmer et al., 2010, 2011; Shorttle et al., 2010; Shorttle and Maclennan, 2011; Ballmer et al. 2013a). For example, any lateral thermal gradient beneath the Hawaiian hot spot will shift the melting zones of fertile and of refractory mantle components relative to each other to contribute to the apparent 'Loa' versus 'Kea' geochemical trends (cf. Ballmer et al., in press).

133.3.7 Plumes in the Context of Mantle Convection and Plate Tectonics

s0235

p0855 Our discussion of plumes and alternative forms of mantle upwelling is set amid the background of larger-scale processes of plate tectonics and mantle convection. The cooling of the oceanic lithosphere ultimately drives mantle convection and plate motion. While the volume of mantle that participates in the plate tectonic cycle is still debated, a consensus model has emerged of moderated whole mantle convection, with significant material exchange across the 660 km discontinuity. Plumes naturally develop from the hot thermal boundary layer at the CMB and are displaced when rising through the convecting mantle (Husson and Conrad, 2012; Olson and Singer, 1985; Richards and Griffiths, 1989; Steinberger, 2000; Whitehead and Luther, 1975).

133.3.7.1 Connection of hot spots with thermochemical structures in the deep mantle

s0240

p0860 An important line of evidence for mantle plume theory is the connection of seismic structures in the deep mantle with occurrences of hot spot volcanism at the surface (Castillo, 1988; Williams et al., 1998). The locations of active hot spots, as well as reconstructed locations of extinct hot spots and LIPs,

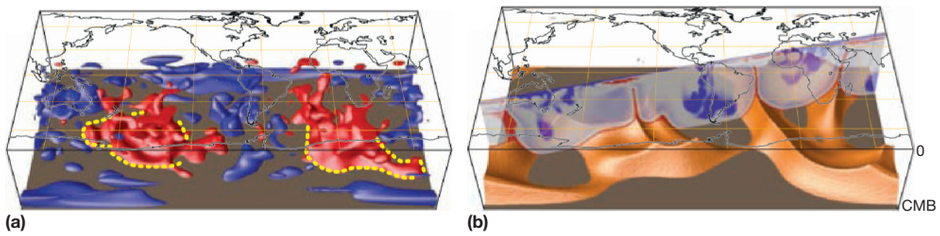

f0145 **Figure 28** From Garnero and McNamara (2008). Comparison of (a) tomographic shear-wave model S20RTS (Ritsema et al., 2004) with (b) a numerical simulation of whole mantle thermochemical convection. Blue and red isosurfaces in (a) denote lower mantle domains that are anomalously fast and slow (±0.6%), respectively. The large, seismically slow regions at the base of the mantle are the LLSVPs. Yellow dashed lines demarcate the steep gradient in shear-wave velocity as evident along the edges of both LLSVPs (Garnero et al., 2007). (b) Modeled chemically dense material (orange isosurfaces) accumulates as piles at the base of the mantle, a possible explanation for the LLSVPs. In cross section, colors denote temperature from red (hot) to blue (cold).

have been shown to be spatially related to the margins of LLSVPs in the lowermost mantle (Burke and Torsvik, 2004; Torsvik et al., 2006, 2010a; **Figures 28(a)** and **29(b)**). This relation holds if the advection of the putative underlying plumes by ambient mantle flow is accounted for (Boschi et al., 2007). The LLSVPs are hot domes or ridges (**Figure 28(b)**) of chemically dense materials (one located beneath Africa, another beneath the South Pacific) with significant topography (500–1000 km) (Garnero and McNamara, 2008; Ishii and Tromp, 1999; Masters et al., 2000; Mosca et al., 2012). Geographic variations seen in OIB geochemistry such as the large-scale DUPAL anomaly (Dupre and Allegre, 1983) have indeed been associated with the LLSVPs (Castillo, 1988; Wen, 2006).

p0865 The origin of these large chemically distinct structures is related to the accretion and chemical differentiation of our planet. For example, they may represent primordial material that is unmodified by subsequent melting, or they may be the residuum of a basal magma ocean as formed very early in the Earth's history (Deschamps et al., 2012; Kellogg et al., 1999; Labrosse et al., 2007; Mukhopadhyay, 2012). Along these lines, the LLSVPs have been identified as good candidates to host the FOZO reservoir, a common member in many hot spot lavas (see **Section 133.3.6.1**). As an alternative, or perhaps in addition to these ancient origins for the LLSVPs, subducted crust composed of dense eclogitic material is expected to settle and accumulate at the base of the mantle (Brandenburg and van Keken, 2007; Brandenburg et al., 2008; Nakagawa et al., 2010). Such a replenishment of the LLSVPs would further strengthen the connection of mantle plumes with LLSVPs, as subduction-related isotope geochemical signatures are common in OIB (e.g., Hofmann, 1997). Both numerical and analogue models indicate that mantle plumes can indeed be anchored by the stable topography provided by high-density layers (such as by the LLSVPs) (Davaille et al., 2002; Jellinek and Manga, 2002; McNamara and Zhong, 2004).

p0870 Global mantle convection models (e.g., McNamara and Zhong, 2005) indicate that any dense thermochemical material would be swept away from subduction zones and toward regions of diffuse upwelling. Using a realistic subduction history and assuming a compositional density difference of ~2%, the dense layer is shaped into structures similar to the imaged LLSVPs (e.g., Steinberger and Torsvik, 2012; **Figure 29**). The predicted diffuse upwellings forming above the LLSVPs may account for the broad dynamic uplift of the overlying lithosphere (i.e., the South Pacific and African Superswells (Adam et al., 2010; Cadio et al., 2011; Hillier and Watts, 2004; Nyblade and Robinson, 1994).

p0875 The details of the organization of such upwelling flow, however, remain to be understood (see also **Chapter 136**). Many models predict upward flow to focus near the crests of the thermochemical structures (Davaille, 1999; McNamara et al., 2010). Such a flow pattern could only be consistent with the spatial patterns of hot spot volcanism if the LLSVPs represented multiple ridges, swept together by ambient mantle flow to form complex structures (**Figure 28(b)**). However, other models show that plume-like upwelling can also occur from the margins of thermochemical structures. According to Steinberger and Torsvik (2012), large-scale mantle flow tends to sweep the thermal boundary layer toward the margins of the LLSVPs to trigger plume ascent. Plume ascent from the margins is further promoted by a lower compressibility in LLSVP than in ambient mantle materials, which causes LLSVPs to form dome-like structures with steep sides, instead of ridgelike features with shallower sloping sides (Tan and Gurnis, 2007; Tan et al., 2011). Seismic constraints are insufficient to distinguish between dome-like and ridgelike geometries for the LLSVPs (cf. Bull et al., 2009; Lassak et al., 2007; Lay and Garnero, 2011).

133.3.7.2 Interaction of plumes with plate tectonic processes s0245

p0880 Not only plate tectonic processes such as slab subduction do influence plume locations by piling up thermochemical material at the base of the mantle (**Figures 28** and 29), but also they can directly interact with individual rising plumes. Recent analogue models (Druken, 2012; Kincaid et al., 2013) show that the regional flow field imposed by a sinking slab (cf. Long and Silver, 2009) can distort plume ascent, thereby strongly altering their surface expressions (**Figure 30**). For example, plume flow is predicted to be guided around a slab edge, as is evident, for example, by Samoan-plume geochemical signatures in the juxtaposed northern Lau back-arc basin (e.g., Jackson et al., 2010; Lupton et al., 2012; Lytle et al., 2012). Such a massive disruption of plume ascent could perhaps also give an explanation for the occurrence of extensive secondary volcanism on the Samoan Islands (cf. Hart et al., 2004; Konter and Jackson, 2012; Koppers et al., 2011b; Natland, 1980).

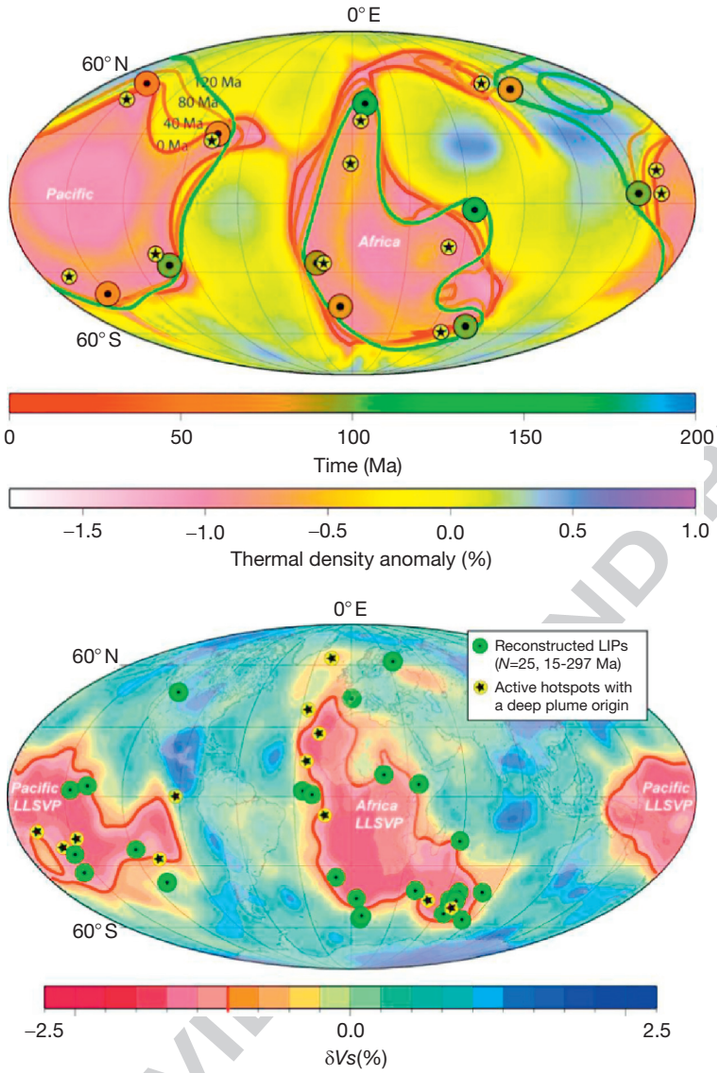

f0150 **Figure 29** Reproduced from B and Antretter M (2006) Conduit diameter and buoyant rising speed of mantle plumes: Implications for the motion of hot spots and shape of plume conduits. *Geochemistry, Geophysics, Geosystems* 7. (top) Representation of their numerical model predictions at 2800 km depth with colors showing thermal density variations (at 0 Ma, i.e., present day; cf. lower color scale) and lines marking the locations of predicted margins of the thermochemical domes (at 120, 80, 40 and 0 Ma). The models are based on subduction locations and fluxes inferred from global plate reconstructions. Large colored circles denote sites, where predicted plume heads first reach the base of the lithosphere (model time: color-coded; cf. upper color scale), corresponding to predicted LIPs. Small yellow circles with stars denote present-day location of plume tails, corresponding to predicted hot spots. Occasionally, a modeled plume disappears or splits into two; therefore, not all predicted LIPs correspond to exactly one predicted hot spot. (bottom) S-wave tomography model SMEAN (Becker and Boschi, 2002) and reconstructed locations of LIPs and present-day hot spot positions (Torsvik et al., 2010a) are shown for comparison.

p0885 Slab–plume interaction is also likely to occur in the western United States. Although this region is well illuminated seismically (see **Section 133.2.5.2**), no consensus model has emerged for the origin of the Columbia River basalt (CRB) and YSRP hot spot track. The seismic images (**Figure 17**) have been interpreted as revealing warm mantle exploiting a slab gap in the remnant Farallon slab and rising through it when the gap first formed, approximately coinciding with CRB emplacement (James et al., 2011). This interpretation is supported by geodynamic modeling (Liu and Stegman, 2011, 2012). However, it remains controversial whether the mantle upwelling just arises from return flow through the slab gap driven by a local gradient in dynamic pressure (James et al., 2011; Liu and Stegman, 2011, 2012) or is rather a mantle plume driven by excess buoyancy of hot material (Darold and Humphreys, 2013; Obrebski et al., 2010; Sigloch, 2011). Dismissing a plume origin altogether appears to be at odds with observations of a deep-rooted low-velocity anomaly beneath Yellowstone, as well as with the coinciding upwarping of the 660 km discontinuity (Schmandt et al., 2012; **Figure 17(b)**).

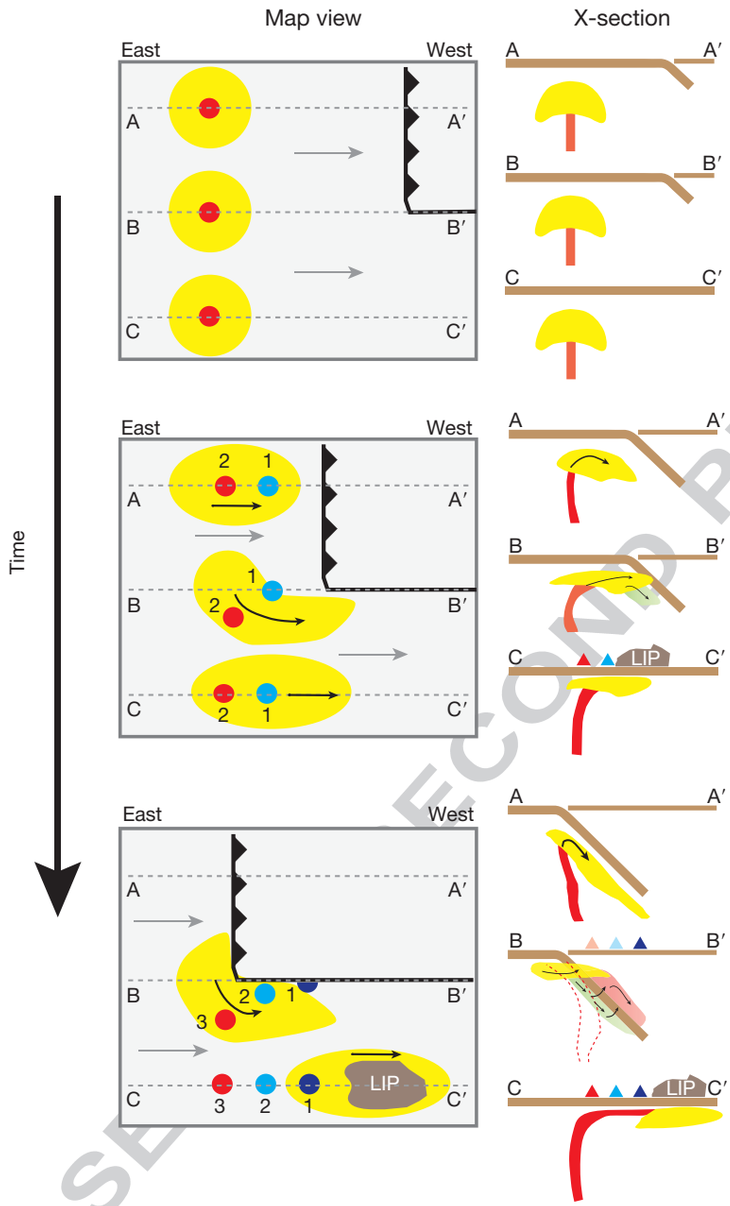

f0155 **Figure 30** From Druken (2012). Cartoons summarizing the results of analogue models of plume–slab interaction in a time series (top to bottom). In map view, left column shows the surface projection of three upwelling plumes in three distinct tectonic configurations (plume–subducting slab, plume–slab edge, and intraplate plume). Projections of the actively upwelling plume tail (i.e., predicted hot spot location) and plume head are denoted red and yellow, respectively. Blue dots in the bottom panels show locations of previous hot spot activity migrated by plate motion with numbers labeling the progression of volcanism. Right column shows vertical cross sections of the plume head (yellow) and tail (red) along the profiles shown in left column with triangles marking the predicted hot spot track. Material displaced into and out of the plane by complex plume–slab edge interaction in cross section B–B′ is denoted light red and light green, respectively.

The complex seismic structure of the anomaly, which continues to challenge any interpretations in the classical framework of plume theory, may be explained by plume bending around slab fragments and/or plume pulsations rising out of the lower mantle (Schmandt et al., 2012). Moreover, Kincaid et al. (2013) argued that some plume material is systematically entrained into the mantle wedge to explain age-progressive volcanism along the HLPs (Figure 8).

Another discussion involves whether segmentation of p0890 the Farallon slab occurred independently of (Sigloch, 2011) or was assisted by the putative Yellowstone plume (Obrebski et al., 2010). For example, the arrival of the plume head may have perturbed the slab enough to cause part of the slab to become convectively unstable, drip downward (i.e., the Farallon 'curtain', FC in Figure 17), and create the gap through which the plume rose (Darold and Humphreys, 2013). In this

scenario, plume material may have been dammed up by the previously intact slab, with the initial burst of plume material through the slab gap perhaps explaining CRB volcanism.

p0895 Slabs are not only able to guide plume ascent but may also trigger mantle upwellings. Small, hydrous plumes have been proposed to rise from the top of the subducted slab to support arc volcanism (Gerya and Yuen, 2003), as well as to hydrate the transition zone (Richard and Bercovici, 2009). Also, slabs stagnating at the base of the upper mantle may sweep material to cause plume-like upwelling and volcanism in the back-arc (Faccenna et al., 2010). In turn, plume heads are able to lubricate or even to actively push plates (Cande and Stegman, 2011; van Hinsbergen et al., 2011).

p0900 Plumes also interact with divergent plate boundaries. For example, the Iceland plume alters plate geometries by inducing ridge jumps and ridge propagators to pin the spreading center to the hot spot (Brozena and White, 1990; Hardarson et al., 1997; Hey et al., 2010; Mittelstaedt et al., 2011; 2012). Similar interactions may have pinned the Réunion hot spot close to the Central Indian Ridge until ~30 Ma (cf. Tiwari et al., 2007).

p0905 In addition, a variety of geochemical and geophysical evidences show that plume material tends to be drawn toward as well as along seafloor spreading centers (e.g., Schilling et al., 1985; Schilling, 1991; Georgen et al., 2001; see also review by Ito et al., 2003). Geodynamic models show that a combination of self-gravitational spreading, sublithospheric topography, and a dynamic pressure low beneath the ridge facilitate this interaction, whereas divergent flow away from the ridge due to seafloor spreading tends to inhibit the interaction (Feighner and Richards, 1995; Ito et al., 1996, 1997; Ribe, 1996; Ribe and Delattre, 1998; Ribe et al., 1995; Sleep, 1996; Yale and Phipps Morgan, 1998). The depleted residue of hot spot melting and the downwelling curtain forming around a plume pancake may choke nearby MOR melting (Singh et al., 2011; Zhou and Dick, 2013).

s0250 133.3.7.3 Lithospheric controls on volcanism

p0910 In addition to their effects on mantle convective processes, the lithospheric plates can control how ascending magmas are focused to form discrete volcanic edifices. The weight of a volcano exerts stresses on the lithosphere that can redirect magma-filled cracks toward a volcano (Müller et al., 2001), but the effects of lithospheric damage (i.e., thermomechanical erosion of magma pathways and/or melting of the wall rock) are essential to stabilize near-vertical melt extraction directly beneath a volcano (Hieronymus and Bercovici, 2001a). Parameterized models of damage-enhanced lithospheric melt permeability predict the formation of chains with realistic volcano spacing, as distal tectonic stresses are perturbed by the load of the volcanic edifices (Hieronymus and Bercovici, 1999; 2000; 2001b). Perturbation by volcanic loading can also explain the volcano patterns in the Hawaiian Islands (Hieronymus and Bercovici, 1999; ten Brink, 1991), which are expressed as a double chain of staggered volcanoes (Jackson et al., 1972).

p0915 Other studies have argued that the lithosphere not only acts as a spatial filter for melts derived from the mantle but also may control the occurrence and timing of volcanic activity itself. An important requirement for this theory is that magmas can be quasi-ubiquitously stabilized in the oceanic asthenosphere (Hirschmann, 2010) or at the base of the oceanic plates (Sakamaki et al., 2013). Such a stabilization has been advocated for to explain the seismic and electric properties of the asthenosphere and/or the sharpness of the lithosphere–asthenosphere boundary (Anderson and Sammis, 1970; Kawakatsu et al., 2009; Naif et al., 2013), an interpretation that however remains controversial (Faul and Jackson, 2005; Karato, 2012, 2013a,b; Karato and Jung, 1998; Stixrude and Lithgow-Bertelloni, 2005). Explaining these geophysical properties and intraplate volcanism at the same time by this mechanism, however, requires a mechanism for melt replenishment.

p0920 Volcanic ridges or island chains have been specifically related to intraplate deformation in response to regional (e.g., Clouard and Gerbault, 2008; Sandwell et al., 1995) and local (e.g., Mittelstaedt and Ito, 2005) tectonic stresses or thermal contraction (Gans et al., 2003; Sandwell and Fialko, 2004). For example, Clouard and Gerbault (2008) argued that regional transtensional stresses associated with the rapid subduction along the Tonga–Kermadec Trench damage the Pacific Plate to allow ascent of magmas along a belt across French Polynesia. Hieronymus and Bercovici (1999, 2000) had shown that perturbation of the stress field by volcanic loading (see preceding text) controls the propagation direction (i.e., parallel to deviatoric tensile stresses) of stress-induced volcanism with opportunities for rejuvenated volcanism on the second volcano of the self-propagating chain. Propagation speed and extent are predicted to be limited by the growth of the volcanic edifices and the abundance of sublithospheric melts, respectively. For example, the availability of melts (if not ubiquitous) as potentially controlled by large-scale mantle convection (e.g., diffuse upwelling beneath the South Pacific Superswell) or more localized asthenospheric upwelling (see **Sections 133.3.3.5–133.3.3.8**) may restrict the final length of the chain.

p0925 Accordingly, discrimination between lithospheric controls and other mechanisms for non-hot spot intraplate volcanism remains challenging. Whereas plume theory provides relatively clear and unique testable predictions in terms of geographic age patterns, predictions related to lithospheric controls, small-scale convection (**Section 133.3.3.5**), buoyant decompression melting (**Section 133.3.3.6**), and shear-driven upwelling (**Section 133.3.3.7**) are generally more complex. Distinguishing between these mechanisms thus requires sufficient geochronological data (and appropriate statistical analysis) and/or additional geophysical constraints (Harmon et al., 2011). Future such efforts are needed to understand whether it is melt production, extraction, or ascent that is the bottleneck that limits volcanic activity in the interior of oceanic as well as continental plates.

133.4 Conclusion

s0255

p0930 In the past few decades, our understanding of hot spots and melting anomalies has seen great advancements. It has been realized that not all melting anomalies are related to hot spot activity and that not all hot spots are necessarily underlain by a mantle plume. Many alternative mechanisms for sustaining mantle melting have been proposed and in some cases have been successfully tested with observations (see **Sections 133.3.3.5–133.3.3.8** and **133.3.7.3**). In particular, non-hot spot volcano

chains are best explained by non-plume mechanisms. Yet, plumes remain a viable explanation for large and long-lived hot spots and many LIPs.

p0935 Classical plume theory makes a range of specific testable predictions, some of which are successful, whereas others fail at a given hot spot. While the most robust predictions of plume theory have been confirmed to at least the first order at many hot spot chains, second-order departures of observations from predictions require revision of the classical concept. These departures may be related to, for example, thermochemical convection, variable mantle properties, and interaction of plumes with large-scale or regional mantle flow. That plumes may indeed rise from the lower mantle has been confirmed by the spatial correlation of hot spots with structures in the deep mantle and, for a subset of hot spots, by regional seismic tomography studies. Future advancements to understand mantle dynamics and composition by studying melting anomalies will require interdisciplinary efforts including geophysicists, geochemists, geologists, and mineral physicists.

Acknowledgments

We thank Dave Bercovici for editorial guidance and comments that helped to greatly improve the manuscript. M.D.B. and G.I. have been supported by NSF grant EAR-1141938.

References

Aarnes I, Svensen H, Connolly JAD, and Podladchikov YY (2010) How contact metamorphism can trigger global climate changes: Modeling gas generation around igneous sills in sedimentary basins. *Geochimica et Cosmochimica Acta* 74: 7179–7195.

Abalos B, Fountain DM, Ibarguchi JIG, and Puelles P (2011) Eclogite as a seismic marker in subduction channels: Seismic velocities, anisotropy, and petrofabric of Cabo Ortegal eclogite tectonites (Spain). *Geological Society of America Bulletin* 123: U439–U477.

Abouchami W, Hofmann AW, Galer SJG, Frey FA, Eisele J, and Feigenson M (2005) Lead isotopes reveal bilateral asymmetry and vertical continuity in the Hawaiian mantle plume. *Nature* 434: 851–856.

Acton GD and Gordon RG (1994) Paleomagnetic tests of Pacific plate reconstructions and implications for motion between hotspots. *Science* 263: 1246–1254.

Adam C and Bonneville A (2005) Extent of the South Pacific Superswell. *Journal of Geophysical Research* 110.

Adam C and Bonneville A (2008) No thinning of the lithosphere beneath northern part of the Cook-Austral volcanic chains. *Journal of Geophysical Research* 113.

Adam C, Vidal V, and Escartin J (2007) 80-Myr history of buoyancy and volcanic fluxes along the trails of the Walvis and St. Helena hotspots (South Atlantic). *Earth and Planetary Science Letters* 261: 432–442.

Adam C, Yoshida M, Isse T, Suetsugu D, Fukao Y, and Barruol G (2010) South Pacific hotspot swells dynamically supported by mantle flows. *Geophysical Research Letters* 37.

Adams A, Nyblade A, and Weeraratne D (2012) Upper mantle shear wave velocity structure beneath the East African plateau: Evidence for a deep, plateauwide low velocity anomaly. *Geophysical Journal International* 189: 123–142.

Afonso JC, Zlotnik S, and Fernandez M (2008) Effects of compositional and rheological stratifications on small-scale convection under the oceans: Implications for the thickness of oceanic lithosphere and seafloor flattening. *Geophysical Research Letters* 35.

Agrusta R, Arcay D, Tommasi A, Davaille A, Ribe N, and Gerya T (2013) Small-scale convection in a plume-fed low-viscosity layer beneath a moving plate. *Geophysical Journal International* 194: 591–610.

Albers M and Christensen UR (1996) The excess temperature of plumes rising from the core-mantle boundary. *Geophysical Research Letters* 23: 3567–3570.

Ali JR, Thompson GM, Zhou MF, and Song XY (2005) Emeishan large igneous province, SW China. *Lithos* 79: 475–489.

Allegre CJ, Birck JL, Capmas F, and Courtillot V (1999) Age of the Deccan traps using ^{187}Re–^{187}Os systematics. *Earth and Planetary Science Letters* 170: 197–204.

Allen MB, Anderson L, Searle RC, and Buslov M (2006) Oblique rift geometry of the West Siberian Basin: Tectonic setting for the Siberian flood basalts. *Journal of the Geological Society* 163: 901–904.

Allen RM, Nolet G, Morgan WJ, et al. (1999) The thin hot plume beneath Iceland. *Geophysical Journal International* 137: 51–63.

Allen RM, Nolet G, Morgan WJ, et al. (2002) Imaging the mantle beneath Iceland using integrated seismological techniques. *Journal of Geophysical Research* 107. http://dx.doi.org/10.1029/2001JB000595.

Allen RM and Tromp J (2005) Resolution of regional seismic models: Squeezing the Iceland anomaly. *Geophysical Journal International* 161: 373–386.

Anderson DL (1989) *Theory of the Earth*, p. 366. Brookline Village, MA: Blackwell.

Anderson DL (1994a) The sublithospheric mantle as the source of continental flood basalts; the case against the continental lithosphere and plume head reservoirs. *Earth and Planetary Science Letters* 123: 269–280.

Anderson DL (1994b) Superplumes or supercontinents? *Geology* 22: 39–42.

Anderson DL (2005) Large igneous provinces, delamination, and fertile mantle. *Elements* 1: 271–275.

Anderson DL and Sammis C (1970) Partial melting in the upper mantle. *Physics of the Earth and Planetary Interiors* 3: 41–50.

Andrews DL, Gordon RG, and Horner-Johnson BC (2006) Uncertainties in plate reconstructions relative to the hotspots: Pacific-hotspot rotations and uncertainties for the past 68 million years. *Geophysical Journal International* 166: 939–951.

Antretter M, Riisager P, Hall S, Zhao X, and Steinberger B (2004) Modelled paleolatitudes for the Louisville hot spot and the Ontong Java Plateau. *Geological Society of America* 299: 21–30, Special Publication.

Aoki I and Takahashi E (2004) Density for MORB eclogite in the upper mantle. *Physics of the Earth and Planetary Interiors* 143–144: 129–143.

Asaadi N, Ribe NM, and Sobouti F (2011) Inferring nonlinear mantle rheology from the shape of the Hawaiian swell. *Nature* 473: U243–U501.

Asimow P and Langmuir CH (2003) The importance of water to oceanic melting regimes. *Nature* 421: 815–820.

Ayalew D, Barbey P, Marty B, Reisberg L, Yirgu G, and Pik R (2002) Source, genesis, and timing of giant ignimbrite deposits associated with Ethiopian continental flood basalts. *Geochimica et Cosmochimica Acta* 66: 1429–1448.

Bagley B and Nyblade AA (2013) Seismic anisotropy in eastern Africa, mantle flow, and the African superplume. *Geophysical Research Letters* 40: 1500–1505.

Ballmer MD, Conrad CP, Smith EI, and Harmon N (2013a) Non-hotspot volcano chains produced by migration of shear-driven upwelling toward the East Pacific Rise. *Geology* 371: 199–202.

Ballmer MD, Ito G, and Cheng C (in press) Thermochemical convection of bilaterally asymmetric plumes and implications for Hawaiian lava composition. In: Carey R, Poland M, Cayol V, and Weis D (eds.) *Hawaiian Volcanism, From Source to Surface. AGU Monograph*.

Ballmer MD, Ito G, van Hunen J, and Tackley PJ (2010) Small-scale sublithospheric convection reconciles geochemistry and geochronology of 'Superplume' volcanism in the western and south Pacific. *Earth and Planetary Science Letters* 290: 224–232.

Ballmer MD, Ito G, van Hunen J, and Tackley PJ (2011) Spatial and temporal variability in Hawaiian hotspot volcanism induced by small-scale convection. *Nature Geoscience* 4: 457–460.

Ballmer MD, Ito G, Wolfe CJ, and Solomon SC (2013b) Double layering of a thermochemical plume in the upper mantle beneath Hawaii. *Earth and Planetary Science Letters* 376: 155–164.

Ballmer MD, van Hunen J, Ito G, Bianco TA, and Tackley PJ (2009) Intraplate volcanism with complex age-distance patterns: A case for small-scale sublithospheric convection. *Geochemistry, Geophysics, Geosystems* 10.

Ballmer MD, van Hunen J, Ito G, Tackley PJ, and Bianco TA (2007) Non-hotspot volcano chains originating from small-scale sublithospheric convection. *Geophysical Research Letters* 34.

Barry TL, Self S, Kelley SP, Reidel S, Hooper P, and Widdowson M (2010) New Ar-40/Ar-39 dating of the Grande Ronde lavas, Columbia River Basalts, USA: Implications for duration of flood basalt eruption episodes. *Lithos* 118: 213–222.

Bastow ID, Stuart GW, Kendall JM, and Ebinger CJ (2005) Upper-mantle seismic structure in a region of incipient continental breakup: Northern Ethiopian rift. *Geophysical Journal International* 162: 479–493.

Becker TW and Boschi L (2002) A comparison of tomographic and geodynamic mantle models. *Geochemistry, Geophysics, Geosystems* 3.

Becker TW, Faccenna C, Humphreys ED, Lowry AR, and Miller MS (2013) Static and dynamic support of western United States topography. *Earth and Planetary Science Letters*. http://dx.doi.org/10.1016/j.epsl.2013.10.012.

Beier C, Haase KM, and Turner SP (2012) Conditions of melting beneath the Azores. *Lithos* 144: 1–11.

Benard F, Callot J-P, Vially R, et al. (2010) The Kerguelen plateau: Records from a long-living/composite microcontinent. *Marine and Petroleum Geology* 27: 633–649.

Benoit MH, Nyblade AA, and VanDecar JC (2006) Upper mantle P-wave speed variations beneath Ethiopia and the origin of the Afar hotspot. *Geology* 34: 329–332.

Bercovici D and Kelly A (1997) The non-linear initiation of diapirs and plume heads. *Physics of the Earth and Planetary Interiors* 101: 119–130.

Bianco TA, Conrad CP, and Smith EI (2011a) Time dependence of intraplate volcanism caused by shear-driven upwelling of low-viscosity regions within the asthenosphere. *Journal of Geophysical Research* 116.

Bianco TA, Ito G, Becker JM, and Garcia MO (2005) Secondary Hawaiian volcanism formed by flexural arch decompression. *Geochemistry, Geophysics, Geosystems* 6: Q08009. http://dx.doi.org/10.01029/02005GC000945.

Bianco TA, Ito G, van Hunen J, Ballmer MD, and Mahoney JJ (2008) Geochemical variation at the Hawaiian hot spot caused by upper mantle dynamics and melting of a heterogeneous plume. *Geochemistry, Geophysics, Geosystems* 9.

Bianco TA, Ito G, van Hunen J, Ballmer MD, and Mahoney JJ (2011b) Geochemical variations at intraplate hot spots caused by variable melting of a veined mantle plume. *Geochemistry, Geophysics, Geosystems* 12.

Bianco TA, Ito G, van Hunen J, Mahoney JJ, and Ballmer MD (2013) Geochemical variations at ridge-centered hotspots caused by variable melting of a veined mantle plume. *Earth and Planetary Science Letters* 371: 191–202.

Biggin AJ, Steinberger B, Aubert J, et al. (2012) Possible links between long-term geomagnetic variations and whole-mantle convection processes. *Nature Geoscience* 5: 526–533.

Bijwaard H and Spakman W (1999) Tomographic evidence for a narrow whole mantle plume below Iceland. *Earth and Planetary Science Letters* 166: 121–126.

Bijwaard H, Spakman W, and Engdahl ER (1998) Closing the gap between regional and global travel time tomography. *Journal of Geophysical Research* 103: 30055–30078.

Bjarnason IT, Silver PG, Rumpker G, and Solomon SC (2002) Shear wave splitting across the Iceland hot spot: Results from the ICEMELT experiment. *Journal of Geophysical Research* 107: 2382. http://dx.doi.org/10.1029/2001JB000916.

Black BA, Elkins-Tanton LT, Rowe MC, and Peate IU (2012) Magnitude and consequences of volatile release from the Siberian Traps. *Earth and Planetary Science Letters* 317: 363–373.

Blackburn TJ, Olsen PE, Bowring SA, et al. (2013) Zircon U–Pb geochronology links the End-Triassic extinction with the Central Atlantic Magmatic Province. *Science* 340: 941–945.

Boehler R (2000) High-pressure experiments and the phase diagram of lower mantle and core materials. *Reviews of Geophysics* 38: 221–245.

Bonatti E and Harrison CGA (1976) Hot lines in the Earth's mantle. *Nature* 263: 402–404.

Bonatti E, Harrison CGA, Fisher DE, et al. (1977a) Easter volcanic chain (southeast Pacific): A mantle hot line. *Journal of Geophysical Research* 82: 2457–2478.

Bonneville A, Dosso L, and Hildenbrand A (2006) Temporal evolution and geochemical variability of the South Pacific superplume activity. *Earth and Planetary Science Letters* 244: 251–269.

Bonneville A, Le Suave R, Audin L, et al. (2002) Arago Seamount: The missing hotspot found in the Austral Islands. *Geology* 30: 1023–1026.

Boschi L, Becker TW, and Steinberger B (2007) Mantle plumes: Dynamic models and seismic images. *Geochemistry, Geophysics, Geosystems* 8.

Boschi L, Becker TW, and Steinberger B (2008) On the statistical significance of correlations between synthetic mantle plumes and tomographic models. *Physics of the Earth and Planetary Interiors* 167: 230–238.

Bourdon B, Joron J-L, Claude-Ivanaj C, and Allegre CJ (1998) U–Th–Pa–Ra systematics for the Grande Comore volcanics: Melting processes in an upwelling plume. *Earth and Planetary Science Letters* 164: 119–133.

Bourdon B, Ribe NM, Stracke A, Saal AE, and Turner SP (2006) Insights into the dynamics of mantle plumes from uranium-series geochemistry. *Nature* 444: 713–717.

Bourdon B, Turner SP, and Ribe NM (2005) Partial melting and upwelling rates beneath the Azores from a U-series isotope perspective. *Earth and Planetary Science Letters* 239: 4256.

Brand U, Posenato R, Came R, et al. (2012) The end-Permian mass extinction: A rapid volcanic CO_2 and CH_4-climatic catastrophe. *Chemical Geology* 322: 121–144.

Brandenburg JP, Hauri EH, van Keken PE, and Ballentine CJ (2008) A multiple-system study of the geochemical evolution of the mantle with force-balanced plates and thermochemical effects. *Earth and Planetary Science Letters* 276: 1–13.

Brandenburg JP and van Keken PE (2007) Deep storage of oceanic crust in a vigorously convecting mantle. *Journal of Geophysical Research* 112.

Breger L, Romanowicz B, and Ng C (2001) The Pacific plume as seen by S, ScS, and SKS. *Geophysical Research Letters* 28: 1859–1862.

Breivik AJ, Mjelde R, Faleide JI, and Murai Y (2006) Rates of continental breakup magmatism and seafloor spreading in the Norway Basin–Iceland plume interaction. *Journal of Geophysical Research – Solid Earth* 111, B07102.

Brozena JM and White RS (1990) Ridge jumps and propagations in the South Atlantic Ocean. *Nature* 348: 149–152.

Brunet D and Yuen DA (2000) Mantle plumes pinched in the transition zone. *Earth and Planetary Science Letters* 178: 13–27.

Bryan SE, Peate IU, Peate DW, et al. (2010) The largest volcanic eruptions on Earth. *Earth-Science Reviews* 102: 207–229.

Buck WR (1986) Small-scale convection induced by passive-rifting: the cause for uplift of rift shoulders. *Earth and Planetary Science Letters* 77: 362–372.

Buck WR and Parmentier EM (1986) Convection beneath young oceanic lithosphere: Implications for thermal structure and gravity. *Journal of Geophysical Research* 91: 1961–1974.

Bull AL, McNamara AK, and Ritsema J (2009) Synthetic tomography of plume clusters and thermochemical piles. *Earth and Planetary Science Letters* 278: 152–162.

Burke K (1996) The African plate. *South African Journal of Geology* 99: 339–409.

Burke K and Torsvik TH (2004) Derivation of Large Igneous Provinces of the past 200 million years from long-term heterogeneities in the deep mantle. *Earth and Planetary Science Letters* 227: 531–538.

Cadio C, Ballmer MD, Panet I, Diament M, and Ribe N (2012) New constraints on the origin of the Hawaiian swell from wavelet analysis of the geoid to topography ratio. *Earth and Planetary Science Letters* 359–360: 40–54.

Cadio C, Panet I, Davaille A, Diament M, Metivier L, and de Viron O (2011) Pacific geoid anomalies revisited in light of thermochemical oscillating domes in the lower mantle. *Earth and Planetary Science Letters* 306: 123–135.

Camp VE and Hanan BB (2008) A plume-triggered delamination origin for the Columbia River Basalt Group. *Geosphere* 4: 480–495.

Campbell IH (2007) Testing the plume theory. *Chemical Geology* 241: 153–176.

Campbell IH and Griffiths RW (1990) Implications of mantle plume structure for the evolution of flood basalts. *Earth and Planetary Science Letters* 99: 79–93.

Campbell IH and Kerr AC (2007) The Great Plume Debate: Testing the plume theory. *Chemical Geology* 241: 149–152.

Cande SC and Stegman DR (2011) Indian and African plate motions driven by the push force of the Reunion plume head. *Nature* 475: 47–52.

Cao Q, van der Hilst RD, de Hoop MV, and Shim SH (2011) Seismic imaging of transition zone discontinuities suggests hot mantle west of Hawaii. *Science* 332: 1068–1071.

Caress DW, McNutt MK, Detrick RS, and Mutter JC (1995) Seismic imaging of hotspot-related crustal underplating beneath the Marquesas Islands. *Nature* 373: 600–603.

Carlson RW, Czamanske G, Fedorenko V, and Ilupin I (2006) A comparison of Siberian meimechites and kimberlites: Implications for the source of high-Mg alkalic magmas and flood basalts. *Geochemistry, Geophysics, Geosystems* 7.

Castillo P (1988) The dupal anomaly as a trace of the upwelling lower mantle. *Nature* 336: 667–670.

Chandler MT, Wessel P, Taylor B, Seton M, Kim S-S, and Hyeong K (2012) Reconstructing Ontong Java Nui: Implications for Pacific absolute plate motion, hotspot drift and true polar wander. *Earth and Planetary Science Letters* 331: 140–151.

Chang HK, Kowsmann RO, Figueiredo AMF, and Bender AA (1992) Tectonics and stratigraphy of the East Brazil Rift system – An overview. *Tectonophysics* 213: 97–138.

Chang S-J and Van der Lee S (2011) Mantle plumes and associated flow beneath Arabia and East Africa. *Earth and Planetary Science Letters* 302: 448–454.

Chauvel C, Maury RC, Blais S, et al. (2012) The size of plume heterogeneities constrained by Marquesas isotopic stripes. *Geochemistry, Geophysics, Geosystems* 13.

Chazey WJ III and Neal CR (2004) Large igneous province magma petrogenesis from source to surface: Platinum-group element evidence from Ontong Java Plateau basalts recovered during ODP legs 130 and 192. In: Fitton JG, Mahoney JJ, Wallace PJ, and Saunders AD (eds.) *Origin and Evolution of the Ontong Java Plateau*, pp. 219–238. London: Geological Society, Special Publications 229.

Chenet A-L, Quidelleur X, Fluteau F, Courtillot V, and Bajpai S (2007) K-40–Ar-40 dating of the Main Deccan large igneous province: Further evidence of KTB age and short duration. *Earth and Planetary Science Letters* 263: 1–15.

Cheng C, Allen RM, Porritt RW, Ballmer MD (in press) Seismic constrains on a double-layered asymmetric whole-mantle plume beneath Hawaii. In Carey R, Poland M, Cayol V, Weis D (eds.) *Hawaiian Volcanism, From Source to Surface, AGU Monograph*.

Christensen U (1984) Instability of a hot boundary-layer and initiation of thermo-chemical plumes. *Annales Geophysicae* 2: 311–319.

Christensen UR and Hofmann AW (1994) Segregation of subducted oceanic crust and the convecting mantle. *Journal of Geophysical Research* 99: 19867–19884.

Clague DA and Dalrymple GB (1987) The Hawaiian-Emperor volcanic chain. In: Decker RW, Wright TL, and Stauffer PH (eds.) *Volcanism in Hawaii*. *U.S. Geological Survey Professional Paper*, vol. 1.

Class C, Goldstein SL, Stute M, Kurz MD, and Schlosser P (2005) Grand Comore Island: A well-constrained "low He-3/He-4" mantle plume. *Earth and Planetary Science Letters* 233: 391–409.

Clift PD, Carter A, and Hurford AJ (1998) The erosional and uplift history of NE Atlantic passive margins: Constraints on a passing plume. *Journal of the Geological Society of London* 155: 787–800.

Clift PD and Turner J (1995) Dynamic support by the Icelandic Plume and vertical tectonics of the Northeast Atlantic continental margins. *Journal of Geophysical Research* 100: 24473–24486.

Clouard V and Bonneville A (2001) How many Pacific hotspots are fed by deep-mantle plumes? *Geology* 29: 695–698.

Clouard V and Bonneville A (2005) Ages of Seamounts, islands, and plateaus on the Pacific plate. In: Foulger G, Natland JH, Presnall DC, and Anderson DL (eds.) *Plumes, Plates, and Paradigms*, pp. 71–90. Boulder, CO: GSA, Special Paper 388.

Clouard V, Bonneville A, and Gillot P-Y (2003) The Tarava Seamounts: A newly characterized hotspot chain on the South Pacific Superswell. *Earth and Planetary Science Letters* 207: 117–130.

Clouard V and Gerbault M (2008) Break-up spots: Could the Pacific open as a consequence of plate kinematics? *Earth and Planetary Science Letters* 265: 195–208.

Coble MA and Mahood GA (2012) Initial impingement of the Yellowstone plume located by widespread silicic volcanism contemporaneous with Columbia River flood basalts. *Geology* 40: 655–658.

Coffin MF (1992) Emplacement and subsidence of Indian Ocean plateaus and submarine ridges. In: Duncan RA, Rea DK, Kidd RB, Rad UV, and Weissel JK (eds.) *Synthesis of Results from Scientific Drilling in the Indian Ocean*. *Geophysical Monograph Series*, 70, pp. 115–125. American Geophysical Union.

Coffin MF and Eldholm O (1993) Scratching the surface: Estimating dimensions of large igneous provinces. *Geology* 21: 515–518.

Coffin MF and Eldholm O (1994) Large igneous provinces: Crustal structure, dimensions, and external consequences. *Reviews of Geophysics* 32: 1–36.

Coffin MF, Pringle MS, Duncan RA, et al. (2002) Kerguelen hotspot magma output since 130 Ma. *Journal of Petrology* 43: 1121–1139.

Cohen RS and O'Nions RK (1982) Identification of recycled continental material in the mantle from Sr, Nd, and Pb isotope investigations. *Earth and Planetary Science Letters* 61: 73–84.

Collier JS, Sansom V, Ishizuka O, Taylor RN, Minshull TA, and Whitmarsh RB (2008) Age of Seychelles–India break-up. *Earth and Planetary Science Letters* 272: 264–277.

Collins JA, Vernon FL, Orcutt JA, and Stephen RA (2002) Upper mantle structure beneath the Hawaiian Swell: Constraints from the ocean seismic network pilot experiment. *Geophysical Research Letters* 29: 1522. http://dx.doi.org/10.1029/2001GL013302.

Coltice N, Bertrand H, Rey P, Jourdan F, Phillips BR, and Ricard Y (2009) Global warming of the mantle beneath continents back to the Archaean. *Gondwana Research* 15: 254–266.

Coltice N, Moreira M, Hernlund J, and Labrosse S (2011) Crystallization of a basal magma ocean recorded by helium and neon. *Earth and Planetary Science Letters* 308: 193–199.

Coltice N, Phillips BR, Bertrand H, Ricard Y, and Rey P (2007) Global warming of the mantle at the origin of flood basalts over supercontinents. *Geology* 35: 391–394.

Coltice N and Ricard Y (1999) Geochemical observations and one layer mantle convection. *Earth and Planetary Science Letters* 174: 125–137.

Condie KC (2001) *Mantle Plumes and Their Record in Earth History,* p. 306. Cambridge, UK: Cambridge University Press.

Connolly JAD and Kerrick DM (2002) Metamorphic controls on seismic velocity of subducted oceanic crust at 100–250 km depth. *Earth and Planetary Science Letters* 204: 61–74.

Conrad CP and Behn MD (2010) Constraints on lithosphere net rotation and asthenospheric viscosity from global mantle flow models and seismic anisotropy. *Geochemistry, Geophysics, Geosystems* 11.

Conrad CP, Bianco TA, Smith EI, and Wessel P (2011) Patterns of intraplate volcanism controlled by asthenospheric shear. *Nature Geoscience* 4: 317–321.

Conrad CP, Wu B, Smith EI, Bianco TA, and Tibbetts A (2010) Shear-driven upwrelling induced by lateral viscosity variations and asthenospheric shear: A mechanism for intraplate volcanism. *Physics of the Earth and Planetary Interiors* 178: 162–175.

Constable S and Heinson G (2004) Hawaiian hot-spot swell structure from seafloor MT sounding. *Tectonophysics* 389: 111–124.

Cordery MJ, Davies GF, and Cambell IH (1997) Genesis of flood basalts from eclogite-bearing mantle plumes. *Journal of Geophysical Research* 102: 20179–20197.

Cornwell DG, Hetenyi G, and Blanchard TD (2011) Mantle transition zone variations beneath the Ethiopian Rift and Afar: Chemical heterogeneity within a hot mantle? *Geophysical Research Letters* 38.

Cottaar S and Romanowicz B (2012) An unusually large ULVZ at the base of the mantle near Hawaii. *Earth and Planetary Science Letters* 355: 213–222.

Courtier AM, Jackson MG, Lawrence JF, et al. (2007) Correlation of seismic and petrologic thermometers suggests deep thermal anomalies beneath hotspots. *Earth and Planetary Science Letters* 264: 308–316.

Courtillot V, Davaille A, Besse J, and Stock J (2003) Three distinct types of hotspots in the Earth's mantle. *Earth and Planetary Science Letters* 205: 295–308.

Courtillot V, Gallet Y, Rocchia R, et al. (2000) Cosmic markers, Ar-40/Ar-39 dating and paleomagnetism of the KT sections in the Anjar Area of the Deccan large igneous province. *Earth and Planetary Science Letters* 182: 137–156.

Courtillot V and Olson P (2007) Mantle plumes link magnetic superchrons to phanerozoic mass depletion events. *Earth and Planetary Science Letters* 260: 495–504.

Courtillot VE and Renne PR (2003) On the ages of flood basalt events. *Comptes Rendus Geoscience* 335: 113–140.

Cox KG (1988) The Karoo province. In: MacDougall JD (ed.) *Continental Flood Basalts*, pp. 239–271. Dordrecht: Kluwer Academic.

Crosby AG and McKenzie D (2009) An analysis of young ocean depth, gravity and global residual topography. *Geophysical Journal International* 178: 1198–1219.

Crough ST (1978) Thermal origin of mid-plate hot-spot swells. *Geophysical Journal of the Royal Astronomical Society* 55: 451–469.

Crough ST (1983) Hotspot swells. *Annual Review of Earth and Planetary Sciences* 11: 165–193.

Crow R, Karlstrom K, Asmerom Y, Schmandt B, Polyak V, and DuFrane SA (2011) Shrinking of the Colorado Plateau via lithospheric mantle erosion: Evidence from Nd and Sr isotopes and geochronology of Neogene basalts. *Geology* 39: 27–30.

Cserepes L, Christensen UR, and Ribe NM (2000) Geoid height versus topography for a plume model of the Hawaiian swell. *Earth and Planetary Science Letters* 178: 29–38.

Cserepes L and Yuen DA (2000) On the possibility of a second kind of mantle plume. *Earth and Planetary Science Letters* 183: 61–71.

Cushman B, Sinton J, Ito G, and Dixon JE (2004) Glass compositions, plume-ridge interaction, and hydrous melting along the Galapagos spreading center, 905 degrees W to 98 degrees W. *Geochemistry, Geophysics, Geosystems* 5: Q08E17. http://dx.doi.org/10.1029/2004GC000709.

d'Acremont E, Leroy S, and Burov EB (2003) Numerical modelling of a mantle plume: The plume head-lithosphere interaction in the formation of an oceanic large igneous province. *Earth and Planetary Science Letters* 206: 379–396.

Darold A and Humphreys E (2013) Upper mantle seismic structure beneath the Pacific Northwest: A plume-triggered delamination origin for the Columbia River flood basalt eruptions. *Earth and Planetary Science Letters* 365: 232–242.

Dasgupta R and Hirschmann MM (2006) Melting in the Earth's deep upper mantle caused by carbon dioxide. *Nature* 440: 659–662.

Dasgupta R, Hirschmann MM, and Smith ND (2007) Partial melting experiments of peridotite CO_2 at 3 GPa and genesis of alkalic ocean island basalts. *Journal of Petrology* 48: 2093–2124.

Dasgupta R, Jackson MG, and Lee C-TA (2010) Major element chemistry of ocean island basalts – Conditions of mantle melting and heterogeneity of mantle source. *Earth and Planetary Science Letters* 289: 377–392.

Davaille A (1999) Simultaneous generation of hotspots and superswells by convection in a heterogeneous planetary mantle. *Nature* 402: 756–760.

Davaille A, Girard F, and LeBars M (2002) How to anchor hotspots in a convecting mantle? *Earth and Planetary Science Letters* 203: 621–634.

Davaille A, Gueslin B, Massmeyer A, and Di Giuseppe E (2013) Thermal instabilities in a yield stress fluid: Existence and morphology. *Journal of Non-Newtonian Fluid Mechanics* 193: 144–153.

Davaille A and Jaupart C (1994) Onset of thermal convection in fluids with temperature-dependent viscosity: Application to the oceanic mantle. *Journal of Geophysical Research* 99: 19853–19866.

Davaille A and Vatteville J (2005) On the transient nature of mantle plumes. *Geophysical Research Letters* 32. http://dx.doi.org/10.1029/2005GL023029.

Davies GF (1999) *Dynamic Earth,* p. 458. Cambridge, UK: Cambridge University Press.
Davies GF (2010) Noble gases in the dynamic mantle. *Geochemistry, Geophysics, Geosystems* 11.
Davis AS, Gray LB, Clague DA, and Hein JR (2002) The Line Islands revisited: New $^{40}Ar/^{39}Ar$ geochronologic evidence for episodes of volcanism due to lithospheric extension. *Geochemistry, Geophysics, Geosystems* 3(3). http://dx.doi.org/10.1029/2001GC000190.
Davis FA, Hirschmann MM, and Humayun M (2011) The composition of the incipient partial melt of garnet peridotite at 3 GPa and the origin of OIB. *Earth and Planetary Science Letters* 308: 380–390.
Day JMD, Pearson DG, Macpherson CG, Lowry D, and Carracedo J-C (2009) Pyroxenite-rich mantle formed by recycled oceanic lithosphere: Oxygen-osmium isotope evidence from Canary Island lavas. *Geology* 37: 555–558.
Deenen MHL, Ruhl M, Bonis NR, et al. (2010) A new chronology for the end-Triassic mass extinction. *Earth and Planetary Science Letters* 291: 113–125.
DeLaughter JE, Stein CA, and Stein S (2005) Hotspots: A view from the swells. In: Foulger GR, Natland JH, Presnall DC and Anderson DL (eds.), *Plates, Plumes, and Paradigms*, pp. 257–278. Geological Society of America. Special Paper 388.
Deschamps F, Cobden L, and Tackley PJ (2012) The primitive nature of large low shear-wave velocity provinces. *Earth and Planetary Science Letters* 349: 198–208.
Deschamps F, Kaminski E, and Tackley PJ (2011) A deep mantle origin for the primitive signature of ocean island basalt. *Nature Geoscience* 4: 879–882.
Desonie DL and Duncan RA (1990) The Cobb-Eickelberg seamount chain: Hotspot volcanism with mid-ocean ridge basalt affinity. *Journal of Geophysical Research* 95: 12697–12711.
Detrick RS and Crough ST (1978) Island subsidence, hot spots, and lithospheric thinning. *Journal of Geophysical Research* 83: 1236–1244.
DiVenere V and Kent DV (1999) Are the Pacific and Indo-Atlantic hotspots fixed? Testing the plate circuit through Antarctica. *Earth and Planetary Science Letters* 170: 105–117.
Dodson A, Kennedy BM, and DePaolo DJ (1997) Helium and neon isotopes in the Imnaha Basalt, Columbia River Basalt Group: Evidence for a Yellowstone plume source. *Earth and Planetary Science Letters* 150: 443–451.
Doin MP and Fleitout L (1996) Thermal evolution of the oceanic lithosphere: An alternative view. *Earth and Planetary Science Letters* 142: 121–136.
Doubrovine PV, Steinberger B, and Torsvik TH (2012) Absolute plate motions in a reference frame defined by moving hot spots in the Pacific, Atlantic, and Indian oceans. *Journal of Geophysical Research* 117.
Doucet S, Weis D, Scoates JS, Debaille V, and Giret A (2004) Geochemical and Hf–Pb–Sr–Nd isotopic constraints on the origin of the Amsterdam–St. Paul (Indian Ocean) hotspot basalts. *Earth and Planetary Science Letters* 218: 179–195.
Druken K (2012) *Plumes-Slab Interaction Driven by Rollback Subduction*, PhD Thesis, University of Rhode Island.
Du Z, Vinnik LP, and Foulger GR (2006) Evidence from P-to-S mantle converted waves for a flat "660-km" discontinuity beneath Iceland. *Earth and Planetary Science Letters* 241: 271–280.
Duggen S, Hoernle KA, Hauff F, Klugel A, Bouabdellah M, and Thirlwall MF (2009) Flow of Canary mantle plume material through a subcontinental lithospheric corridor beneath Africa to the Mediterranean. *Geology* 37: 283–286.
Dumoulin C, Choblet G, and Doin MP (2008) Convective interactions between oceanic lithosphere and asthenosphere: Influence of a transform fault. *Earth and Planetary Science Letters* 274: 301–309.
Duncan RA (1978) Geochronology of basalts from the Ninetyeast Ridge and continental dispersion in the Eastern Indian Ocean. *Journal of Volcanology and Geothermal Research* 4: 283–305.
Duncan RA (1984) Age progressive volcanism in the New England Seamounts and the opening of the Central Atlantic Ocean. *Journal of Geophysical Research* 89: 9980–9990.
Duncan RA (1991) Age distribution of volcanism along aseismic ridges in the eastern Indian Ocean. *Proceedings of the Ocean Drilling Program Scientific Results* 121, pp. 507–517. College Station, TX: Ocean Drilling Program.
Duncan RA (2002) A time frame for construction of the Kerguelen Plateau and Broken Ridge. *Journal of Petrology* 43: 1109–1119.
Duncan RA, Backman J, Peterson LC, et al. (1990) The volcanic record of the Reunion hotspot. *Proceedings of the Ocean Drilling Program – Scientific Results* 115: 3–10.
Duncan RA and Clague DA (1985) Pacific plate motion recorded by linear volcanic chains. In: Nairn AEM, Stehli FG, and Uyeda S (eds.) *The Ocean Basins and Margins*, pp. 89–121. New York: Plenum Press.
Duncan RA and Hargraves RB (1984) Caribbean region in the mantle reference frame. In: Bonini W, et al. (eds.) *The Caribbean–South American Plate Boundary and Regional Tectonic. Geological Society of America Memoir*, vol. 162, pp. 89–121. Geological Society of America.
Duncan RA and Keller R (2004) Radiometric ages for basement rocks from the Emperor Seamounts, ODP Leg 197. *Geochemistry, Geophysics, Geosystems* 5: Q08L03. http://dx.doi.org/10.1029/2004GC000704.
Duncan RA and Richards MA (1991) Hotspots, mantle plumes, flood basalts, and true polar wander. *Reviews of Geophysics* 29–1: 31–50.
Dupre B and Allegre CJ (1983) Pb–Sr isotope variation in Indian-Ocean basalts and mixing phenomena. *Nature* 303: 142–146.
Dziewonski AM, Lekic V, and Romanowicz BA (2010) Mantle anchor structure: An argument for bottom up tectonics. *Earth and Planetary Science Letters* 299: 69–79.
Ebinger CJ and Sleep NH (1998) Cenozoic magmatism throughout East Africa resulting from impact of a single plume. *Nature* 395: 788–791.
Elkins-Tanton LT (2007) Continental magmatism, volatile recycling, and a heterogeneous mantle caused by lithospheric gravitational instabilities. *Journal of Geophysical Research* 112.
Elkins-Tanton LT and Hager BH (2005) Giant meteoroid impacts can cause volcanism. *Earth and Planetary Science Letters* 239: 219–232.
Ellam RM and Stuart FM (2004) Coherent He–Nd–Sr isotope trends in high $^{3}He/^{4}He$ basalts: Implications for a common reservoir, mantle heterogeneity and convection. *Earth and Planetary Science Letters* 228: 511–523.
Elliot DH and Fleming TH (2004) Occurrence and dispersal of magmas in the Jurassic Ferrar Large igneous province, Antarctica. *Gondwana Research* 7: 223–237.
Emerick CM and Duncan RA (1982) Age progressive volcanism in the Comores Archipelago, western Indian Ocean and implications for Somali plate tectonics. *Earth and Planetary Science Letters* 60: 415–428.
Encarnacion J, Fleming TH, Elliot DH, and Eales HV (1996) Synchronous emplacement of Ferrar and Karoo dolerites and the early breakup of Gondwana. *Geology* 24: 535–538.
Ernst RE (2007) Mafic-ultramafic large igneous provinces (LIPs): Importance of the pre-mesozoic record. *Episodes* 30: 108–114.
Ernst RE and Baragar WRA (1992) Evidence from magnetic fabric for the flow pattern of magma in the Mackenzie Giant Radiating Dyke Swarm. *Nature* 356: 511–513.
Ernst RE and Buchan KL (eds.) (2001) *Mantle Plumes: Their Identification through Time*, p. 593. Boulder, CO: Geological Society of America.
Ernst RE and Buchan KL (2003) Recognizing mantle plumes in the geological record. *Annual Review of Earth and Planetary Sciences* 31: 469–523.
Ewart A, Marsh JS, Milner SC, Duncan AR, Kamber BS, and Armstrong RA (2004) Petrology and geochemistry of Early Cretaceous bimodal continental flood volcanism of the NW Etendeka, Namibia: Part 1, Introduction, mafic lavas and re-evaluation of mantle source components. *Journal of Petrology* 45: 59–105.
Faccenna C, Becker TW, Lallemand S, Lagabrielle Y, Funiciello F, and Piromallo C (2010) Subduction-triggered magmatic pulses: A new class of plumes? *Earth and Planetary Science Letters* 299: 54–68.
Falloon TJ, Danyushevsky LV, Ariskin A, Green DH, and Ford CE (2007) The application of olivine geothermometry to infer crystallization temperatures of parental liquids: Implications for the temperature of MORB magmas. *Chemical Geology* 241: 207–233.
Farnetani CG (1997) Excess temperature of mantle plumes: The role of chemical stratification of D" *Geophysical Research Letters* 24: 1583–1586.
Farnetani CG and Hofmann AW (2009) Dynamics and internal structure of a lower mantle plume conduit. *Earth and Planetary Science Letters* 282: 314–322.
Farnetani CG and Hofmann AW (2010) Dynamics and internal structure of the Hawaiian plume. *Earth and Planetary Science Letters* 295: 231–240.
Farnetani CG, Hofmann AW, and Class C (2012) How double volcanic chains sample geochemical anomalies from the lowermost mantle. *Earth and Planetary Science Letters* 359–360: 240–247.
Farnetani CG, Legras B, and Tackley PJ (2002) Mixing and deformations in mantle plumes. *Earth and Planetary Science Letters* 196: 1–15.
Farnetani CG and Richards MA (1995) Thermal entrainment and melting in mantle plumes. *Earth and Planetary Science Letters* 133: 251–267.
Farnetani CG and Samuel H (2005) Beyond the thermal plume hypothesis. *Geophysical Research Letters* 32: L07311. http://dx.doi.org/10.1029/02005GL022360.
Faul UH and Jackson I (2005) The seismological signature of temperature and grain size variations in the upper mantle. *Earth and Planetary Science Letters* 234: 119–134.
Fee D and Dueker K (2004) Mantle transition zone topography and structure beneath the Yellowstone hotspot. *Geophysical Research Letters* 31: L18603. http://dx.doi.org/10.1029/12004GL020636.
Feigenson MD, Carr MJ, Maharaj SV, Juliano S, and Bolge LL (2004) Lead isotope composition of Central American volcanoes: Influence of the Galapagos plume. *Geochemistry, Geophysics, Geosystems* 5: Q06001. http://dx.doi.org/10.1029/02003GC000621.

Feighner MA and Richards MA (1995) The fluid dynamics of plume-ridge and plume-plate interactions: An experimental investigation. *Earth and Planetary Science Letters* 129: 171–182.

Ferguson DJ, Maclennan J, Bastow ID, et al. (2013) Melting during late-stage rifting in Afar is hot and deep. *Nature* 499: 70–73.

Fitton JG and Godard M (2004) Origin and evolution of magmas on the Ontong Java Plateau. In: Fitton JG, Mahoney JJ, Wallace PJ, and Saunders AD (eds.) *Origin and Evolution of the Ontong Java Plateau*, pp. 151–178. London: Geological Society, Special Publications 229.

Fitton JG, Mahoney JJ, Wallace PJ, and Saunders AD (eds.) (2004) *Origin and Evolution of the Ontong Java Plateau*, p. 374. London: Geological Society.

Flament N, Rey PF, Coltice N, Dromart G, and Olivier N (2011) Lower crustal flow kept Archean continental flood basalts at sea level. *Geology* 39: 1159–1162.

Fodor RV and Hanan BB (2000) Geochemical evidence for the Trindade hotspot trace: Columbia Seamount ankaramite. *Lithos* 51: 293–304.

Fontaine FR, Hooft EEE, Burkett PG, Toomey DR, Solomon SC, and Silver PG (2005) Shear-wave splitting beneath the Galapagos archipelago. *Geophysical Research Letters* 32.

Forsyth DW, Harmon N, Scheirer DS, and Duncan RA (2006) Distribution of recent volcanism and the morphology of seamounts and ridges in the GLIMPSE study area: Implications for the lithospheric cracking hypothesis for the origin of intraplate, non-hot spot volcanic chains. *Journal of Geophysical Research* 111.

Forte AM, Quere S, Moucha R, et al. (2010) Joint seismic–geodynamic–mineral physical modelling of African geodynamics: A reconciliation of deep-mantle convection with surface geophysical constraints. *Earth and Planetary Science Letters* 295: 329–341.

Fouch MJ (2012) The Yellowstone hotspot: Plume or not? *Geology* 40: 479–480.

Foulger G and Jurdy DM (eds.) (2007) *Plates, Plumes, and Planetary Processes*, p. 997. Geological Society of America.

Foulger G, Natland J, Presnall D, and Anderson DL (eds.) (2006) *Plates, Plumes, and Paradigms*, p. 861. Geological Society of America.

Foulger GR, Pritchard MJ, Julian BR, et al. (2001) Seismic tomography shows that upwelling beneath Iceland is confined to the upper mantle. *Geophysical Journal International* 146: 504–530.

Frey FA, Coffin MF, Wallace PJ, et al. (2000) Origin and evolution of a submarine large igneous province; the Kerguelen Plateau and Broken Ridge, southern Indian Ocean. *Earth and Planetary Science Letters* 176: 73–89.

Frey FA, Suen CJ, and Stockman HW (1985) The Ronda high-temperature peridotite – Geochemistry and petrogenesis. *Geochimica et Cosmochimica Acta* 49: 2469–2491.

Frey FA, Weis D, Borisova AY, and Xu G (2002) Involvement of continental crust in the formation of the Cretaceous Kerguelen Plateau: New perspectives from ODP Leg 120 sites. *Journal of Petrology* 43: 1207–1239.

Gallacher RJ and Bastow ID (2012) The development of magmatism along the Cameroon Volcanic Line: Evidence from teleseismic receiver functions. *Tectonics* 31.

Ganino C and Arndt NT (2009) Climate changes caused by degassing of sediments during the emplacement of large igneous provinces. *Geology* 37: 323–326.

Gans KD, Wilson DS, and Macdonald KC (2003) Pacific Plate gravity lineaments: Diffuse extension or thermal contraction? *Geochemistry, Geophysics, Geosystems* 4: 1074. http://dx.doi.org/10.1029/2002GC000465.

Garcia MO, Swinnard L, Weis D, et al. (2010) Petrology, geochemistry and geochronology of Kaua'i Lavas over 4.5 Myr: Implications for the origin of rejuvenated volcanism and the evolution of the Hawaiian plume. *Journal of Petrology* 51: 1507–1540.

Garnero EJ, Lay T, and McNamara AK (2007) Implications of lower mantle structural heterogeneity for existence and nature of whole mantle plumes. In: Foulger GR and Jurdy DM (eds.) *The Origin of Melting Anomalies: Plates, Plumes and Planetary Processes*, pp. 79–102. Boulder, CO: Geological Society of America, Special Paper 430.

Garnero EJ and McNamara AK (2008) Structure and dynamics of Earth's lower mantle. *Science* 320: 626–628.

Geldmacher J, Hoefig TW, Hauff F, Hoernle K, Garbe-Schoenberg D, and Wilson DS (2013) Influence of the Galapagos hotspot on the East Pacific Rise during Miocene superfast spreading. *Geology* 41: 183–186.

Geldmacher J, Hoernle K, van der Bogaard P, Duggen S, and Werner R (2005) New Ar-40/Ar-39 age and geochemical data from seamounts in the Canary and Madeira volcanic provinces: Support for the mantle plume hypothesis. *Earth and Planetary Science Letters* 237: 85–101.

Gente P, Dyment J, Maia M, and Goslin J (2003) Interaction between the Mid-Atlantic Ridge and the Azores hot spot during the last 85 Myr: Emplacement and rifting of the hot spot-derived plateaus. *Geochemistry, Geophysics, Geosystems* 4: 8514. http://dx.doi.org/10.1029/2003GC000527.

Georgen JE, Lin J, and Dick HJB (2001) Evidence from gravity anomalies for interactions of the Marion and Bouvet hotspots with the Southwest Indian Ridge: Effects of transform offsets. *Earth and Planetary Science Letters* 187: 283–300.

Gerya TV and Yuen DA (2003) Rayleigh–Taylor instabilities from hydration and melting propel "cold plumes" at subduction zones. *Earth and Planetary Science Letters* 212: 47–62.

Ghatak A and Basu AR (2011) Vestiges of the Kerguelen plume in the Sylhet Traps, northeastern India. *Earth and Planetary Science Letters* 308: 52–64.

Gibson SA, Thompson RN, Weska R, Dickin AP, and Leonardos OH (1997) Late Cretaceous rift-related upwelling and melting of the Trindade starting mantle plume head beneath western Brazil. *Contributions to Mineralogy and Petrology* 126: 303–314.

Gill RCO, Holm PM, and Nielsen TFD (1995) Was a short-lived Baffin Bay plume active prior to initiation of the present Icelandic plume? Clues from the high-Mg picrites of West Greenland. *Lithos* 34: 27–39.

Gill RCO, Pedersen AK, and Larsen JG (1992) Tertiary picrites from West Greenland: Melting at the periphery of a plume? In: Storey BC, Alabaster T, and Pankhurst RJ (eds.) *Magmatism and the Causes of Continental Break-up*, pp. 335–348. London: Geological Society, Special Publication 68.

Giordano G, Lucci F, Phillips D, Cozzupoli D, and Runci V (2012) Stratigraphy, geochronology and evolution of the Mt. Melbourne volcanic field (North Victoria Land, Antarctica). *Bulletin of Volcanology* 74: 1985–2005.

Gladczenko TP, Coffin MF, and Eldholm O (1997) Crustal structure of the Ontong Java Plateau: Modeling of new gravity and existing seismic data. *Journal of Geophysical Research* 102: 22711–22729.

Goes S, Spakman W, and Bijwaard H (1999) A lower mantle source for central European volcanism. *Science* 286: 1928–1931.

Gogus OH and Pysklywec RN (2008a) Mantle lithosphere delamination driving plateau uplift and synconvergent extension in eastern Anatolia. *Geology* 36: 723–726.

Gogus OH and Pysklywec RN (2008b) Near-surface diagnostics of dripping or delaminating lithosphere. *Journal of Geophysical Research* 113.

Gonnermann HM and Mukhopadhyay S (2009) Preserving noble gases in a convecting mantle. *Nature* 459: 560–563.

Goodwillie AM (1995) Short-wavelength gravity lineations and unusual flexure results at the Puka Puka volcanic ridge system. *Earth and Planetary Science Letters* 136: 297–314.

Graham DW (2002) Noble gas isotope geochemistry of mid-ocean ridge and ocean island basalts: Characterization of mantle source reservoirs. In: Porcelli D, Ballentine CJ, and Wieler R (eds.) *Noble Gases in Geochemistry and Cosmochemistry*. *Reviews in Mineralogy and Geochemistry*, vol. 47, pp. 247–318. Washington, DC: Mineralogical Society of America.

Graham DW, Johnson KTM, Priebe LD, and Lupton JE (1999) Hotspot-ridge interaction along the Southeast Indian Ridge near Amsterdam and St. Paul islands: Helium isotope evidence. *Earth and Planetary Science Letters* 167: 297–310.

Grand SP, van der Hilst RD, and Widiyantoro S (1997) Global seismic tomography: A snapshot of convection in the mantle. *Geological Society of America Today* 7: 1–7.

Green DH, Falloon TJ, Eggins SM, and Yaxley GM (2001) Primary magmas and mantle temperatures. *European Journal Of Mineralogy* 13: 437–451.

Griffin TJ and McDougall I (1975) Geochronology of the cainozoic McBride Volcanic Province, Northern Queensland. *Journal of the Geological Society of Australia* 22: 387–396.

Griffiths RW (1986) Thermals in extremely viscous fluids, including the effects of temperature-dependent viscosity. *Journal of Fluid Mechanics* 166: 115–138.

Griffiths RW and Campbell IH (1990) Stirring and structure in mantle starting plumes. *Earth and Planetary Science Letters* 99: 66–78.

Griffiths RW and Campbell IH (1991) On the dynamics of long-lived plume conduits in the convecting mantle. *Earth and Planetary Science Letters* 103: 214–227.

Grigne C, Labrosse S, and Tackley PJ (2007) Convection under a lid of finite conductivity: Heat flux scaling and application to continents. *Journal of Geophysical Research* 112.

Gripp AE and Gordon RG (2002) Young tracks of hotspots and current plate velocities. *Geophysical Journal International* 150: 321–361.

Guillou H, Carracedo JC, Paris R, and Torrado FJP (2004) Implications for the early shield-stage evolution of Tenerife from K/Ar ages and magnetic stratigraphy. *Earth and Planetary Science Letters* 222: 599–614.

Guillou H, Maury RC, Blais S, et al. (2005) Age progression along the Society hotspot chain (French Polynesia) based on new unspiked K–Ar ages. *Bulletin De La Societe Geologique De France* 176: 135–150.

Gurenko AA, Sobolev AV, Hoernle KA, Hauff F, and Schmincke H-U (2009) Enriched, HIMU-type peridotite and depleted recycled pyroxenite in the Canary plume: A mixed-up mantle. *Earth and Planetary Science Letters* 277: 514–524.

Haase KM, Devey CW, and Goldstein SL (1996) Two-way exchange between the Easter mantle plume and the Easter microplate spreading axis. *Nature* 382: 344–346.

Hales TC, Abt DL, Humphreys ED, and Roering JU (2005) A lithospheric instability origin for Columbia River flood basalts and Wallowa Mountains uplift in northeast Oregon. *Nature* 438: 842–845.

Halliday AN, Lee DC, Tommasini S, et al. (1995) Incompatible trace-elements in OIB and MORB and source enrichment in the sub-oceanic mantle. *Earth and Planetary Science Letters* 133: 379–395.

Hames WE, Renne PR, and Ruppel C (2000) New evidence for geologically instantaneous emplacement of earliest Jurassic Central Atlantic magmatic province basalts on the North American margin. *Geology* 28: 859–862.

Hanan BB and Graham DW (1996) Lead and helium isotope evidence from oceanic basalts for a common deep source of mantle plumes. *Science* 272: 991–995.

Hansen SE and Nyblade AA (2013) The deep seismic structure of the Ethiopia/Afar hotspot and the African superplume. *Geophysical Journal International* 194: 118–124.

Hansen SE, Nyblade AA, and Benoit MH (2012) Mantle structure beneath Africa and Arabia from adaptively parameterized P-wave tomography: Implications for the origin of Cenozoic Afro-Arabian tectonism. *Earth and Planetary Science Letters* 319: 23–34.

Hanyu T, Tatsumi Y, Senda R, et al. (2011) Geochemical characteristics and origin of the HIMU reservoir: A possible mantle plume source in the lower mantle. *Geochemistry, Geophysics, Geosystems* 12.

Hardarson BS, Fitton JG, Ellam RM, and Pringle MS (1997) Rift relocation—A geochemical and geochronological investigation of a paleo-rift in northwest Iceland. *Earth and Planetary Science Letters* 153: 181–196.

Hardebol NJ, Pysklywec RN, and Stephenson R (2012) Small-scale convection at a continental back-arc to craton transition: Application to the southern Canadian Cordillera. *Journal of Geophysical Research* 117.

Harmon N, Forsyth DW, and Scheirer DS (2006) Analysis of gravity and topography in the GLIMPSE study region: Isostatic compensation and uplift of the Sojourn and Hotu Matua Ridge systems. *Journal of Geophysical Research* 111.

Harmon N, Forsyth DW, Weeraratne DS, Yang Y, and Webb SC (2011) Mantle heterogeneity and off axis volcanism on young Pacific lithosphere. *Earth and Planetary Science Letters* 311: 306–315.

Harris RN and McNutt MK (2007) Heat flow on hot spot swells: Evidence for fluid flow. *Journal of Geophysical Research* 112.

Hart SR, Coetzee M, Workman RK, et al. (2004) Genesis of the Western Samoa seamount province: Age, geochemical fingerprint and tectonics. *Earth and Planetary Science Letters* 227: 3756.

Hart SR, Hauri EH, Oschmann LA, and Whitehead JA (1992) Mantle plumes and entrainment: Isotopic evidence. *Science* 256: 517–520.

Hart SR, Schilling J-G, and Powell JL (1973) Basalts from Iceland and along the Reykjanes Ridge: Sr isotope geochemistry. *Nature* 246: 104–107.

Hauri E (1996) Major-element variability in the Hawaiian mantle plume. *Nature* 382: 415–419.

Hawkesworth C, Kelley S, Turner S, le Roex A, and Storey B (1999) Mantle processes during Gondwana break-up and dispersal. *Journal of African Earth Sciences* 28: 239–261.

Haxby WF and Weissel JK (1986) Evidence for small-scale mantle convection from Seasat altimeter data. *Journal of Geophysical Research* 91: 3507–3520.

He B, Xu YG, Chung SL, Xiao L, and Wang Y (2003) Sedimentary evidence for a rapid, kilometer-scale crustal doming prior to the eruption of the Emeishan flood basalts. *Earth and Planetary Science Letters* 213: 391–405.

Heintz M, Debayle E, and Vauchez A (2005) Upper mantle structure of the South American continent and neighboring oceans from surface wave tomography. *Tectonophysics* 406: 115–139.

Hekinian R, Stoffers P, and Cheminee J-L (eds.) (2004) *Oceanic Hotspots*. New York: Springer.

Helffrich G (2000) Topography of the transition zone seismic discontinuities. *Reviews of Geophysics* 38: 141–158.

Helffrich G, Faria B, Fonseca JFBD, Lodge A, and Kaneshima S (2010) Transition zone structure under a stationary hot spot: Cape Verde. *Earth and Planetary Science Letters* 289: 156–161.

Helmberger D, Ni SD, Wen LX, and Ritsema J (2000) Seismic evidence for ultralow-velocity zones beneath Africa and eastern Atlantic. *Journal of Geophysical Research* 105: 23865–23878.

Helmberger DV, Wen L, and Ding X (1998) Seismic evidence that the source of the Iceland hotspot lies at the core–mantle boundary. *Nature* 396: 248–251.

Hendrie DB, Kusznir NJ, Morley CK, and Ebinger CJ (1994) Cenozoic extension in Northern Kenya – A quantitative model of rift basin development in the Turkana region. *Tectonophysics* 236: 409–438.

Hernlund JW, Stevenson DJ, and Tackley PJ (2008a) Buoyant melting instabilities beneath extending lithosphere: 2. Linear analysis. *Journal of Geophysical Research* 113.

Hernlund JW, Tackley PJ, and Stevenson DJ (2008b) Buoyant melting instabilities beneath extending lithosphere: 1. Numerical models. *Journal of Geophysical Research* 113.

Herzberg C (2004a) Geodynamic information in peridotite petrology. *Journal of Petrology* 45: 2507–2530.

Herzberg C (2004b) Partial melting below the Ontong Java Plateau. In: Fitton JG, Mahoney JJ, Wallace PJ, and Saunders AD (eds.) *Origin and Evolution of the Ontong Java Plateau, Special publications 229*, pp. 179–184. London: Geological Society.

Herzberg C (2006) Petrology and thermal structure of the Hawaiian plume from Mauna Kea volcano. *Nature* 444: 605–609.

Herzberg C (2011) Identification of source lithology in the Hawaiian and Canary Islands: Implications for origins. *Journal of Petrology* 52: 113–146.

Herzberg C, Asimow PD, Arndt N, et al. (2007) Temperatures in ambient mantle and plumes: Constraints from basalts, picrites, and komatiites. *Geochemistry, Geophysics, Geosystems* 8.

Herzberg C and Gazel E (2009) Petrological evidence for secular cooling in mantle plumes. *Nature* 458: U619–U683.

Herzberg C and O'Hara MJ (2002) Plume-associated ultramafic magmas of Phanerozoic age. *Journal of Petrology* 43: 1857–1883.

Hey R, Martinez F, Hoskuldsson A, and Benediktsdottir A (2010) Propagating rift model for the V-shaped ridges south of Iceland. *Geochemistry, Geophysics, Geosystems* 11.

Hieronymus CF and Bercovici D (1999) Discrete alternating hotspot islands formed by interaction of magma transport and lithospheric flexure. *Nature* 397: 604–607.

Hieronymus CF and Bercovici D (2000) Non-hotspot formation of volcanic chains: Control of tectonic and flexural stresses on magma transport. *Earth and Planetary Science Letters* 181: 539–554.

Hieronymus CF and Bercovici D (2001a) Focusing of eruptions by fracture wall erosion. *Geophysical Research Letters* 28: 1823–1826.

Hieronymus CF and Bercovici D (2001b) A theoretical model of hotspot volcanism: Control on volcanic spacing and patterns via magma dynamics and lithospheric stresses. *Journal of Geophysical Research* 106: 683–702.

Hillier JK and Watts AB (2004) "Plate-like" subsidence of the East Pacific Rise-South Pacific superswell system. *Journal of Geophysical Research* 109.

Hirano N, Kawamura K, Hattori M, Saito K, and Ogawa Y (2001) A new type of intra-plate volcanism: Young alkali-basalts discovered from the subducting Pacific Plate, northern Japan Trench. *Geophysical Research Letters* 28: 2719–2722.

Hirano N, Koppers AAP, Takahashi A, Fujiwara T, and Nakanishi M (2008) Seamounts, knolls and petit-spot monogenetic volcanoes on the subducting Pacific Plate. *Basin Research* 20: 543–553.

Hirose K, Fei Y, Ma Y, and Ho-Kwang M (1999) The fate of subducted basaltic crust in the Earth's lower mantle. *Nature* 387: 53–56.

Hirose K and Kushiro I (1993) Partial melting of dry peridotites at high-pressures – Determination of compositions of melts segregated from peridotite using aggregates of diamond. *Earth and Planetary Science Letters* 114: 477–489.

Hirschmann MM (2010) Partial melt in the oceanic low velocity zone. *Physics of the Earth and Planetary Interiors* 179: 60–71.

Hirschmann MM, Asimow PD, Ghiorso MS, and Stolper EM (1999) Calculation of peridotite partial melting from thermodynamic models of minerals and melts. III. Controls on isobaric melt production and the effect of water on melt production. *Journal of Petrology* 40: 831–851.

Hirschmann MM, Kogiso T, Baker MB, and Stolper EM (2003) Alkalic magmas generated by partial melting of garnet pyroxenite. *Geology* 31: 481–484.

Hirth G and Kohlstedt DL (1996) Water in the oceanic upper mantle: Implications for rheology, melt extraction, and the evolution of the lithosphere. *Earth and Planetary Science Letters* 144: 93–108.

Hoernle K, Hauff F, and van den Bogaard P (2004) 70 m.y. history (139–69 Ma) for the Caribbean large igneous province. *Geology* 32: 697–700.

Hoernle K, Hauff F, van den Bogaard P, et al. (2010) Age and geochemistry of volcanic rocks from the Hikurangi and Manihiki oceanic Plateaus. *Geochimica et Cosmochimica Acta* 74: 7196–7219.

Hoernle K, van den Bogaard P, Werner R, et al. (2002) Missing history (16–71 Ma) of the Galapagos hotspot: Implications for the tectonic and biological evolution of the Americas. *Geology* 30: 795–798.

Hofmann AW (1997) Mantle geochemistry: The message from oceanic volcanism. *Nature* 385: 219–229.

Hofmann AW and White WM (1982) Mantle plumes from ancient oceanic crust. *Earth and Planetary Science Letters* 57: 421–436.

Hofmann C, Courtillot V, Feraud G, et al. (1997) Timing of the Ethiopian flood basalt event and implications for plume birth and global change. *Nature* 389: 838–841.

Hofmann C, Feraud G, and Courtillot V (2000) Ar-40/Ar-39 dating of mineral separates and whole rocks from the Western Ghats lava pile: Further constraints on duration and age of the Deccan traps. *Earth and Planetary Science Letters* 180: 13–27.

Holm PM, Gill RCO, Pedersen AK, et al. (1993) The tertiary picrites of West Greenland: Contributions from "Icelandic" and other sources. *Earth and Planetary Science Letters* 115: 227–244.

Hooft EEE, Toomey DR, and Solomon SC (2003) Anomalously thin transition zone beneath the Galapagos hotspot. *Earth and Planetary Science Letters* 216: 55–64.

Hooper P, Widdowson M, and Kelley S (2010) Tectonic setting and timing of the final Deccan flood basalt eruptions. *Geology* 38: 839–842.

Hooper PR (1997) The Columbia River flood basalt province: Current status. In: Mahoney JJ and Coffin MF (eds.) *Large Igneous Provinces: Continental, Oceanic, and Planetary Flood Volcanism*. *Geophysical Monograph*, 100, pp. 1–27. Washington, DC: AGU.

Hooper PR, Binger GB, and Lees KR (2002) Ages of the Steens and Columbia River flood basalts and their relationship to extension-related calc-alkalic volcanism in eastern Oregon. *Geological Society of America Bulletin* 114: 43–50.

Hopper JR, Dahl-Jensen T, Holbrook WS, et al. (2003) Structure of the SE Greenland margin from seismic reflection and refraction data: Implications for nascent spreading center subsidence and asymmetric crustal accretion during North Atlantic opening. *Journal of Geophysical Research* 108: 2269.

Houseman GA, McKenzie DP, and Molnar P (1981) Convective instability of a thickened boundary-layer and its relevance for the thermal evolution of continental convergent belts. *Journal of Geophysical Research* 86: 6115–6132.

Houser C and Williams Q (2010) Reconciling Pacific 410 and 660 km discontinuity topography, transition zone shear velocity patterns, and mantle phase transitions. *Earth and Planetary Science Letters* 296: 255–266.

Huang J (2008) Controls on entrainment of a dense chemical layer by thermal plumes. *Physics of the Earth and Planetary Interiors* 166: 175–187.

Huang J, Fu R, and Ke F (2010) Influence of gradational compositional layering on plume entrainment and its implication for geochemistry. *Physics of the Earth and Planetary Interiors* 178: 6879.

Huang J, Zhong S, and van Hunen J (2003) Controls on sublithospheric small-scale convection. *Journal of Geophysical Research* 108. http://dx.doi.org/10.1029/2003JB002456.

Huang S, Hall PS, and Jackson MG (2011) Geochemical zoning of volcanic chains associated with Pacific hotspots. *Nature Geoscience* 4: 874–878.

Huckfeldt M, Courtier AM, and Leahy GM (2013) Implications for the origin of Hawaiian volcanism from a converted wave analysis of the mantle transition zone. *Earth and Planetary Science Letters* 373: 194–204.

Huerta AD, Nyblade AA, and Reusch AM (2009) Mantle transition zone structure beneath Kenya and Tanzania: More evidence for a deep-seated thermal upwelling in the mantle. *Geophysical Journal International* 177: 1249–1255.

Humphreys ER and Niu Y (2009) On the composition of ocean island basalts (OIB): The effects of lithospheric thickness variation and mantle metasomatism. *Lithos* 112: 118–136.

Hung SH, Shen Y, and Chiao LY (2004) Imaging seismic velocity structure beneath the Iceland hot spot: A finite frequency approach. *Journal of Geophysical Research* 109: B08305. http://dx.doi.org/10.1029/02003JB002889.

Hunt AC, Parkinson IJ, Harris NBW, Barry TL, Rogers NW, and Yondon M (2012) Cenozoic volcanism on the Hangai Dome, Central Mongolia: Geochemical evidence for changing melt sources and implications for mechanisms of melting. *Journal of Petrology* 53: 19131942.

Husson L and Conrad CP (2012) On the location of hotspots in the framework of mantle convection. *Geophysical Research Letters* 39.

Hwang YK, Ritsema J, van Keken PE, Goes S, and Styles E (2011) Wavefront healing renders deep plumes seismically invisible. *Geophysical Journal International* 187: 273–277.

Ingle S and Coffin MF (2004) Impact origin for the greater Ontong Java Plateau? *Earth and Planetary Science Letters* 218: 123–134.

Ingle S, Ito G, Mahoney JJ, et al. (2010) Mechanisms of geochemical and geophysical variations along the western Galapagos Spreading Center. *Geochemistry, Geophysics, Geosystems* 11.

Irifune T, Sekine T, Ringwood AE, and Hibberson WO (1986) The eclogite-garnetite transformations at high pressure and some geophysical implications. *Earth and Planetary Science Letters* 77: 245–256.

Ishii M and Tromp J (1999) Normal-mode and free-air gravity constraints on lateral variations in velocity and density of Earth's mantle. *Science* 285: 1231–1236.

Ito E and Takahashi E (1989) Postspinel transformations in the system Mg_2SiO_4-Fe_2SiO_4 and some geophysical implications. *Journal of Geophysical Research* 94: 10637–10646.

Ito G and Clift P (1998) Subsidence and growth of Pacific Cretaceous plateaus. *Earth and Planetary Science Letters* 161: 85–100.

Ito G, Lin J, and Gable C (1997) Interaction of mantle plumes and migrating midocean ridges: Implications for the Galapagos plume-ridge system. *Journal of Geophysical Research* 102: 15403–15417.

Ito G, Lin J, and Gable CW (1996) Dynamics of mantle flow and melting at a ridge-centered hotspot: Iceland and the Mid-Atlantic Ridge. *Earth and Planetary Science Letters* 144: 53–74.

Ito G, Lin J, and Graham D (2003) Observational and theoretical studies of the dynamics of mantle plume-mid-ocean ridge interaction. *Reviews of Geophysics* 41: 1017. http://dx.doi.org/10.1029/2002RG000117.

Ito G and Mahoney J (2006) Melting a high $^3He/^4He$ source in a heterogeneous mantle. *Geochemistry, Geophysics, Geosystems* 7: Q05010. http://dx.doi.org/10.1029/02005GC001158.

Ito G and Mahoney JJ (2005a) Flow and melting of a heterogeneous mantle: 1.Method and importance to the geochemistry of ocean island and mid-ocean ridge basalts. *Earth and Planetary Science Letters* 230: 29–46.

Ito G and Mahoney JJ (2005b) Flow and melting of a heterogeneous mantle: 2. Implications for a chemically nonlayered mantle. *Earth and Planetary Science Letters* 230: 47–63.

Ito G, McNutt M, and Gibson RL (1995) Crustal structure of the Tuamotu Plateau, 15°S, and implications for its origin. *Journal of Geophysical Research* 100: 8097–8114.

Ito G, Shen Y, Hirth G, and Wolfe CJ (1999) Mantle flow, melting, and dehydration of the Iceland mantle plume. *Earth and Planetary Science Letters* 165: 81–96.

Ivanov BA and Melosh HJ (2003) Impacts do not initiate volcanic eruptions: Eruptions close to the crater. *Geology* 31: 869–872.

Jackson ED, Silver EA, and Dalrymple GB (1972) Hawaiian-Emperor chain and its relation to Cenozoic circumpacific tectonics. *Geological Society of America Bulletin* 83: 601–618.

Jackson I (ed.) (1998) *The Earth's Mantle, Composition, Structure, and Evolution*, p. 566. Cambridge, UK: Cambridge University Press.

Jackson MG and Dasgupta R (2008) Compositions of HIMU, EM1, and EM2 from global trends between radiogenic isotopes and major elements in ocean island basalts. *Earth and Planetary Science Letters* 276: 175–186.

Jackson MG, Hart SR, Konter JG, et al. (2010) Samoan hot spot track on a "hot spot highway": Implications for mantle plumes and a deep Samoan mantle source. *Geochemistry, Geophysics, Geosystems* 11.

Jackson MG, Weis D, and Huang S (2012) Major element variations in Hawaiian shield lavas: Source features and perspectives from global ocean island basalt (OIB) systematics. *Geochemistry, Geophysics, Geosystems* 13.

James DE, Fouch MJ, Carlson RW, and Roth JB (2011) Slab fragmentation, edge flow and the origin of the Yellowstone hotspot track. *Earth and Planetary Science Letters* 311: 124–135.

Janney PE, Macdougall JD, Natland JH, and Lynch MA (2000) Geochemical evidence from the Pukapuka volcanic ridge system for a shallow enriched mantle domain beneath the South Pacific Superswell. *Earth and Planetary Science Letters* 181: 47–60.

Jellinek AM and Manga M (2002) The influence of the chemical boundary layer on the fixity, spacing and lifetime of mantle plumes. *Nature* 418: 760–763.

Jellinek AM and Manga M (2004) Links between long-lived hot spots, mantle plumes, D", and plate tectonics. *Reviews of Geophysics* 42: RG3002. http://dx.doi.org/10.1029/2003RG000144.

Jha K, Parmentier EM, and Morgan JP (1994) The role of mantle depletion and melt-retention buoyancy in spreading-center segmentation. *Earth and Planetary Science Letters* 125: 221–234.

Jones AP, Price GD, Price NJ, DeCarli PS, and Clegg RA (2002a) Impact induced melting and the development of large igneous provinces. *Earth and Planetary Science Letters* 202: 551–561.

Jones SM, White N, and Maclennan J (2002b) V-shaped ridges around Iceland: Implications for spatial and temporal patterns of mantle convection. *Geochemistry, Geophysics, Geosystems* 3: 1059. http://dx.doi.org/10.1029/2002GC000361.

Jordahl KA, McNutt MK, and Caress DW (2004) Multiple episodes of volcanism in the Southern Austral Islands: Flexural constraints from bathymetry, seismic reflection, and gravity data. *Journal of Geophysical Research* 109.

Jordan TH (1979) Mineralogies, densities and seismic velocities of garnet lherzolites and their geophysical implications. In: Boyd FR and Meyer HOA (eds.) *Mantle*

Sample: Inclusions in Kimberlites and Other Volcanics, pp. 1–13. Washington, DC: American Geophysical Union.

Jourdan F, Feraud G, Bertrand H, et al. (2004) The Karoo triple junction questioned: Evidence from Jurassic and Proterozoic Ar-40/Ar-39 ages and geochemistry of the giant Okavango dyke swarm (Botswana). *Earth and Planetary Science Letters* 222: 989–1006.

Jourdan F, Feraud G, Bertrand H, et al. (2005) Karoo large igneous province: Brevity, origin, and relation to mass extinction questioned by new Ar-40/Ar-39 age data. *Geology* 33: 745–748.

Jourdan F, Feraud G, Bertrand H, Watkeys MK, Kampunzu AB, and Le Gall B (2006) Basement control on dyke distribution in Large Igneous Provinces: Case study of the Karoo triple junction. *Earth and Planetary Science Letters* 241: 307–322.

Jourdan F, Marzoli A, Bertrand H, et al. (2009) Ar-40/Ar-39 ages of CAMP in North America: Implications for the Triassic-Jurassic boundary and the K-40 decay constant bias. *Lithos* 110: 167–180.

Kaminski E and Jaupart C (2003) Laminar starting plumes in high-Prandtl-number fluids. *Journal of Fluid Mechanics* 478: 287–298.

Karato S-i (2012) On the origin of the asthenosphere. *Earth and Planetary Science Letters* 321: 95–103.

Karato S-i (2013a) Does partial melting explain geophysical anomalies? *Physics of the Earth and Planetary Interiors* 228: 300–306.

Karato S-i (2013b) Theory of isotope diffusion in a material with multiple species and its implications for hydrogen-enhanced electrical conductivity in olivine. *Physics of the Earth and Planetary Interiors* 219: 49–54.

Karato S and Jung H (1998) Water, partial melting and the origin of the seismic low velocity and high attenuation zone in the upper mantle. *Earth and Planetary Science Letters* 157: 193–207.

Kawakatsu H, Kumar P, Takei Y, et al. (2009) Seismic evidence for sharp lithosphere-asthenosphere boundaries of oceanic plates. *Science* 324: 499–502.

Keller G, Adatte T, Gardin S, Bartolini A, and Bajpai S (2008) Main Deccan volcanism phase ends near the K-T boundary: Evidence from the Krishna-Godavari Basin, SE India. *Earth and Planetary Science Letters* 268: 293–311.

Keller RA, Graham DW, Farley KA, Duncan RA, and Lupton E (2004) Cretaceous-to-recent record of elevated He-3/He-4 along the Hawaiian-Emperor volcanic chain. *Geochemistry, Geophysics, Geosystems* 5.

Kellogg LH, Hager B, and van der Hilst R (1999) Compositional stratification in the deep mantle. *Science* 99: 276–289.

Kellogg LH and King SD (1997) The effect of temperature dependent viscosity on the structure of new plumes in the mantle: Results of a finite element model in a spherical, axisymmetric shell. *Earth and Planetary Science Letters* 148: 13–26.

Kelly A and Bercovici D (1997) The clustering of rising diapirs and plume heads. *Geophysical Research Letters* 24: 201–204.

Kent AJR, Stolper EM, Francis D, Woodhead J, Frei R, and Eiler J (2004) Mantle heterogeneity during the formation of the North Atlantic Igneous Province: Constraints from trace element and Sr-Nd-Os-O isotope systematics of Baffin Island picrites. *Geochemistry, Geophysics, Geosystems* 5: Q11004. http://dx.doi.org/10.1029/12004GC000743.

Kent RW, Pringle MS, Muller RD, Sauders AD, and Ghose NC (2002) $^{40}Ar/^{39}Ar$ geochronology of the Rajmahal basalts, India, and their relationship to the Kerguelen Plateau. *Journal of Petrology* 43: 1141–1153.

Kent W, Saunders AD, Kempton PD, and Ghose NC (1997a) Rajmahal Basalts, Eastern India: Mantle sources and melt distribution at a volcanic rifted margin. In: Mahoney JJ and Coffin MF (eds.) *Large Igneous Provinces: Continental, Oceanic and Planetary Flood Volcanism*. *Geophysical Monograph*, 100, pp. 114–123, 145–182. Washington, DC: American Geophysical Union.

Keyser M, Ritter JRR, and Jordan M (2002) 3D shear-wave velocity structure of the Eifel Plume, Germany. *Earth and Planetary Science Letters* 203: 59–82.

Kidder DL and Worsley TR (2010) Phanerozoic Large Igneous Provinces (LIPs), HEATT (Haline Euxinic Acidic Thermal Transgression) episodes, and mass extinctions. *Palaeogeography, Palaeoclimatology, Palaeoecology* 295: 162–191.

Kieffer B, Arndt N, Lapierre H, et al. (2004) Flood and shield basalts from Ethiopia: Magmas from the African superswell. *Journal of Petrology* 45: 793–834.

Kincaid C, Druken KA, Griffiths RW, and Stegman DR (2013) Bifurcation of the Yellowstone plume driven by subduction-induced mantle flow. *Nature Geoscience* 6: 395–399.

King S and Anderson DL (1998) Edge-driven convection. *Earth and Planetary Science Letters* 160: 289–296.

King SD (2007) Hotspots and edge-driven convection. *Geology* 35: 223–226.

King SD and Anderson DL (1995) An alternative mechanism of flood basalt formation. *Earth and Planetary Science Letters* 136: 269–279.

King SD and Ritsema J (2000) African hot spot volcanism: Small-scale convection in the upper mantle beneath cratons. *Science* 290: 1137–1140.

Klein EM and Langmuir CH (1987) Global correlations of ocean ridge basalt chemistry with axial depth and crustal thickness. *Journal of Geophysical Research* 92: 8089–8115.

Koch FW, Wiens DA, Nyblade AA, et al. (2012) Upper-mantle anisotropy beneath the Cameroon Volcanic Line and Congo Craton from shear wave splitting measurements. *Geophysical Journal International* 190: 75–86.

Kogiso T and Hirschmann MM (2006) Partial melting experiments of bimineralic eclogite and the role of recycled mafic oceanic crust in the genesis of ocean island basalts. *Earth and Planetary Science Letters* 249: 188–199.

Kogiso T, Hirschmann MM, and Frost DJ (2003) High-pressure partial melting of garnet pyroxenite: Possible mafic lithologies in the source of ocean island basalts. *Earth and Planetary Science Letters* 216: 603–617.

Kogiso T, Hirschmann MM, and Reiners PW (2004) Length scales of mantle heterogeneities and their relationship to ocean island basalt geochemistry. *Geochimica et Cosmochimica Acta* 68: 345–360.

Kokfelt TF, Hoernle K, and Hauff F (2003) Upwelling and melting of the Iceland Plume from radial variation of (super 238) U- (super 230) Th disequilibria in postglacial volcanic rocks. *Earth and Planetary Science Letters* 214: 167–186.

Kono M (1980) Paleomagnetism of DSDP Leg 55 basalts and implications for the tectonics of the Pacific plate. In: Jackson ED (ed.) *Initial Reports of the Deep Sea Drilling Project*, vol. 55, pp. 737–752.

Konter JG, Hanan BB, Blichert-Toft J, Koppers AAP, Plank T, and Staudigel H (2008) One hundred million years of mantle geochemical history suggest the retiring of mantle plumes is premature. *Earth and Planetary Science Letters* 275: 285–295.

Konter JG and Jackson MG (2012) Large volumes of rejuvenated volcanism in Samoa: Evidence supporting a tectonic influence on late-stage volcanism. *Geochemistry, Geophysics, Geosystems* 13.

Koornneef JM, Stracke A, Bourdon B, et al. (2012) Melting of a two-component source beneath Iceland. *Journal of Petrology* 53: 127–157.

Koppers AA, Staudigel H, Pringle MS, and Wijbrans JR (2003) Short-lived and discontinuous intraplate volcanism in the South Pacific: Hot spots or extensional volcanism. *Geochemistry, Geophysics, Geosystems* 4: 1089. http://dx.doi.org/10.1029/2003GC000533.

Koppers AAP, Duncan RA, and Steinberger B (2004) Implications of a nonlinear $^{40}Ar/^{39}Ar$ age progression along the Louisville seamount trail for models of fixed and moving hot spots. *Geochemistry, Geophysics, Geosystems* 5: Q06L02. http://dx.doi.org/10.1029/2003GC000671.

Koppers AAP, Gowen MD, Colwell LE, et al. (2011a) New Ar-40/Ar-39 age progression for the Louisville hot spot trail and implications for inter-hot spot motion. *Geochemistry, Geophysics, Geosystems* 12.

Koppers AAP, Russell JA, Jackson MG, Konter J, Staudigel H, and Hart SR (2008) Samoa reinstated as a primary hotspot trail. *Geology* 36: 435–438.

Koppers AAP, Russell JA, Roberts J, et al. (2011b) Age systematics of two young en echelon Samoan volcanic trails. *Geochemistry, Geophysics, Geosystems* 12.

Koppers AAP and Staudigel H (2005) Asynchronous bends in Pacific seamounts trails: A case for extensional volcanism? *Science* 307: 904–907.

Koppers AAP, Staudigel H, Morgan JP, and Duncan RA (2007) Nonlinear (40)Ar/(39)Ar age systematics along the Gilbert Ridge and Tokelau Seamount Trail and the timing of the Hawaii-Emperor Bend. *Geochemistry, Geophysics, Geosystems* 8.

Koppers AAP, Staudigel H, Wijbrans JR, and Pringle MS (1998) The Magellan Seamount Trail: Implications for Cretaceous hotspot volcanism and absolute Pacific Plate motion. *Earth and Planetary Science Letters* 163: 53–68.

Koppers AAP and Watts AB (2010) Intraplate seamounts as a window into deep Earth processes. *Oceanography* 23: 42–57.

Koppers AAP, Yamazaki T, Geldmacher J, et al. (2012) Limited latitudinal mantle plume motion for the Louisville hotspot. *Nature Geoscience* 5: 911–917.

Korenaga J (2004) Mantle mixing and continental breakup magmatism. *Earth and Planetary Science Letters* 218: 463–473.

Korenaga J (2005) Why did not the Ontong Java Plateau form subaerially? *Earth and Planetary Science Letters* 234: 385–399.

Korenaga J (2011) Velocity-depth ambiguity and the seismic structure of large igneous provinces: A case study from the Ontong Java Plateau. *Geophysical Journal International* 185: 1022–1036.

Korenaga J and Jordan TH (2004) Physics of multiscale convection in Earth's mantle: Evolution of sublithospheric convection. *Journal of Geophysical Research* 109. http://dx.doi.org/10.1029/2003JB002464.

Korenaga J and Kelemen PB (2000) Major element heterogeneity in the mantle source of the North Atlantic igneous province. *Earth and Planetary Science Letters* 184: 251–268.

Korenaga J and Sager WW (2012) Seismic tomography of Shatsky Rise by adaptive importance sampling. *Journal of Geophysical Research* 117.

Krishna KS, Abraham H, Sager WW, et al. (2012) Tectonics of the Ninetyeast Ridge derived from spreading records in adjacent oceanic basins and age constraints of the ridge. *Journal of Geophysical Research* 117.

Kumagai I, Davaille A, and Kurita K (2007) On the fate of thermally buoyant mantle plumes at density interfaces. *Earth and Planetary Science Letters* 254: 180–193.

Kumagai I, Davaille A, Kurita K, and Stutzmann E (2008) Mantle plumes: Thin, fat, successful, or failing? Constraints to explain hot spot volcanism through time and space. *Geophysical Research Letters* 35.

Kuroda J, Ogawa NO, Tanimizu M, et al. (2007) Contemporaneous massive subaerial volcanism and late cretaceous Oceanic Anoxic Event 2. *Earth and Planetary Science Letters* 256: 211–223.

Labrosse S, Hernlund JW, and Coltice N (2007) A crystallizing dense magma ocean at the base of the Earth's mantle. *Nature* 450: 866–869.

Langmuir CH, Klein EM, and Plank T (1992) Petrological systematics of mid-ocean ridge basalts: Constraints on melt generation beneath ocean ridges. In: Phipps Morgan J, Blackman DK, and Sinton JM (eds.) *Mantle Flow and Melt Generation at Mid-Ocean Ridges*. *Geophysical Monograph*, vol. 71, pp. 183–280. Washington, DC: American Geophysical Union.

Lanyon R, Varne R, and Crawford AJ (1993) Tasmanian Tertiary basalts, the Balleny plume, and opening of the Tasman Sea (Southwest Pacific Ocean). *Geology* 21: 555–558.

Larsen TB and Yuen DA (1997) Ultrafast upwelling bursting through the upper mantle. *Earth and Planetary Science Letters* 146: 393–399.

Larsen TB, Yuen DA, and Storey M (1999) Ultrafast mantle plumes and implications for flood basalt volcanism in the Northern Atlantic region. *Tectonophysics* 311: 31–43.

Laske G, Markee A, Orcutt JA, et al. (2011) Asymmetric shallow mantle structure beneath the Hawaiian Swell-evidence from Rayleigh waves recorded by the PLUME network. *Geophysical Journal International* 187: 1725–1742.

Laske G and Masters G (1997) A global digital map of sediment thickness. *EOS, Transactions American Geophysical Union* 78(Fall Meeting Supplement): F483.

Laske G, Phipps Morgan J, and Orcutt JA (2007) The Hawaiian SWELL pilot experiment-evidence for lithosphere rejuvenation from ocean bottom surface wave data. In: Foulger GR and Jurdy DM (eds.) *Plates, Plumes, and Planetary Processes*, pp. 209–233. Geological Society of America.

Lassak TM, McNamara AK, and Zhong S (2007) Influence of thermochemical piles on topography at Earth's core-mantle boundary. *Earth and Planetary Science Letters* 261: 443–455.

Lawrence JF and Shearer PM (2008) Imaging mantle transition zone thickness with SdS-SS finite-frequency sensitivity kernels. *Geophysical Journal International* 174: 143–158.

Lawver LA and Mueller RD (1994) Iceland hotspot track. *Geology* 22: 311–314.

Lay T and Garnero EJ (2011) Deep mantle seismic modeling and imaging. In: Jeanloz R and Freeman KH (eds.) *Annual Review of Earth and Planetary Sciences*, 39, pp. 91–123. Palo Alto, CA: Annual Reviews.

Le Pourhiet L, Gurnis M, and Saleeby J (2006) Mantle instability beneath the Sierra Nevada mountains in California and Death Valley extension. *Earth and Planetary Science Letters* 251: 104–119.

Lecheminant AN and Heaman LM (1989) Mackenzie igneous events, Canada – Middle Proterozoic hotspot magmatism associated with ocean opening. *Earth and Planetary Science Letters* 96: 38–48.

Lee C-TA, Luffi P, Hoeink T, Li J, Dasgupta R, and Hernlund J (2010) Upside-down differentiation and generation of a 'primordial' lower mantle. *Nature* 463: U102–U930.

Lee C-TA, Luffi P, Plank T, Dalton H, and Leeman WP (2009) Constraints on the depths and temperatures of basaltic magma generation on Earth and other terrestrial planets using new thermobarometers for mafic magmas. *Earth and Planetary Science Letters* 279: 20–33.

Lee CTA, Lenardic A, Cooper CM, Niu F, and Levander A (2005) The role of chemical boundary layers in regulating the thickness of continental and oceanic thermal boundary layers (vol. 230, p. 379, 2005). *Earth and Planetary Science Letters* 234: 297–298.

Legendre C, Maury RC, Blais S, Guillou H, and Cotten J (2006) Atypical hotspot chains: Evidence for a secondary melting zone below the Marquesas (French Polynesia). *Terra Nova* 18: 210–216.

Lei JS and Zhao DP (2006) A new insight into the Hawaiian plume. *Earth and Planetary Science Letters* 241: 438–453.

Lekic V, Cottaar S, Dziewonski A, and Romanowicz B (2012) Cluster analysis of global lower mantle tomography: A new class of structure and implications for chemical heterogeneity. *Earth and Planetary Science Letters* 357: 68–77.

Lenardic A and Jellinek AM (2009) Tails of two plume types in one mantle. *Geology* 37: 127–130.

Leng W and Gurnis M (2012) Shape of thermal plumes in a compressible mantle with depth- dependent viscosity. *Geophysical Research Letters* 39.

Leng W and Zhong S (2008) Controls on plume heat flux and plume excess temperature. *Journal of Geophysical Research* 113.

Levander A, Schmandt B, Miller MS, et al. (2011) Continuing Colorado plateau uplift by delamination-style convective lithospheric downwelling. *Nature* 472: U461–U540.

Li A and Detrick RS (2003) Azimuthal anisotropy and phase velocity beneath Iceland: Implication for plume-ridge interaction. *Earth and Planetary Science Letters* 214: 153165.

Li A and Detrick RS (2006) Seismic structure of Iceland from Rayleigh wave inversions and geodynamic implications. *Earth and Planetary Science Letters* 241: 901–912.

Li X, Kind R, Priestley K, et al. (2000) Mapping the Hawaiian plume conduit with converted seismic waves. *Nature* 405: 938–941.

Li X, Kind R, Yuan X, Woelbern I, and Hanka W (2004) Rejuvenation of the lithosphere by the Hawaiian Plume. *Nature* 427: 827–829.

Li XQ, Kind R, and Yuan XH (2003) Seismic study of upper mantle and transition zone beneath hotspots. *Physics of the Earth and Planetary Interiors* 136: 79–92.

Lin S-C and van Keken PE (2006a) Deformation, stirring and material transport in thermochemical plumes. *Geophysical Research Letters* 33.

Lin S-C and van Keken PE (2006b) Dynamics of thermochemical plumes: 1. Plume formation and entrainment of a dense layer. *Geochemistry, Geophysics, Geosystems* 7: Q02006. http://dx.doi.org/10.1029/02005GC001071.

Lin SC, Kuo BY, Chiao LY, and van Keken PE (2005) Thermal plume models and melt generation in East Africa: A dynamic modeling approach. *Earth and Planetary Science Letters* 237: 175–192.

Lin SC and van Keken PE (2005) Multiple volcanic episodes of flood basalts caused by thermochemical mantle plumes. *Nature* 436: 250–252.

Lin SC and van Keken PE (2006c) Dynamics of thermochemical plumes: 2. Complexity of plume structures and its implications for mapping mantle plumes. *Geochemistry, Geophysics, Geosystems* 7: Q03003. http://dx.doi.org/10.1029/02005GC001072.

Lipman PW and Glazner AF (1991) Introduction to middle tertiary cordilleran volcanism – Magma sources and relations to regional tectonics. *Journal of Geophysical Research* 96: 13193–13199.

Lithgow-Bertelloni C, Richards MA, Conrad CP, and Griffiths RW (2001) Plume generation in natural thermal convection at high Rayleigh and Prandtl numbers. *Journal of Fluid Mechanics* 434: 1–21.

Liu L and Stegman DR (2011) Segmentation of the Farallon slab. *Earth and Planetary Science Letters* 311: 1–10.

Liu L and Stegman DR (2012) Origin of Columbia River flood basalt controlled by propagating rupture of the Farallon slab. *Nature* 482: U386–U1508.

Lodge A and Helffrich G (2006) Depleted swell root beneath the Cape Verde Islands. *Geology* 34: 449–452.

Long MD and Silver PG (2009) Mantle flow in subduction systems: The subslab flow field and implications for mantle dynamics. *Journal of Geophysical Research* 114.

Long MD, Till CB, Druken KA, et al. (2012) Mantle dynamics beneath the Pacific Northwest and the generation of voluminous back-arc volcanism. *Geochemistry, Geophysics, Geosystems* 13.

Lupton JE, Arculus RJ, Evans LJ, and Graham DW (2012) Mantle hotspot neon in basalts from the Northwest Lau Back-arc Basin. *Geophysical Research Letters* 39.

Lustrino M and Wilson M (2007) The circum-Mediterranean anorogenic Cenozoic igneous province. *Earth-Science Reviews* 81: 1–65.

Lynch MA (1999) Linear ridge groups: Evidence for tensional cracking in the Pacific Plate. *Journal of Geophysical Research* 104: 29321–29333.

Lytle ML, Kelley KA, Hauri EH, Gill JB, Papia D, and Arculus RJ (2012) Tracing mantle sources and Samoan influence in the northwestern Lau back-arc basin. *Geochemistry, Geophysics, Geosystems* 13.

Mackay LM, Turner J, Jones SM, and White NJ (2005) Cenozoic vertical motions in the Moray Firth Basin associated with initiation of the Iceland Plume. *Tectonics* 24.

Maclennan J, McKenzie D, and Gronvold K (2001) Plume-driven upwelling under central Iceland. *Earth and Planetary Science Letters* 194: 67–82.

Macnab R, Verhoef J, Roest W, and Arkani-Hamed J (1995) New database documents the magnetic character of the Arctic and North Atlantic. *EOS, Transactions of the American Geophysical Union* 76(45): 449.

Mahoney JJ and Coffin MF (eds.) (1997) *Large Igneous Provinces: Continental, Oceanic and Planetary Flood Volcanism,* p. 438. Washington, DC: American Geophysical Union.

Mahoney JJ, Duncan RA, Tejada MLG, Sager WW, and Bralower TJ (2005) Jurassic-Cretaceous boundary age and mid-oceanic-ridge-type mantle source for Shatsky Rise. *Geology* 33: 185–188.

Mahoney JJ, Fitton JG, Wallace PJ, et al. (2001) Proceedings of the Ocean Drilling Program, Initial Reports, 192 (online). http://www-odp.tamu.edu/publications/192IR7192ir.htm.

Mahoney JJ, Jones WB, Frey FA, Salters VJ, Pyle DG, and Davies HL (1995) Geochemical characteristics of lavas from Broken Ridge, the Naturaliste Plateau and southernmost Kerguelen plateau: Cretaceous plateau volcanism in the SE Indian Ocean. *Chemical Geology* 120: 315–345.

Mahoney JJ, Storey M, Duncan RA, Spencer KJ, and Pringle M (1993) Geochemistry and age of the Ontong Java Plateau. In: Pringle M, Sager W, Sliter W, and Stein S (eds.) *The Mesozoic Pacific: Geology, Tectonics, and Volcanism. Geophysical Monograph Seriese,* 77, pp. 233–261. Washington, DC: AGU.

Maia M, Ackermand D, Dehghani GA, et al. (2000) The Pacific-Antarctic Ridge-Foundation Hotspot interaction: A case study of a ridge approaching a hotspot. *Marine Geology* 167: 61–84.

Maia M, Hemond C, and Gente P (2001) Contrasted interactions between plume, upper mantle, and lithosphere: Foundation chain case. *Geochemistry, Geophysics, Geosystems* 2.

Mallik A and Dasgupta R (2012) Reaction between MORB-eclogite derived melts and fertile peridotite and generation of ocean island basalts. *Earth and Planetary Science Letters* 329: 97–108.

Manga M (1997) Interactions between mantle diapirs. *Geophysical Research Letters* 24: 1871–1874.

Marks KM and Sandwell DT (1991) Analysis of geoid height versus topography for oceanic plateaus and swells using nonbiased linear-regression. *Journal of Geophysical Research* 96: 8045–8055.

Marske JP, Pietruszka AJ, Weis D, Garcia MO, and Rhodes JM (2007) Rapid passage of a small-scale mantle heterogeneity through the melting regions of Kilauea and Mauna Loa Volcanoes. *Earth and Planetary Science Letters* 259: 34–50.

Marzoli A, Jourdan F, Puffer JH, et al. (2011) Timing and duration of the Central Atlantic magmatic province in the Newark and Culpeper basins, eastern USA. *Lithos* 122: 175–188.

Marzoli A, Piccirillo EM, Renne PR, et al. (2000) The Cameroon volcanic line revisited: Petrogenesis of continental basaltic magmas from lithospheric and asthenospheric mantle sources. *Journal of Petrology* 41: 87–109.

Marzoli A, Renne PR, Piccirillo EM, Ernesto M, Bellieni G, and De Min A (1999) Extensive 200-million-year-old continental flood basalts of the Central Atlantic Magmatic Province. *Science* 284: 616–618.

Massmeyer A, Di Giuseppe E, Davaille A, Rolf T, and Tackley PJ (2013) Numerical simulation of thermal plumes in a Herschel-Bulkley fluid. *Journal of Non-Newtonian Fluid Mechanics* 195: 32–45.

Masters G, Laske G, Bolton H, and Dziewonski A (2000) The relative behavior of shear velocity, bulk sound speed, and compressional velocity in the mantle: Implications for chemical and thermal structure. In: *Earth's Deep Interior: Mineral Physics and Tomography from the Atomic to the Global Scale. Geophysical Monograph Series*, 117, pp. 63–87. Washington, DC: AGU.

Matyska C, Moser J, and Yuen DA (1994) The potential influence of radiative heat transfer on the formation of megaplumes in the lower mantle. *Earth and Planetary Science Letters* 125: 255–266.

Matyska C and Yuen DA (2005) The importance of radiative heat transfer on superplumes in the lower mantle with the new post-perovskite phase change. *Earth and Planetary Science Letters* 234: 71–81.

Matyska C and Yuen DA (2006) Lower mantle dynamics with the post-perovskite phase change, radiative thermal conductivity, temperature- and depth-dependent viscosity. *Physics of the Earth and Planetary Interiors* 154: 196–207.

Matyska C, Yuen DA, Wentzcovitch RM, and Qzkova H (2011) The impact of variability in the rheological activation parameters on lower-mantle viscosity stratification and its dynamics. *Physics of the Earth and Planetary Interiors* 188: 1–8.

Mayborn KR and Lesher CE (2004) Paleoproterozoic mafic dike swarms of northeast Laurentia: Products of plumes or ambient mantle? *Earth and Planetary Science Letters* 225: 305–317.

McDougall I and Duncan RA (1988) Age progressive volcanism in the Tasmantid Seamounts. *Earth and Planetary Science Letters* 89: 207–220.

McDougall I, Verwoerd W, and Chevallier L (2001) K-Ar geochronology of Marion Island, Southern Ocean. *Geological Magazine* 138: 1–17.

McKenzie D (1984) The generation and compaction of partially molten rock. *Journal of Petrology* 25: 713–765.

McKenzie D and Bickle MJ (1988) The volume and composition of melt generated by extension of the lithosphere. *Journal of Petrology* 29: 625–679.

McNamara AK, Garnero EJ, and Rost S (2010) Tracking deep mantle reservoirs with ultra-low velocity zones. *Earth and Planetary Science Letters* 299: 1–9.

McNamara AK and Zhong SJ (2004) The influence of thermochemical convection on the fixity of mantle plumes. *Earth and Planetary Science Letters* 222: 485–500.

McNamara AK and Zhong SJ (2005) Thermochemical structures beneath Africa and the Pacific Ocean. *Nature* 437: 1136–1139.

McNutt M (1988) Thermal and mechanical properties of the Cape Verde Rise. *Journal of Geophysical Research* 93: 2784–2794.

McNutt M and Bonneville A (2000) A shallow, chemical origin for the Marquesas Swell. *Geochemistry, Geophysics, Geosystems* 1.

McNutt MK (1998) Superswells. *Reviews of Geophysics* 36: 211–244.

McNutt MK (2002) Heat flow variations over Hawaiian swell controlled by near-surface processes, not plume properties. *Geophysical Monograph* 128: 364–365.

McNutt MK, Caress DW, Reynolds J, Jordahl KA, and Duncan RA (1997) Failure of plume theory to explain midplate volcanism in the southern Austral Island. *Nature* 389: 479–482.

McNutt MK and Fischer KM (1987) The South Pacific Superswell. In: Keating GH, Fryer P, Batiza R, and Boehlert GW (eds.) *Seamounts, Islands, and Atolls. Geophysical Monograph,* 43, Washington, DC: AGU.

McNutt MK and Judge AV (1990) The Superswell and mantle dynamics beneath the South Pacific. *Science* 248: 969–975.

McNutt MK, Winterer EL, Sager WW, Natland JH, and Ito G (1990) The Darwin Rise: A cretaceous superswell? *Geophysical Research Letters* 17: 1101–1104.

Meert JG and Tamrat E (2006) Paleomagnetic evidence for a stationary Marion hotspot: Additional paleomagnetic data from Madagascar. *Gondwana Research* 10: 340–348.

Mege D and Korme T (2004) Dyke swarm emplacement in the Ethiopian large igneous province: Not only a matter of stress. *Journal of Volcanology and Geothermal Research* 132: 283–310.

Meibom A, Sleep NH, Zahnle K, and Anderson DL (2005) Models for noble gasses in mantle geochemistry: Some observations and alternatives. In: *Plumes, Plates, and Paradigms*, pp. 347–363. Geological Society of America, Special paper 388.

Menzies M, Baker J, Chazot G, and Al'Kadasi M (1997) Evolution of the Red Sea volcanic margin, Western Yemen. In: Mahoney JJ and Coffin MF (eds.) *Large Igneous Provinces: Continental, Oceanic, and Planetary Flood Volcanism. Geophysical Monograph,* 100, pp. 29–43. Washington, DC: American Geophysical Union.

Mihalffy P, Steinberger B, and Schmeling H (2008) The effect of the large-scale mantle flow field on the Iceland hotspot track. *Tectonophysics* 447: 5–18.

Milelli L, Fourel L, and Jaupart C (2012) A lithospheric instability origin for the Cameroon Volcanic Line. *Earth and Planetary Science Letters* 335: 80–87.

Minor DR and Mukasa SB (1997) Zircon U-Pb and hornblende Ar-40-Ar-39 ages for the Dufek layered mafic intrusion, Antarctica: Implications for the age of the Ferrar large igneous province. *Geochimica et Cosmochimica Acta* 61: 2497–2504.

Minshull TA, Lane CI, Collier JS, and Whitmarsh RB (2008) The relationship between rifting and magmatism in the northeastern Arabian Sea. *Nature Geoscience* 1: 463–467.

Missenard Y and Cadoux A (2012) Can Moroccan Atlas lithospheric thinning and volcanism be induced by Edge-Driven Convection? *Terra Nova* 24: 27–33.

Mittelstaedt E, Ito G, and van Hunen J (2011) Repeat ridge jumps associated with plume-ridge interaction, melt transport, and ridge migration. *Journal of Geophysical Research* 116.

Mittelstaedt E, Soule S, Harpp K, et al. (2012) Multiple expressions of plume-ridge interaction in the Galapagos: Volcanic lineaments and ridge jumps. *Geochemistry, Geophysics, Geosystems* 13.

Mittelstaedt EL and Ito G (2005) Plume-ridge interaction, lithospheric stresses, and origin of near-ridge volcanic lineaments. *Geochemistry, Geophysics, Geosystems* 6: Q06002. http://dx.doi.org/10.1029/02004GC000860.

Mjelde R, Wessel P, and Mueller RD (2010) Global pulsations of intraplate magmatism through the Cenozoic. *Lithosphere* 2: 361–376.

Molnar P and Stock J (1987) Relative motions of hotspots in the Pacific, Atlantic and Indian Oceans since late Cretaceous time. *Nature* 327: 587–591.

Montelli R, Nolet G, Dahlen FA, and Masters G (2006) A catalogue of deep mantle plumes: New results from finite-frequency tomography. *Geochemistry, Geophysics, Geosystems* 7.

Montigny R, Ngounouno I, and Deruelle B (2004) K-Ar ages of magmatic rocks from the Garoua rift: Their place in the frame of the 'Cameroun Line'. *Comptes Rendus Geoscience* 336: 1463–1471.

Moore WB, Schubert G, and Tackley P (1998) Three-dimensional simulations of plume-lithosphere interaction at the Hawaiian swell. *Science* 279: 1008–1011.

Morgan WJ (1971) Convection plumes in the lower mantle. *Nature* 230: 42–43.

Morgan WJ (1972) Plate motions and deep mantle convection. *Geological Society of America Memoir* 132: 7–22.

Morgan WJ (1978) Rodriguez, Darwin, Amsterdam,. . ., A second type of hotspot island. *Journal of Geophysical Research* 83: 5355–5360.

Morgan WJ (1983) Hotspot tracks and the early rifting of the Atlantic. *Tectonophysics* 94: 123–139.

Morley CK, Wescott WA, Stone DM, Harper RM, Wigger ST, and Karanja FM (1992) Tectonic evolution of The Northern Kenyan rift. *Journal of the Geological Society* 149: 333–348.

Mosar J, Lewis G, and Torsvik TH (2002) North Atlantic sea-floor spreading rates; implications for the Tertiary development of inversion structures of the Norwegian-Greenland Sea. *Geological Society of London* 159: 503–515.

Mosca I, Cobden L, Deuss A, Ritsema J, and Trampert J (2012) Seismic and mineralogical structures of the lower mantle from probabilistic tomography. *Journal of Geophysical Research* 117.

Mueller RD, Roest WR, and Royer J-Y (1998) Asymmetric sea-floor spreading caused by ridge-plume interactions. *Nature* 396: 455–459.

Mukhopadhyay S (2012) Early differentiation and volatile accretion recorded in deep-mantle neon and xenon. *Nature* 486: U101–U124.

Müller JR, Ito G, and Martel SJ (2001) Effects of volcano loading on dike propagation in an elastic half-space. *Journal of Geophysical Research* 106: 11101–11113.

Müller RD, Roest WR, Royer J-Y, Gahagan LM, and Sclater JG (1993a) *A digital age map of the ocean floor*. Scripps Institution of Oceanography, Reference Series.

Müller RD, Royer J-Y, and Lawver LA (1993b) Revised plate motions relative to the hotspots from combined Atlantic and Indian Ocean hotspot tracks. *Geology* 21: 275–278.

Mutter JC and Zehnder CM (1988) Deep crustal structure and magmatic processes: The inception of seafloor spreading in the Norwegian-Greenland Sea. In: Moron AC and Parson LM (eds.) *Early Tertiary Volcanism and the Opening of the NE Atlantic 39*, pp. 35–48. Geological Society of America, Special Publication.

Nadin PA, Kusznir NJ, and Cheadle MJ (1997) Early Tertiary plume uplift of the North Sea and Faeroe-Shetland basins. *Earth and Planetary Science Letters* 148: 109–127.

Naif S, Key K, Constable S, and Evans RL (2013) Melt-rich channel observed at the lithosphere-asthenosphere boundary. *Nature* 495: 356–359.

Nakagawa T, Tackley PJ, Deschamps F, and Connolly JAD (2010) The influence of MORB and harzburgite composition on thermo-chemical mantle convection in a 3-D spherical shell with self-consistently calculated mineral physics. *Earth and Planetary Science Letters* 296: 403–412.

Nakakuki T, Yuen DA, and Honda S (1997) The interaction of plumes with the transition zone under continents and oceans. *Earth and Planetary Science Letters* 146: 379–391.

Nakanishi M, Sager WW, and Klaus A (1999) Magnetic lineations within Shatsky Rise, northwest Pacific Ocean: Implications for hot spot-triple junction interaction and oceanic plateau formation. *Journal of Geophysical Research* 104: 7539–7556.

Nataf H-C (2000) Seismic imaging of mantle plumes. *Annual Review of Earth and Planetary Sciences* 28: 391–417.

Nataf HC and VanDecar J (1993) Seismological detection of a mantle plume? *Nature* 364: 115120.

Natland JH (1980) The progression of volcanism in the Samoan linear volcanic chain. *American Journal of Science* 280A: 709–735.

Neal CR, Mahoney JJ, and Chazey WJ (2002) Mantle sources and the highly variable role of continental lithosphere in basalt petrogenesis of the Kerguelen Plateau and Broken Ridge LIP: Results from ODP Leg 183. *Journal of Petrology* 43: 1177–1205.

Neal CR, Mahoney JJ, Kroenke LW, Duncan RA, and Petterson MG (1997) The Ontong Java Plateau. In: Mahoney JJ and Coffin MF (eds.) *Large Igneous Provinces: Continental, Oceanic, and Planetary Flood Volcanism. Geophysical Monograph*, vol. 100, pp. 183–216. Washington, DC: American Geophysical Union.

Nelson ST and Tingey DG (1997) Time-transgressive and extension-related basaltic volcanism in southwest Utah and vicinity. *Geological Society of America Bulletin* 109: 1249–1265.

Ni SD, Helmberger DV, and Tromp J (2005) Three-dimensional structure of the African superplume from waveform modelling. *Geophysical Journal International* 161: 283–294.

Ni SD, Tan E, Gurnis M, and Helmberger D (2002) Sharp sides to the African superplume. *Science* 296: 1850–1852.

Nicolaysen K, Frey FA, Hodges KV, Weis D, and Giret A (2000) $^{40}Ar/^{39}Ar$ geochronology of flood basalts from the Kerguelen Archipelago, southern Indian Ocean: Implications for Cenozoic eruption rates of the Kerguelen plume. *Earth and Planetary Science Letters* 174: 313–328.

Nielsen TK and Hopper JR (2004) From rift to drift: Mantle melting during continental breakup. *Geochemistry, Geophysics, Geosystems* 5.

Nielsen TK, Larsen HC, and Hopper JR (2002) Contrasting rifted margin styles south of Greenland; implications for mantle plume dynamics. *Earth and Planetary Science Letters* 200: 271–286.

Niu F, Solomon SC, Silver PG, Suetsugu D, and Inoue H (2002a) Mantle transition-zone structure beneath the South Pacific Superswell and evidence for a mantle plume underlying the Society Hotspot. *Earth and Planetary Science Letters* 198: 371–380.

Niu Y, Collerson KD, Batiza R, Wendt I, and Regelous M (1999) The origin of E-type MORB at ridges far from mantle plumes: The East Pacific Rise at 11°20'N. *Journal of Geophysical Research* 104: 7067–7087.

Niu Y, Regelous M, Wendt IJ, Batiza R, and O'Hara MJ (2002b) Geochemistry of near-EPR seamounts: Importance of source vs. process and the origin of enriched mantle component. *Earth and Planetary Science Letters* 199: 327–345.

Niu Y, Waggoner G, Sinton JM, and Mahoney JJ (1996) Mantle source heterogeneity and melting processes beneath seafloor spreading centers: The East Pacific Rise 18°-19°S. *Journal of Geophysical Research* 101: 27711–27733.

Nolet G, Allen R, and Zhao D (2007) Mantle plume tomography. *Chemical Geology* 241: 248–263.

Norton IO (2000) Global hotspot reference frames and plate motion. In: Richards MA, Gordon RG, and van der Hilst RD (eds.) *The History and Dynamics of Global Plate Motions. Geophysical Monograph*, vol. 121, pp. 339–357. Washington, DC: AGU.

Nyblade AA (2011) The upper-mantle low-velocity anomaly beneath Ethiopia, Kenya, and Tanzania: Constraints on the origin of the African superswell in eastern Africa and plate versus plume models of mantle dynamics. *Geological Society of America Special Papers* 478: 37–50.

Nyblade AA and Robinson SW (1994) The African superswell. *Geophysical Research Letters* 21: 765–768.

O'Connor JM and Duncan RA (1990) Evolution of the Walvis Ridge-Rio Grande Rise hot spot system: Implications for African and South American plate motions over plumes. *Journal of Geophysical Research* 95: 17475–17502.

O'Connor JM, Jokat W, le Roex AP, et al. (2012) Hotspot trails in the South Atlantic controlled by plume and plate tectonic processes. *Nature Geoscience* 5: 735–738.

O'Connor JM and Roex APL (1992) South Atlantic hot spot-plume systems: 1. Distribution of volcanism in time and space. *Earth and Planetary Science Letters* 113: 343–364.

O'Connor JM, Steinberger B, Regelous M, et al. (2013) Constraints on past plate and mantle motion from new ages for the Hawaiian-Emperor Seamount Chain. *Geochemistry, Geophysics, Geosystems* 14: 4564–4584.

O'Connor JM, Stoffers P, van den Bogaard P, and McWilliams M (1999) First seamount age evidence for significantly slower African Plate motion since 19 to 30 Ma. *Earth and Planetary Science Letters* 171: 575–589.

O'Connor JM, Stoffers P, and Wijbrans JR (2002) Pulsing of a focused mantle plume: Evidence from the distribution of Foundation Chain hotspot volcanism. *Geophysical Research Letters* 29(9): 4.

O'Connor JM, Stoffers P, and Wijbrans JR (2004) The Foundation Chain: Inferring hotspot-plate interaction from a weak seamount trail. In: Hekinian R, Stoffers P, and Cheminee J-L (eds.) *Oceanic Hotspots*, pp. 349–374. Springer.

O'Neill C, Müller D, and Steinberger B (2005) On the uncertainties in hot spot reconstructions and the significance of moving hot spot reference frames. *Geochemistry, Geophysics, Geosystems* 6: Q04003. http://dx.doi.org/10.1029/02004GC000784.

O'Reilly SY and Griffin WL (1988) Mantle Metasomatism beneath western Victoria, Australia.1. Metasomatic Processes in Cr-diopside Lherzolites. *Geochimica et Cosmochimica Acta* 52: 433–447.

Obrebski M, Allen RM, Xue M, and Hung S-H (2010) Slab-plume interaction beneath the Pacific Northwest. *Geophysical Research Letters* 37.

Ogden DE and Sleep NH (2012) Explosive eruption of coal and basalt and the end-Permian mass extinction. *Proceedings of the National Academy of Sciences of the United States of America* 109: 59–62.

Olson P (1990) Hot spots, swells and mantle plumes. In: Ryan MP (ed.) *Magma Transport and Storage*, pp. 33–51. New York: Wiley.

Olson P and Christensen U (1986) Solitary wave propagation in a fluid conduit within a viscous matrix. *Journal of Geophysical Research: Solid Earth* 91: 6367–6374.

Olson P, Schubert G, and Anderson C (1987) Plume formation in the D"-layer and the roughness of the core-mantle boundary. *Nature* 327: 409–413.

Olson P, Schubert G, and Anderson C (1993) Structure of axisymmetric mantle plumes. *Journal of Geophysical Research: Solid Earth* 98: 6829–6844.

Olson P, Schubert G, Anderson C, and Goldman P (1988) Plume formation and lithosphere erosion: A comparison of laboratory and numerical experiments. *Journal of Geophysical Research* 93: 15065–15084.

Olson P and Singer H (1985) Creeping plumes. *Journal of Fluid Mechanics* 158: 511–531.

Operto S and Charvis P (1996) Deep structure of the southern Kerguelen Plateau (southern Indian Ocean) from ocean bottom seismometer wide-angle seismic data. *Journal of Geophysical Research* 101: 25077–25103.

Oxburgh ER and Parmentier EM (1977) Compositional and density stratification in oceanic lithosphere-causes and consequences. *Geological Society of London* 133: 343–355.

Ozawa A, Tagami T, and Garcia MO (2005) Unspiked K-Ar dating of the Honolulu rejuvenated and Ko'olau shield volcanism on O'ahu, Hawai'i. *Earth and Planetary Science Letters* 232: 1–11.

Paczkowski K, Bercovici D, Landuyt W, and Brandon MT (2012) Drip instabilities of continental lithosphere: Acceleration and entrainment by damage. *Geophysical Journal International* 189: 717–729.

Pankhurst RJ, Leat PT, Sruoga P, et al. (1998) The Chon Aike province of Patagonia and related rocks in West Antarctica: A silicic large igneous province. *Journal of Volcanology and Geothermal Research* 81: 113–136.

Pankhurst RJ, Riley TR, Fanning CM, and Kelley SP (2000) Episodic silicic volcanism in Patagonia and the Antarctic Peninsula: Chronology of magmatism associated with the break-up of Gondwana. *Journal of Petrology* 41: 605–625.

Pares JM and Moore TC (2005) New evidence for the Hawaiian hotspot plume motion since the Eocene. *Earth and Planetary Science Letters* 237: 951–959.

Park Y and Nyblade AA (2006) P-wave tomography reveals a westward dipping low velocity zone beneath the Kenya Rift. *Geophysical Research Letters* 33.

Parkinson IJ, Shaefer BF, and Arculus RJ (2002) A lower mantle origin for the world's biggest LIP? A high precision Os isotope isochron from Ontong Java Plateau basalts drilled on ODP Leg 192. *Geochimica et Cosmochimica Acta* 66: A580.

Parman SW, Kurz MD, Hart SR, and Grove TL (2005) Helium solubility in olivine and implications for high $^{3}He/^{4}He$ in ocean island basalts. *Nature* 437(7062): 1140–1143.

Parnell-Turner RE, White NJ, Maclennan J, Henstock TJ, Murton BJ, and Jones SM (2013) Crustal manifestations of a hot transient pulse at 60°N beneath the Mid-Atlantic Ridge. *Earth and Planetary Science Letters* 363: 109–120.

Parsons B and Daly S (1983) The relationship between surface-topography, gravity-anomalies, and temperature structure of convection. *Journal of Geophysical Research* 88: 1129–1144.

Passier ML and Snieder RK (1996) Correlation between shear wave upper mantle structure and tectonic surface expressions: Application to central and southern Germany. *Journal of Geophysical Research* 101: 25293–25304.

Payne JL and Clapham ME (2012) End-permian mass extinction in the oceans: An ancient analog for the twenty-first century? In: Jeanloz R (ed.) *Annual Review of Earth and Planetary Sciences*, vol 40, pp. 89–111.

Peate DW (1997) The Parana-Etendeka provinces. In: Mahoney JJ and Coffin MF (eds.) *Large Igneous Provinces: Continental, Oceanic, and Planetary Flood Volcanism*. *Geophysical Monograph,* 100, pp. 217–246. Washington, DC: American Geophysical Union.

Pertermann M and Hirschmann MM (2003) Partial melting experiments on a MORB-like pyroxenite between 2 and 3 GPa: Constraints on the presence of pyroxenite in basalt source regions from solidus locations and melting rate. *Journal of Geophysical Research* 108(B2). http://dx.doi.org/10.1029/2000JB 000118.

Peto MK, Mukhopadhyay S, and Kelley KA (2013) Heterogeneities from the first 100 million years recorded in deep mantle noble gases from the Northern Lau Back-arc Basin. *Earth and Planetary Science Letters* 369: 13–23.

Petterson MG (2004) The geology of north and central Malaita, Solomon Islands: The thickest and most accessible part of the world's largest (Ontong Java) oceanic plateau. In: Fitton JG, Mahoney JJ, Wallace PJ, and Saunders AD (eds.) *Origin and evolution of the Ontong Java Plateau, Special publications 229*, pp. 63–82. London: Geological Society.

Phipps Morgan J (1999) Isotope topology of individual hotspot basalt arrays: Mixing curves or melt extraction trajectories. *Geochemistry, Geophysics, Geosystems* 1. http://dx.doi.org/10.1029/1999GC000004.

Phipps Morgan J (2001) Thermodynamics of pressure release melting of a veined plum pudding mantle. *Geochemistry, Geophysics, Geosystems* 2. http://dx.doi.org/10.1029/2000GC000049.

Phipps Morgan J, Morgan WJ, and Price E (1995a) Hotspot melting generates both hotspot volcanism and a hotspot swell. *Journal of Geophysical Research* 100: 8045–8062.

Phipps Morgan J, Morgan WJ, Zhang YS, and Smith WHF (1995b) Observational hints for a plume-fed, suboceanic asthenosphere and its role in mantle convection. *Journal of Geophysical Research* 100: 12753–12767.

Pietruszka AJ, Rubin KH, and Garcia MO (2001) (super 226) Ra- (super 230) Th- (super 238) U disequilibria of historical Kilauea lavas (1790–1982) and the dynamics of mantle melting within the Hawaiian Plume. *Earth and Planetary Science Letters* 186: 15–31.

Pik R, Deniel C, Coulon C, Yirgu G, Hofmann C, and Ayalew D (1998) The northwestern Ethiopian Plateau flood basalts. Classification and spatial distribution of magma types. *Journal of Volcanology and Geothermal Research* 81: 91–111.

Pilet S, Baker MB, and Stolper EM (2008) Metasomatized lithosphere and the origin of alkaline lavas. *Science* 320: 916–919.

Pilet S, Ulmer P, and Villiger S (2010) Liquid line of descent of a basanitic liquid at 1.5 Gpa: Constraints on the formation of metasomatic veins. *Contributions to Mineralogy and Petrology* 159: 621–643.

Pilidou S, Priestley K, Debayle E, and Gudmundsson O (2005) Rayleigh wave tomography in the North Atlantic: High resolution images of the Iceland, Azores and Eifel mantle plumes. *Lithos* 79: 453–474.

Pilidou S, Priestley K, Gudnmundsson O, and Debayle E (2004) Upper mantle S-wave speed heterogeneity and anisotropy beneath the North Atlantic from regional surface wave tomography: The Iceland and Azores plumes. *Geophysical Journal International* 159: 1057–1076.

Poore H, White N, and Maclennan J (2011) Ocean circulation and mantle melting controlled by radial flow of hot pulses in the Iceland plume. *Nature Geoscience* 4: 558–561.

Portnyagin M, Hoernle K, and Savelyev D (2009) Ultra-depleted melts from Kamchatkan ophiolites: Evidence for the interaction of the Hawaiian plume with an oceanic spreading center in the Cretaceous? *Earth and Planetary Science Letters* 287: 194–204.

Presnall DC, Gudfinnsson GH, and Walter MJ (2002) Generation of mid-ocean ridge basalts at pressures from 1 to 7 GPa. *Geochimica et Cosmochimica Acta* 66: 2073–2090.

Priestley K and Tilmann F (1999) Shear-wave structure of the lithosphere above the Hawaiian hot spot from two-station Rayleigh wave phase velocity measurements. *Geophysical Research Letters* 26: 1493–1496.

Putirka KD (2005) Mantle potential temperatures at Hawaii, Iceland, and the mid-ocean ridge system, as inferred from olivine phenocrysts: Evidence for thermally driven mantle plumes. *Geochemistry, Geophysics, Geosystems* 6: Q05L08. http://dx.doi.org/10.1029/2005GC000915.

Putirka KD, Perfit M, Ryerson FJ, and Jackson MG (2007) Ambient and excess mantle temperatures, olivine thermometry, and active vs. passive upwelling. *Chemical Geology* 241: 177–206.

Putirka KD, Ryerson FJ, Perfit M, and Ridley WI (2011) Mineralogy and composition of the oceanic mantle. *Journal of Petrology* 52: 279–313.

Raddick MJ, Parmentier EM, and Scheirer DS (2002) Buoyant decompression melting: A possible mechanisms for intra plate volcanism. *Journal of Geophysical Research* 107: 2228. http://dx.doi.org/10.1029/2001JB000617.

Ramalho R, Helffrich G, Cosca M, Vance D, Hoffmann D, and Schmidt DN (2010) Episodic swell growth inferred from variable uplift of the Cape Verde hotspot islands. *Nature Geoscience* 3: 774–777.

Ray JS, Mahoney JJ, Duncan RA, Ray J, Wessel P, and Naar DF (2012) Chronology and geochemistry of Lavas from the Nazca ridge and Easter Seamount chain: An similar to 30 Myr hotspot record. *Journal of Petrology* 53: 1417–1448.

Raymond C, Stock JM, and Cande SC (2000) Fast Paleogene motion of the Pacific hotspots from revised global plate circuit constraints. The history and dynamics of global plate motions. *AGU Geophysical Monograph* 121: 359–375.

Reichow MK, Pringle MS, Al'Mukhamedov AI, et al. (2009) The timing and extent of the eruption of the Siberian Traps large igneous province: Implications for the end-Permian environmental crisis. *Earth and Planetary Science Letters* 277: 9–20.

Reichow MK, Saunders AD, White RV, Al'Mukhamedov AL, and Medvedev AY (2005) Geochemistry and petrogenesis of basalts from the West Siberian basin: An extension of the Permo-Triassic Siberian Traps, Russia. *Lithos* 79: 425–452.

Reid MR, Bouchet RA, Blichert-Toft J, et al. (2012) Melting under the Colorado Plateau, USA. *Geology* 40: 387–390.

Reiners PW (2002) Temporal-compositional trends in intraplate basalt eruptions: Implications for mantle heterogeneity and melting processes. *Geochemistry, Geophysics, Geosystems* 3: 1011. http://dx.doi.org/10.1029/2002GC000250.

Renne PR, Deckart K, Ernesto M, Feraud G, and Piccirillo EM (1996) Age of the Ponta Grossa dike swarm (Brazil), and implications to Parana flood volcanism. *Earth and Planetary Science Letters* 144: 199–211.

Retallack GJ (2013) Permian and Triassic greenhouse crises. *Gondwana Research* 24: 90–103.

Reusch AM, Nyblade AA, Tibi R, et al. (2011) Mantle transition zone thickness beneath Cameroon: Evidence for an upper mantle origin for the Cameroon Volcanic Line. *Geophysical Journal International* 187: 1146–1150.

Reusch AM, Nyblade AA, Wiens DA, et al. (2010) Upper mantle structure beneath Cameroon from body wave tomography and the origin of the Cameroon Volcanic Line. *Geochemistry, Geophysics, Geosystems* 11.

Reyners M, Eberhart-Phillips D, and Bannister S (2011) Tracking repeated subduction of the Hikurangi Plateau beneath New Zealand. *Earth and Planetary Science Letters* 311: 165171.

Ribe N (1996) The dynamics of plume-ridge interaction 2. Off-ridge plumes. *Journal of Geophysical Research* 101: 16195–16204.

Ribe N, Christensen UR, and Theissing J (1995) The dynamics of plume-ridge interaction, 1: Ridge-centered plumes. *Earth and Planetary Science Letters* 134: 155–168.

Ribe N and Delattre WL (1998) The dynamics of plume-ridge interaction, 3: The effects of ridge migration. *Geophysical Journal International* 133: 511–518.

Ribe NM and Christensen UR (1994) Three-dimensional modelling of plume-lithosphere interaction. *Journal of Geophysical Research* 99: 669–682.

Ribe NM and Christensen UR (1999) The dynamical origin of Hawaiian volcanism. *Earth and Planetary Science Letters* 171: 517–531.

Ribe NM, Davaille A, and Christensen UR (2007) Fluid dynamics of mantle plumes. In: Ritter J and Christensen U (eds.) *Mantle Plumes – A Multidisciplinary Approach*, p. 148. New York: Springer.

Ribe NM and de Valpine DP (1994) The global hotspot distribution and instability of D" *Geophysical Research Letters* 21: 1507–1510.

Richard GC and Bercovici D (2009) Water-induced convection in the Earth's mantle transition zone. *Journal of Geophysical Research* 114.

Richards MA, Duncan RA, and Courtillot VE (1989) Flood basalts and hotspot tracks: Plume heads and tails. *Science* 246: 103–107.

Richards MA and Griffiths RW (1989) Thermal entrainment by deflected mantle plumes. *Nature* 342: 900–902.

Richter FM (1973) Convection and the large-scale circulation of the mantle. *Journal of Geophysical Research* 78: 8735–8745.

Richter FM and McKenzie DP (1981) On some consequences and possible causes of layered mantle convection. *Journal of Geophysical Research* 86: 6133–6142.

Rickers F, Fichtner A, and Trampert J (2013) The Iceland-Jan Mayen plume system and its impact on mantle dynamics in the North Atlantic region: Evidence from full-waveform inversion. *Earth and Planetary Science Letters* 367: 39–51.

Ritsema J and Allen RM (2003) The elusive mantle plume. *Earth and Planetary Science Letters* 207: 1–12.

Ritsema J, Deuss A, van Heijst HJ, and Woodhouse JH (2011) S40RTS: a degree-40 shear- velocity model for the mantle from new Rayleigh wave dispersion, teleseismic traveltime and normal-mode splitting function measurements. *Geophysical Journal International* 184: 1223–1236.

Ritsema J, van Heijst HJ, and Woodhouse JH (1999) Complex shear velocity structure beneath Africa and Island. *Science* 286: 1925–1928.

Ritsema J, van Heijst HJ, and Woodhouse JH (2004) Global transition zone tomography. *Journal of Geophysical Research* 109.

Ritter JRR, Jordan M, Christensen UR, and Achauer U (2001) A mantle plume below the Eifel volcanic fields, Germany. *Earth and Planetary Science Letters* 186: 7–14.

Ritzwoller MH, Shapiro NM, and Zhong S-J (2004) Cooling history of the Pacific lithosphere. *Earth and Planetary Science Letters* 226: 69–84.

Roberge J, Wallace PJ, White RV, and Coffin MF (2005) Anomalous uplift and subsidence of the Ontong Java Plateau inferred from CO_2 contents of submarine basaltic glasses. *Geology* 33: 501–504.

Roberge J, White RV, and Wallace PJ (2004) Volatiles in submarine basaltic glasses from the Ontong Java Plateau (ODP Leg 192): Implications for magmatic processes and source region compositions. In: Fitton JG, Mahoney JJ, Wallace PJ, and Saunders AD (eds.) *Origin and Evolution of the Ontong Java Plateau*, pp. 239–258. London: Geological Society, Special Publications 229.

Rogers GC (1982) Oceanic plateaus as meteorite impact signatures. *Nature* 299: 341–342.

Rooney TO, Herzberg C, and Bastow ID (2012) Elevated mantle temperature beneath East Africa. *Geology* 40: 27–30.

Roy AB (2003) Geological and geophysical manifestations of the Reunion Plume-Indian lithosphere interactions: Evidence from northwest India. *Gondwana Research* 6: 487–500.

Rychert CA, Laske G, Harmon N, and Shearer PM (2013) Seismic imaging of melt in a displaced Hawaiian plume. *Nature Geoscience* 6: 657–660.

Saal AE, Hart SR, Shimizu N, Hauri EH, and Layne GD (1998) Pb isotopic variability in melt inclusions from oceanic island basalt, Polynesia. *Science* 282: 1481–1484.

Saffman PG and Taylor GI (1958) The penetration of a fluid into a porous medium of Hele-Shaw cell containing a more viscous liquid. *Proceedings of the Royal Society of London* A245: 312–329.

Sager WW (2005) What built Shatsky Rise, a mantle plume or ridge tectonics? In: Foulger G, Natland JH, Presnall DC, and Anderson DL (eds.) *Plumes, Plates, and Paradigms Special Paper 388*. Boulder, CO: Geological Society of America.

Sager WW, Kim J, Klaus A, Nakanishi M, and Khankishieva LM (1999) Bathymetry of Shatsky Rise, northwest Pacific Ocean: Implications for ocean plateau development at a triple junction. *Journal of Geophysical Research: Solid Earth* 104: 7557–7576.

Sager WW, Lamarch AJ, and Kopp C (2005) Paleomagnetic modeling of seamounts near the Hawaiian-Emperor bend. *Tectonophysics* 405: 121–140.

Sager WW, Zhang J, Korenaga J, et al. (2013) An immense shield volcano within the Shatsky Rise oceanic plateau, northwest Pacific Ocean. *Nature Geoscience* 6: 976–981, advance online publication.

Sakamaki T, Suzuki A, Ohtani E, et al. (2013) Ponded melt at the boundary between the lithosphere and asthenosphere. *Nature Geoscience* 6: 1041–1044.

Sallares V, Charvis P, Flueh ER, and Bialas J (2005) Seismic structure of the Carnegie ridge and the nature of the Galapagos hotspot. *Geophysical Journal International* 161: 763–788.

Salters VJM and Dick HJB (2002) Mineralogy of the mid-ocean-ridge basalt source from neodymium and isotopic composition of abyssal peridotites. *Nature* 418: 68–72.

Saltzer RL and Humphreys ED (1997) Upper mantle P wave velocity structure of the eastern Snake River Plain and its relationship to geodynamic models of the region. *Journal of Geophysical Research* 102: 11829–11841.

Samuel H and Bercovici D (2006) Oscillating and stagnating plumes in the Earth's lower mantle. *Earth and Planetary Science Letters* 248: 90–105.

Sandwell D and Fialko Y (2004) Warping and cracking of the Pacific plate by thermal contraction. *Journal of Geophysical Research* 109: B10411. http://dx.doi.org/10.1029/12004JB0003091.

Sandwell DT, Winterer EL, Mammerickx J, et al. (1995) Evidence for diffuse extension of the Pacific plate from Pukapuka ridges and cross-grain gravity lineations. *Journal of Geophysical Research* 100: 15087–15099.

Saunders AD, England RW, Relchow MK, and White RV (2005) A mantle plume origin for the Siberian traps: Uplift and extension in the West Siberian Basin, Russia. *Lithos* 79: 407–424.

Saunders AD, Fitton JG, Kerr AC, Norry MJ, and Kent RW (1997) The North Atlantic igneous province. In: Mahoney JJ and Coffin MF (eds.) *Large Igneous Provinces: Continental, Oceanic, and Planetary Flood Volcanism*. *Geophysical Monograph*, vol. 100, pp. 45–94. Washington, DC: American Geophysical Union.

Saunders AD, Jones SM, Morgan LA, Pierce KL, Widdowson M, and Xu YG (2007) Regional uplift associated with continental large igneous provinces: The roles of mantle plumes and the lithosphere. *Chemical Geology* 241: 282–318.

Schaller MF, Wright JD, and Kent DV (2011) Atmospheric P-CO_2 perturbations associated with the central atlantic magmatic province. *Science* 331: 1404–1409.

Schaller MF, Wright JD, Kent DV, and Olsen PE (2012) Rapid emplacement of the Central Atlantic Magmatic Province as a net sink for CO_2. *Earth and Planetary Science Letters* 323: 27–39.

Schaltegger U, Guex J, Bartolini A, Schoene B, and Ovtcharova M (2008) Precise U-Pb age constraints for end-Triassic mass extinction, its correlation to volcanism and Hettangian post-extinction recovery. *Earth and Planetary Science Letters* 267: 266–275.

Schilling J-G (1971) Sea floor evolution: Rare earth evidence. *Philosophical Transactions of the Royal Society of London A* 268A: 663–706.

Schilling J-G (1973) Iceland mantle plume: Geochemical study of Reykjanes Ridge. *Nature* 242: 565–571.

Schilling J-G (1991) Fluxes and excess temperatures of mantle plumes inferred from their interaction with migrating mid-ocean ridges. *Nature* 352: 397–403.

Schilling J-G, Thompson G, Kingsley R, and Humphris S (1985) Hotspot-migrating ridge interaction in the South Atlantic. *Nature* 313: 187–191.

Schmandt B, Dueker K, Humphreys E, and Hansen S (2012) Hot mantle upwelling across the 660 beneath Yellowstone. *Earth and Planetary Science Letters* 331: 224–236.

Schmandt B and Humphreys E (2010) Complex subduction and small-scale convection revealed by body-wave tomography of the western United States upper mantle. *Earth and Planetary Science Letters* 297: 435–445.

Schmerr N (2012) The gutenberg discontinuity: Melt at the lithosphere-asthenosphere boundary. *Science* 335: 1480–1483.

Schmerr N, Garnero E, and McNamara A (2010) Deep mantle plumes and convective upwelling beneath the Pacific Ocean. *Earth and Planetary Science Letters* 294: 143–151.

Schubert G, Masters G, Olson P, and Tackley P (2004) Superplumes or plume clusters? *Physics of the Earth and Planetary Interiors* 146: 147–162.

Schubert G and Olson P (1989) Solitary waves in mantle plumes. *Journal of Geophysical Research* 94: 9523–9532.

Schubert G, Turcotte DL, and Olson P (2001) *Mantle Convection in the Earth and Planets*, p. 940. Cambridge: Cambridge University Press.

Schulte P, Alegret L, Arenillas I, et al. (2010) The chicxulub asteroid impact and mass extinction at the cretaceous-paleogene boundary. *Science* 327: 1214–1218.

Schutt DL and Lesher CE (2006) Effects of melt depletion on the density and seismic velocity of garnet and spinel lherzolite. *Journal of Geophysical Research* 111.

Scott DR and Stevenson DJ (1989) A self-consistent model for melting, magma migration and buoyancy-driven circulation beneath mid-ocean ridges. *Journal of Geophysical Research* 94: 2973–2988.

Scott DR, Stevenson DJ, and Whitehead JA (1986) Observations of solitary waves in a viscously deformable pipe. *Nature* 319: 759–761.

Self S, Widdowson M, Thordarson T, and Jay AE (2006) Volatile fluxes during flood basalt eruptions and potential effects on the global environment: A Deccan perspective. *Earth and Planetary Science Letters* 248: 518–532.

Sharma M (1997) Siberian traps. In: Mahoney JJ and Coffi MF (eds.) *Large Igneous Provinces: Continental, Oceanic, and Planetary Flood Volcanism*. *Geophysical Monograph*, 100, pp. 273–296. Washington, DC: American Geophysical Union.

Sharp WD and Clague DA (2006) 50-Ma initiation of Hawaiian-Emperor bend records major change in Pacific plate motion. *Science* 313: 1281–1284.

Shellnutt JG, Denyszyn SW, and Mundil R (2012) Precise age determination of mafic and felsic intrusive rocks from the Permian Emeishan large igneous province (SW China). *Gondwana Research* 22: 118–126.

Shellnutt JG and Jahn BM (2011) Origin of Late Permian Emeishan basaltic rocks from the Panxi region (SW China): Implications for the Ti-classification and spatial-compositional distribution of the Emeishan flood basalts. *Journal of Volcanology and Geothermal Research* 199: 85–95.

Shen Y and Forsyth DW (1995) Geochemical constraints on initial and final depths of melting beneath mid-ocean ridges. *Journal of Geophysical Research* 100: 2211–2237.

Shen Y, Solomon SC, Bjarnason IT, et al. (2002) Seismic evidence for a tilted mantle plume and north-south mantle flow beneath Iceland. *Earth and Planetary Science Letters* 197: 261–272.

Shen Y, Solomon SC, Bjarnason IT, and Wolfe C (1998) Seismic evidence for a lower mantle origin of the Iceland plume. *Nature* 395: 62–65.

Shervais JW and Hanan BB (2008) Lithospheric topography, tilted plumes, and the track of the Snake River-Yellowstone hot spot. *Tectonics* 27.

Sheth HC (2005) from deccan to reunion: No trace of a mantle plume. In: Foulger G, Natland JH, Presnall DC, and Anderson DL (eds.) *Plumes, Plates, and Paradigms Special Paper 388*, pp. 477–501. Geological Society of America.

Shorttle O and Maclennan J (2011) Compositional trends of Icelandic basalts: Implications for short-length scale lithological heterogeneity in mantle plumes. *Geochemistry, Geophysics, Geosystems* 12.

Shorttle O, Maclennan J, and Jones SM (2010) Control of the symmetry of plume-ridge interaction by spreading ridge geometry. *Geochemistry, Geophysics, Geosystems* 11.

Sigloch K (2011) Mantle provinces under North America from multifrequency P wave tomography. *Geochemistry, Geophysics, Geosystems* 12.

Sikora PJ and Bergen JA (2004) Lower Cretaceous planktonic foraminiferal and nannofossil biostratigraphy of Ontong Java Plateau sites from DSDP Leg 30 and ODP Leg 192. In: Fitton JG, Mahoney JJ, Wallace PJ, and Saunders AD (eds.) *Origin and evolution of the Ontong Java Plateau, Special Publications 229*, pp. 83–112. London: Geological Society.

Silva IGN, Weis D, Scoates JS, and Barling J (2013) The ninetyeast ridge and its relation to the kerguelen, Amsterdam and St. Paul hotspots in the Indian ocean. *Journal of Petrology* 54: 1177–1210.

Simmons NA, Forte AM, and Grand SP (2006) Constraining mantle flow with seismic and geodynamic data: A joint approach. *Earth and Planetary Science Letters* 246: 109–124.

Sims KWW, DePaolo DJ, Murrell MT, et al. (1999) Porosity of the melting zone and variations in the solid mantle upwelling rate beneath Hawaii: Inferences from U-238-Th-230-Ra-226 and U-235-Pa-231 disequilibria. *Geochimica et Cosmochimica Acta* 63: 4119–4138.

Singh SC, Carton H, Chauhan AS, et al. (2011) Extremely thin crust in the Indian Ocean possibly resulting from Plume-Ridge Interaction. *Geophysical Journal International* 184: 29–42.

Sinton CW, Christie DM, and Duncan RA (1996) Geochronology of the Galapagos seamounts. *Journal of Geophysical Research* 101: 13689–13700.

Sinton CW, Duncan RA, and Denyer P (1997) Nicoya Peninsula, Costa Rica: A single suite of Caribbean oceanic plateau magmas. *Journal of Geophysical Research* 102: 15507–15520.

Skilbeck JN and Whitehead JA (1978) Formation of discrete islands in linear island chains. *Nature* 272: 499–501.

Slater L, Jull M, McKenzie D, and Gronvold K (1998) Deglaciation effects on mantle melting under Iceland: Results from the northern volcanic zone. *Earth and Planetary Science Letters* 164: 151–164.

Sleep NH (1990) Hotspots and mantle plumes: Some phenomenology. *Journal of Geophysical Research* 95: 6715–6736.

Sleep NH (1996) Lateral flow of hot plume material ponded at sublithospheric depths. *Journal of Geophysical Research* 101: 28065–28083.

Sleep NH (2006) Mantle plumes from top to bottom. *Earth-Science Reviews* 77: 231–271.

Sleep NH (2007) Edge-modulated stagnant-lid convection and volcanic passive margins. *Geochemistry, Geophysics, Geosystems* 8.

Sleep NH (2008) Channeling at the base of the lithosphere during the lateral flow of plume material beneath flow line hot spots. *Geochemistry, Geophysics, Geosystems* 9.

Sleep NH (2011) Seismically observable features of mature stagnant-lid convection at the base of the lithosphere: Some scaling relationships. *Geochemistry, Geophysics, Geosystems* 12.

Smallwood JR and White RS (2002) Ridge-plume interaction in the North Atlantic and its influence on continental breakup and seafloor spreading. *Geological Society* 197: 15–37, Special Publications.

Smirnov AV and Tarduno JA (2010) Co-location of eruption sites of the Siberian Traps and North Atlantic Igneous Province: Implications for the nature of hotspots and mantle plumes. *Earth and Planetary Science Letters* 297: 687–690.

Smith RB and Braile LW (1994) The Yellowstone hotspot. *Journal of Volcanology and Geothermal Research* 61: 121–187.

Smith WHF and Sandwell DT (1997) Global seafloor topography from satellite altimetry and ship depth soundings. *Science* 277: 1957–1962.

Sobolev AV, Hofmann AW, Bruegmann G, Batanova VG, and Kuzmin DV (2008) A quantitative link between recycling and osmium isotopes. *Science* 321: 536.

Sobolev AV, Hofmann AW, Kuzmin DV, et al. (2007) The amount of recycled crust in sources of mantle-derived melts. *Science* 316: 412–417.

Sobolev AV, Hofmann AW, Sobolev SV, and Nikogosian IK (2005) An olivine-free mantle source of Hawaiian shield basalts. *Nature* 434: 590–597.

Sobolev AV, Krivolutskaya NA, and Kuzmin DV (2009) Petrology of the parental melts and mantle sources of Siberian trap magmatism. *Petrology* 17: 253–286.

Sobolev SV, Sobolev AV, Kuzmin DV, et al. (2011) Linking mantle plumes, large igneous provinces and environmental catastrophes. *Nature* 477: U312–U380.

Spandler C, Yaxley G, Green DH, and Rosenthal A (2008) Phase relations and melting of anhydrous k-bearing eclogite from 1200 to 1600 °C and 3 to 5 GPa. *Journal of Petrology* 49: 771–795.

Sparks DW, Parmentier EM, and Morgan JP (1993) Three-dimensional mantle convection beneath a segmented spreading center: Implications for along-axis variations in crustal thickness and gravity. *Journal of Geophysical Research* 98: 21977–21995.

Staudigel H, Park KH, Pringle MS, Rubenstone JL, Smith WHF, and Zindler A (1991) The longevity of the South Pacific isotopic and thermal anomaly. *Earth and Planetary Science Letters* 102: 24–44.

Stein CA and Stein S (1992) A model for the global variation in oceanic depth and heat flow with lithospheric age. *Nature* 359: 123–129.

Stein CA and Stein S (1993) Constraints on Pacific midplate swells from global depth-age and heat flow-age models. In: Pringle M, Sager W, Sliter W, and Stein S (eds.) *The Mesozoic Pacific. Geophysical Monograph*, vol. 76, pp. 53–76. American Geophysical Union.

Stein CA and Stein S (1994) Constraints on hydrothermal heat flux through the oceanic lithosphere from global heat flow. *Journal of Geophysical Research* 99: 3081–3095.

Stein CA and Stein S (2003) Mantle plumes: Heat-flow near Iceland. *Astronomy and Geophysics* 44: 8–10.

Steinberger B (2000) Plumes in a convecting mantle: Models and observations for individual hotspots. *Journal of Geophysical Research* 105: 11127–11152.

Steinberger B and Antretter M (2006) Conduit diameter and buoyant rising speed of mantle plumes: Implications for the motion of hot spots and shape of plume conduits. *Geochemistry, Geophysics, Geosystems* 7.

Steinberger B, Sutherland R, and O'Connell RJ (2004) Prediction of Emperor-Hawaii seamount locations from a revised model of global plate motion and mantle flow. *Nature* 430: 167–173.

Steinberger B and Torsvik TH (2012) A geodynamic model of plumes from the margins of Large Low Shear Velocity Provinces. *Geochemistry, Geophysics, Geosystems* 13.

Stewart K and Rogers N (1996) Mantle plume and lithosphere contributions to basalts from southern Ethiopia. *Earth and Planetary Science Letters* 139: 195–211.

Stewart K, Turner S, Kelley S, Hawkesworth C, Kirstein L, and Mantovani M (1996) 3-D, (super 40) Ar- (super 39) Ar geochronology in the Parana continental flood basalt province. *Earth and Planetary Science Letters* 143: 95–109.

Stixrude L and Lithgow-Bertelloni C (2005) Mineralogy and elasticity of the oceanic upper mantle: Origin of the low-velocity zone. *Journal of Geophysical Research* 110.

Storey M, Duncan RA, and Tegner C (2007) Timing and duration of volcanism in the North Atlantic Igneous Province: Implications for geodynamics and links to the Iceland hotspot. *Chemical Geology* 241: 264–281.

Storey M, Mahoney JJ, and Saunders AD (1997) Cretaceous basalts in Madagascar and the transition between plume and continental lithosphere mantle sources. In: Mahoney JJ and Coffin MF (eds.) *Large Igneous Provinces: Continental, Oceanic, and Planetary Flood Volcanism. Geophysical Monograph*, 100, pp. 95–122. Washington, DC: American Geophysical Union.

Stracke A, Zindler A, Salters VJM, et al. (2003) Theistareykir revisited. *Geochemistry, Geophysics, Geosystems* 4: 8507. http://dx.doi.org/10.1029/2001GC000201.

Stuart FM, Lass-Evans S, Fitton JG, and Ellam RM (2003) High $^{3}He/^{4}He$ ratios in pictritic basalts from Baffin Island and the role of a mixed reservoir in mantle plumes. *Nature* 424: 57–59.

Styles E, Goes S, van Keken PE, Ritsema J, and Smith H (2011) Synthetic images of dynamically predicted plumes and comparison with a global tomographic model. *Earth and Planetary Science Letters* 311: 351–363.

Suetsugu D, Isse T, Tanaka S, et al. (2009) South Pacific mantle plumes imaged by seismic observation on islands and seafloor. *Geochemistry, Geophysics, Geosystems* 10.

Sun Y, Lai X, Wignall PB, et al. (2010) Dating the onset and nature of the Middle Permian Emeishan large igneous province eruptions in SW China using conodont biostratigraphy and its bearing on mantle plume uplift models. *Lithos* 119: 20–33.

Svensen H, Corfu F, Polteau S, Hammer O, and Planke S (2012) Rapid magma emplacement in the Karoo Large Igneous Province. *Earth and Planetary Science Letters* 325: 1–9.

Svensen H, Planke S, Polozov AG, et al. (2009) Siberian gas venting and the end-Permian environmental crisis. *Earth and Planetary Science Letters* 277: 490–500.

Tackley PJ (2011) Living dead slabs in 3-D: The dynamics of compositionally-stratified slabs entering a "slab graveyard" above the core-mantle boundary. *Physics of the Earth and Planetary Interiors* 188: 150–162.

Tackley PJ and Stevenson DJ (1993) A mechanism for spontaneous self-perpetuating volcanism on terrestrial planets. In: Stone DB and Runcorn SK (eds.) *Flow and Creep in the Solar System: Observations, Modeling and Theory*, pp. 307–321. Norwell, MA: Kluwer Academic.

Takahashi E (2002) The Hawaiian plume and magma genesis. *Geophysical Monograph* 128: 347–348.

Takahashi E and Kushiro I (1983) Melting of a dry peridotite at high-pressures and basalt magma genesis. *American Mineralogist* 68: 859–879.

Takahashi E, Nakajima K, and Wright TL (1998) Origin of the Columbia Rivers basalts: Melting model of a heterogeneous plume head. *Earth and Planetary Science Letters* 162: 63–80.

Takazawa E, Frey FA, Shimizu N, and Obata M (2000) Whole rock compositional variations in an upper mantle peridotite (Horoman, Hokkaido, Japan): Are they consistent with a partial melting process? *Geochimica et Cosmochimica Acta* 64: 695–716.

Tan E and Gurnis M (2007) Compressible thermochemical convection and application to lower mantle structures. *Journal of Geophysical Research* 112.

Tan E, Leng W, Zhong S, and Gurnis M (2011) On the location of plumes and lateral movement of thermochemical structures with high bulk modulus in the 3-D compressible mantle. *Geochemistry, Geophysics, Geosystems* 12.

Tanaka S, Obayashi M, Suetsugu D, et al. (2009) P-wave tomography of the mantle beneath the South Pacific Superswell revealed by joint ocean floor and islands broadband seismic experiments. *Physics of the Earth and Planetary Interiors* 172: 268–277.

Tarduno J, Bunge H-P, Sleep N, and Hansen U (2009) The Bent Hawaiian-Emperor hotspot track: Inheriting the mantle wind. *Science* 324: 50–53.

Tarduno JA, Duncan RA, Scholl DW, et al. (2003) The Emperor Seamounts; southward motion of the Hawaiian Hotspot plume in Earth's mantle. *Science* 301: 1064–1069.

Tarduno JA and Gee J (1995) Large-scale motion between Pacific and Atlantic hotspots. *Nature* 378: 477–480.

Tarduno JA, Sliter WV, Kroenke LW, et al. (1991) Rapid formation of Ontong Java Plateau by Aptian mantle plume volcanism. *Science* 254: 399–403.

Tauzin B, Debayle E, and Wittlinger G (2008) The mantle transition zone as seen by global Pds phases: No clear evidence for a thin transition zone beneath hotspots. *Journal of Geophysical Research* 113.

Taylor B (2006) The single largest oceanic plateau: Ontong Java-Manihiki-Hikurangi. *Earth and Planetary Science Letters* 241: 372–380.

Tejada MLG, Mahoney JJ, Castillo PR, Ingle SP, Sheth HC, and Weis D (2004) Pin-pricking the elephant: Evidence on the origin of the Ontong Java Plateau from Pb-Sr-Hf-Nd isotopic characteristics of ODP Leg 192. In: Fitton JG, Mahoney JJ, Wallace PJ, and Saunders AD (eds.) *Origin and Evolution of the Ontong Java Plateau, Special Publications 229*, pp. 133–150. London: Geological Society.

Tejada MLG, Mahoney JJ, Duncan RA, and Hawkins MP (1996) Age and geochemistry of basement and alkalic rocks of Malaita and Santa Isabel, Solomon Islands, southern margin of Ontong Java Plateau. *Journal of Petrology* 37: 361–394.

Tejada MLG, Mahoney JJ, Neal CR, Duncan RA, and Petterson MG (2002) Basement geochemistry and geochronology of central Malaita and Santa Isabel, Solomon Islands, southern margin of Ontong Java Plateau. *Journal of Petrology* 37: 449–484.

ten Brink U (1991) Volcano spacing and plate rigidity. *Geology* 19: 397–400.

Thompson RN and Gibson SA (1991) Subcontinental mantle plumes, hotspots and preexisting thinspots. *Journal of the Geological Society* 148: 973–977.

Thorne MS, Garnero EJ, and Grand SP (2004) Geographic correlation between hot spots and deep mantle lateral shear-wave velocity gradients. *Physics of the Earth and Planetary Interiors* 146: 4763.

Tian Y and Zhao D (2012) P-wave tomography of the western United States: Insight into the Yellowstone hotspot and the Juan de Fuca slab. *Physics of the Earth and Planetary Interiors* 200: 72–84.

Till CB, Elkins-Tanton LT, and Fischer KM (2010) A mechanism for low-extent melts at the lithosphere-asthenosphere boundary. *Geochemistry, Geophysics, Geosystems* 11.

Tilmann FJ, Benz HM, Priestley KF, and Okubo PG (2001) P-wave velocity structure of the uppermost mantle beneath Hawaii from traveltime tomography. *Geophysical Journal International* 146: 594–606.

Tiwari VM, Grevemeyer I, Singh B, and Morgan JP (2007) Variation of effective elastic thickness and melt production along the Deccan-Reunion hotspot track. *Earth and Planetary Science Letters* 264: 9–21.

To A, Romanowicz B, Capdeville Y, and Takeuchi N (2005) 3D effects of sharp boundaries at the borders of the African and Pacific Superplumes: Observation and modeling. *Earth and Planetary Science Letters* 233: 137–153.

Toomey DR, Hooft EEE, and Detrick R (2001) Crustal thickness variations and internal structure of the Galapagos Archipelago. *EOS, Transactions of the American Geophysical Union* 82(47), Fall Meeting Supplement, Abstract T42B-0939.

Torsvik TH, Burke K, Steinberger B, Webb SJ, and Ashwal LD (2010a) Diamonds sampled by plumes from the core-mantle boundary. *Nature* 466: U100–U352.

Torsvik TH, Smethurst MA, Burke K, and Steinberger B (2006) Large igneous provinces generated from the margins of the large low-velocity provinces in the deep mantle. *Geophysical Journal International* 167: 1447–1460.

Torsvik TH, Steinberger B, Gurnis M, and Gaina C (2010b) Plate tectonics and net lithosphere rotation over the past 150 My. *Earth and Planetary Science Letters* 291: 106–112.

Torsvik TH, Van der Voo R, Preeden U, et al. (2012) Phanerozoic polar wander, palaeogeography and dynamics. *Earth-Science Reviews* 114: 325–368.

Torsvik TH, Van der Voo R, and Redfield TF (2002) Relative hotspot motions versus true polar wander. *Earth and Planetary Science Letters* 202: 185–200.

Tosi N and Yuen DA (2011) Bent-shaped plumes and horizontal channel flow beneath the 660 km discontinuity. *Earth and Planetary Science Letters* 312: 348–359.

Trampert J, Deschamps F, Resovsky J, and Yuen D (2004) Probabilistic tomography maps chemical heterogeneities throughout the lower mantle. *Science* 306: 853–856.

Trumbull RB, Vietor T, Hahne K, Wackerle R, and Ledru P (2004) Aeromagnetic mapping and reconnaissance geochemistry of the Early Cretaceous Henties Bay-Outjo dike swarm, Etendeka Igneous Province, Namibia. *Journal of African Earth Sciences* 40: 17–29.

Turner DL, Jarrard RD, and Forbes RB (1980) Geochronology and origin of the Pratt-Welker seamount chain, Gulf of Alaska: A new pole of rotation for the Pacific plate. *Journal of Geophysical Research* 85: 6547–6556.

Turner S, et al. (1994) Magmatism and continental bread-up in the South Atlantic: High precision ^{40}Ar-^{39}Ar geochronology. *Earth and Planetary Science Letters* 121: 333–348.

Uenzelmann-Neben G, Schmidt DN, Niessen F, and Stein R (2012) Intraplate volcanism off South Greenland: Caused by glacial rebound? *Geophysical Journal International* 190: 1–7.

van Ark E and Lin J (2004) Time variation in igneous volume flux of the Hawaii-Emperor seamount chain. *Journal of Geophysical Research* 109: B11401. http://dx.doi.org/10.1029/2003JB002949.

van der Hilst RD and Karason H (1999) Compositional heterogeneity in the bottom 1000 kilometers of Earth's mantle: Toward a hybrid convection model. *Science* 283: 1885–1888.

van Hinsbergen DJJ, Steinberger B, Doubrovine PV, and Gassmoeller R (2011) Acceleration and deceleration of India-Asia convergence since the Cretaceous: Roles of mantle plumes and continental collision. *Journal of Geophysical Research* 116.

van Hunen J and Zhong S (2003) New insight in the Hawaiian plume swell dynamics from scaling laws. *Geophysical Research Letters* 30: 1785. http://dx.doi.org/10.1029/2003GL017646.

van Hunen J, Zhong SJ, Shapiro NM, and Ritzwoller MH (2005) New evidence for dislocation creep from 3-D geodynamic modeling of the Pacific upper mantle structure. *Earth and Planetary Science Letters* 238: 146–155.

van Keken PE (1997) Evolution of starting mantle plumes: A comparison between numerical and laboratory models. *Earth and Planetary Science Letters* 148: 1–11.

van Keken PE, Davaille A, and Vatteville J (2013) Dynamics of a laminar plume in a cavity: The influence of boundaries on the steady state stem structure. *Geochemistry, Geophysics, Geosystems* 14: 158–178.

van Keken PE and Gable CW (1995) The interaction of a plume with a rheological boundary: A comparison between two- and three-dimensional models. *Journal of Geophysical Research* 100: 20291–20302.

van Wijk JW, Baldridge WS, van Hunen J, et al. (2010) Small-scale convection at the edge of the Colorado Plateau: Implications for topography, magmatism, and evolution of Proterozoic lithosphere. *Geology* 38: 611–614.

van Wijk JW, Huismans RS, ter Voorde M, and Cloetingh S (2001) Melt generation at volcanic continental margins: No need for a mantle plume? *Geophysical Research Letters* 28: 3995–3998.

Vandamme D, Courtillot V, Besse J, and Montinny R (1991) Paleomagnetism and age determinations of the Deccan Traps (India): Results of a Nagpur-Bombay traverse and review of earlier work. *Reviews of Geophysics* 29: 159–190.

VanDecar JC, James DE, and Assumpcao M (1995) Seismic evidence for a fossil mantle plume beneath South America and implications for plate driving forces. *Nature* 378: 25–31.

Vatteville J, van Keken PE, Limare A, and Davaille A (2009) Starting laminar plumes: Comparison of laboratory and numerical modeling. *Geochemistry, Geophysics, Geosystems* 10.

Vdovin O, Rial JA, Levshin AL, and Ritzwoller MH (1999) Group-velocity tomography of South America and the surrounding oceans. *Geophysical Journal International* 136: 324–340.

Verati C, Rapaille C, Feraud G, Marzoli A, Bertrand H, and Youbi N (2007) Ar-40/Ar-39 ages and duration of the Central Atlantic Magmatic Province volcanism in Morocco and Portugal and its relation to the Triassic-Jurassic boundary. *Palaeogeography, Palaeoclimatology, Palaeoecology* 244: 308–325.

Vidal V and Bonneville A (2004) Variations of the Hawaiian hot spot activity revealed by variations in magma production rate. *Journal of Geophysical Research* 109. http://dx.doi.org/10.1029/2003JB002559.

Villagomez DR, Toomey DR, Hooft EEE, and Solomon SC (2007) Upper mantle structure beneath the Galapagos Archipelago from surface wave tomography. *Journal of Geophysical Research* 112.

Vinnik L, Silveira G, Kiselev S, Farra V, Weber M, and Stutzmann E (2012) Cape Verde hotspot from the upper crust to the top of the lower mantle. *Earth and Planetary Science Letters* 319: 259–268.

Vlastelic I and Dosso L (2005) Initiation of a plume-ridge interaction in the South Pacific recorded by high-precision Pb isotopes along Hollister Ridge. *Geochemistry, Geophysics, Geosystems* 6.

Waite GP, Smith RB, and Allen RM (2006) V-P and V-S structure of the Yellowstone hot spot from teleseismic tomography: Evidence for an upper mantle plume. *Journal of Geophysical Research* 111.

Walker KT, Bokelmann GHR, Klemperer SL, and Bock G (2005) Shear-wave splitting around the Eifel hotspot: Evidence for a mantle upwelling. *Geophysical Journal International* 163: 962–980.

Wang S and Wang R (2001) Current plate velocities relative to hotspots: Implications for hotspot motion, mantle viscosity and global reference frame. *Earth and Planetary Science Letters* 189: 133–140.

Watson S and McKenzie D (1991) Melt generation by plumes – A study of Hawaiian volcanism. *Journal of Petrology* 32: 501–537.

Watts AB, Weissel JK, Duncan RA, and Larson RL (1988) Origin of the Louisville ridge and its relationship to the Eltanin fracture zone system. *Journal of Geophysical Research* 93: 3051–3077.

Weeraratne DS, Forsyth DW, Yang Y, and Webb SC (2007) Rayleigh wave tomography beneath intraplate volcanic ridges in the South Pacific. *Journal of Geophysical Research* 112.

Weis D, Frey FA, Schlich R, et al. (2002) Trace of the Kerguelen mantle plume: Evidence from seamounts between the Kerguelen Archipelago and Heard Island, Indian Ocean. *Geochemistry, Geophysics, Geosystems* 3.

Weis D, Garcia MO, Rhodes JM, Jellinek M, and Scoates JS (2011) Role of the deep mantle in generating the compositional asymmetry of the Hawaiian mantle plume. *Nature Geoscience* 4: 831–838.

Wen L (2006) A compositional anomaly at the Earth's core-mantle boundary as an anchor to the relatively slowly moving surface hotspots and as source to the DUPAL anomaly. *Earth and Planetary Science Letters* 246: 138–148.

Werner R, Hoernle K, van den Bogaard P, Ranero C, von Huene R, and Korich D (1999) Drowned 14-m.y.-old Galapagos Archipelago off the coast of Costa Rica: Implications for tectonic and evolutionary models. *Geology* 27: 499–502.

Wessel P (1993) Observational constraints on models of the Hawaiian hot spot swell. *Journal of Geophysical Research* 98: 16095–16104.

Wessel P and Kroenke LW (2008) Pacific absolute plate motion since 145 Ma: An assessment of the fixed hot spot hypothesis. *Journal of Geophysical Research* 113.

Wessel P and Kroenke LW (2009) Observations of geometry and ages constrain relative motion of Hawaii and Louisville plumes. *Earth and Planetary Science Letters* 284: 467–472.

Wessel P and Smith WHF (1995) New version of the Generic Mapping Tools released. *EOS, Transactions of the American Geophysical Union* 76: 329.

West JD, Fouch MJ, Roth JB, and Elkins-Tanton LT (2009) Vertical mantle flow associated with a lithospheric drip beneath the Great Basin. *Nature Geoscience* 2: 438–443.

White R and McKenzie D (1989) Magmatism at rift zones: The generation of volcanic continental margins and flood basalts. *Journal of Geophysical Research* 94: 7685–7729.

White RS (1988) A hot-spot model for early Tertiary volcanism in the N Atlantic. *Geological Society* 39: 3–13, special publications.

White RS (1997) Rift-plume interaction in the North Atlantic. *Philosophical Transactions of the Royal Society of London, Series A* 355: 319–339.

White RS, Bown JW, and Smallwood JR (1995) The temperature of the Iceland plume and origin of outward propagating V-shaped ridges. *Journal of the Geological Society* 152: 1039–1045.

White RS and McKenzie D (1995) Mantle plumes and flood basalts. *Journal of Geophysical Research* 100: 17543–17585.

Whitehead JA and Helfrich KR (1988) Wave transport of deep mantle material. *Nature* 336: 59–61.

Whitehead JA and Luther DS (1975) Dynamics of laboratory diapir and plume models. *Journal of Geophysical Research* 80: 705–717.

Whiteside JH, Olsen PE, Kent DV, Fowell SJ, and Et-Touhami M (2007) Synchrony between the Central Atlantic magmatic province and the Triassic-Jurassic mass-extinction event? *Palaeogeography, Palaeoclimatology, Palaeoecology* 244: 345–367.

Whittaker JM, Mueller RD, Leitchenkov G, et al. (2007) Major Australian-Antarctic plate reorganization at Hawaiian-Emperor bend time. *Science* 318: 83–86.

Williams Q, Revenaugh J, and Garnero E (1998) A correlation between ultra-low basal velocities in the mantle and hot spots. *Science* 281: 546–549.

Wilson JT (1963) A possible origin of the Hawaiian Islands. *Canadian Journal of Physics* 41: 863–870.

Wilson JT (1973) Mantle plumes and plate motions. *Tectonophysics* 19: 149–164.

Wolfe C, Bjarnason IT, VanDecar JC, and Solomon SC (1997) Seismic structure of the Iceland mantle plume. *Nature* 385: 245–247.

Wolfe CJ, Solomon SC, Laske G, et al. (2009) Mantle shear-wave velocity structure beneath the hawaiian hot spot. *Science* 326: 1388–1390.

Wolfe CJ, Solomon SC, Laske G, et al. (2011) Mantle P-wave velocity structure beneath the Hawaiian hotspot. *Earth and Planetary Science Letters* 303: 267–280.

Wolfe CJ, Solomon SC, Silver PG, VanDecar JC, and Russo RM (2002) Inversion of body- wave delay times for mantle structure beneath the Hawaiian Islands: Results from the PELENET experiment. *Earth and Planetary Science Letters* 198: 129–145.

Wolff JA, Ramos FC, Hart GL, Patterson JD, and Brandon AD (2008) Columbia River flood basalts from a centralized crustal magmatic system. *Nature Geoscience* 1: 177–180.

Xu J-F, Suzuki K, Xu Y-G, Mei H-J, and Li J (2007) Os, Pb, and Nd isotope geochemistry of the Permian Emeishan continental flood basalts: Insights into the source of a large igneous province. *Geochimica et Cosmochimica Acta* 71: 2104–2119.

Xu W, Lithgow-Bertelloni C, Stixrude L, and Ritsema J (2008) The effect of bulk composition and temperature on mantle seismic structure. *Earth and Planetary Science Letters* 275: 70–79.

Xu Y, Chung S-L, Jahn B-M, and Wu G (2001) Petrologic and geochemical constraints on the petrogenesis of Permian-Triassic Emeishan flood basalts in southwestern China. *Lithos* 58: 145–168.

Xu Y, He B, Chung S-L, Menzies MA, and Frey FA (2004) Geologic, geochemical, and geophysical consequences of plume involvement in the Emeishan flood-basalt province. *Geology* 32: 917–920.

Xue M and Allen RM (2005) Asthenospheric channeling of the Icelandic upwelling: Evidence from seismic anisotropy. *Earth and Planetary Science Letters* 235: 167–182.

Yale MM and Phipps Morgan J (1998) Asthenosphere flow model of hotspot-ridge interactions: A comparison of Iceland and Kerguelen. *Earth and Planetary Science Letters* 161: 45–56.

Yamamoto M, Morgan JP, and Morgan WJ (2007) Global plume-fed asthenosphere flow-II: Application to the geochemical segmentation of mid-ocean ridges. In: Foulger GR and Jurdy DM (eds.) *Plates, Plumes, and Planetary Processes, GSA Special Paper 430:* Geological Society of America.

Yang T and Shen Y (2005) P-wave velocity structure of the crust and uppermost mantle beneath Iceland from local earthquake tomography. *Earth and Planetary Science Letters* 235: 597–609.

Yang T, Shen Y, van der Lee S, Solomon SC, and Hung S-H (2006) Upper mantle structure beneath the Azores hotspot from finite-frequency seismic tomography. *Earth and Planetary Science Letters* 250: 11–26.

Yasuda A and Fujii T (1994) Melting phase relations of an anhydrous mid-ocean ridge basalt from 3 to 20 GPa: Implications for the behavior of subducted oceanic crust in the mantle. *Journal of Geophysical Research* 99: 9401–9414.

Yaxley GM and Green DH (1998) Reactions between eclogite and peridotite: Mantle refertilization by subduction of oceanic crust. *Schweizerische Mineralogische und Petrographische Mitteilungen* 78: 243255.

Yuan HY and Dueker K (2005) Teleseismic P-wave tomogram of the Yellowstone plume. *Geophysical Research Letters* 32: L07304. http://dx.doi.org/10.01029/02004GL022056.

Zhang J and Green HW (2007) Experimental investigation of eclogite rheology and its fabrics at high temperature and pressure. *Journal of Metamorphic Geology* 25: 97–115.

Zhang T, Lin J, and Gao J (2011) Interactions between hotspots and the Southwest Indian Ridge during the last 90 Ma: Implications on the formation of oceanic plateaus and intra-plate seamounts. *Science China-Earth Sciences* 54: 1177–1188.

Zhao D (2007) Seismic images under 60 hotspots: Search for mantle plumes. *Gondwana Research* 12: 335–355.

Zheng L, Yang Z, Tong Y, and Yuan W (2010) Magnetostratigraphic constraints on two-stage eruptions of the Emeishan continental flood basalts. *Geochemistry, Geophysics, Geosystems* 11.

Zhong H, Campbell IH, Zhu W-G, et al. (2011) Timing and source constraints on the relationship between mafic and felsic intrusions in the Emeishan large igneous province. *Geochimica et Cosmochimica Acta* 75: 1374–1395.

Zhong H, Zhu W-G, Chu Z-Y, He D-F, and Song X-Y (2007) Shrimp U-Pb zircon geochronology, geochemistry, and Nd-Sr isotopic study of contrasting granites in the Emeishan large igneous province, SW China. *Chemical Geology* 236: 112–133.

Zhong SJ and Watts AB (2002) Constraints on the dynamics of mantle plumes from uplift of the Hawaiian Islands. *Earth and Planetary Science Letters* 203: 105–116.

Zhou H and Dick HJB (2013) Thin crust as evidence for depleted mantle supporting the Marion Rise. *Nature* 494: 195–200.

Zhou Z, Malpas J, Song XY, et al. (2002) A temporal link between the Emeishan large igneous province (SW China) and the end-Guadalupian mass extinction. *Earth and Planetary Science Letters* 196: 113–122.

Zindler A and Hart S (1986) Chemical geodynamics. *Annual Review of Earth and Planetary Sciences* 14: 493–571.

Zlotnik S, Afonso JC, Diez P, and Fernandez M (2008) Small-scale gravitational instabilities under the oceans: Implications for the evolution of oceanic lithosphere and its expression in geophysical observables. *Philosophical Magazine* 88: 3197–3217.

TGP2: 00133

Non-Print Items

Abstract:

This chapter describes the progress that has been made over the past decades in understanding observations of large-scale melting anomalies that are not readily explained by plate tectonic theory. Fundamental observations include the volume and geochemistry of flood basalts and ocean island basalts, the age progression of volcano chains, the geometry of hotspot swells, and the seismic imaging of crust and mantle structures. Observations of a subset of melting anomalies can be explained by classical plume theory, in which buoyancy-driven upwellings rise through the entire mantle to cause massive flood basalt volcanism that is trailed by an age-progressive hotspot volcano chain. However, a range of observations call for significant extensions to classical theory, and some sites of excess volcanism are better explained by alternative mechanisms, such as small-scale convection or shear-driven upwelling, than by plume theory. Detailed studies of upwelling and melting can provide constraints for heat and material fluxes through the mantle and provide a better understanding of the long-term thermal and chemical evolution of the Earth's interior.

Keywords: Decompression melting; Dynamic topography; Flood basalts; Hotspot; Hotspot swell; Intraplate volcanism; Large igneous provinces; Mantle plumes; Ocean island basalts; Seismic mantle tomography; Shear-driven upwelling; Small-scale convection; Thermochemical convection

Author and Co-author Contact Information:

Maxim D. Ballmer
Department of Geology and Geophysics
SOEST
University of Hawaii
Honolulu
HI
USA
E-mail: ballmer@hawaii.edu

Earth Life Science Institute
Tokyo Institute of Technology
Meguro-ku
Tokyo
Japan

Peter E. van Keken
Earth and Environmental Sciences
University of Michigan
Ann Arbor
MI
USA
E-mail: keken@umich.edu

Garrett Ito
Department of Geology and Geophysics
SOEST
University of Hawaii
Honolulu
HI
USA
E-mail: gito@hawaii.edu